PTR-MS MOBILE LABORATORY VAPOR MONITORING MONTHLY REPORT – MONTH 5

Report No. 53005-81-RPT-048
Revision 0
January 1, 2019 – February 9, 2019

Prepared for:

Washington River Protection Solutions, LLC
P.O. Box 850
Richland, WA 99352

Subcontract 53005, Release 81

Prepared by:
TerraGraphics Environmental Engineering, Inc.
2926 E. Ainsworth St.
Pasco, WA 99301

TerraGraphics
www.terragraphics.com

Approval Form

Prepared by:

Date: 10/25/2019

Tyler Williams

Reviewed by:

Date: 10/25/2019

Matthew Erickson, Ph.D.

Approved by:

Date: 10/25/2019

Rich Westberg

Record of Revision

Revision	Date	Pages/Sections Changed	Brief Description
0	10/2019	All	Original Issue

Table of Contents

Appendices

Figures

Tables

Acronyms and Abbreviations

ALS	Australian Laboratory Services
AME	Automated Measurement and Evaluation
ANOVA	Analysis of Variance
AOP	Abnormal Operating Procedure
ASTM	American Society of Testing and Materials
CI	Confidence Interval
COPC	Chemical of Potential Concern
DNPH	Dinitrophenylhydrazine
DOE	U.S. Department of Energy
DR	Deficiency Report
FY	Fiscal Year
HPLC	High Performance Liquid Chromatography
MCP	Multi-channel Plate
MDL	Method Detection Limit
ML	Mobile Laboratory (Mobile Vapor Monitoring Laboratory)
NDEA	N-nitrosodiethylamine
NDMA	N-nitrosodimethylamine
NEMA	N-nitrosomethylethylamine
NIOSH	National Institute of Occupational Safety and Health
NMOR	N-nitrosomorpholine
OEL	Occupational Exposure Limit
OSC	Organosulfur Compound
PNNL	Pacific Northwest National Laboratory
ppbv	parts per billion by volume
ppmv	parts per million by volume
pptv	parts per trillion by volume
PTR-MS	Proton Transfer Reaction – Mass Spectrometer
PTR-TOF	Proton Transfer Reaction – Time of Flight
QA	Quality Assurance
R&D	Research and Development
RL	Reporting Limit
SME	Subject Matter Expert

SSR	Solid State Relay
TIC	Tentatively Identified Compound
VOC	Volatile Organic Compound
WRPS	Washington River Protection Solutions, LLC

Executive Summary

In support of the Hanford Vapor Monitoring, Detection, and Remediation Project, Washington River Protection Solutions, LLC has subsidized the implementation of a mobile vapor monitoring laboratory developed by TerraGraphics Environmental Engineering, Inc. (Statement of Work #306312, "Mobile Laboratory Services and Lease"). The contract secures services associated with the lease and operation of the Mobile Laboratory designed specifically for trace gas analysis based on the Proton Transfer Reaction – Mass Spectrometer and supplemental analytical instruments. Operation of the Mobile Laboratory will be at the discretion of Washington River Protection Solutions, LLC and will be conducted to support a variety of projects including continuing background studies, fugitive emissions, waste disturbing activities, leading indicator studies, and general area sampling. Other applications of the Mobile Laboratory will be determined as needed by Washington River Protection Solutions, LLC.

This report covers operations and testing activities between January 1, 2019, and February 9, 2019. During this period, operations and testing activities included maintenance activities, septic investigation, AP Tank Farm pump removal, and completion of the fourth and final leg of a background study.

For the majority of Month 5, the Mobile Laboratory was used for the measurement of volatile organic compounds during a 24-day background study between January 14, 2019, and February 9, 2019. As this was a continuation of a four-part seasonal study, six previously selected sites were monitored on a rotating basis for sixteen chemicals of potential concern including nitrosamines, furans, and ammonia. The technical basis for this study is the same as the previous background studies performed by TerraGraphics and RJ Lee Group, Inc. Five sampling locations were chosen within the secured Hanford area and one site within the City of Kennewick to represent a site with heavy traffic and mixed commercial use.

The Mobile Laboratory supported the AP Pump Removal activities that occurred on January 24, 2019. The Mobile Laboratory performed area monitoring of AP Farm during partial and complete removal of the pump.

In support of Washington River Protection Solutions LLC's fugitive emissions team, the Mobile Laboratory participated in a short-term investigation to characterize septic odors in the 200 East area of the Hanford Site on January 30, 2019.

During Month 5, the Proton Transfer Reaction – Mass Spectrometer experienced instrumentation issues that caused baseline sensitivity to drift upward. The issue was documented in a deficiency report, DR19-001, and managed by Mobile Laboratory staff. As a result, method detection limits were adjusted upward by Mobile Laboratory subject matter experts and data analysts to levels sufficient to reduce uncertainty to acceptable levels.

1.0 DESCRIPTION OF TESTS CONDUCTED

During Month 5, spanning the dates of January 1, 2019, to February 9, 2019, the Mobile Laboratory (ML) was deployed for the measurement of volatile organic compounds (VOCs) after ML maintenance, modifications, operational testing, and continuous training were performed. During this period, three testing campaigns were conducted on the Hanford Site (Figure 1-1). These tests detailed in Section 5.0 included septic analysis, AP pump removal, and a background study. Table 1-1 provides a summary of tests and activities conducted during Month 5.

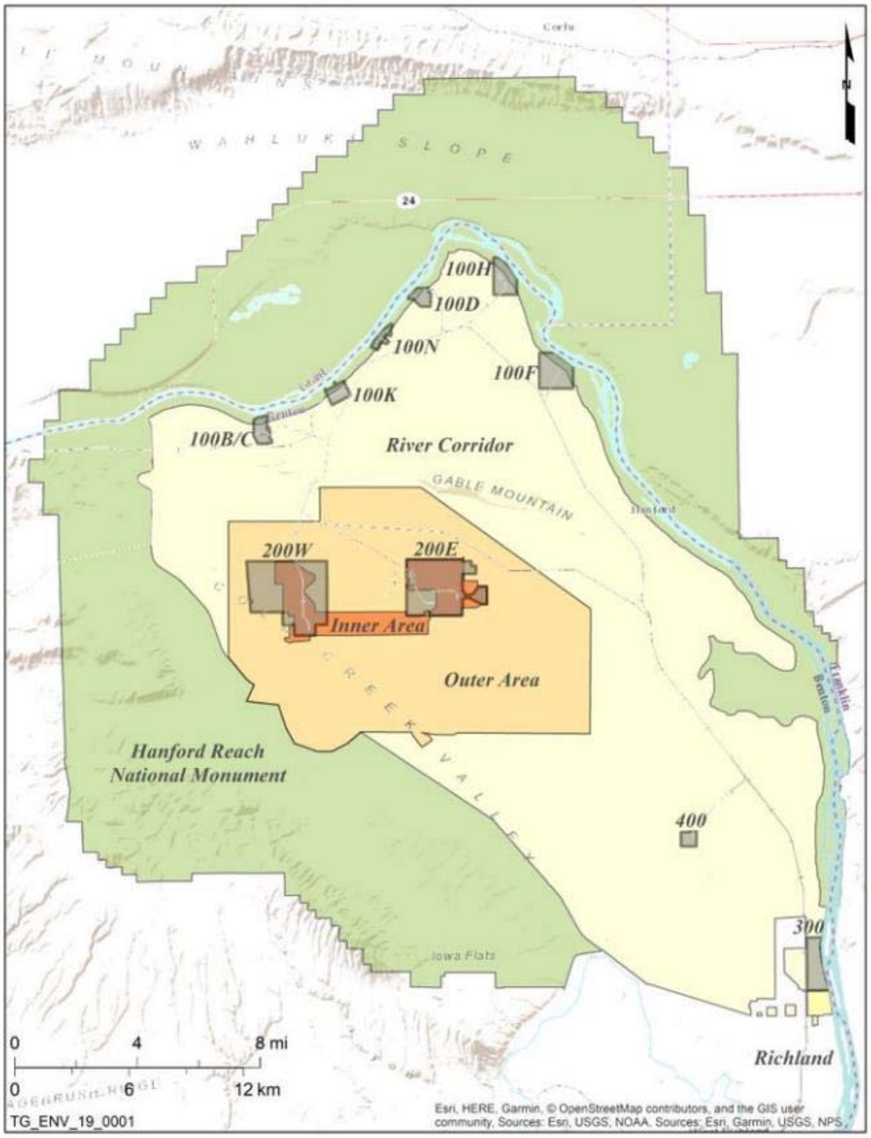

Figure 1-1. Hanford Site.

Table 1-1. Summary of Month 5 Testing and Operational Activities.

Week	Date	Activity
22	01/02/2019	ML Modifications and Testing
	01/03/2019	ML Modifications and Testing
	01/04/2019	ML Modifications and Testing
23	01/07/2019	ML Modifications and Testing
	01/08/2019	ML Modifications and Testing
	01/09/2019	ML Personnel Training
	01/10/2019	ML Modifications and Testing
	01/11/2019	ML Modifications and Testing
24	01/14/2019	Site 1 (Stationary Monitoring)
	01/15/2019	Site 2 (Stationary Monitoring)
	01/16/2019	Site 3 (Stationary Monitoring)
	01/17/2019	Site 4 (Stationary Monitoring)
	01/18/2019	Site 5 (Stationary Monitoring)
	01/19/2019	Site 6 (Stationary Monitoring)
	01/20/2019	Site 1 (Stationary Monitoring)
25	01/21/2019	Site 2 (Stationary Monitoring)
	01/22/2019	Site 3 (Stationary Monitoring)
	01/23/2019	Site 4 (Stationary Monitoring)
	01/24/2019	AP Pump Removal Monitoring & MCP Module Installation
	01/25/2019	ML Modifications & Calibration
	01/26/2019	Site 1 (Stationary Monitoring)
	01/27/2019	Site 2 (Stationary Monitoring)
26	01/28/2019	Site 3 (Stationary Monitoring)
	01/29/2019	Site 4 (Stationary Monitoring)
	01/30/2019	Fugitive Emissions & Site 5 (Stationary Monitoring)
	01/31/2019	Site 6 (Stationary Monitoring)
	02/01/2019	Site 1 (Stationary Monitoring)
	02/02/2019	Site 2 (Stationary Monitoring)
	02/03/2019	Site 3 (Stationary Monitoring)
27	02/04/2019	Site 4 (Stationary Monitoring)
	02/05/2019	Site 5 (Stationary Monitoring)
	02/06/2019	Site 6 (Stationary Monitoring)
	02/07/2019	Site 3 (Stationary Monitoring)
	02/08/2019	Site 5 (Stationary Monitoring)
	02/09/2019	Site 6 (Stationary Monitoring)

Beyond monitoring, the tasks conducted during this period were performed to support proper function of the instruments in the ML. These tasks include calibrations, troubleshooting, verifications, and maintenance.

This report is structured based on reporting requirements, as defined in the original statement of work (SOW 306312, "Mobile Laboratory Services and Lease").

1.1 Description of Background Study

The field campaign, referred to as the background study, was performed in accordance with 66409-RPT-007, *Mobile Laboratory Operational Project Test Plan FY2019 (Test Plan).* The study included 24 days of sampling at six pre-determined sampling sites four days each on a revolving schedule. This study is a continuation of Fiscal Year (FY)17 sampling activities where samples were taken over a six-week period encompassing six sites of interest with repeated visits to each location throughout the test period. The goal of the background study is to provide a comprehensive spatial and temporal study of chemicals of potential concern (COPCs) background concentrations both on and off the Hanford Site.

The sampling locations chosen for this study are listed below.

- **Site 1:** Hanford Central Plateau northwest of the 200W Tank Farm, chosen as an upwind location from the central Hanford Plateau.
- **Site 2:** Southern end of the 200W Tank Farms.
- **Site 3:** Near the Corner of 4th and Buffalo; west of the 242-A Evaporator. This site is historically known for the occurrence of several Abnormal Operating Procedure (AOP-015) Events.
- **Site 4:** Downwind of the AN Tank Farm.
- **Site 5**: Southwest of the Waste Treatment Facility.
- **Site 6:** Near the intersection of US-395 and Clearwater Avenue in Kennewick WA. This site represents heavy traffic and mixed commercial activity.

The background study focused on nineteen compounds from the Hanford COPC list; four nitrosamines, fourteen furans, and ammonia. Several furans are exact isomers of each other, therefore the number of unique signals focused on during the background study campaign totaled sixteen. Additional details regarding the nature, results, and conclusion of this study are provided in Section 5.4. Contained in that section is an assessment of study completeness along with an assessment of ML measurements to confirmatory sample measurements.

1.2 Description of Septic Analysis

Under the direction of Washington River Protection Solutions, LLC's (WRPS') Fugitive Emissions Team, the ML was operated in the 200 East area of the Hanford Site on January 30, 2019, as part of a short-term investigation of septic odors. The ML was stationed at the southwest corner of AP Tank Farm, downwind of a septic tank and drain field to the north of the farm. Measurements were made with no issues and a multi-compound profile was produced for this analysis which is detailed in Section 5.1.

1.3 Description of AP Pump Removal

Under the direction of WRPS' Tank Farms Project Team, the ML operated in the 200 East area on January 24, 2019, in an effort to support AP Pump Removal. The ML was positioned downwind of the AP Pump while tank farm workers performed removal activities. The ML performed area monitoring of AP Farm during partial and complete removal of the pump. Measurements were collected with no issue and results from this operation are detailed in Section 5.2.

2.0 MEASUREMENT SYSTEM DESIGN

This section describes the sampling methods, instrumentation, and confirmatory measurements used during this monitoring period.

2.1 Sampling Methods

The following sections detail the sampling methods utilized during the monitoring periods that occurred in Month 5.

2.1.1 Design of Sampling System

The ML is housed in a Chevrolet®[1] 4500 14' Box Truck equipped with a 5.2L diesel engine. The box has been fully insulated to allow for the ML to maintain comfortable working temperatures for the Operators and the instrumentation. The ML has the option of utilizing either shore power or onboard diesel generator power for operation of the instruments. During Month 5, while the ML was located at the TerraGraphics shop, shore power was utilized. The ML was powered by the generator at all deployed locations during Month 5. When deployed for septic tank monitoring, the ML used both the mast and the side port to perform air sampling. The mast was utilized for sampling for the duration of the background study sampling.

The layout of the ML and the sampling system is shown in the following drawings:

- 66409-18-ML-003, *Sampling Manifold Sketch*; and
- 66409-18-ML-004, *Mobile Lab Schematics*.

2.1.1.1 Proton Transfer Reaction – Mass Spectrometer Sampling

The Proton Transfer Reaction – Time of Flight (PTR-TOF) 6000 X2 is the latest trace VOC analyzer from IONICON®[2]. The PTR-TOF 6000 X2 is used to quantify COPCs from the sampled air. The sampled air enters the Proton Transfer Reaction – Mass Spectrometer (PTR-MS) drift tube. In the drift tube, VOCs undergo chemical ionization via a fast proton transfer reaction using the reagent ion, hydronium. The hydronium is produced from water vapor via a series of reactions in the hollow cathode PTR-MS ion source. This is a soft ionization method and VOC fragmentation is minimized. These ionized compounds and hydronium then travel through the drift tube to the transfer lens system, subsequently entering the TOF-MS where they are separated by mass and monitored. The signal from the TOF-MS is used to identify the VOCs based on their mass, as well as to calculate individual compound concentration based on the ratio of compound signal to hydronium signal.

---

[1] Chevrolet is a registered trademark of General Motors, LLC, Detroit, Michigan.
[2] IONICON is a registered trademark of Ionicon Analytik Gesellschaft m.b.H., Innsbruck, Austria.

2.1.1.2 DAQFactory Sampling

DAQFactory®[3] is a data acquisition and automation software from AzeoTech that allows users to design custom applications with control and automatic output settings. In the ML, DAQFactory controls the sampling system through valves and flow controllers for the LI-COR®[4] CO_2 monitor, Picarro Ammonia Analyzer, Airmar®[5] Weather Station, and the PTR-TOF.

2.2 Instrumentation and Methods Used

The following sections detail the instrumentation and methods utilized during the monitoring periods that occurred in Month 5.

2.2.1 Proton Transfer Reaction – Mass Spectrometer

Measurements performed by the ML during Month 5 utilized the IONICON® PTR-TOF 6000 X2 system. The mass resolution of the PTR-TOF 6000 is sufficient to resolve COPCs with high confidence (i.e., furan from isoprene) while other compounds have interferences which can potentially compromise their reliable detection and quantification. A full discussion of the reliability of COPC detection and quantification as performed by a PTR-TOF 4000, an instrument with less resolution, can be found in *Fiscal Year 2017 Mobile Laboratory Vapor Monitoring at the Hanford Site: Monitoring During Waste Disturbing Activities and Background Study*, September 2017. A brief summary of the instrument and its underlying chemistry that leads to the sensitive detection of vapor components will be provided herein. The general layout of the instrument is shown in Figure 2-1.

---

[3] DAQFactory is a registered trademark of Azeotech, Inc., Ashland, Oregon.
[4] LI-COR is a registered trademark of LI-COR, Inc., Lincoln, Nebraska.
[5] Airmar is a registered trademark of Airmar Technology Corporation, Milford, New Hampshire.

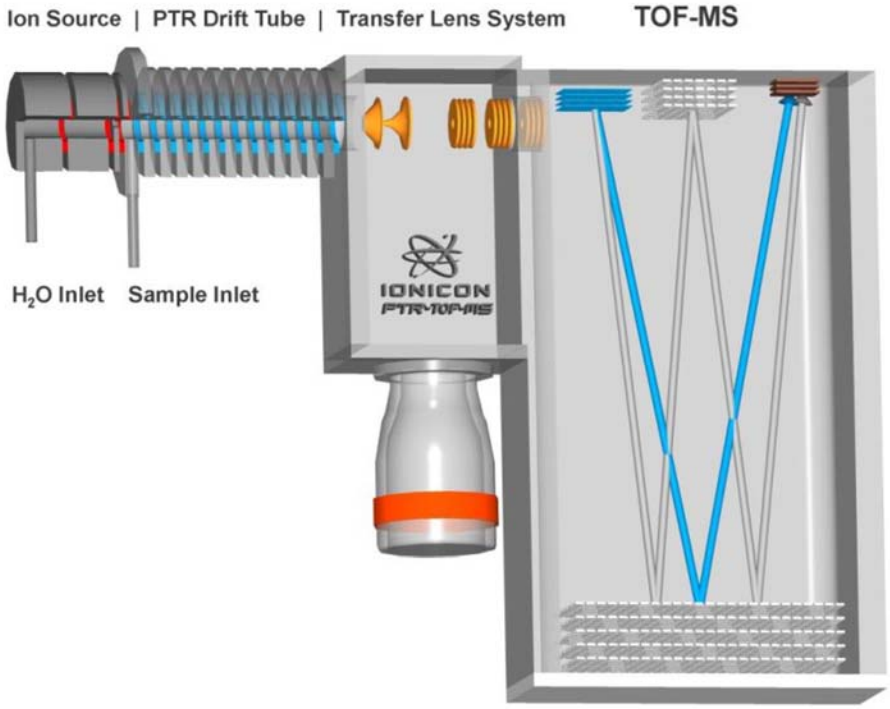

Figure 2-1. The General Configuration of an IONICON Proton Transfer Reaction – Time of Flight Instrument.

The VOCs are measured by chemical ionization, where the reagent ion H_3O^+ ionizes organics via a fast proton transfer reaction (R1).

$$R + H_3O^+ \rightarrow RH^+ + H_2O \qquad \text{(R1)}$$

These reactions are normally non-dissociative, although there are some compounds that fragment to smaller ions upon protonation. The reaction takes place in a drift tube where the sample air stream reacts with H_3O^+ ions produced by a hollow cathode ion source. The number of ions counted per second for the reagent ion and protonated sample ion are monitored and used for the determination of estimated concentrations according to Equation 1.

$$[R] = \frac{1}{kt}\left(\frac{I_{RH+}}{I_{H3O+}}\right)\frac{\varepsilon_{RH+}}{\varepsilon_{H3O+}} \qquad (1)$$

where k is the ion–molecule rate constant (molecules cm^{-3} s^{-1}), t is the reaction time (~ 100 microseconds), I_{RH+} and I_{H3O+} are the respective ion count rates, and ε_{RH+} and ε_{H3O+} are the ion transmission efficiencies through the TOF. It is important to note that estimated concentrations of compounds can be determined directly from Equation 1 (the “kinetic approach” to quantification). There is no need for the analysis of authentic standards and the generation of calibration curves. The system is essentially self-correcting as all measurements are made with respect to the ion count rate of the reagent ion.

The mixing ratio X of the organic R in the sample air is then determined by:

$$X_R\ (ppbV) = \frac{[R]}{[AIR]_{drift}} \times 1 \times 10^9 \qquad (2)$$

where *[AIR]* is the number density of air (molecules/cm^3) in the drift tube given the drift tube pressure (typically ~ 2.4 mbar) and temperature (typically ~ 50°C).

The PTR-MS technology has been used in numerous applications around the world with hundreds of peer review publications appearing in the literature over the past 20 years. Even though the technology is widely used in the research arena and has proven to be indispensable for many applications, there is no standard method among the United States regulatory agencies such as the U.S. Environmental Protection Agency, ASTM®[7], and NIOSH®[8]. The end user of the technology is expected to provide the "best practice" in its use by adhering to established operational parameters governed by the scope of the project and the nature of the sample(s) to be measured.

The kinetic approach provides quantitative estimates based on the use of relative ion signals of target compounds versus that of the reagent ion with an applied reaction rate constant found in the literature. This approach was chosen over the use of calibration standards due to the challenges associated with obtaining stable calibration mixtures for the Hanford COPC list. All H_3O^+ related quantification performed in this background study was accomplished by the kinetic approach. The NO^+ mode quantification applies the method described in the 53005-81-RPT-039, *PTR-MS-Mobile Laboratory Monitoring Monthly Report – Month 4*.

2.2.2 Carbon Dioxide Monitor

Carbon dioxide is not a COPC; however, monitoring CO_2 is necessary for correlation of vapor signals to combustion processes or other sources. There are numerous combustion sources near the sampling sites of the background study including diesel and gas generators, all-terrain vehicles with no catalytic converters, and diesel and gasoline vehicles. These contribute VOCs to the vapor burden and are readily observed by the PTR-MS. It is necessary to distinguish these VOCs from tank farm related emissions resulting from normal work-related activities.

The CO_2 monitor used in the TerraGraphics ML was the LI-COR Model 850A. The Li-850A is an absolute, non-dispersive infrared gas analyzer based upon a single path, dual wavelength infrared detection system. It is a low-maintenance, high-performance monitoring solution that gives accurate, stable readings over a wide range of environmental conditions. It has a range of 0-20,000 ppm (0-2%), low power consumption (4 W after power-up), and 1-second signal averaging to allow for real-time source apportionment (i.e., monitoring vehicle exhaust or other combustion sources on-the-fly). The instrument operates on a gas flow of less than 1 liter per minute.

---

[7] ASTM is a registered trademark of American Society for Testing and Materials, West Conshohocken, Pennsylvania.

[8] NIOSH is a registered trademark of U.S. Department of Health and Human Services, Bethesda, Maryland.

It is interfaced to the ML's internal gas manifold at the same location as the PTR-MS sampling port to ensure that both instruments are simultaneously measuring the same source. The data from the CO_2 monitor are used to predict when VOC measurements from the PTR-MS come from combustion sources.

The CO_2 monitor used during the background study and sewer sampling was operated using a factory calibration. Periodic checks of the unit were made with zero air and ambient background air (ambient atmospheric CO_2 levels are approximately 400 ppm), and a certified reference standard to ensure continued system operation. The system has a continuous direct readout which can be displayed on the DAQFactory monitor in real time to aid in real-time decision making by the field analysts.

2.2.3 Ammonia Monitor

Ammonia is a compound on the COPC list of particular importance. It is believed to be associated with all high-level waste storage tanks on the Hanford Site and as such was identified as a key leading indicator for up to 43 COPCs in Pacific Northwest National Laboratory (PNNL) publication 27449, *FY18 Leading Indicator Phase 2 Report*. The global average background for ammonia is between 5-7 parts per billion by volume (ppbv). Previous studies of ammonia levels on the Hanford Site indicate the expected measurement range should be in the low ppbv range. Although relatively easy to measure at the parts per million by volume (ppmv) level, its measurement at the low ppbv level with high temporal resolution is not trivial. The purpose of measuring trace levels of NH_3 is the correlation of vapor data from the PTR-MS to actual tank emissions. A measured vapor plume containing elevated COPCs with the same time correlation as an ammonia plume is reasonable evidence of a tank emission.

The ammonia monitor used was a Picarro Model G2103 that is capable of measuring NH_3 with parts per trillion by volume (pptv) sensitivity. It is a sophisticated time-based measurement system that uses a laser to quantify spectral features of gas phase molecules in an optical cavity. It is based on cavity ring down spectroscopy. Gas phase spectroscopy measurements are subject to temperature and pressure fluctuations. The Picarro system features a ± 0.005°C temperature stability and ± 0.0002 atm pressure stability to ensure low noise and high accuracy measurements. Sample flow rate to the instrument was provided by an external pump at 0.8 liters per minute at 760 Torr.

The analyzer is interfaced to the ML main sample stream to ensure the instrument measured the same gas sample as the PTR-MS and CO_2 monitor. The system outputs real-time data to a monitor, records data to its internal computer, and uses the ML Wi-Fi connection to automatically synchronize to a clock service. Daily data sets are retrieved and backed up similar to the other data collection instruments.

2.2.4 Weather Station

The weather station used in the ML is an Airmar 200WX-IPx7 with a control unit mounted in the server cabinet and the transducer mounted on the sampling mast located above the roof of the van. Real-time display of the output is visible on the DAQFactory monitor to aid field analysts in making sampling decisions in the field. The output data are fed to the server with a clock time stamp that is synchronized to the other monitoring systems in the laboratory. The functions and outputs of the station include:

- Apparent wind speed and angle,
- True wind speed and angle,
- Air temperature,
- Barometric pressure,
- 2D Magnetic compass heading,
- Heading relative to true north, and
- Global positioning system (GPS).

The weather station transmitted data continuously at 2-second intervals to DAQFactory.

2.3 Confirmatory Measurements

Although PTR-MS has exceptional response time, sensitivity, and is an excellent instrument for quantification, it suffers from the inability to make qualitative determinations of complex samples. Alternate analytical methods can provide important supporting evidence of the qualitative assignments made while interpreting the PTR-MS data as well as quantification validation of some COPCs. The Gas Chromatograph – Mass Spectrometer, High Performance Liquid Chromatograph (HPLC)/MS/MS, HPLC and GC methods used to support and confirm PTR-MS were performed using well-established methodology by accredited laboratories. Within the context of this study, the three confirmatory methods that were utilized were NIOSH Method 2522, “Nitrosamines,” modified; EPA TO-17, “Volatile Organic Compounds,” modified; and EPA TO-11A, “Determination of Formaldehyde in Ambient Air Using Adsorbent Cartridge Followed by High Performance Liquid Chromatography (HPLC).”

The ML has an onboard confirmatory sample collection system that allows up to four samples to be collected simultaneously through the same sampling inlet used by the PTR-MS and the other analytical equipment in the truck. This allows the ML Operators to collect co-located confirmatory samples simultaneously with the PTR-MS, carbon dioxide, and ammonia analyzer.

The confirmatory sampling strategy and analyte list for this background study was designed with the following objectives in mind:

1. The chemical is generally present in high enough concentrations in the background studies to be detected, under reasonable sampling times, by the confirmatory methods;
2. Chemical is in the calibration list for at least one of the confirmatory methods; and
3. Chemical is quantified by PTR-MS and if possible, a COPC.

Commercially available traditional laboratory analytical techniques do not analyze for a large number of the COPCs. Every attempt was made to find laboratory subcontract support for as large a number of the COPCs as possible. However, in most cases, it was not feasible or possible for laboratories to analyze for the majority of the COPCs. In total, ten COPCs were analyzed quantitatively using valid confirmatory method full calibrations. Two more COPCs, furan and acetonitrile, were analyzed for by tentatively identified compound (TIC).

The frequency and duration of the sampling was designed to produce duplicates for each method utilized for each of the six background sites. For this reason, both accuracy and precision data can be evaluated. Also, one blank per ten samples analyzed was performed.

By the very nature of the experiment, the concentrations measured during the background study are very low, and in most cases, below the reporting limits or detection limits. The list analyzed, utilizing three analytical methods and covering a broad range of analytes, was chosen to accomplish the objectives above.

Since limited information can be gathered from results that are less than the laboratory and PTR-MS reporting limits, sampling times and volumes were chosen based on the laboratory detection limit and the estimated background concentration determined from previous studies.

It should be emphasized that any results reported below laboratory or PTR-MS reporting limits or TICs must be considered qualitative.

3.0 CALIBRATION METHODS AND CALIBRATION GASES USED

Table 3-1, shown below, highlights the type, identification number, and expiration date for each gas standard cylinder employed by the ML for calibration purposes during Month 5.

Table 3-1. Calibrated Gases in use During Month 5.

Cylinder	**ID#**	**Exp. Date**
Carbon Dioxide	77-401243203-1	07/13/2026
Ammonia	48-401233442-1	06/21/2019
Zero-air	Lot #: 2181802 (115421, C5438107, T-2768, 330-662, KI428)	06/29/2019
VOC	160-401265983-1	02/28/2019
O_2	SG UHPOX337	08/28/2019
N_2	13 3177 94	08/28/2019

During periods of deployment, Mobile Laboratory personnel operate under Report No. 66409-RPT-004, *Mobile Laboratory Operational Procedure*, which states that at least once during the scheduled shift, ML Operators perform a user-initiated zero-air and sensitivity check on the LI-COR, Picarro, and PTR-MS instruments. If a zero-air or sensitivity check fails, the ML Operators are instructed to inform the WRPS Project Manager, TerraGraphics Senior Scientist/Subject Matter Expert (SME), TerraGraphics Quality Assurance Representative, and TerraGraphics Project Manager. In the event that any recorded result in the procedure fails to conform to the acceptance criteria listed, the Quality Assurance Representative is notified, and the steps outlined in TG-DOE-QAP-002-1502, “Control of Nonconforming Processes,” are followed.

Zero-air checks performed on each of the ML instruments provides a diagnostic look at instrument background and verifies the sampling system has no contamination. Sensitivity checks are performed using a single point standard concentration which must be quantified within an accepted degree of accuracy to verify that the instruments are functioning properly.

Tables 3-2 through 3-7 display the zero-air and sensitivity checks performed daily during the Winter Background Study.

Table 3-2. Zero-air Checks for the LI-COR CO_2 Monitor.

Date	Time	Instrument Check	Observed Result (ppm)	Expected Result (ppm)	Pass/Fail
01/14/2019	08:34	Zero	2.77	<50	Pass
01/15/2019	08:13	Zero	2.91	<50	Pass
01/16/2019	08:08	Zero	2.5	<50	Pass
01/17/2019	08:55	Zero	2.64	<50	Pass
01/18/2019	07:55	Zero	2.74	<50	Pass
01/19/2019	08:10	Zero	2.38	<50	Pass
01/20/2019	07:27	Zero	2.5	<50	Pass
01/21/2019	08:14	Zero	2.3	<50	Pass
01/22/2019	08:29	Zero	2.19	<50	Pass
01/23/2019	07:36	Zero	2.25	<50	Pass
01/24/2019	07:50	Zero	2.20	<50	Pass
01/26/2019	07:09	Zero	1.94	<50	Pass
01/27/2019	07:55	Zero	2.1	<50	Pass
01/28/2019	08:22	Zero	2.12	<50	Pass
01/29/2019	08:15	Zero	2.2	<50	Pass
01/30/2019	09:00	Zero	2.33	<50	Pass
01/31/2019	11:19	Zero	2.3	<50	Pass
02/01/2019	09:47	Zero	2.2	<50	Pass
02/02/2019	08:14	Zero	2.3	<50	Pass
02/03/2019	07:46	Zero	2.03	<50	Pass
02/04/2019	08:27	Zero	1.9	<50	Pass
02/05/2019	12:31	Zero	1.9	<50	Pass
02/06/2019	10:01	Zero	2.02	<50	Pass
02/07/2019	08:42	Zero	1.97	<50	Pass
02/08/2019	09:03	Zero	2.18	<50	Pass
02/09/2019	09:40	Zero	1.70	<50	Pass

Table 3-3. Sensitivity Checks for the LI-COR CO_2 Monitor.

Date	Time	Instrument Check	Observed Result (ppm)	Expected Result (ppm)	% Difference	Acceptance Criteria (%)	Pass/Fail
01/14/2019	08:34	Sensitivity	362	384	5.7	20	Pass
01/15/2019	08:13	Sensitivity	360	384	6	20	Pass
01/16/2019	08:24	Sensitivity	358	384	6.7	20	Pass
01/17/2019	08:55	Sensitivity	358	384	6.8	20	Pass
01/18/2019	07:55	Sensitivity	359	385	7	20	Pass
01/19/2019	08:10	Sensitivity	358	384	6.7	20	Pass
01/20/2019	07:27	Sensitivity	358	384	6.7	20	Pass
01/21/2019	08:14	Sensitivity	358	384	7.8	20	Pass
01/22/2019	08:29	Sensitivity	358	384	6.7	20	Pass
01/23/2019	07:36	Sensitivity	360	384	6.3	20	Pass
01/24/2019	07:52	Sensitivity	359	384	6.5	20	Pass
01/26/2019	07:09	Sensitivity	354	385	8.05	20	Pass
01/27/2019	07:55	Sensitivity	357	384	7	20	Pass
01/28/2019	08:22	Sensitivity	358	384	6.8	20	Pass
01/29/2019	08:15	Sensitivity	359	384	6.5	20	Pass
01/30/2019	09:00	Sensitivity	358	384	6.8	20	Pass
01/31/2019	11:19	Sensitivity	358	384	9.1	20	Pass
02/01/2019	09:47	Sensitivity	359	384	6.5	20	Pass
02/02/2019	08:16	Sensitivity	358	385	7.01	20	Pass
02/03/2019	07:51	Sensitivity	359	384	6.5	20	Pass
02/04/2019	08:27	Sensitivity	359	384	6.5	20	Pass
02/05/2019	12:32	Sensitivity	358	384	6.8	20	Pass
02/06/2019	10:02	Sensitivity	385	358	7.5	20	Pass
02/07/2019	08:44	Sensitivity	360	385	6.49	20	Pass
02/08/2019	09:04	Sensitivity	359	385	6.7	20	Pass
02/09/2019	09:42	Sensitivity	358	385	7.01	20	Pass

Table 3-4. Zero-air Checks for the Proton Transfer Reaction – Mass Spectrometer.

Date	Time	Instrument Check	Observed Result (ppbv)	Expected Result (ppbv)	Pass/Fail
01/14/2019	08:38	Zero	0.47	<0.5	Pass
01/15/2019	08:15	Zero	0.80	<0.5	Fail
01/16/2019	07:24	Zero	0.27	<0.5	Pass
01/17/2019	08:57	Zero	0.22	<0.5	Pass
01/18/2019	07:59	Zero	0.24	<0.5	Pass
01/19/2019	08:12	Zero	0.25	<0.5	Pass
01/20/2019	07:29	Zero	0.25	<0.5	Pass
01/21/2019	08:17	Zero	0.25	<0.5	Pass
01/22/2019	08:35	Zero	0.25	<0.5	Pass
01/23/2019	07:47	Zero	0.25	<0.5	Pass
01/24/2019	07:59	Zero	0.20	<0.5	Pass
01/26/2019	07:14	Zero	0.30	<0.5	Pass
01/27/2019	07:58	Zero	0.25	<0.5	Pass
01/28/2019	08:36	Zero	0.26	<0.5	Pass
01/29/2019	08:18	Zero	0.25	<0.5	Pass
01/30/2019	09:24	Zero	0.28	<0.5	Pass
01/31/2019	11:22	Zero	0.25	<0.5	Pass
02/01/2019	09:48	Zero	0.25	<0.5	Pass
02/02/2019	08:26	Zero	0.27	<0.5	Pass
02/03/2019	07:52	Zero	0.22	<0.5	Pass
02/04/2019	08:40	Zero	0.25	<0.5	Pass
02/05/2019	12:41	Zero	0.22	<0.5	Pass
02/06/2019	10:12	Zero	0.20	<0.5	Pass
02/07/2019	08:51	Zero	0.20	<0.5	Pass
02/08/2019	09:11	Zero	0.23	<0.5	Pass
02/09/2019	09:50	Zero	0.20	<0.5	Pass

Table 3-5. Sensitivity Checks for the Proton Transfer Reaction – Mass Spectrometer.

Date	Time	Instrument Check	Observed Result (ppbv)	Expected Result (ppbv)	% Difference	Acceptance Criteria (%)	Pass/Fail
01/14/2019	08:38	Sensitivity	17.5	9.6	82	30	Fail
01/15/2019	08:15	Sensitivity	18.0	9.6	87	30	Fail
01/16/2019	07:35	Sensitivity	8.8	9.6	8.3	30	Pass
01/17/2019	09:00	Sensitivity	7.8	9.6	18.8	30	Pass
01/18/2019	08:00	Sensitivity	7.9	9.6	17.7	30	Pass
01/19/2019	08:12	Sensitivity	7.9	9.6	17.7	30	Pass
01/20/2019	07:29	Sensitivity	8.0	9.6	16.6	30	Pass
01/21/2019	08:33	Sensitivity	8.0	9.6	16.6	30	Pass
01/22/2019	08:36	Sensitivity	8.0	9.6	16.6	30	Pass
01/23/2019	07:57	Sensitivity	8.2	9.6	14.6	30	Pass
01/24/2019	08:10	Sensitivity	8.1	9.6	15.5	30	Pass
01/26/2019	07:21	Sensitivity	8.39	9.6	12.6	30	Pass
01/27/2019	07:58	Sensitivity	8.4	9.6	12.5	30	Pass
01/28/2019	08:42	Sensitivity	8.5	9.6	11.5	30	Pass
01/29/2019	08:32	Sensitivity	8.7	9.6	9.3	30	Pass
01/30/2019	09:26	Sensitivity	8.73	9.6	9.1	30	Pass
01/31/2019	11:22	Sensitivity	8.6	9.6	11.1	30	Pass
02/01/2019	09:48	Sensitivity	8.7	9.6	9.3	30	Pass
02/02/2019	08:34	Sensitivity	8.93	9.6	6.98	30	Pass
02/03/2019	08:08	Sensitivity	8.69	9.6	9.47	30	Pass
02/04/2019	08:40	Sensitivity	8.75	9.6	8.8	30	Pass
02/05/2019	12:30	Sensitivity	8.8	9.6	8.3	30	Pass
02/06/2019	10:12	Sensitivity	8.67	9.6	9.6	30	Pass
02/07/2019	09:03	Sensitivity	8.6	9.6	10.4	30	Pass
02/08/2019	09:19	Sensitivity	8.62	9.6	10.2	30	Pass
02/09/2019	10:00	Sensitivity	8.6	9.6	10.4	30	Pass

Table 3-6. Zero-air Checks for the Picarro Ammonia Analyzer.

Date	Time	Instrument Check	Observed Result (ppb)	Expected Result (ppb)	Pass/Fail
01/14/2019	08:24	Zero	5.0	<20	Pass
01/15/2019	08:17	Zero	5.5	<20	Pass
01/16/2019	07:38	Zero	2.4	<20	Pass
01/17/2019	08:27	Zero	15.0	<20	Pass
01/18/2019	07:35	Zero	5.9	<20	Pass
01/19/2019	08:14	Zero	6.3	<20	Pass
01/20/2019	07:30	Zero	6.0	<20	Pass
01/21/2019	08:15	Zero	5.3	<20	Pass
01/22/2019	08:32	Zero	6.0	<20	Pass
01/23/2019	07:35	Zero	6.0	<20	Pass
01/24/2019	07:33	Zero	6.5	<20	Pass
01/26/2019	07:09	Zero	6.1	<20	Pass
01/27/2019	07:56	Zero	5	<20	Pass
01/28/2019	08:21	Zero	5	<20	Pass
01/29/2019	08:15	Zero	5.5	<20	Pass
01/30/2019	09:00	Zero	5	<20	Pass
01/31/2019	11:22	Zero	6.4	<20	Pass
02/01/2019	09:49	Zero	6.3	<20	Pass
02/02/2019	07:52	Zero	8.33	<20	Pass
02/03/2019	07:30	Zero	6.4	<20	Pass
02/04/2019	08:26	Zero	5.7	<20	Pass
02/05/2019	12:29	Zero	6.4	<20	Pass
02/06/2019	10:04	Zero	7.5	<20	Pass
02/07/2019	08:25	Zero	5.7	<20	Pass
02/08/2019	08:45	Zero	6.5	<20	Pass
02/09/2019	09:23	Zero	7.5	<20	Pass

Table 3-7. Sensitivity Checks for the Picarro Ammonia Analyzer.

Date	Time	Instrument Check	Observed Result (ppb)	Expected Result (ppb)	% Difference	Acceptance Criteria (%)	Pass/Fail
01/14/2019	08:24	Sensitivity	3450	3250	6.15	20	Pass
01/15/2019	08:17	Sensitivity	3525	3250	8	20	Pass
01/16/2019	08:06	Sensitivity	3470	3250	6.7	20	Pass
01/17/2019	08:58	Sensitivity	3520	3250	8.3	20	Pass
01/18/2019	07:41	Sensitivity	3460	3250	6.5	20	Pass
01/19/2019	08:14	Sensitivity	3540	3250	8.9	20	Pass
01/20/2019	07:30	Sensitivity	3600	3250	10	20	Pass
01/21/2019	08:15	Sensitivity	3570	3250	9.8	20	Pass
01/22/2019	08:32	Sensitivity	3590	3250	10	20	Pass
01/23/2019	07:35	Sensitivity	3620	3250	11.4	20	Pass
01/24/2019	07:45	Sensitivity	3600	3250	10.76	20	Pass
01/26/2019	07:09	Sensitivity	3510	3250	8.0	20	Pass
01/27/2019	07:56	Sensitivity	3610	3250	11	20	Pass
01/28/2019	08:21	Sensitivity	3600	3250	10.8	20	Pass
01/29/2019	08:15	Sensitivity	3625	3250	11.5	20	Pass
01/30/2019	09:00	Sensitivity	3640	3250	12	20	Pass
01/31/2019	11:22	Sensitivity	3630	3250	11.6	20	Pass
02/01/2019	09:49	Sensitivity	3725	3250	14.6	20	Pass
02/02/2019	08:05	Sensitivity	3454	3265	5.79	20	Pass
02/03/2019	07:40	Sensitivity	3607	3250	10.9	20	Pass
02/04/2019	08:26	Sensitivity	3660	3250	12.6	20	Pass
02/05/2019	12:30	Sensitivity	3702	3250	13.9	20	Pass
02/06/2019	10:04	Sensitivity	3667	3250	12.8	20	Pass
02/07/2019	08:36	Sensitivity	3670	3250	12.9	20	Pass
02/08/2019	08:55	Sensitivity	3625	3250	11.5	20	Pass
02/09/2019	09:34	Sensitivity	3588	3250	10.4	20	Pass

4.0 MEASUREMENT UNCERTAINTY AND KNOWN SOURCES OF ERROR

The sections below discuss the measurement uncertainty associated with each instrument employed in the ML, as well as a study conducted to quantify the Method Detection Limits (MDLs) of the PTR-MS.

4.1.1 Proton Transfer Reaction – Mass Spectrometer

All standards/zeroes performed by the field team to verify the accuracy of the instrument were recorded in 66409-RPT-004. DR19-001 describes the PTR-MS standards/zeroes performed on January 14, 2019, and January 15, 2019, that fell outside of the acceptable administrative limits due to a change in transmission efficiency on the PTR-MS. See Appendix C for the full deficiency report. Nonconformance Reports NCR-19-001 and NCR-19-002 detail the issue of intermittent periods of increased instrument baseline. During these periods, the detection limit would increase, and the moving baseline could be misinterpreted as an actual shift in concentrations. The sensitivity remains the same and there is no risk of a false negative occurring.

4.1.2 Carbon Dioxide Monitor

The LI-COR CO_2 Analyzer had no specific errors associated within the timeframe covered in this monthly report. All standards/zeroes performed by the field team and reported in this summary to verify the accuracy of the instrument fell within acceptable administrative limits (±20%). The measurement accuracy of a properly calibrated instrument listed in the LI-COR factory specifications is ±3% of reading.

4.1.3 Ammonia Monitor

The Picarro G2103 Ammonia Monitor had no specific errors associated within the timeframe covered in this monthly report. Further detail regarding the errors associated with measuring ammonia using a Picarro instrument is discussed in *Fiscal Year 2017 Mobile Laboratory Vapor Monitoring at the Hanford Site: Monitoring During Waste Disturbing Activities and Background Study*, September 2017. All standards/zeroes associated with data reported in this summary performed by the field team to verify the accuracy of the instrument fell within acceptable administrative limits (±20%). The measurement accuracy of a calibrated instrument listed in the Picarro factory specifications is ±5% of reading.

4.1.4 Weather Station

The Airmar 200WX-IPx7 Weather Station had no specific errors associated within the timeframe covered in this monthly report. The Airmar 150 WX Weather Station is factory calibrated and is not user calibrated. The manual does not recommend periodic calibration. This is described in 66409-RPT-003, *Mobile Laboratory Operational Acceptance Testing Plan*.

4.2 Method Detection Limit Study

In order to gain insight into the limits of detection of the PTR-TOF 6000 X2, all zero air checks run on the instrument from January 14, 2019, to February 9, 2019, were analyzed. A total of 26 zero-air checks were run during this time period. Each zero-air check result was the average concentration of each individual species over a roughly 3-minute period of time, which consisted of roughly 100 data points, taken at 2 Hz.

The MDLs were calculated by taking the mean and standard deviation of the data collected during each zero-air check for each compound detected. This considers the variance (or noise) present in the real-time data.

$$\mu = \frac{\sum_{i=1}^{n} x_i}{n}$$

$$\sigma = \sqrt{\frac{\sum_{i=1}^{n}(x_i - \mu)^2}{n}}$$

Next, the mean value for all zero-air check results for each compound was calculated.

$$\mu_T = \frac{\sum_{i=1}^{n} \mu_i}{n}$$

Using propagation of error, the standard deviations were combined. This was done by taking the square root of the average of the squares of each calculated standard deviation, i.e., the root of the average of the variances.

$$\sigma_T = \sqrt{\frac{\sum_{i=1}^{n} \sigma_i^2}{n}}$$

This ensured that the variances attributed to the discrete points of 2 Hz data were conserved. If a standard deviation of the mean of means was taken, the variance taken into account would include the variance between calculated averages as well.

The mean of the 26 sample dataset was then added to the standard deviation for the 26 sample, zero-air dataset was multiplied by the 1-tailed Student's t-value for 25 degrees of freedom at 95% CI, i.e., 2.15. This provided the MDLs for each compound detected by the PTR-TOF 6000 X2. As a conservative approach, an additional factor of 3 was then applied to the MDLs to obtain the Reporting Limits (RLs).

Additionally, throughout the course of the resolution of DR19-001, MDL and RL values were increased to compensate for the increase of signal noise caused by instrument performance issues. These values were validated using data from January 14, 2019, which was found to be representative of the extent of the instrument issues, with collaboration from the SME to ensure that the RLs were conservative enough to address the performance issues without overly hindering the PTR-MS's ability to detect hits above background signal. This effectively covers all dates associated with the Winter FY19 Background Study.

Calculated MDLs and RLs for each COPC and odor compound are shown in the table below.

Table 4-1. Method Detection Limits and Reporting Limits for Chemicals of Potential Concern. (2 Sheets)

COPC Name	OEL (ppbv)	MDL (ppbv)	RL (ppbv)
formaldehyde	300	0.01	0.03
methanol	200000	1.302	3.906
acetonitrile	20000	1.839	5.517
acetaldehyde	25000	0.07	0.21
ethylamine	5000	2.07	6.21
1,3-butadiene	1000	0.055	0.165
propanenitrile	6000	0.122	0.366
2-propenal	100	0.121	0.363
1-butanol + butenes	20000	0.314	0.942
methyl isocyanate	20	0.149	0.447
methyl nitrite	100	0.061	0.183
furan	1	0.117	0.351
butanenitrile	8000	0.053	0.159
but-3-en-2-one + 2,3-dihydrofuran + 2,5-dihydrofuran	200, 1, 1	0.04	0.12
butanal	25000	0.034	0.102
NDMA	0.3	0.063	0.189
benzene	500	0.02	0.06
2,4-pentadienenitrile + pyridine	300, 1000	0.23	0.69
2-methylene butanenitrile	30	0.084	0.252
2-methylfuran	1	0.05	0.15
pentanenitrile	6000	0.046	0.138
3-methyl-3-buten-2-one + 2-methyl-2-butenal	20, 30	0.029	0.087
NEMA	0.3	0.048	0.144
2,5-dimethylfuran	1	0.027	0.081
hexanenitrile	6000	0.035	0.105

Table 4-1. Method Detection Limits and Reporting Limits for Chemicals of Potential Concern. (2 Sheets)

COPC Name	OEL (ppbv)	MDL (ppbv)	RL (ppbv)
2-hexanone (MBK)	5000	0.029	0.087
NDEA	0.1	0.03	0.09
butyl nitrite + 2-nitro-2-methylpropane	100, 300	0.023	0.069
2,4-dimethylpyridine	500	0.106	0.318
2-propylfuran + 2-ethyl-5-methylfuran	1	0.031	0.093
heptanenitrile	6000	0.035	0.105
4-methyl-2-hexanone	500	0.029	0.087
NMOR	0.6	0.032	0.096
butyl nitrate	2500	0.017	0.051
2-ethyl-2-hexenal + 4-(1-methylpropyl)-2,3-dihydrofuran+ 3-(1,1-dimethylethyl)-2,3-dihydrofuran	100, 1, 1	0.019	0.057
6-methyl-2-heptanone	8000	0.032	0.096
2-pentylfuran	1	0.028	0.084
biphenyl	200	0.029	0.087
2-heptylfuran	1	0.031	0.093
1,4-butanediol dinitrate	50	0.136	0.408
2-octylfuran	1	0.184	0.552
1,2,3-propanetriol 1,3-dinitrate	50	0.013	0.039
PCB	1000	0.132	0.396
6-(2-furanyl)-6-methyl-2-heptanone	1	0.139	0.417
furfural acetophenone	1	0.025	0.075

Calculated MDLs and RLs for each odor-causing compound are shown in the table below.

Table 4-2. Method Detection Limits and Reporting Limits for Odor-Causing Compounds.

Odor Name	**MDL (ppbv)**	**RL (ppbv)**
methyl mercaptan	0.137	0.411
dimethyl sulfide; ethanethiol	0.107	0.321
allyl mercaptan	0.177	0.531
1-propanethiol; Isopropyl mercaptan	0.469	1.407
2-butene-1-thiol	0.18	0.54
Diethyl Sulfide; 2-methylpropane-2-thiol	0.529	1.587
thiopropanal sulfuroxide	0.046	0.138
dimethyl disulfide	0.186	0.558
1-pentanethiol; 2,2-dimethylpropane-1-thiol	0.048	0.144
benzenethiol	0.019	0.057
diallyl sulfide	0.034	0.102
methyl propyl disulfide	0.022	0.066
methylbenzenethiol	0.103	0.309
dimethyl trisulfide	0.022	0.066
(1-oxoethyl) thiophene	0.276	0.828
(1-oxopropyl) thiophene	0.028	0.084
dipropyl disulfide	0.018	0.054
methyl propyl trisulfide	0.047	0.141
dimethyl tetrasulfide	0.027	0.081
dipropyl trisulfide	0.132	0.396
diphenyl sulfide	0.014	0.042

It is worth noting that while the RLs are calculated with the purpose of applying them to the data to reduce the likelihood of false positives at low concentrations, these calculated RLs will not be applied retroactively to the data discussed in this monthly report.

Measured values below the RL but above the MDL are an estimate only. Values below the MDL should be treated with care as they have no quantitative significance.

5.0 TEST RESULTS

This section details the test results found during this month's monitoring activities.

5.1 Maintenance Activities

During Month 5, there were 7 days spent on maintenance-related activities for the ML. These activities included planned preventative and corrective maintenance as well as selective reagent ionization testing. All activities were performed to improve the ML's function and overall data collection capabilities. Activities performed on the ML during the first two weeks of January 2019 are presented in Table 5-1.

Table 5-1. Mobile Laboratory Maintenance Activities.

Week	Date	Activity
22	01/02/2019	Updated configuration inside ML, pump installation, wiring, and installation of new heated line.
	01/03/2019	Installation of updated sampling system, instrument software programming, wiring, and instrument tubing.
	01/04/2019	Wrapped heated line and solid-state relay (SSR), network cables were installed, instrument software programming.
23	01/07/2019	Completed installation of new heated line, instrument software programming, tray built to mount Variacs®[9].
	01/08/2019	NO^+ automated mode switching tested, training in programming instrument software, tested ML equipment and instruments.
	01/09/2019	Personnel trained via mock deployment.
	01/10/2019	Investigated issue with circuit 21, installed side panel to LI-COR, and SSR was wired to temperature controllers.
	01/11/2019	Wired SSR backups for heated lime system, prepared ML and shop for ML deployment.

5.2 AP Pump Removal

On January 24, 2019, the ML supported WRPS' Tank Farm Projects' Team during the removal of a pump in the AP Farm, by conducting area monitoring.

The ML's main objective during the removal process was to monitor potential releases of COPCs by staying downwind of the AP pump removal activities. The ML Operators observed AP Pump Removal work from approximately 9:05 am to 12:35 pm. Additional insights are given by focusing on that period in several time traces for several representative species. Figure 5-1 shows the location of the ML during the monitoring period and Figure 5-2 provides meteorological information obtained from the ML mounted weather station for the time period of sampling for the AP Pump Removal.

---

[9] Variac is a registered trademark of Instrument Service and Equipment, Inc., Cleveland, Ohio.

Figure 5-1. Mobile Laboratory Location for the Duration of the Monitoring Period.

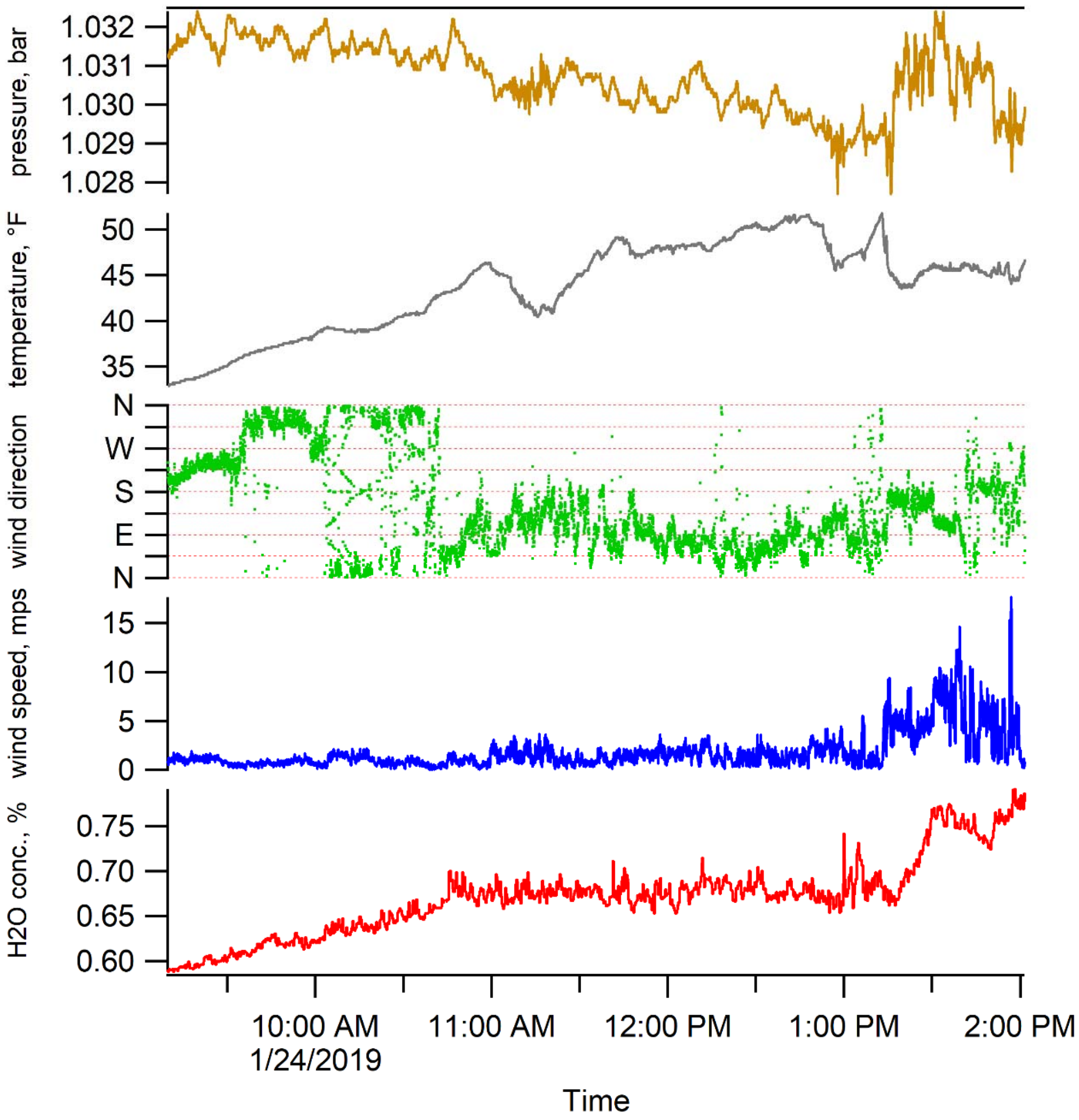

Figure 5-2. Weather Data.

Meteorological conditions were calm during the pump removal with winds between 2-4 mps and temperature rising from 34˚F – 50˚F. Mild and consistent wind conditions provide confidence in monitoring the ambient air near the work location.

5.2.1 Discussion of Test Activities and Observations – AP Pump Removal

Continuous air monitoring was performed using the PTR-MS, LICOR CO_2 Monitor, Picarro Ammonia Monitor, and Weather Station. Confirmatory air samples were not collected for this day.

Table 5-2 gives the concentrations and statistical information for all species monitored before, during and after the AP pump removal.

Table 5-2. Statistical Information for the Monitoring Period of January 24, 2019. (2 Sheets)

COPC #	COPC Name	OEL (ppb)	MDL (ppb)	Ave. (ppb)	St. Dev. (ppb)	Rel St. Dev. (%)	Max. (ppb)	Median (ppb)
1	ammonia	25000	0.010	10.705	2.503	23.386	21.918	9.990
2	formaldehyde	300	1.302	<1.302	N/A	N/A	4.992	<1.302
3	methanol	200000	1.839	3.439†	0.703	20.444	9.390	3.207
4	acetonitrile	20000	0.070	<0.070	N/A	N/A	0.643	<0.070
5	acetaldehyde	25000	2.070	<2.070	N/A	N/A	19.100	<2.070
6	ethylamine	5000	0.055	<0.055	N/A	N/A	0.083	<0.055
7	1,3-butadiene	1000	0.122	<0.122	N/A	N/A	5.965	<0.122
8	propanenitrile	6000	0.121	<0.121	N/A	N/A	2.490	<0.121
9	2-propenal	100	0.314	<0.314	N/A	N/A	2.095	<0.314
10	1-butanol + butenes	20000	0.149	<0.149	N/A	N/A	14.433	<0.149
11	methyl isocyanate	20	0.061	<0.061	N/A	N/A	0.172	<0.061
12	methyl nitrite	100	0.117	<0.117	N/A	N/A	1.014	<0.117
13	furan	1	0.053	<0.053	N/A	N/A	0.231	<0.053
14	butanenitrile	8000	0.040	<0.040	N/A	N/A	1.170	<0.040
15	but-3-en-2-one + 2,3-dihydrofuran + 2,5-dihydrofuran	200, 1, 1	0.034	0.039†	0.052	132.488	N/A*	N/A*
16	butanal	25000	0.063	0.078†	0.039	50.143	0.439	0.067
17	NDMA**	0.3	0.020	<0.020	N/A	N/A	0.059	<0.020
18	benzene	500	0.230	<0.230	N/A	N/A	25.294	<0.230
19	2,4-pentadienenitrile + pyridine	300, 1000	0.084	<0.084	N/A	N/A	1.673	<0.084
20	2-methylene butanenitrile	300	0.050	<0.050	N/A	N/A	0.220	<0.050
21	2-methylfuran	1	0.046	<0.046	N/A	N/A	0.270	<0.046
22	pentanenitrile	6000	0.029	<0.029	N/A	N/A	0.450	<0.029
23	3-methyl-3-buten-2-one + 2-methyl-2-butenal	20, 30	0.048	<0.048	N/A	N/A	0.300	<0.048
24	NEMA**	0.3	0.027	<0.027	N/A	N/A	0.051	<0.027
25	2,5-dimethylfuran	1	0.035	<0.035	N/A	N/A	0.122	<0.035
26	hexanenitrile	6000	0.029	<0.029	N/A	N/A	0.241	<0.029
27	2-hexanone (MBK)	5000	0.030	<0.030	N/A	N/A	0.060	<0.030
28	NDEA**	0.1	0.023	<0.023	N/A	N/A	0.031	<0.023
29	butyl nitrite + 2-nitro-2-methylpropane	100, 300	0.106	<0.106	N/A	N/A	0.428	<0.106
30	2,4-dimethylpyridine	500	0.031	<0.031	N/A	N/A	3.993	<0.031

Table 5-2. Statistical Information for the Monitoring Period of January 24, 2019. (2 Sheets)

COPC #	COPC Name	OEL (ppb)	MDL (ppb)	Ave. (ppb)	St. Dev. (ppb)	Rel St. Dev. (%)	Max. (ppb)	Median (ppb)
31	2-propylfuran + 2-ethyl-5-methylfuran	1	0.035	<0.035	N/A	31	0.074	<0.035
32	heptanenitrile	6000	0.029	<0.029	N/A	N/A	0.128	<0.029
33	4-methyl-2-hexanone	500	0.032	<0.032	N/A	N/A	0.066	<0.032
34	NMOR**	0.6	0.017	<0.017	N/A	N/A	1.191	<0.017
35	butyl nitrate	2500	0.019	<0.019	N/A	N/A	0.033	<0.019
36	2-ethyl-2-hexenal + 4-(1-methylpropyl)-2,3-dihydrofuran + 3-(1,1-dimethylethyl)-2,3-dihydrofuran	100, 1, 1	0.032	<0.032	N/A	N/A	0.058	<0.032
37	6-methyl-2-heptanone	8000	0.028	<0.028	N/A	N/A	0.041	<0.028
38	2-pentylfuran	1	0.029	<0.029	N/A	N/A	0.063	<0.029
39	biphenyl	200	0.031	<0.031	N/A	N/A	0.038	<0.031
40	2-heptylfuran	1	0.136	<0.136	N/A	N/A	0.125	<0.136
41	1,4-butanediol dinitrate	50	0.184	<0.184	N/A	N/A	0.050	<0.184
42	2-octylfuran	1	0.013	<0.013	N/A	N/A	0.042	<0.013
43	1,2,3-propanetriol 1,3-dinitrate	50	0.132	<0.132	N/A	N/A	0.036	<0.132
44	PCB	1000	0.139	<0.139	N/A	N/A	0.052	<0.139
45	6-(2-furanyl)-6-methyl-2-heptanone	1	0.025	<0.025	N/A	N/A	0.036	<0.025
46	furfural acetophenone	1	0.119	<0.119	N/A	N/A	0.102	<0.119

N/A*	The maximum peak value for but-3-en-2-one + 2,3 dihydrofuran + 2,5 dihydrofuran was 0.698 ppb and the median value was <0.034 ppb. The PTR-MS results for but-3-en-2-one + 2,3 dihydrofuran + 2,5 dihydrofuran are not compared to OEL concentrations because: 1) the result is suspect due to a known biogenic interferant (methacrolein) that is expected to be in concentrations that occasionally exceed the dihydrofuran OEL, and 2) this combination of COPCs have OEL concentrations that differ by a factor of 200, which provide widely variant bases for these numbers.
**	Nitrosamine results are suspect due to isobaric interferants causing positive bias that have been encountered during previous background [53005-81-RPT-007, *PTR-MS Mobile Laboratory Vapor Monitoring Background Study, (3/18/2018 – 4/20/2018)*, and *Fiscal Year 2017 Mobile Laboratory Vapor Monitoring at the Hanford Site: Monitoring During Waste Disturbing Activities and Background Study*, RJ Lee Group, Inc.].
ND	COPC Averages below the MDL.
†	COPC Averages between the RL and the MDL.
🟥	COPC Averages >100% of the OEL.
🟧	COPC Averages 50-100% of the OEL.
🟨	COPC Averages 10-50% of the OEL.

Table 5-1 shows that COPC average concentrations over the entire period monitored were less than MDLs, which are 1-3 orders of magnitude lower than occupational exposure limits (OELs). In the two cases where COPCs were detected above MDLs, the averages did not exceed the RL.

5.2.2 Identification of Vapor Sources and Quantitative Analysis of Vapor Composition

To quantify the presence of any significant vapor source during the AP pump removal, focused analysis of representative species during the pump removal time period, approximately 9:05am to 12:35 pm, was performed and presented in the following figures and discussion.

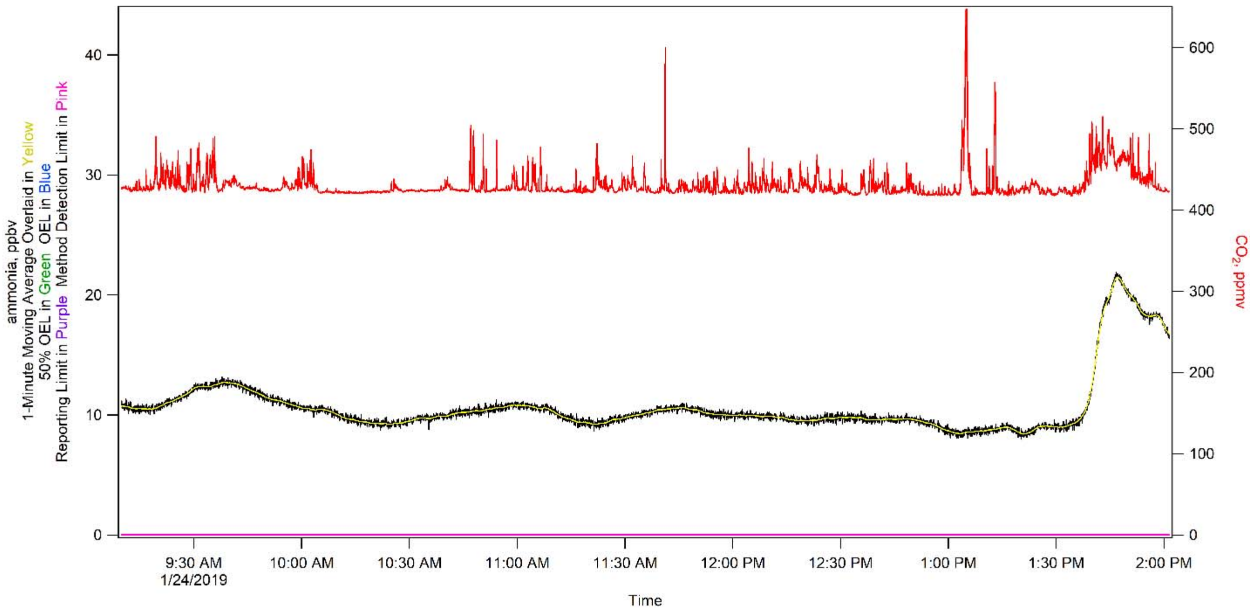

Figure 5-3. Ammonia.

Figure 5-3 shows the time trace for ammonia along with CO$_2$. The level for ammonia stayed around 10-12 ppb for the entire AP pump removal period, well below the OEL of 25,000 ppb. No apparent correlation with the pump removal, approximately 9:05am to 12:35 pm, was observed.

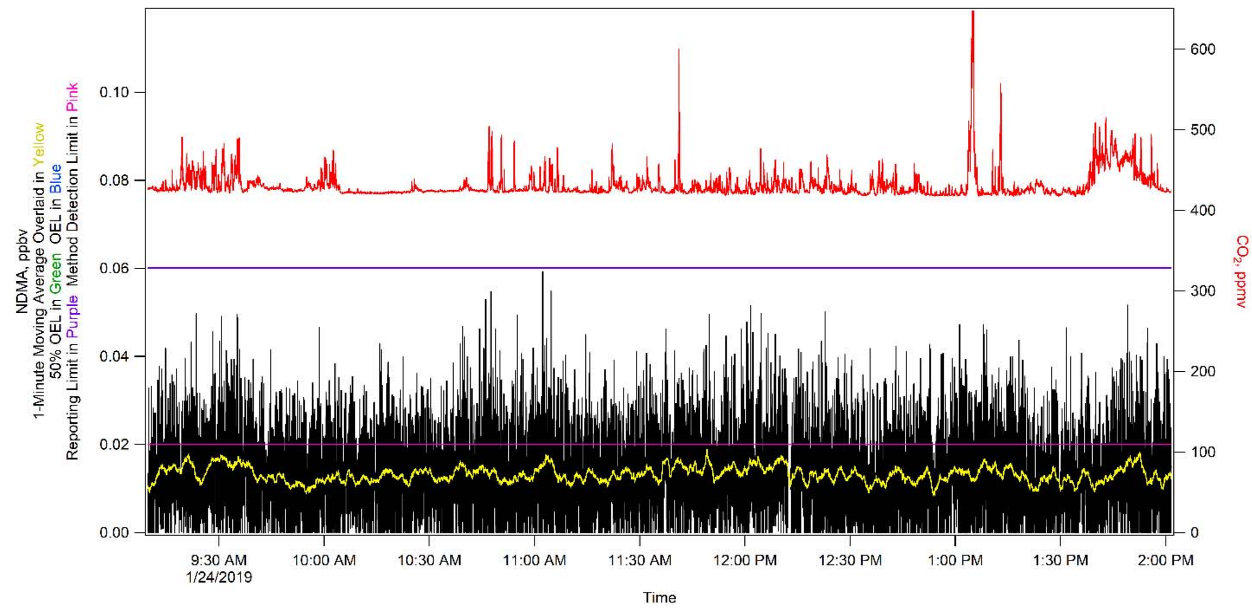

Figure 5-4. N-nitrosodimethylamine (NDMA).

Figure 5-4 shows the time trace for NDMA and CO_2 including the period of AP pump removal. There is no signal above the MDL indicating no significant if any release of NDMA during the AP pump removal. The same lack of signal was observed for most species including other nitrosamines and the larger furans.

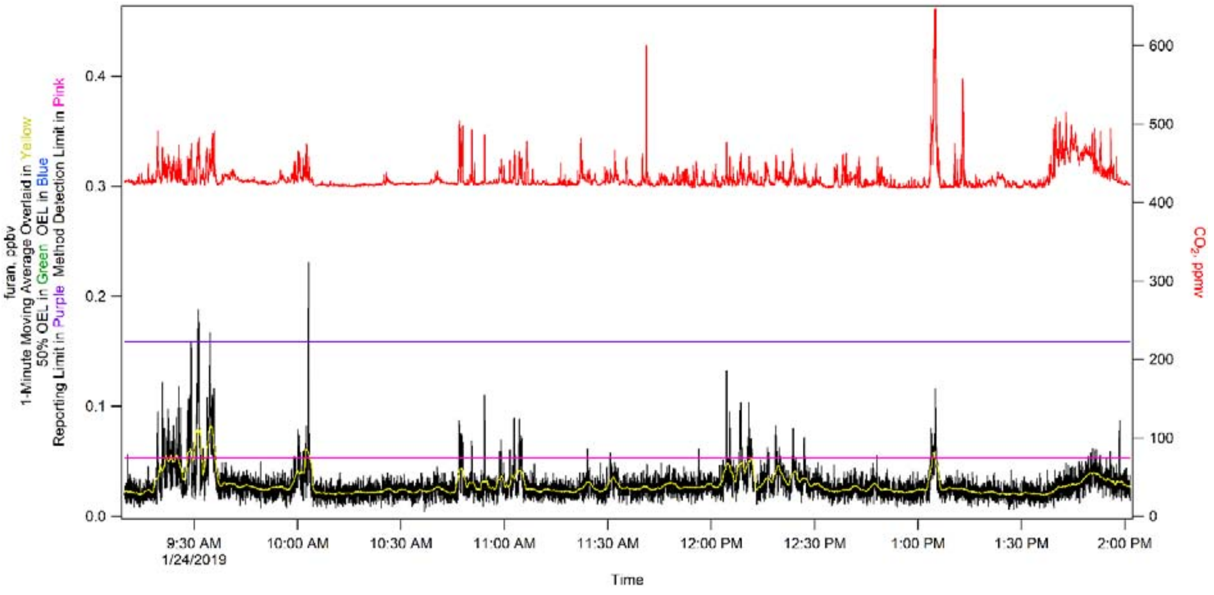

Figure 5-5. Furan.

Figure 5-5 shows the time dependent signal for furan and CO_2. The furan signal shows more variation than observed for ammonia, NDMA, and most other species with brief spikes above the MDL and a few above the reporting limit.

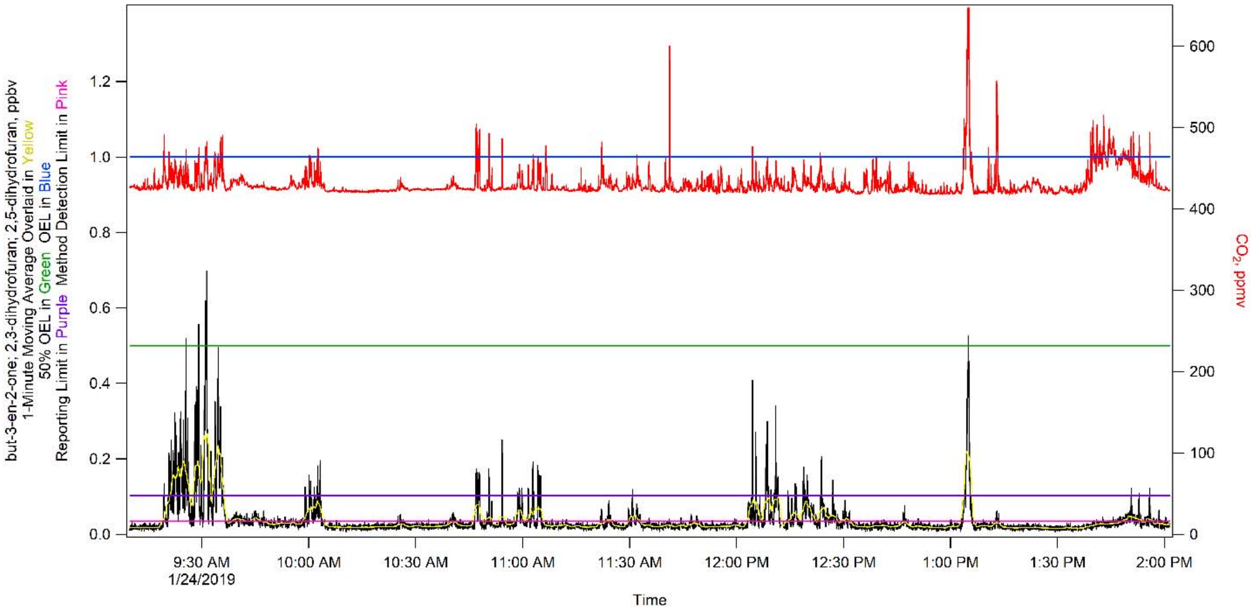

Figure 5-6. but-3-en-2-one + 2,3-dihydrofuran + 2,5-dihydrofuran.

Figure 5-6 shows the similar time response for the isobaric species but-3-en-2-one, 2,3-dihydrofuran, and 2,5-dihydrofuran in this case with times of consistent signal above the MDL, acute detections above the RL, and a small number of spikes above the 50% OEL. Figure 5-6 displays the OEL for 2,3-dihydrofuran and 2,5-dihydrofuran.

5.2.3 Detailed Analysis of Test Data – AP Pump Removal Conclusions

While small temporal excursions were observed during the AP pump removal, the lack of similar response in other known tank farm headspace species such as ammonia suggests that there may be another variable source responsible for these signals. Additionally, the calm meteorological conditions observed during the pump removal would not have impacted the detection of other known headspace species through unique mixing or dispersion.

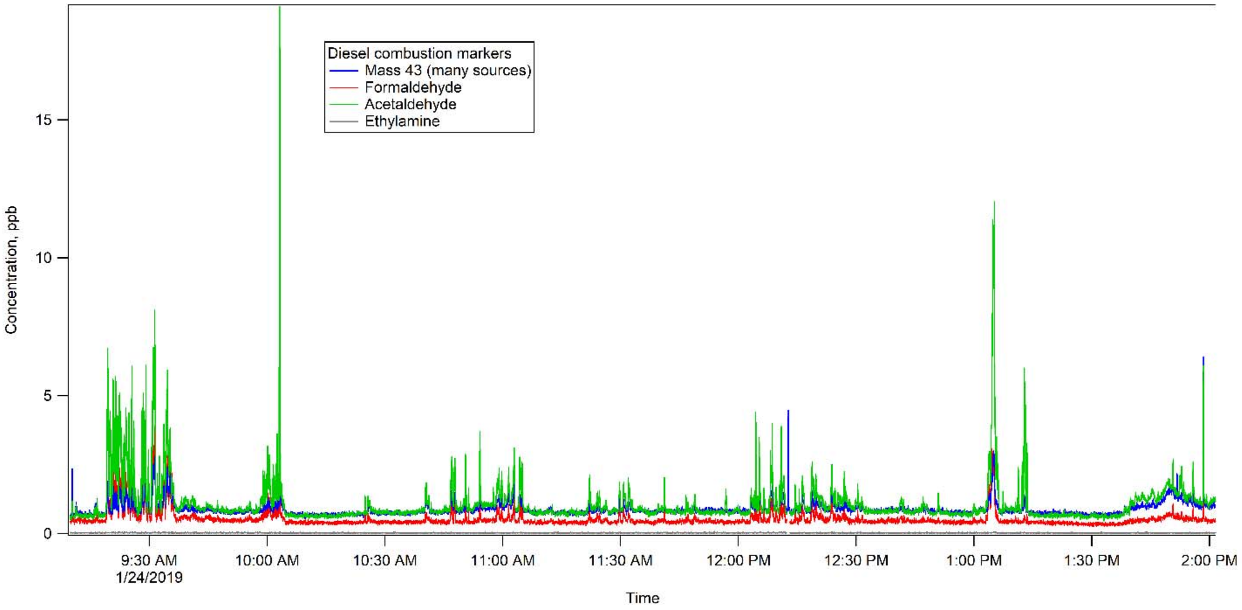

Figure 5-7. Diesel Combustion Markers.

Figure 5-7 shows the time response of several diesel combustion markers during the same time period. It is readily apparent that there is a strong correlation between the time response of the diesel combustion markers and the time response for furan and similar species. Furans are well known to be present as diesel combustion products and have been observed by the ML in the exhaust from its own and other diesel generators.

There was no apparent correlation between the COPCs monitored during the AP pump removal period. The variations observed in furan and other species correlate strongly with the variations in diesel combustion markers; therefore, they are most likely due to diesel generators or vehicles operating in the vicinity and upwind of the ML.

5.3 Septic Analysis

On January 30, 2019, the ML was deployed to sample 2607-E12 septic system tank emissions, located in the 200 East Area of the Hanford Site. Figure 5-8 shows the location of the septic tank during this investigation.

Figure 5-8. Mobile Laboratory Location for the Duration of the Monitoring Period.

Figure 5-9 provides a summary of the meteorological conditions during analysis of septic tank gases. As shown, conditions were moderate with pressure ranging and temperature between 1.0200 and 1.0212 mps and 31.6°F and 32.8°F, respectively.

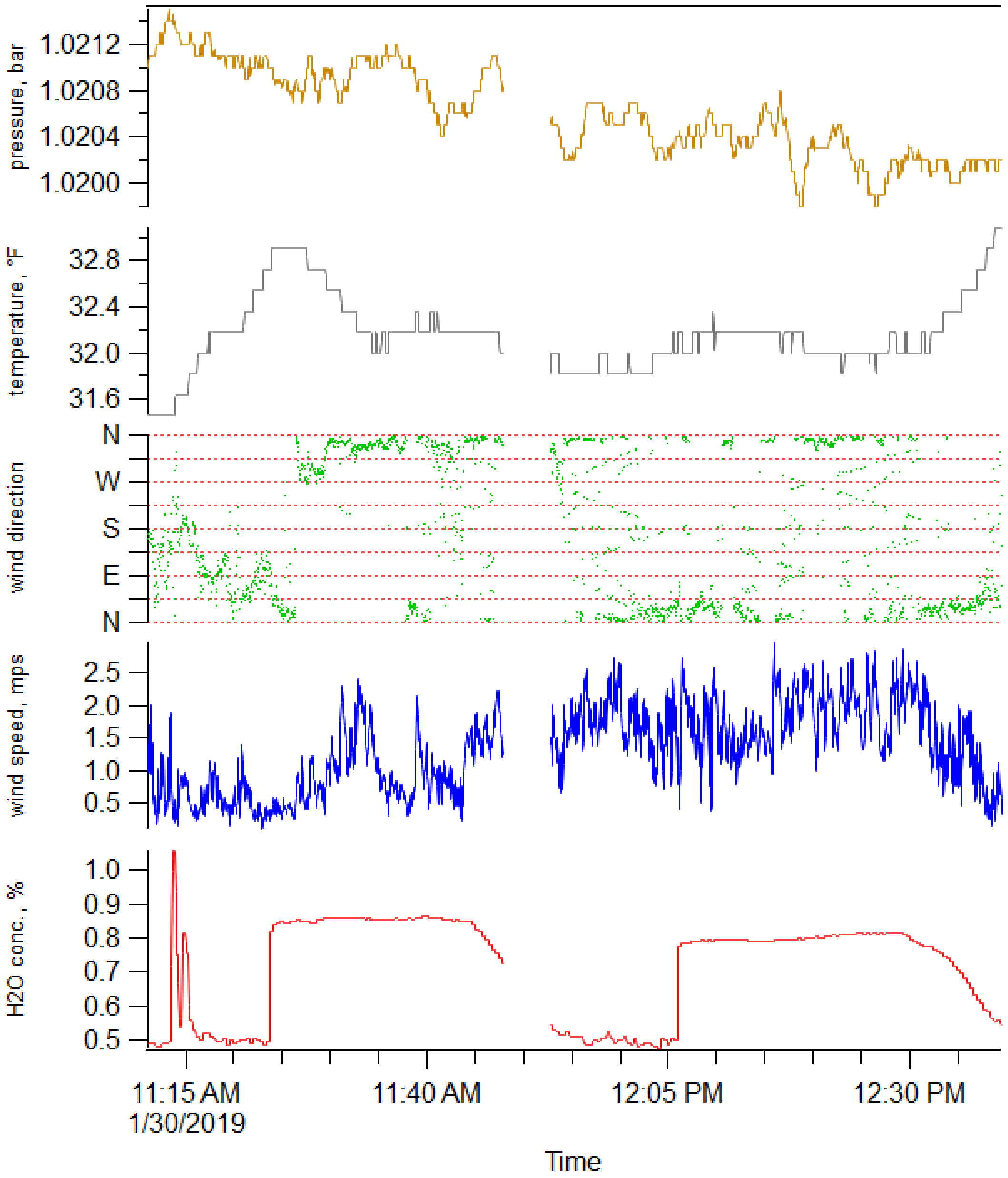

Figure 5-9. Weather Data.

5.3.1 Discussion of Test Activities and Observations – Septic

As directed by WRPS fugitive emissions team, one of the main objectives was to determine if there are any larger compounds previously unobserved. This was accomplished by implementing a new sampling method. Three sample lines were inserted into the septic tank at three different levels to provide the ability to stratify septic tank vapors at high, mid, and low levels. There is potential for stratification of species based on the molecular weight of the compound with heavier species accumulating more at the lower level. Figure 5-10 provides a picture of the different sample lines. The mid-level is ~2' away from both the high and low levels, meaning the high level is ~4' above the low level.

Figure 5-10. Setup of the Three Level Sampling Lines used for Testing Septic Composition on January 30, 2019.

Table 5-3 gives the concentrations and statistical information for all species monitored before, during and after the septic investigation.

Table 5-3. Odor Statistical Information for the Monitoring Period of January 30, 2019.

Odor #	Odor Compound Name	Ave. (ppb)	St. Dev. (ppb)	Rel St. Dev (%)	Max. (ppb)	Median (ppb)
1	methyl mercaptan	108.812	101.939	93.684	227.697	186.546
2	Dimethylsulfide + ethanethiol	20.744	19.670	94.826	58.813	31.530
3	allyl mercaptan	1.226	1.066	86.931	6.850	1.223
4	1-propanethiol + isopropyl mercaptan	0.695	0.655	94.255	1.891	1.048
5	2-butene-1-thiol	0.332	0.290	87.315	0.979	0.482
6	diethyl sulfide + 2-methylpropane-2-thiol	5.727	5.230	91.321	14.812	9.064
7	thiopropanal sulfuroxide	0.345	0.316	91.430	0.922	0.528
8	dimethyl disulfide	2.579	2.448	94.919	7.169	4.101
9	1-pentanethiol + 2,2-dimethylpropane-1-thiol	0.054	0.077	141.994	0.332	0.011
10	benzenethiol	0.008	0.011	145.462	0.075	0.002
11	diallyl sulfide	0.013	0.021	164.913	0.130	0.000
12	methyl propyl disulfide	0.006	0.012	208.454	0.090	0.000
13	methylbenzenethiol	0.072	0.024	33.688	0.145	0.071
14	dimethyl trisulfide	0.353	0.288	81.686	1.006	0.519
15	(1-oxoethyl) thiophene	0.048	0.037	75.687	0.212	0.048
16	(1-oxopropyl) thiophene	0.028	0.018	63.022	0.101	0.029
17	dipropyl disulfide	0.075	0.048	63.467	0.241	0.060
18	methyl propyl trisulfide	0.015	0.016	105.232	0.067	0.012
19	dimethyl tetrasulfide	0.031	0.009	30.026	0.078	0.031
20	dipropyl trisulfide	0.014	0.019	135.743	0.090	0.003
21	diphenyl sulfide	0.016	0.012	77.538	0.059	0.016

5.3.2 Identification of Vapor Sources and Quantitative Analysis of Vapor Composition – Septic

Figure 5-11 is a time-series of methyl mercaptan and nominal m/z 299. In previous reports, methyl mercaptan was identified as one of the largest constituents within the septic emissions. Nominal m/z 299 was identified during analysis further in the report but was included because it emphasizes the changes in different levels well. The test started by sampling from the side inlet, which was not inside of the septic tank. This was done to establish an ambient background level to compare the septic constituents. The different levels were sampled for ~5 minutes each with the exception of the last period of high level sampling which occurred for approximately 10 minutes. Fingerprint analysis at all three levels was performed using the same parameters from previous reports. To be included within the fingerprint, the species had to have a response of at least 0.05 ppbv and have a relative abundance 0.5% within the overall signal. This does mean that there could be the presence of species at low levels that are missed by this analysis. For long term comparison, it is important to keep the analysis parameters the same, so additional analysis beyond developing the fingerprints will be conducted to investigate the presence of low concentration species.

It is important to point out that sampling within the septic tank resulted in higher concentrations than typical for this type of testing. When monitoring high concentrations, the PTR-MS can become saturated with signal when a species produces an extremely high response. This is not the ideal scenario for PTR-MS monitoring since response is non-linear when saturated and quantification becomes an underestimate. This was the first attempt at sampling in this manner and there was no mechanism available to reduce the risk of saturation. Due to this potential for saturation, the results could be slightly skewed and under quantify species with high response. Based on analysis for previous reports, the most likely candidates are methyl mercaptan, dihydrogen sulfide, and the organosulfur compound (OSC) fragment at m/z 93. In the time since this test, a sample dilution system has been developed and tested that would allow for minimizing the potential for saturation for future sampling of this type.

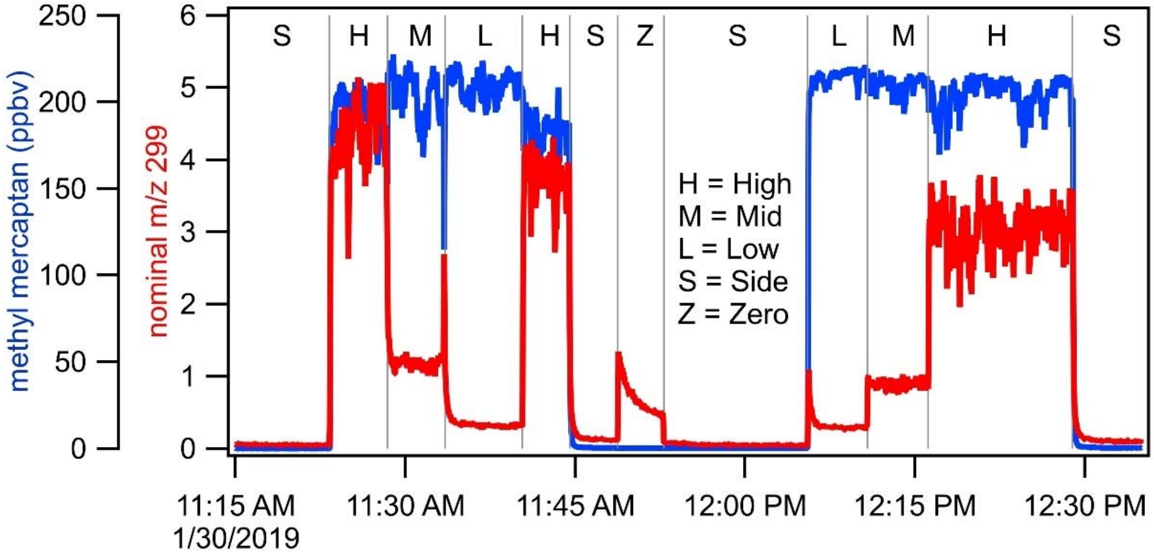

Figure 5-11. Methyl Mercaptan and Nominal m/z 299 During Septic Testing on January 30, 2019.

Figure 5-12 shows the septic fingerprint observed at the high level. The largest responses were at methyl mercaptan and the OSC fragment at m/z 93. There was also prominent response from dihydrogen sulfide, dimethyl sulfide + ethanethiol, and nominal m/z 145. One of the more interesting features is the response of heavier species at nominal m/z 201, 297, and 299. This is the first observation of a response at this high of an m/z during septic sampling. Further research is needed before these responses can be attributed to a specific analyte, but its presence suggests that heavier species are present within septic emissions. It was hypothesized that after emission, heavier species within septic plumes will remain low to the ground and travel longer distances under favorable meteorological conditions. Identifying heavy compounds within the septic emissions will provide valuable information for future testing that would include downwind septic monitoring to test the hypothesis.

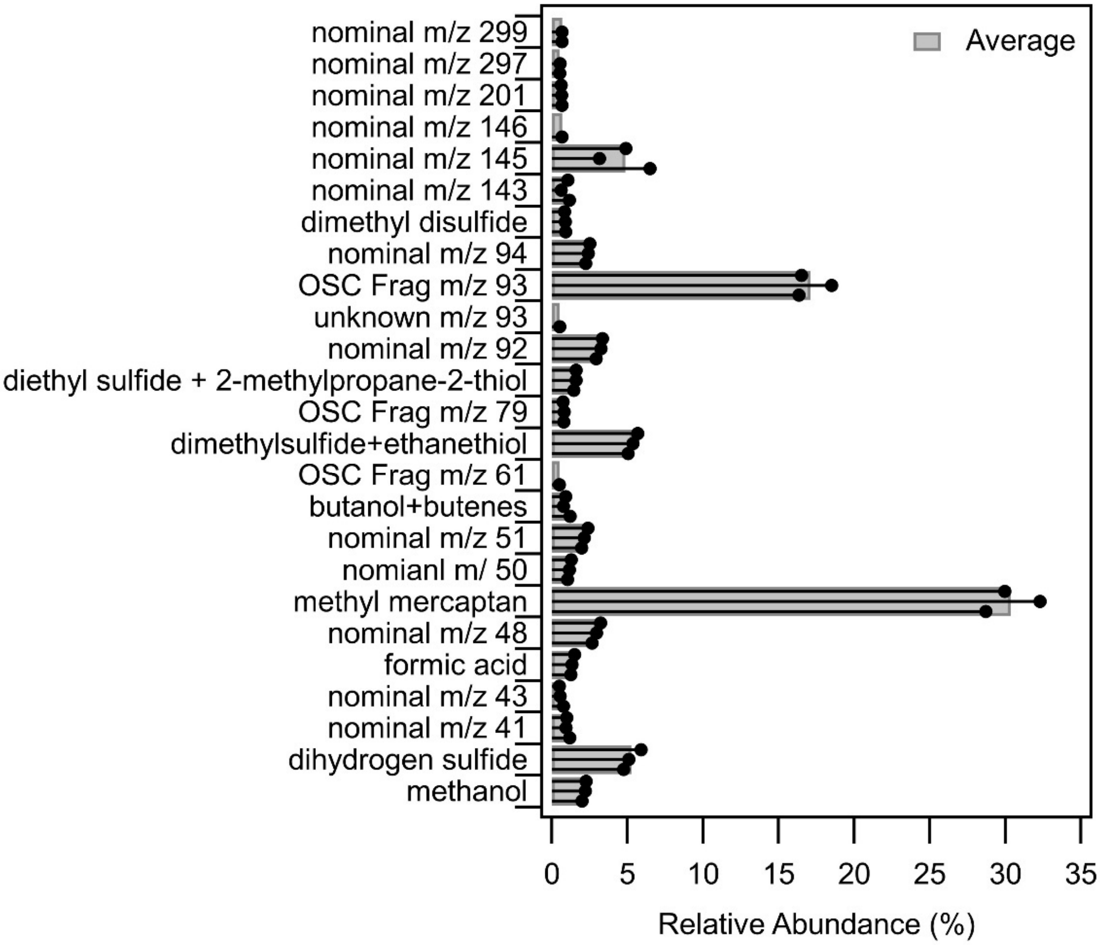

Figure 5-12. Septic Fingerprint at the High Level.

Figure 5-13 shows the septic fingerprint observed at the mid-level. Just like at the high level, the largest responses were at methyl mercaptan and the OSC fragment at m/z 93 with dihydrogen sulfide and dimethyl sulfide + ethanethiol having a prominent presence. There is also a signal at nominal m/ 145 but it is much more suppressed compared to the high level. There is also a lack of response from the nominal m/z 201, 297, and 299 species within the fingerprint. The hypothesis was that there may be some stratification of species within the septic tank, with heavier species accumulating more near the bottom. The lack of heavier response at the mid-level compared to the high level suggests that the opposite is happening with a larger presence of heavy species near the top. It is unclear what mechanism would cause this, but it is important to note that the heavy species response at the high level was reasonably minimal. There could be some mixing dynamics that are not understood within the septic tank that results in a small accumulation of the heavy species near the top.

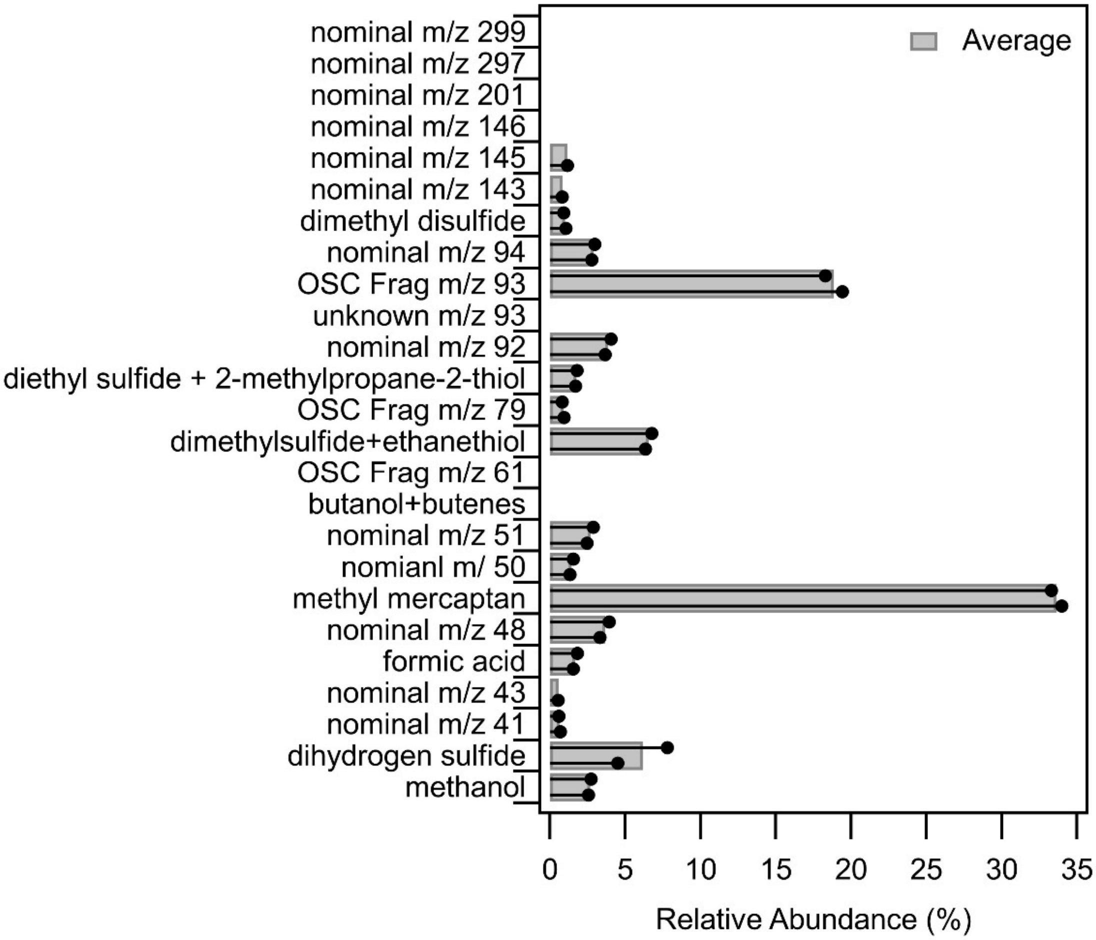

Figure 5-13. Septic Fingerprint at the Mid-level.

Figure 5-14 shows the septic fingerprint observed at the low level. The primary responses were methyl mercaptan and the OSC fragment at m/z 93 coupled with signal from dihydrogen sulfide and dimethyl sulfide + ethanethiol, as observed in the mid and high levels. As with the mid-level, there is no response of heavier species at the low level. This further suggests that stratification does not occur as expected and the mixing mechanism within the septic tank is not well understood.

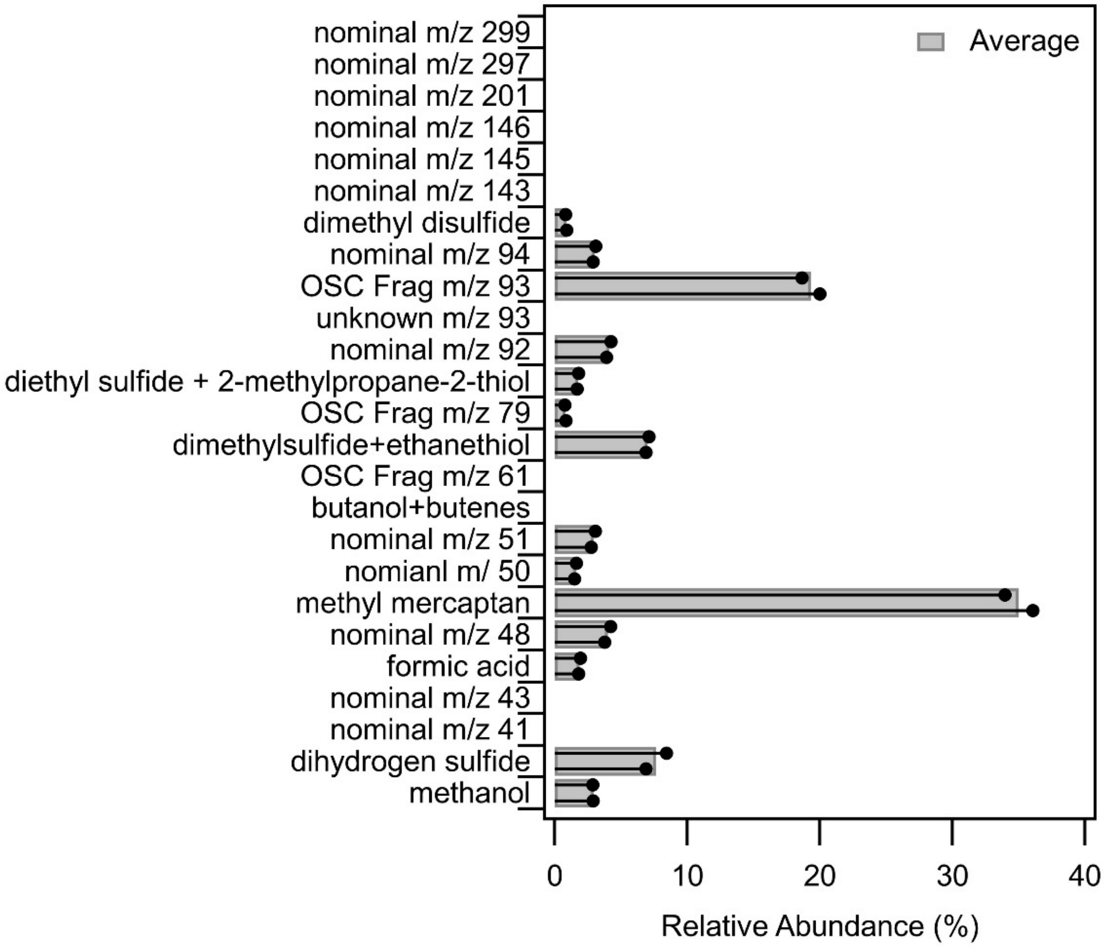

Figure 5-14. Septic Fingerprint at the Low Level.

Figure 5-15 shows the average septic fingerprint for all three levels. Overall, the fingerprints are nearly identical and it appears that the height of sampling has little or negligible effect on the composition. The septic fingerprint at the three levels ranges from 34% to 38% methyl mercaptan, 19% to 21% OSC fragment at m/z 93, 5% to 9% dihydrogen sulfide, and 6% to 8% dimethyl sulfide + ethanethiol. These four species comprise 65% to 75% of the septic fingerprint. While only the high level saw heavier species contribute at least 0.5% to the relative abundance, the response at nominal m/z 145 may provide additional insight. It contributes approximately 5.5% to the high level fingerprint, a little over 1% to the mid-level fingerprint, and is not present within the low level fingerprint. This does suggest there is a gradient in nominal m/z 145, but it is the only species that shows this behavior within the fingerprints. This points out one limitation of the fingerprint analysis and the purpose of this type of analysis should be reiterated. Generating these source fingerprints provides an easy metric for determining the prominent and unique species from a source that can help identify and distinguish it from other sources. It focuses on the most abundant species since those are the most likely to be detected in a plume that has traveled longer distances or diluted by larger amounts These prominent and unique species are important, but that does not mean that secondary, low abundance species do not carry importance. Therefore, analysis beyond fingerprint development was performed to identify and investigate the behavior of species not captured within the fingerprint.

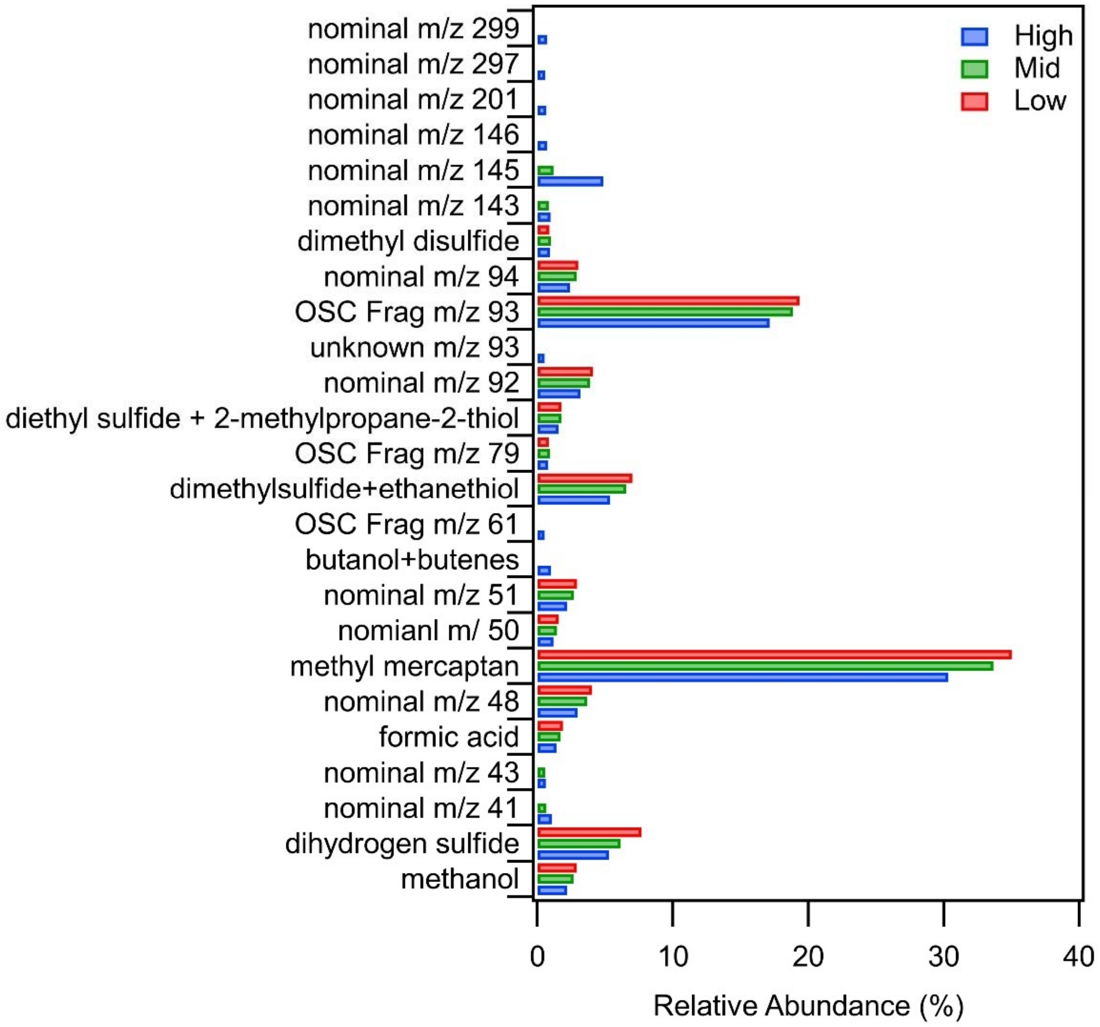

Figure 5-15. Comparison of Septic Fingerprints at the Three Levels.

Referring to Figure 5-11, nominal m/z 299 was used to help distinguish the sampling at the different levels. However, the fingerprint analysis at the different levels concluded that m/z 299 is not prominent enough within the low and mid-levels to contribute meaningfully to their fingerprints. The time-series in Figure 5-11 clearly shows a response higher than ambient levels at m/z 299. While it is not important from a fingerprint standpoint, it does suggest the presence of heavier species at all three levels. Further analysis was performed to identify the presence of species regardless of its contribution to the overall abundance.

Figure 5-16 shows a mass spectrum of the septic gas observed at the high level. The y-axis is in log scale so the response at a wide range of magnitudes can be observed since the response at methyl mercaptan (m/z 49) would skew the scale and make the low concentration responses invisible. The lower limit of the axis is also set at 0.05 ppbv, which is the cutoff point for the fingerprint analysis. The x-axis is the m/z value of the species. Previous figures were changed to list the representative species rather than an m/z, but the order in which they appear is numeric. For Figure 5-16, the highest responses are methyl mercaptan (m/z 49) and the OSC frag at m/z 93 as shown previously. This also shows the presence of heavier species more clearly. The responses around m/z 201, 297, and 299 are clearly visible, but there are clusters of peaks from m/z 221 to 227, m/z 239 to 241, and m/z 281 to 285. The highest response in each of these ranges occurred at m/z 223, 239, and 281, respectively. There are clearly other heavy species within the septic tank, but they are not above the 0.5% abundance contribution to be considered important from a fingerprint standpoint. Due to this low abundance and magnitude within the septic tank, detection of these species in a diluted plume emitted from this source is unlikely. Another potential complication with heavier masses is their transmission through the sample lines. The molecular weight of a species is often representative of its ability to be transmitted through sample lines with higher molecular weight typically meaning reduced transmission. This is often caused by loss of analyte as it sticks to the inner walls of the sample line and reduces the signal. In addition, a larger molecular weight typically means a higher potential for fragmentation. This would result in increased signal at a lower m/z than would be expected and is difficult to estimate without extensive testing and access to a certified source of the species. This line loss and fragmentation could mean an underestimation of the heavy species present within the septic tank, but future research and testing is required to increase our confidence with this dynamic.

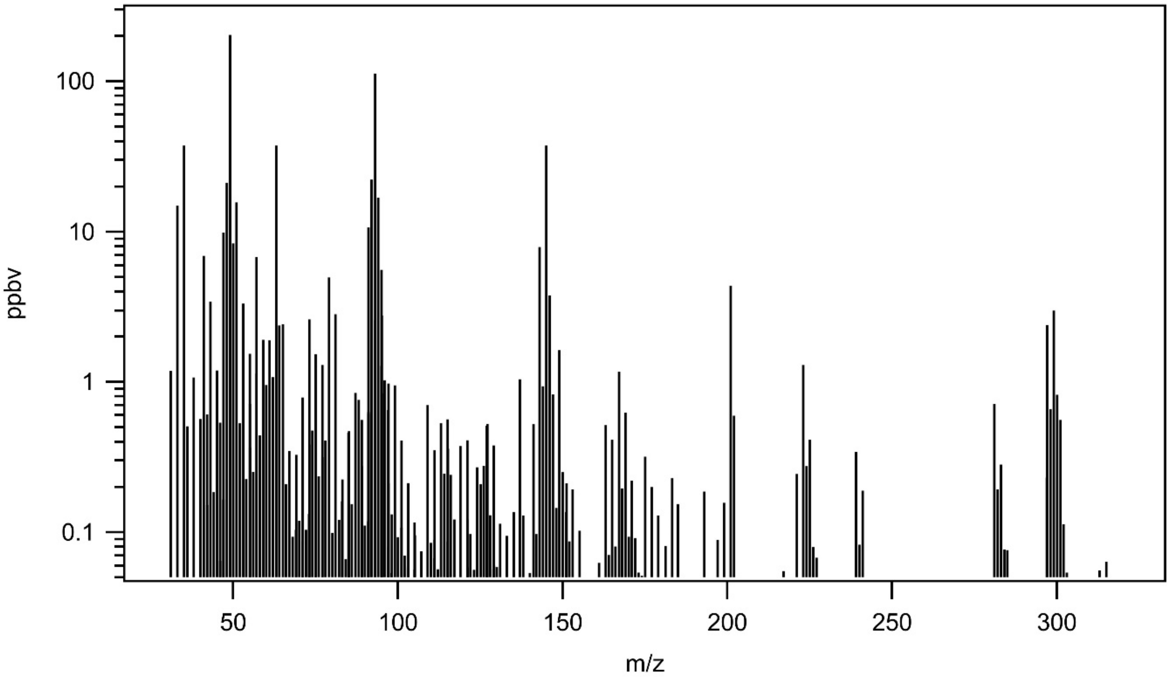

Figure 5-16. Mass Spectra of Septic Gas Constituents Monitored from the High Sample Port.

5.3.3 Detailed Analysis of Test Data – Septic

To look further at the heavy species, the response at m/z 201, 223, 239, 281, 297, and 299 were explored at the different levels. Just to note, m/z 223 is where diethyl phthalate responds, but there is no evidence to attribute the response in the septic emissions to it at this point. Figure 5-17 shows the time series of these ions during the testing. While not present in large quantities considering the sampling is directly in the source, they were all observed at each of the three levels. As mentioned earlier, m/z 145 showed a negative gradient with concentrations decreasing with height. All the ions in Figure 5-17 show the same behavior. To reiterate, this is the opposite of the hypothesis and the mechanism driving this gradient is currently not understood. The transition between the different levels can also suggest some properties of the species responsible for the signal. At m/z 281, 297, and 299, the transition between levels is sharp and seems to adjust quickly to stabilize at the new concentration. This would suggest that the species in question has good transmission through the lines with minimal line loss associated with conditioning. Alternatively, at m/z 201, 223, and 239, there seems to be a slower transition when switching between the three levels, especially with m/z 201. This would suggest that there are some conditioning effects and the species in question has a higher aptitude to adhere to the walls of the sample line. Based on this difference in transmission, the signals at m/z 201, 223, and 239 are probably from a different category of species and have a different chemical structure. Another interesting feature in Figure 5-16 occurs around 11:50 when the PTR-MS sampled zero air. The signals at m/z 281, 297, and 299 saw increases instead of decreases. It appears that there is a potential contaminant within the zero air system resulting in an increase at these ions. It is unknown what species would cause this and further investigation is needed to determine if this contaminant can be removed or accounted for.

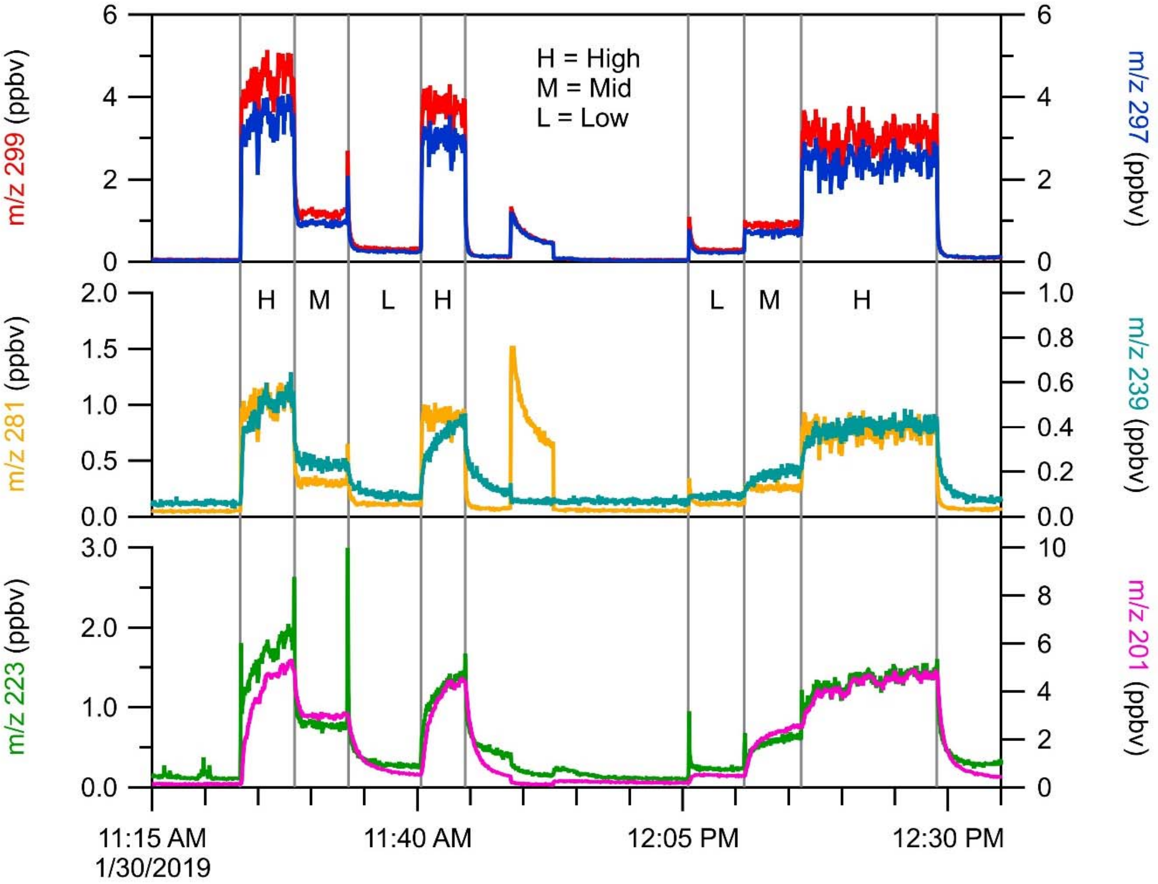

Figure 5-17. Time-series of Heavier Species at the Different Sampling Heights.

Previous reports have included analysis of septic emissions so comparing the results over time can aid in the understanding of the source and reveal behavior not easily captured over short time scales. Figure 5-18 shows the average septic fingerprint developed during 53005-81-RPT-027, *PTR-MS Mobile Laboratory Vapor Monitoring Monthly Report – Month 2*, and 53005-81-RPT-039 along with the combined average septic fingerprint of all three sampling levels in this Month 5 report. While the fingerprints are all from the same source, the sampling methods were different. Month 2 focused on tracking and monitoring the septic plumes downwind from the source. Month 4 sampling occurred at the top of the tank with the lid closed. The Month 4 and Month 5 sampling method is very similar to the Month 2 method yet varying enough that differences are expected.

For all three fingerprints, methyl mercaptan, dihydrogen sulfide, and OSC frag at m/z 93 comprise a majority of the relative abundance, but their individual contributions vary greatly. Month 2 is shifted towards dihydrogen sulfide as the dominant constituent while methyl mercaptan is dominant during Months 4 and 5. Dihydrogen sulfide is the second most abundant in Month 4, but it is relatively suppressed in Month 5. The OSC frag at m/z 93 shows a much larger presence during Month 5 than both Months 2 and 4 where it has a relatively minor contribution compared to methyl mercaptan and dihydrogen sulfide. This demonstrates the consistency of these three signals as the most important components within the fingerprints, but the relative differences in abundance show that there is variability from the source. It is unclear the mechanism that results in this variability in abundance but continued monitoring of septic emissions under similar and new conditions is required to further our understanding.

Month 2 and Month 5 both observed the presence of some heavier species but not at the same ions. There are multiple reasons this could have occurred. Since Month 2 sampling was performed downwind there is a reasonable chance that there is influence from other nearby sources mixing with the septic plume and generating a response at the heavy ions. In addition, the Month 5 sampling within the septic tank provided a better scenario to observe heavier species which may not effectively travel downwind or are present in too low of a concentration to be monitored downwind. It is interesting that heavier species were not observed during Month 4 since the sampling method was similar to Month 5. This could be a function of the Month 4 sampling requiring more modification and shifting of the sample inlet that it perturbed the septic emissions resulting in the difference. The possibility of the emissions being different based on time of day, week, or year cannot be ignored, but continued monitoring under different conditions will help the understanding of the temporal effects.

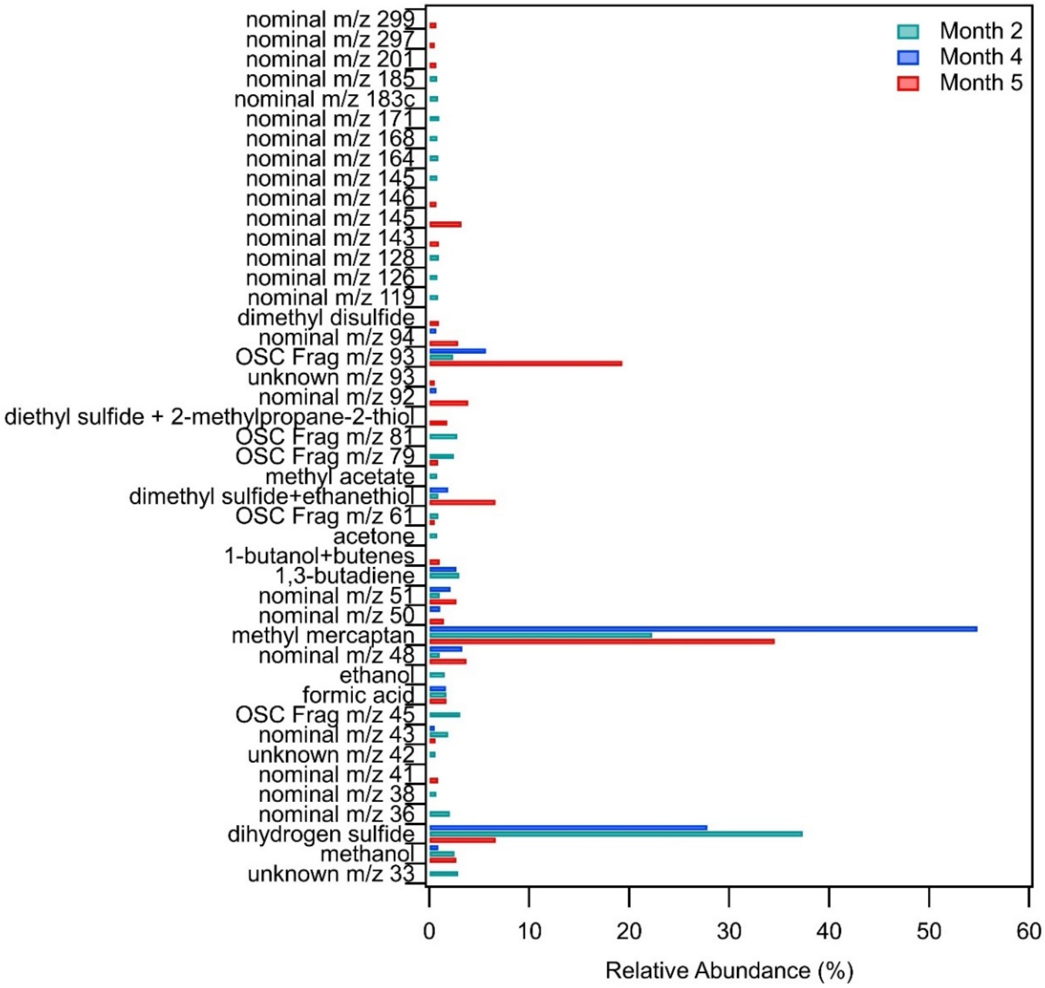

Figure 5-18. Comparison Average Septic Fingerprints Developed for the Months 2, 4, and 5 Reports.

5.4 Background Study

This subsection details the winter background study conducted from January 14, 2019, through February 9, 2019. Test completeness and general observations are documented in Section 5.4.1, followed by an analysis of background vapor composition, with a detailed assessment of the test data and confirmatory sampling measurements in the final subsection.

5.4.1 Discussion of Test Activities and Observations – Background

This subsection presents the winter background test activities through examination of completeness and provides validation observations through a comparison of ML data to confirmatory samples.

5.4.1.1 Completeness of Test Activities

The Test Plan prescribes the required monitoring parameters and data collection tasks necessary to conduct the fall background study that would produce results and conclusions as part of a seasonal comprehensive background study.

From an executory perspective, the study required 24 days of sampling ambient air at six pre-determined locations on and off the Hanford Site (corresponding to locations sampled during previous segments of the study), between January 14, 2019, and February 9, 2019, for durations of 22 to 23 hours per site. Figure 5-19 shows all the background locations. Table 5-4 shows the completed schedule of background sampling, which corresponds identically to the projected schedule from the Test Plan.

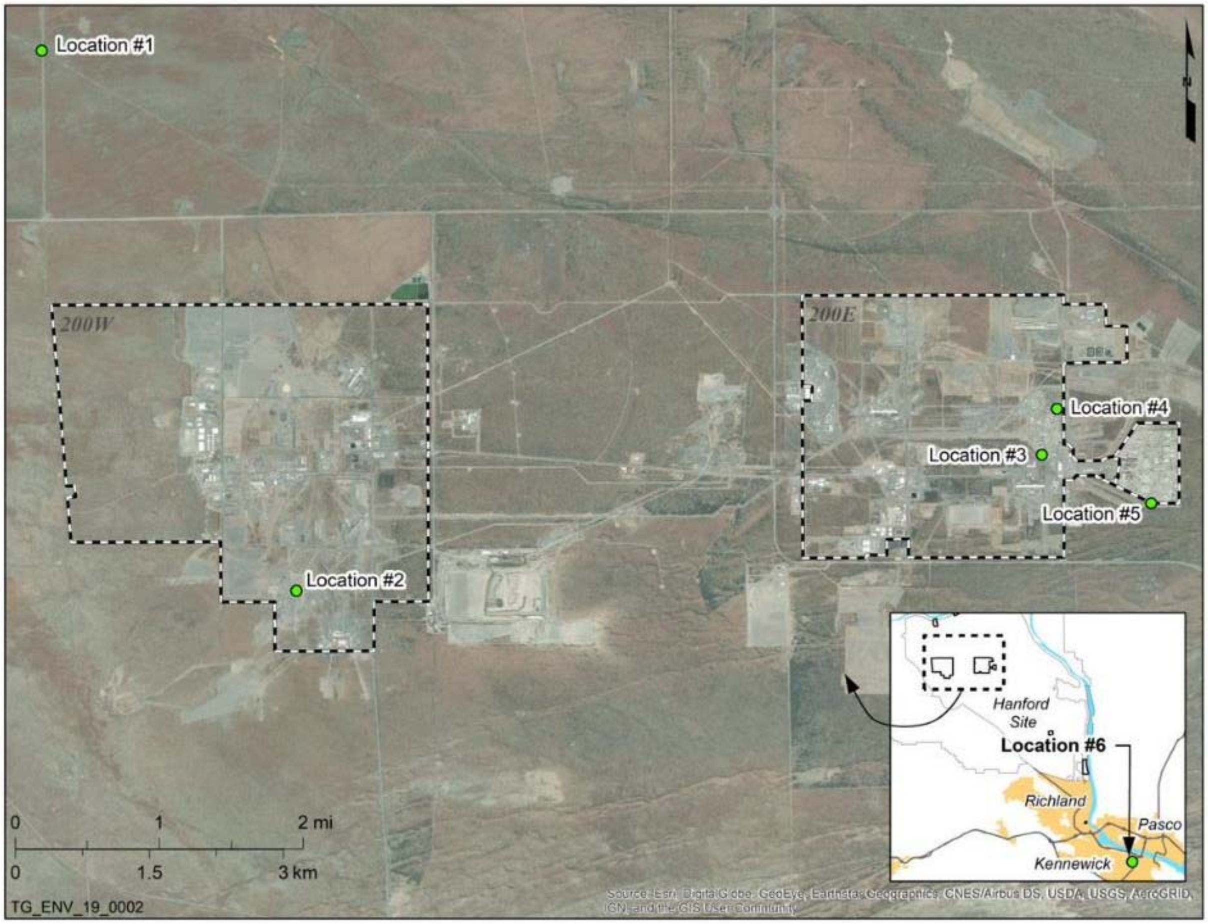

Figure 5-19. Fall 2018 Background Study Locations.

Table 5-4. Background Study Schedule Overview.

Start Date	Start Time	Stop Date	Stop Time	Hours	Site 1	Site 2	Site 3	Site 4	Site 5	Site 6
01/14/2019	07:38	01/15/2019	07:05	23 hr 27 min	X					
01/15/2019	07:52	01/16/2019	07:10	23 hr 18 min		X				
01/16/2019	08:18	01/17/2019	07:04	22 hr 46 min			X			
01/17/2019	08:00	01/18/2019	07:00	23 hr				X		
01/18/2019	07:28	01/19/2019	06:47	23 hr 19 min					X	
01/19/2019	08:10	01/20/2019	06:06	21 hr 56 min						X
01/20/2019	07:26	01/21/2019	07:20	23 hr 54 min	X					
01/21/2019	08:12	01/22/2019	07:05	22 hr 53 min		X				
01/22/2019	08:49	01/23/2019	06:55	22 hr 6 min			X			
01/23/2019	07:16	01/24/2019	07:08	23 hr 52 min				X		
01/24/2019	09:05	01/24/2019	13:07	4 hr 2 min	AP Pump Removal					
01/25/2019	08:12	01/25/2019	12:53	4 hr 41 min	Calibration & Testing of new MCP Module					
01/26/2019	09:34	01/27/2019	07:05	21 hr 31 min	X					
01/27/2019	07:46	01/28/2019	07:30	23 hr 44 min		X				
01/28/2019	08:08	01/29/2019	07:05	22 hr 57 min			X			
01/29/2019	08:13	01/30/2019	08:10	23 hr 57 min				X		
01/30/2019	08:35	01/31/2019	09:05	24 hr 30 min					X	
01/31/2019	11:19	02/01/2019	07:50	20 hr 31 min						X
02/01/2019	09:47	02/02/2019	07:21	21 hr 34 min	X					
02/02/2019	08:31	02/03/2019	06:57	22 hr 26 min		X				
02/03/2019	07:41	02/04/2019	07:00	23 hr 19 min			X			
02/04/2019	08:24	02/05/2019	11:20	26 hr 56 min				X		
02/05/2019	11:56	02/06/2019	09:00	21 hr 4 min					X	
02/06/2019	10:00	02/07/2019	07:50	21 hr 50 min						X
02/07/2019	09:23	02/08/2019	08:10	22 hr 47 min			X			
02/08/2019	08:38	02/09/2019	08:56	24 hr 18 min					X	
02/09/2019	10:26	02/10/2019	07:45	21 hr 19 min						X
Number of Days					4	4	5	4	4	4

As planned, the winter background study was executed to meet the temporal requirements at the planned locations for the prescribed durations.

Detailed data collection and reporting requirements were prescribed in 66409-RPT-007. Table 5-3 lists the required COPCs. 66409-RPT-007 required summary-level reporting of all COPCs measurable by the PTR-MS with attention on the compounds in Table 5-5 due to the difficulty of measuring them with standard analytical methods. The COPCs in Table 5-5 were successfully measured for the duration of the fall background study and summaries of those results are presented in Section 5.3, as well as other compounds detected by the PTR-MS during this campaign.

Table 5-5. List of Applicable Chemicals of Potential Concern.

COPC	OEL (ppb)
Ammonia	25000
Furan	1
But-3-en-2-one + 2,3-dihydrofuran + 2,5-dihydrofuran	200, 1, 1
NDMA	0.3
2-methylefuran	1
NEMA	0.3
2,5-dimethylfuran	1
NDEA	0.1
2-propylfuran + 2-ethyl-5-methylfuran	1
NMOR	0.6
2-ethyl-2-hexenal + 4-(1-methylpropyl)-2,3-dihydrofuran + 3-(1,1-dimethylethyl)-2,3-dihydrofuran	1
2-pentylfuran	1
2-heptylfuran	1
2-octylfuran	1
6-(2-furanyl)-6-methyl-2-heptanone	1
furfural acetophenone	1

5.4.1.2 Validation Observations from Confirmatory Samples

A standard quality control tool deployed in environmental sampling plans is the collection and analysis of split samples to validate both sample collection and analytical techniques. In lieu of using a second PTR-MS to validate ML measurements, standard sampling media and standard laboratory methods for confirmation and validation of ML PTR-MS results were performed. Three confirmatory methods were prescribed in the Test Plan and were utilized by TerraGraphics during the fall background study:

1. NIOSH Method 2522 modified (Thermosorb®[10]/N, solid sorbent tube sampling);

---

[10] Thermosorb is a registered trademark of Ellutia Limited, Cambridgeshire, United Kingdom.

2. EPA TO-17 modified (Carbotrap®[11] 300, thermal desorption tube sampling); and

3. EPA TO-11A [Dinitrophenylhydrazine (DNPH) sorbent tubes].

Confirmatory measurements were required in duplicate by each analytical method at a rate of one per every ten samples with a blank collected and analyzed every 20 samples. Because of the difficulty measuring the COPC list of interest (Table 5-5), a secondary list of compounds was selected for confirmatory measurements. Confirmatory compounds along with detection and volume requirements are shown in Table 5-6.

Table 5-6. List of Compounds for Confirmatory Analysis.

Method	**Species**	**ALS Detection Limit (ug)**	**Estimated Background Concentration (ug/m^3)**	**Mass per 1 Liter (ug/L)**	**Flow Rate (L/min)**	**Recommended Sampling Time (Minutes)**
TO-17	1,3-butadiene	0.025	1.1	0.0011	0.250	45
	acetonitrile	0.025	0.08	0.00008	0.250	596
	benzene	0.025	0.32	0.00032	0.250	157
	2-hexanone	0.025	0.2	0.0002	0.250	245
	acetone	0.025	1.19	0.00119	0.250	42
	toluene	0.025	0.19	0.00119	0.250	266
	m,p-xylene	0.025	0.22	0.00022	0.250	231
	o-xylene	0.025	0.22	0.00022	0.250	231
	ethylbenzene	0.025	0.22	0.00022	0.250	231
	styrene	0.025	0.11	0.00011	0.250	470
TO-11A	acetaldehyde	0.05	0.36	0.00036	1.0	278
	butanal	0.05	0.29	0.00029	1.0	340
	2-propenal	0.05	0.23	0.00023	1.0	437
	acetone	0.05	1.15	0.00115	1.0	87
NIOSH 2522	NDEA	0.01	0.08	0.00008	1.0	240
	NDMA	0.01	0.15	0.00015	1.0	132
	NEMA	0.01	0.11	0.00011	1.0	185
	NMOR	0.01	0.05	0.00005	1.0	422

---

[11] Carbotrap is a registered trademark of Sigma-Aldrich Co., LLC, St. Louis, Missouri.

Australian Laboratory Services (ALS) was selected to perform analysis of the confirmatory samples for compounds listed in Table 5-4, with the added direction of reporting any TICs.

Once analyzed, these samples were compared, where possible, to the average PTR-MS signal observed over the same time period the samples were collected. Air sample collection on the alternative media occurred once daily per site. Carbotrap-300 samples were generally collected over the course of 360 minutes, while Thermosorb/N and DNPH cartridges were generally collected over the course of 180 minutes. Confirmatory samples were collected and analyzed from each of the six sites per the Test Plan requirement of one confirmatory sample for every two days of monitoring at each site for each of the three analytical methods. The frequency and duration of the sampling was designed to produce duplicates for each method utilized for each of the six background sites. For this reason, both accuracy and precision data can be evaluated. Also, one blank per ten samples analyzed was performed.

By the very nature of the experiment, the concentrations measured during the background study are very low, and in most cases, below the reporting limits or MDLs. Since limited information can be gathered from results that are less than the laboratory and PTR-MS reporting limits, sampling times and volumes were chosen based on the laboratory detection limit and the estimated background concentration determined from previous studies. The chemical list was chosen based on available standard analysis, overlap with the COPC list, and the likelihood of the chemicals to be greater than the laboratory and PTR-MS reporting limits. Despite the limitations of the subcontract laboratory analyte list, samples were able to be analyzed for ten COPCs with full calibration, and two others using TICs. The ML data along with confirmatory sampling data is provided in Appendix A.

5.4.1.3 Comparison to Carbotrap-300 TO-17 Results

Table A-2 in Appendix A provides all Carbotrap-300 samples taken over the course of the winter background study while Table 5-5 summarizes a subset of results for confirmatory sample comparison of PTR-MS to EPA Compendium TO-17. Very little quantitative confidence can be ascribed to results below either the PTR-MS or Laboratory RL. Thus, results that are summarized here are those where the ALS result is above the RL and where the PTR-MS result is above the MDL.

The 192 analytical measurements attempted on the 16 (includes one blank and two duplicates) Carbotrap-300 samples were sent to ALS for laboratory testing. 68% of the measurements made by ALS were reported as not detectable above the reporting limit. 73% of the measurements made by the ML were reported as not detectable above the MDL. Out of those sample locations where analytes were detected above reporting limits for both methods, three compounds (acetone, benzene, and toluene) were detected at frequencies and levels substantial enough to be analyzed for comparative precision. Table 5-7 shows the results of a simple precision analysis between TO-17 and PTR-MS.

Table 5-7. Precision of Proton Transfer Reaction – Mass Spectrometer and TO-17 Using Carbotrap-300.

Constituent	Number of Duplicates Evaluated	Number of Duplicate Measurements*	Percent Out of Limits (>20%)	Range of Out-of-Limit RPD
Benzene	16	4	100%	36 – 47%
Acetone	16	11	81%	47 – 111%
Toluene	16	10	100%	55 – 150%

* Duplicates with both results greater than ALS reporting limits or PTR-MS MDL.

Due to the elevated level of baseline noise during this monitoring period, which caused PTR-MS MDLs to be increased above normal operating thresholds, PTR-MS levels of detection were similar to those produced by TO-17 analysis. As a result, both methods produced similar numbers of detections. Due to the low abundance of many of the TO-17 compounds (Table 5-5) in the background study area, confirmation of PTR-MS results with standard sampling and analysis techniques will continue to be difficult. Because PTR-MS data used in this comparison is greater than the MDLs but less than the RLs, there is a moderate level of uncertainty associated with the results leading to poor precision with TO-17 results.

5.4.1.4 Comparison to Dinitrophenylhydrazine TO-11 Results

Table A-3 in Appendix A provides all DNPH samples taken over the course of the winter background study while Table 5-6 summarizes a subset of results for confirmatory sample comparison of PTR-MS to EPA Compendium TO-11a. Very little quantitative confidence can be ascribed to results below either the PTR-MS or Laboratory RL. Thus, results that are summarized here are those where the ALS result is above the RL and where the PTR-MS result is above the MDL. Some acetone results in Table 5-6 are included that ALS reported below their RL because acetone was also analyzed by TO-17 (Table 5-5 and Appendix A, Table A-2) and it is interesting to look at the behavior of acetone by all three methods.

The 76 analytical measurements attempted on the 16 (includes one blank and two duplicates) DNPH samples were sent to ALS for laboratory testing. A total of 46% of the measurements made by ALS were reported as not detectable above the reporting limit. Conversely, only 82% of the measurements made by the ML were reported as not detectable above the MDL. Out of those sample locations where analytes were detected above RL for TO-11 and MDL for PTR-MS, one compound (acetone) was detected at frequencies and levels substantial enough to be analyzed for comparative precision. Table 5-8 shows the results of a simple precision analysis between TO-11a and PTR-MS.

Table 5-8. Precision of Proton Transfer Reaction – Mass Spectrometer and TO-11a Using LpDNPH.

Constituent	Number of Duplicates Evaluated	Number of Duplicate Measurements*	Percent Out of Limits (>20%)	Range of Out-of-Limit RPD
Acetone	16	11	100%	21 – 128%

*Duplicates with both results greater than reporting limits.

Due to the elevated level of baseline noise during this monitoring period which caused PTR-MS MDLs to be increased above normal operating thresholds, PTR-MS levels of detection were greater than those produced by TO-11 analysis. As a result, PTR-MS produced fewer detections during this monitoring period. Due to the low abundance of many of the TO-11a compounds (Table 5-6) in the background study area, confirmation of PTR-MS results with standard sampling and analysis techniques will continue to be difficult. Because PTR-MS data used in this comparison are greater than the MDLs but less than the RLs, there is a moderate level of uncertainty associated with the results leading to poor precision with TO-11 results.

5.4.1.5 Comparison of Thermosorb/N NIOSH 2522 Results

Table A-4 in Appendix A provides all Thermosorb-N samples taken over the course of the winter background study as confirmatory sample comparison of PTR-MS to NIOSH Method 2522. Very little quantitative confidence can be ascribed to results below either the PTR-MS or Laboratory RL. No results were reported by ALS above the RL for the four nitrosamine compounds of interest:

1. N-nitrosodimethylamine (NDMA),
2. N- nitrosodiethylamine (NDEA),
3. N-nitrosomorpholine (NMOR), and
4. N-nitrosomethylethylamine (NEMA).

The 64 analytical measurements attempted on the 16 (includes one blank and two duplicates) Thermosorb/N samples were sent to ALS for laboratory testing. One hundred percent of the measurements made by ALS were reported as not detectable above the RL. Similarly none of the measurements made by the ML were reported as not detectable above the RL. The lack of detections by PTR-MS is partly attributed to the elevated level of baseline noise during this monitoring period which caused PTR-MS MDLs to be increased above normal operating thresholds. Because no samples produced results using both testing methods, no comparative precision analysis was performed.

5.4.2 Identification of Vapor Sources, Quantitative Analysis of Vapor Composition and Summary of Background Results

This section is typically reserved for description and analysis of chemical makeup of observed vapor sources, emissions, or plumes. The nature of this study is to provide information as part of a four-part, comprehensive background study of vapors at ambient concentrations. Summaries of the results for the six sampling sites are presented in the following subsection.

Total average concentrations of COPCs at each site over the course of the fall background study are listed in the following tables, along with figures depicting locations for background data collection. The values shown in the site summary tables below are based on the aggregate of all measurements taken at each individual study site across four separate monitoring days.

5.4.2.1 Summary of Site 1

The location of the ML at Site 1, which is approximately one mile northwest of the 200 West Area of the Hanford Site, is displayed in Figure 5-20. Summary statistics including compound average concentrations as well as maximum concentrations observed over the fall background study period are shown in Table 5-9.

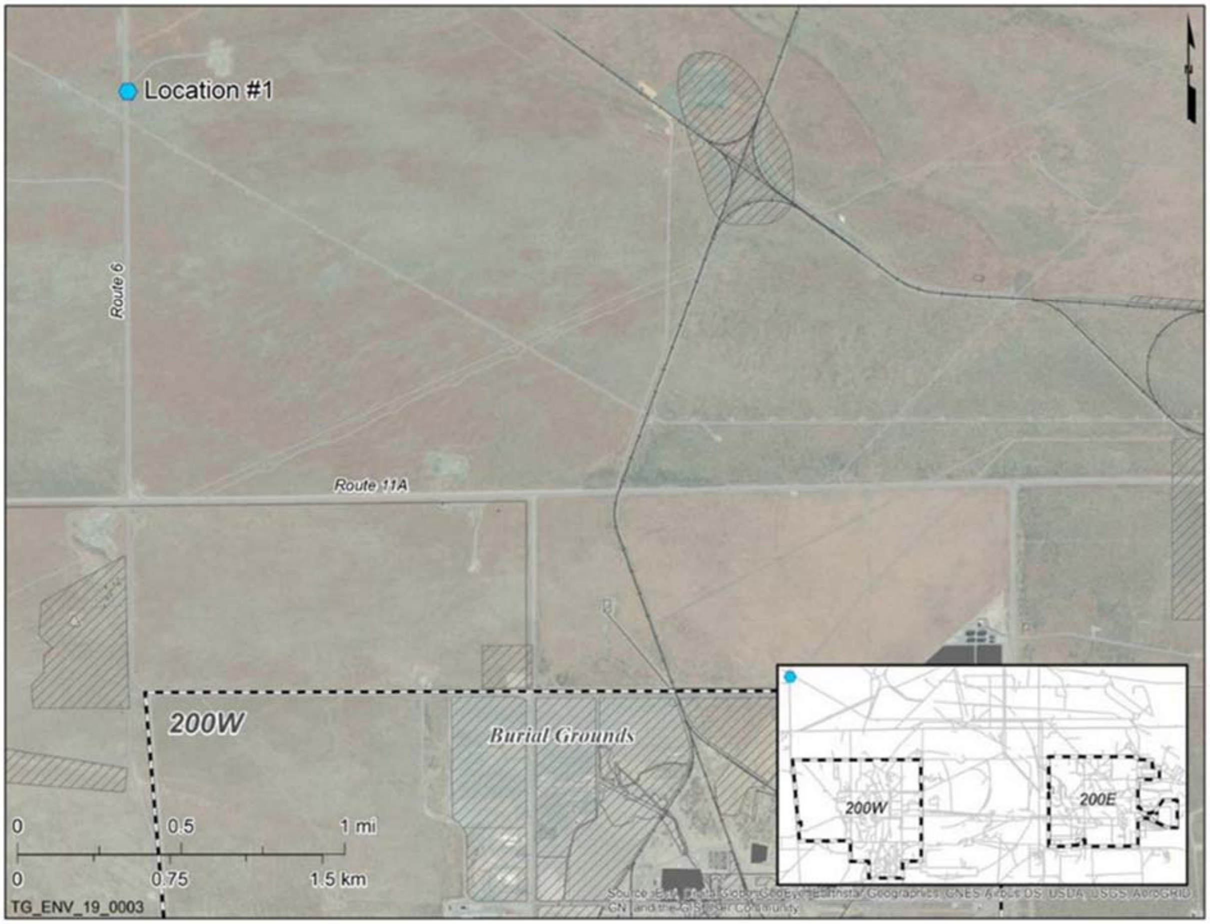

Figure 5-20. Mobile Laboratory Site 1 for the Duration of the Monitoring Period.

Table 5-9. Summary of Site 1 Proton Transfer Reaction – Mass Spectrometer Observations of Chemical of Potential Concern. (2 Sheets)

COPC Name	OEL (ppbv)	Average (ppbv)	Max (ppbv)
ammonia	25000	5.259	9.569
formaldehyde	300	0.315	6.396
methanol	200000	2.458	7.058
acetonitrile	20000	0.037	0.157
acetaldehyde	25000	0.474	2.997
ethylamine	5000	0.045	0.671
1,3-butadiene	1000	0.019	0.283
propanenitrile	6000	0.052	0.282
2-propenal	100	0.052	0.751
1-butanol + butenes	20000	0.050	0.215
methyl isocyanate	20	0.035	0.205
methyl nitrite	100	0.085	0.503
furan	1	0.028	0.139
butanenitrile	8000	0.024	0.144
but-3-en-2-one + 2,3-dihydrofuran + 2,5-dihydrofuran	200, 1, 1	0.018	0.197
butanal	25000	0.044	0.129
NDMA	0.3	0.011	0.096
benzene	500	0.114	0.413
2,4-pentadienenitrile + pyridine	300, 1000	0.055	0.279
2-methylene butanenitrile	300	0.039	0.201
2-methylfuran	1	0.025	0.127
pentanenitrile	6000	0.020	0.116
3-methyl-3-buten-2-one + 2-methyl-2-butenal	20, 30	0.021	0.119
NEMA	0.3	0.012	0.092
2,5-dimethylfuran	1	0.018	0.103
hexanenitrile	6000	0.019	0.120
2-hexanone (MBK)	5000	0.018	0.100
NDEA	0.1	0.011	0.105
butyl nitrite + 2-nitro-2-methylpropane	100, 300	0.058	0.286
2,4-dimethylpyridine	500	0.018	0.135
2-propylfuran + 2-ethyl-5-methylfuran	1	0.016	0.087
heptanenitrile	6000	0.018	0.106

Table 5-9. Summary of Site 1 Proton Transfer Reaction – Mass Spectrometer Observations of Chemical of Potential Concern. (2 Sheets)

COPC Name	OEL (ppbv)	Average (ppbv)	Max (ppbv)
4-methyl-2-hexanone	500	0.017	0.096
NMOR	0.6	0.003	0.052
butyl nitrate	2500	0.011	0.078
2-ethyl-2-hexenal + 4-(1-methylpropyl)-2,3-dihydrofuran + 3-(1,1-dimethylethyl)-2,3-dihydrofuran	100, 1, 1	0.018	0.101
6-methyl-2-heptanone	8000	0.018	0.100
2-pentylfuran	1	0.023	0.097
biphenyl	200	0.015	0.113
2-heptylfuran	1	0.076	0.386
1,4-butanediol dinitrate	50	0.026	0.147
2-octylfuran	1	0.002	0.049
1,2,3-propanetriol 1,3-dinitrate	50	0.001	0.063
PCB	1000	0.031	0.163
6-(2-furanyl)-6-methyl-2-heptanone	1	0.017	0.109
furfural acetophenone	1	0.080	0.417

5.4.2.2 Summary of Site 2

The location of the ML at Site 2, near the S-SX Tank Farms in the 200 West Area of the Hanford Site, is displayed in Figure 5-21. Summary statistics including compound average concentrations as well as maximum concentrations observed over the fall background study period are shown in Table 5-10.

Figure 5-21. Mobile Laboratory Site 2 for the Duration of the Monitoring Period.

Table 5-10. Summary of Site 2 Proton Transfer Reaction – Mass Spectrometer Observations of Chemicals of Potential Concern. (2 Sheets)

COPC Name	OEL (ppbv)	Average (ppbv)	Max (ppbv)
ammonia	25000	4.369	10.604
formaldehyde	300	0.324	1.853
methanol	200000	2.509	13.184
acetonitrile	20000	0.036	8.251
acetaldehyde	25000	0.434	14.718
ethylamine	5000	0.043	0.131
1,3-butadiene	1000	0.016	0.378
propanenitrile	6000	0.043	0.824
2-propenal	100	0.048	1.115
1-butanol + butenes	20000	0.045	0.729
methyl isocyanate	20	0.029	0.133
methyl nitrite	100	0.071	0.632
furan	1	0.024	0.152
butanenitrile	8000	0.019	0.311
but-3-en-2-one + 2,3-dihydrofuran + 2,5-dihydrofuran	200, 1, 1	0.015	0.199
butanal	25000	0.042	0.186
NDMA	0.3	0.008	0.055
benzene	500	0.094	1.174
2,4-pentadienenitrile + pyridine	300, 1000	0.047	0.169
2-methylene butanenitrile	300	0.033	0.135
2-methylfuran	1	0.020	0.161
pentanenitrile	6000	0.016	0.141
3-methyl-3-buten-2-one + 2-methyl-2-butenal	20, 30	0.017	0.155
NEMA	0.3	0.009	0.045
2,5-dimethylfuran	1	0.014	0.135
hexanenitrile	6000	0.015	0.081
2-hexanone (MBK)	5000	0.015	0.060
NDEA	0.1	0.008	0.043
butyl nitrite + 2-nitro-2-methylpropane	100, 300	0.047	0.400
2,4-dimethylpyridine	500	0.015	0.137
2-propylfuran + 2-ethyl-5-methylfuran	1	0.012	0.087
heptanenitrile	6000	0.014	0.060

Table 5-10. Summary of Site 2 Proton Transfer Reaction – Mass Spectrometer Observations of Chemicals of Potential Concern. (2 Sheets)

COPC Name	OEL (ppbv)	Average (ppbv)	Max (ppbv)
4-methyl-2-hexanone	500	0.014	0.061
NMOR	0.6	0.003	0.055
butyl nitrate	2500	0.008	0.049
2-ethyl-2-hexenal + 4-(1-methylpropyl)-2,3-dihydrofuran + 3-(1,1-dimethylethyl)-2,3-dihydrofuran	100, 1, 1	0.014	0.059
6-methyl-2-heptanone	8000	0.014	0.055
2-pentylfuran	1	0.019	0.075
biphenyl	200	0.012	0.057
2-heptylfuran	1	0.059	0.168
1,4-butanediol dinitrate	50	0.021	0.068
2-octylfuran	1	0.002	0.047
1,2,3-propanetriol 1,3-dinitrate	50	0.001	0.049
PCB	1000	0.025	0.076
6-(2-furanyl)-6-methyl-2-heptanone	1	0.013	0.049
furfural acetophenone	1	0.063	0.167

5.4.2.3 Summary of Site 3

The location of the ML at Site 3, just west of the 242-A Evaporator in the 200 East area of the Hanford Site, is displayed in Figure 5-22. Summary statistics including compound average concentrations as well as maximum concentrations observed over the fall background study period are shown in Table 5-11.

Figure 5-22. Mobile Laboratory Site 3 for the Duration of the Monitoring Period.

Table 5-11. Summary of Site 3 Proton Transfer Reaction – Mass Spectrometer Observations of Chemicals of Potential Concern. (2 Sheets)

COPC Name	OEL (ppbv)	Average (ppbv)	Max (ppbv)
ammonia	25000	5.722	12.567
formaldehyde	300	0.303	1.058
methanol	200000	2.533	12.428
acetonitrile	20000	0.030	2.032
acetaldehyde	25000	0.491	3.177
ethylamine	5000	0.047	0.176
1,3-butadiene	1000	0.013	0.180
propanenitrile	6000	0.042	0.256
2-propenal	100	0.051	0.620
1-butanol + butenes	20000	0.046	0.631
methyl isocyanate	20	0.029	0.106
methyl nitrite	100	0.072	0.550
furan	1	0.024	0.113
butanenitrile	8000	0.019	0.171
but-3-en-2-one + 2,3-dihydrofuran + 2,5-dihydrofuran	200, 1, 1	0.016	0.160
butanal	25000	0.043	0.143
NDMA	0.3	0.007	0.056
benzene	500	0.125	1.418
2,4-pentadienenitrile + pyridine	300, 1000	0.045	0.159
2-methylene butanenitrile	300	0.030	0.099
2-methylfuran	1	0.021	0.112
pentanenitrile	6000	0.016	0.061
3-methyl-3-buten-2-one + 2-methyl-2-butenal	20, 30	0.018	0.105
NEMA	0.3	0.008	0.049
2,5-dimethylfuran	1	0.016	0.082
hexanenitrile	6000	0.014	0.060
2-hexanone (MBK)	5000	0.015	0.054
NDEA	0.1	0.008	0.048
butyl nitrite + 2-nitro-2-methylpropane	100, 300	0.044	0.140
2,4-dimethylpyridine	500	0.016	0.387
2-propylfuran + 2-ethyl-5-methylfuran	1	0.013	0.064
heptanenitrile	6000	0.013	0.052

Table 5-11. Summary of Site 3 Proton Transfer Reaction – Mass Spectrometer Observations of Chemicals of Potential Concern. (2 Sheets)

COPC Name	OEL (ppbv)	Average (ppbv)	Max (ppbv)
4-methyl-2-hexanone	500	0.013	0.051
NMOR	0.6	0.003	0.061
butyl nitrate	2500	0.008	0.043
2-ethyl-2-hexenal + 4-(1-methylpropyl)-2,3-dihydrofuran + 3-(1,1-dimethylethyl)-2,3-dihydrofuran	100, 1, 1	0.014	0.053
6-methyl-2-heptanone	8000	0.014	0.052
2-pentylfuran	1	0.018	0.060
biphenyl	200	0.011	0.054
2-heptylfuran	1	0.057	0.184
1,4-butanediol dinitrate	50	0.020	0.074
2-octylfuran	1	0.002	0.051
1,2,3-propanetriol 1,3-dinitrate	50	0.001	0.053
PCB	1000	0.023	0.079
6-(2-furanyl)-6-methyl-2-heptanone	1	0.012	0.052
furfural acetophenone	1	0.060	0.194

5.4.2.4 Summary of Site 4

The location of the ML at Site 4, east of the AN and C Tank Farms in the 200 East area of the Hanford Site, is displayed in Figure 5-23. Summary statistics including compound average concentrations as well as maximum concentrations observed over the fall background study period are shown in Table 5-12.

Figure 5-23. Mobile Laboratory Site 4 for the Duration of the Monitoring Period.

Table 5-12. Summary of Site 4 Proton Transfer Reaction – Mass Spectrometer Observations of Chemicals of Potential Concern. (2 Sheets)

COPC Names	OEL (ppbv)	Averages (ppbv)	Max (ppbv)
ammonia	25000	4.106	6.420
formaldehyde	300	4.180	11.113
methanol	200000	0.913	5.003
acetonitrile	20000	2.143	18.660
acetaldehyde	25000	0.140	1.118
ethylamine	5000	0.335	3.698
1,3-butadiene	1000	0.037	0.385
propanenitrile	6000	0.022	1.152
2-propenal	100	0.040	0.542
1-butanol + butenes	20000	0.048	1.335
methyl isocyanate	20	0.041	1.391
methyl nitrite	100	0.038	1.242
furan	1	0.051	0.922
butanenitrile	8000	0.020	0.505
but-3-en-2-one + 2,3-dihydrofuran + 2,5-dihydrofuran	200, 1, 1	0.017	0.204
butanal	25000	0.024	0.447
NDMA	0.3	0.037	0.368
benzene	500	0.029	0.377
2,4-pentadienenitrile; pyridine	300, 1000	0.103	3.792
2-methylene butanenitrile	300	0.039	0.871
2-methylfuran	1	0.025	0.335
pentanenitrile	6000	0.018	0.460
3-methyl-3-buten-2-one + 2-methyl-2-butenal	20, 30	0.015	0.294
NEMA	0.3	0.014	0.377
2,5-dimethylfuran	1	0.009	0.294
hexanenitrile	6000	0.014	0.413
2-hexanone (MBK)	5000	0.014	0.338
NDEA	0.1	0.013	0.253
butyl nitrite + 2-nitro-2-methylpropane	100, 300	0.018	1.060
2,4-dimethylpyridine	500	0.033	0.411
2-propylfuran + 2-ethyl-5-methylfuran	1	0.013	0.348
heptanenitrile	6000	0.012	0.369

Table 5-12. Summary of Site 4 Proton Transfer Reaction – Mass Spectrometer Observations of Chemicals of Potential Concern. (2 Sheets)

COPC Names	OEL (ppbv)	Averages (ppbv)	Max (ppbv)
4-methyl-2-hexanone	500	0.013	0.326
NMOR	0.6	0.010	0.043
butyl nitrate	2500	0.004	0.253
2-ethyl-2-hexenal + 4-(1-methylpropyl)-2,3-dihydrofuran + 3-(1,1-dimethylethyl)-2,3-dihydrofuran	100, 1, 1	0.009	0.326
6-methyl-2-heptanone	8000	0.013	0.327
2-pentylfuran	1	0.014	0.299
biphenyl	200	0.015	0.345
2-heptylfuran	1	0.023	1.445
1,4-butanediol dinitrate	50	0.042	0.606
2-octylfuran	1	0.013	0.054
1,2,3-propanetriol 1,3-dinitrate	50	0.002	0.055
PCB	1000	0.008	0.623
6-(2-furanyl)-6-methyl-2-heptanone	1	0.019	0.420
furfural acetophenone	1	0.025	1.737

5.4.2.5 Summary of Site 5

The location of the ML at Site 5, south of the Waste Treatment Plant in the 200 East area of the Hanford Site, is displayed in Figure 5-24. Summary statistics including compound average concentrations as well as maximum concentrations observed over the fall background study period are shown in Table 5-13.

Figure 5-24. Mobile Laboratory Site 5 for the Duration of the Monitoring Period.

Table 5-13. Summary of Site 5 Proton Transfer Reaction – Mass Spectrometer Observations of Chemical of Potential Concern. (2 Sheets)

COPC Names	OEL (ppbv)	Average (ppbv)	Max (ppbv)
ammonia	25000	8.590	23.023
formaldehyde	300	0.379	5.094
methanol	200000	2.688	99.662
acetonitrile	20000	0.034	0.910
acetaldehyde	25000	0.632	7.210
ethylamine	5000	0.045	0.188
1,3-butadiene	1000	0.033	1.685
propanenitrile	6000	0.038	0.727
2-propenal	100	0.071	1.153
1-butanol + butenes	20000	0.061	4.249
methyl isocyanate	20	0.027	0.135
methyl nitrite	100	0.071	0.924
furan	1	0.023	0.166
butanenitrile	8000	0.017	0.342
but-3-en-2-one + 2,3-dihydrofuran + 2,5-dihydrofuran	200, 1, 1	0.022	0.309
butanal	25000	0.061	0.987
NDMA	0.3	0.008	0.060
benzene	500	0.146	8.768
2,4-pentadienenitrile + pyridine	300, 1000	0.040	0.610
2-methylene butanenitrile	300	0.025	0.126
2-methylfuran	1	0.023	0.182
pentanenitrile	6000	0.014	0.145
3-methyl-3-buten-2-one + 2-methyl-2-butenal	20, 30	0.020	0.172
NEMA	0.3	0.008	0.056
2,5-dimethylfuran	1	0.016	0.112
hexanenitrile	6000	0.012	0.092
2-hexanone (MBK)	5000	0.014	0.110
NDEA	0.1	0.006	0.042
butyl nitrite + 2-nitro-2-methylpropane	100, 300	0.037	0.251
2,4-dimethylpyridine	500	0.016	1.153
2-propylfuran + 2-ethyl-5-methylfuran	1	0.012	0.075
heptanenitrile	6000	0.011	0.062

Table 5-13. Summary of Site 5 Proton Transfer Reaction – Mass Spectrometer Observations of Chemical of Potential Concern. (2 Sheets)

COPC Names	OEL (ppbv)	Average (ppbv)	Max (ppbv)
4-methyl-2-hexanone	500	0.013	0.130
NMOR	0.6	0.004	0.361
butyl nitrate	2500	0.007	0.053
2-ethyl-2-hexenal + 4-(1-methylpropyl)-2,3-dihydrofuran + 3-(1,1-dimethylethyl)-2,3-dihydrofuran	100, 1, 1	0.012	0.053
6-methyl-2-heptanone	8000	0.012	0.053
2-pentylfuran	1	0.016	0.063
biphenyl	200	0.009	0.044
2-heptylfuran	1	0.046	0.181
1,4-butanediol dinitrate	50	0.016	0.086
2-octylfuran	1	0.002	0.043
1,2,3-propanetriol 1,3-dinitrate	50	0.001	0.039
PCB	1000	0.019	0.077
6-(2-furanyl)-6-methyl-2-heptanone	1	0.010	0.058
furfural acetophenone	1	0.047	0.198

5.4.2.6 Summary of Site 6

The location of the ML at Site 6, an urban location in Kennewick, WA at the corner of Clearwater avenue and U.S. Highway 395, is displayed in Figure 5-25. Summary statistics including compound average concentrations as well as maximum concentrations observed over the fall background study period are shown in Table 5-14.

Source: Esri, DigitalGlobe, GeoEye, Earthstar Geographics, CNES/Airbus DS, USDA, USGS, AeroGRID, IGN, and the GIS User Community

Figure 5-25. Mobile Laboratory Site 6 for the Duration of the Monitoring Period.

Table 5-14. Summary of Site 6 Proton Transfer Reaction – Mass Spectrometer Observations for Chemicals of Potential Concern. (2 Sheets)

COPC Names	OEL (ppbv)	Average (ppbv)	Max (ppbv)
ammonia	25000	10.282	21.413
formaldehyde	300	0.391	2.140
methanol	200000	3.088	40.808
acetonitrile	20000	0.044	1.695
acetaldehyde	25000	0.872	9.558
ethylamine	5000	0.055	0.161
1,3-butadiene	1000	0.038	2.135
propanenitrile	6000	0.053	1.664
2-propenal	100	0.113	2.667
1-butanol + butenes	20000	0.117	10.002
methyl isocyanate	20	0.032	0.235
methyl nitrite	100	0.091	1.099
furan	1	0.046	0.263
butanenitrile	8000	0.022	0.686
but-3-en-2-one + 2,3-dihydrofuran + 2,5-dihydrofuran	200, 1, 1	0.027	0.472
butanal	25000	0.068	0.288
NDMA	0.3	0.006	0.056
benzene	500	0.311	10.614
2,4-pentadienenitrile + pyridine	300, 1000	0.051	0.715
2-methylene butanenitrile	300	0.028	0.104
2-methylfuran	1	0.043	0.246
pentanenitrile	6000	0.015	0.213
3-methyl-3-buten-2-one + 2-methyl-2-butenal	20, 30	0.028	0.267
NEMA	0.3	0.007	0.076
2,5-dimethylfuran	1	0.025	0.145
hexanenitrile	6000	0.013	0.087
2-hexanone (MBK)	5000	0.014	0.056
NDEA	0.1	0.006	0.041
butyl nitrite + 2-nitro-2-methylpropane	100, 300	0.040	0.129
2,4-dimethylpyridine	500	0.028	1.962
2-propylfuran + 2-ethyl-5-methylfuran	1	0.018	0.092
heptanenitrile	6000	0.011	0.054

Table 5-14. Summary of Site 6 Proton Transfer Reaction – Mass Spectrometer Observations for Chemicals of Potential Concern. (2 Sheets)

COPC Names	OEL (ppbv)	Average (ppbv)	Max (ppbv)
4-methyl-2-hexanone	500	0.013	0.057
NMOR	0.6	0.006	0.274
butyl nitrate	2500	0.009	0.125
2-ethyl-2-hexenal + 4-(1-methylpropyl)-2,3-dihydrofuran + 3-(1,1-dimethylethyl)-2,3-dihydrofuran	100, 1, 1	0.013	0.057
6-methyl-2-heptanone	8000	0.011	0.045
2-pentylfuran	1	0.017	0.053
biphenyl	200	0.010	0.043
2-heptylfuran	1	0.046	0.153
1,4-butanediol dinitrate	50	0.016	0.066
2-octylfuran	1	0.002	0.043
1,2,3-propanetriol 1,3-dinitrate	50	0.001	0.040
PCB	1000	0.018	0.067
6-(2-furanyl)-6-methyl-2-heptanone	1	0.010	0.045
furfural acetophenone	1	0.046	0.150

5.4.3 Detailed Analysis of Test Data

The data collected during the Winter FY18 background study were used to draw comparisons between the following:

- Fall FY18 Background Study Data and co-collected confirmatory samples on alternative media;
- Data collected at differing sites; and
- Fall FY18 Background Study Data, Spring FY18 Background Study Data and FY17 Background Study Data.

5.4.3.1 Site Comparisons

In order to obtain an estimate of the true background concentration of COPCs at each study site, each data set was visually scanned for the longest continuous period of time with few or no signal spikes above the noise. An average was taken for this time period, which varied depending on monitoring location and other environmental factors, for each day of the background study. These averages were then sorted by study site (four data points per site) and averaged again to produce a single average and standard deviation value for each study site, per COPC.

The purpose of using this method was to attempt to disregard all short-duration local sources that could skew the estimate of the background concentration. This ensures that the comparison between site averages is truly a meaningful like-for-like comparison of bulk background concentrations that is not heavily biased towards local emissions, which, in many cases, are likely to be vehicle exhaust.

For many compounds, background concentrations across sites are very comparable. In general, the site that seemed to be the most statistically different from the others was Site 6. This is further supported by the generally much larger standard deviations produced by averaging study days at Site 6. The result was that Site 6 is also observed to be the study site with the highest variability. It is hypothesized that this is due to the much larger and unpredictable array of influences acting on a more urban site such as Site 6. Site 1 also experienced a considerable amount of variability in measurements taken, while it appeared that Site 4 measurements experienced the least amount of variability.

From the perspective of individual chemicals, ammonia marginally saw the greatest average background at Site 5, but had much greater variability at Site 6. Furan experienced both the highest background average and the highest variability at Site 6. NDMA had high variability across all sites, where in all cases the relative standard deviation (RSD) exceeded 33% of the average background concentration. The background average for 2-methylfuran was highest at Site 6, but a very nearly identical average was obtained for Site 1 as well. Highest background concentrations of NEMA were observed at Site 1, but all NEMA averages have relatively high variability, implying inconsistent background temporally. 2,5-dimethylfuran was observed to be the highest at Site 1. For NDEA background concentrations for Sites 1-4 were relatively consistent, with Sites 5 and 6 being slightly lower. However, NDEA saw the greatest variability at Site 3 by a fair margin, with an RSD of 54.7%. The NMOR background average observations were relatively consistently low, with the lowest background average obtained at Site 5. 2-pentylfuran, 2-heptylfuran, 6-(2-furanyl)-6-methyl-2-heptanone, and furfural acetophenone background averages all were observed to follow similar trends, with higher averages obtained at Sites 1 through 4, and lowest averages observed at Sites 5 and 6. For 2-heptylfuran, 6-(2-furanyl)-6-methyl-2-heptanone, and furfural acetophenone specifically, variability at Site 3 was the highest.

Table 5-15 below highlights the average background concentration and relative standard deviations for those periods for the 16 COPC signals, by site. The bar plots for the remaining COPCs detected by PTR-MS are located in Appendix B.

Table 5-15. Background Averages and Relative Standard Deviations by Study Site for Background Study Chemicals of Potential Concern.

Analyte	Site 1		Site 2		Site 3		Site 4		Site 5		Site 6	
	Avg. (ppbv)	RSD (%)	Avg. (ppbv)	RSD (%)	Avg. (ppbv)	RSD (%)	Avg. (ppbv)	RSD (%)	Avg. (ppbv)	RSD (%)	Avg. (ppbv)	RSD (%)
ammonia	5.929	55.3	3.707	36.0	4.455	34.6	5.293	14.2	6.558	21.1	6.534	54.3
furan	0.022	19.1	0.019	9.3	0.021	18.5	0.019	19.3	0.017	12.0	0.027	39.1
but-3-en-2-one + 2,3-dihydrofuran + 2,5-dihydrofuran	0.015	25.9	0.012	17.6	0.013	26.4	0.014	35.0	0.012	33.5	0.015	30.7
NDMA	0.007	47.7	0.007	41.0	0.006	71.6	0.007	33.9	0.006	66.9	0.005	78.0
2-methylfuran	0.020	23.9	0.016	19.8	0.018	19.4	0.017	25.3	0.015	21.1	0.021	21.9
NEMA	0.008	38.4	0.007	36.4	0.007	63.2	0.008	31.6	0.006	51.8	0.006	45.2
2,5-dimethylfuran	0.015	19.2	0.011	17.8	0.013	25.9	0.012	24.1	0.012	30.0	0.013	18.8
NDEA	0.007	24.9	0.007	29.6	0.007	54.7	0.007	23.9	0.005	40.0	0.005	28.1
2-propylfuran + 2-ethyl-5-methylfuran	0.012	14.9	0.010	16.4	0.011	31.1	0.011	26.1	0.009	31.3	0.011	30.3
NMOR	0.003	5.3	0.003	11.0	0.003	14.5	0.003	18.1	0.002	7.6	0.003	15.4
2-ethyl-2-hexenal + 4-(1-methylpropyl)-2,3-dihydrofuran + 3-(1,1-dimethylethyl)-2,3-dihydrofuran	0.014	27.3	0.012	24.5	0.012	41.8	0.012	25.5	0.010	32.7	0.010	23.5
2-pentylfuran	0.021	41.5	0.015	37.9	0.015	43.6	0.016	34.7	0.012	39.6	0.012	37.7
2-heptylfuran	0.051	21.8	0.048	26.5	0.050	48.2	0.050	24.4	0.040	35.9	0.038	27.5
2-octylfuran	0.002	19.1	0.002	23.9	0.002	14.8	0.002	9.0	0.002	11.1	0.002	13.4
6-(2-furanyl)-6-methyl-2-heptanone	0.011	21.4	0.010	27.5	0.011	49.3	0.011	23.0	0.008	35.3	0.008	26.1
furfural acetophenone	0.053	21.8	0.051	27.1	0.052	49.7	0.052	24.0	0.041	33.9	0.039	26.8

5.4.4 Background Study Statistical Analysis and Conclusions

To assess differences between sampling locations an analysis of variance, ANOVA (a statistical method in which the variation in a set of observations is divided into distinct components), is typically performed. However, for an ANOVA test to be valid, the variances in each population must be similar. Figure 5-26 plots the hourly averages and medians for furan measured at each of the six study sites. As can be clearly seen in this figure, the data variance (or spread) is quite different at each site. As expected, the Bartlett test indicated a significant difference in these variances. As a result, a regular ANOVA test will be suspect.

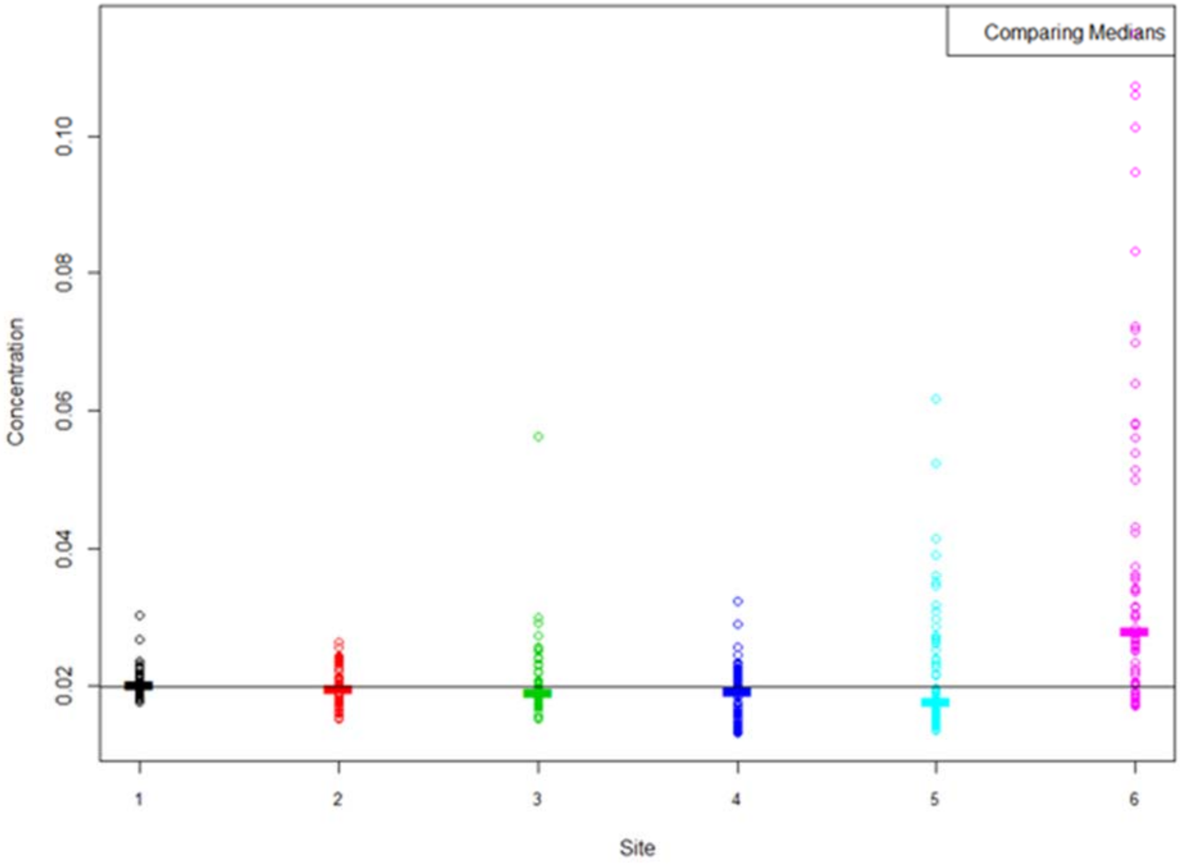

Figure 5-26. Dissimilar Variances in Hourly Average Furan Concentrations (ppbv) by Sites.

Since the variances are statistically different, a Kruskal-Wallis test is a more reliable way to determine whether a significant difference exists between background concentrations at the different test sites. A pairwise Dunn's test was also performed to assess statistical differences between pairs of sites for each chemical compound. The results of the Kruskal Wallis and Dunn's pairwise comparison tests are presented in this section for the combined furans.

Combined furans were selected for statistical analysis instead of individual furans to streamline reporting and summarize the combined effects of furan exposure. Furans that are confidently measured by the PTR-MS were included in the combined furan analysis as follows:

- Furan;
- 2-methylfuran;
- 2,5-dimethylfuran;
- 2-propylfuran, and 2-ethyl-5-methylfuran (isobaric, measured as one ion signal);
- 2-pentylfuran;
- 2-heptylfuran;
- 2-octylfuran;
- 6-(2-furanyl)-6methyl-2-heptanone; and
- 4-(1-methylpropyl)-2,3-dihydrofuran and 3-(1,1-dimethylethyl)-2,3-dihydrofuran (isobaric, measured as one ion signal, also inseparable from 2-ethyl-2-hexenal).

For consistency with prior background studies, 3-(2-furanyl)-1-phenyl-2-propen-1-one was not included in the combined furan analysis as it was not included in prior studies.

5.4.4.1 Site Comparison

The p-value is defined as the probability of obtaining a result equal to or “more extreme” than what was actually observed, when the null hypothesis is true. In this case, the null hypothesis is that “there is no difference between the vapor concentrations at each of the sites.” If a 95% confidence limit is established, the null Hypothesis must be rejected when the p-value is less than 0.05. The Kruskal-Wallis test produced a p-value of 2.78014227e-13, which clearly indicates that there are significant differences in concentrations between the different sites as shown below.

non-parametric tests

```
        Kruskal-Wallis rank sum test

data:  Combined Furans by Site
Kruskal-Wallis chi-squared = 67.91588772, df = 5, p-value =
0.000000000000278014227
```

By visual inspection, Figure 5-27 shows that the site with the highest average furan concentration is Site 6 (395 and Clearwater). The most notable observation from the data is that all sites had relatively low combined furan concentrations on average, compared to the OEL of 1 ppbv for furan. Each site’s median concentration across all hourly averages (thick colored bars) was less than 15% of the OEL, while the overall median (thin black line) was less than 10% of the OEL. Additionally, no single hourly average combined furan concentration (colored circles) exceeded 35% of the OEL.

.

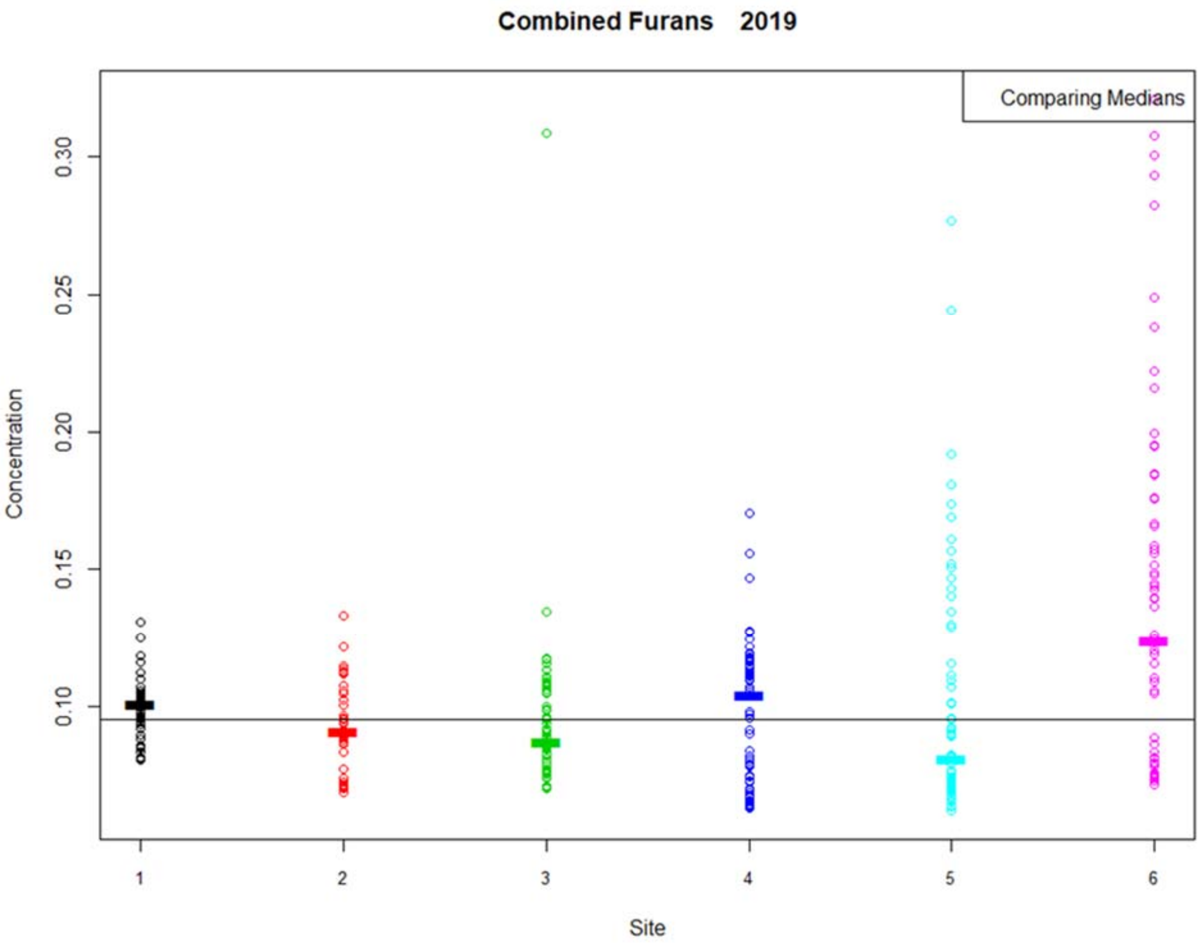

Figure 5-27. Median of Hourly Averages of Combined Furan Concentrations (ppbv) by Site.

The pairwise Dunn's Test results for the combined furan signals measured during the background study are shown in Table 5-16. This test was run for each pair of study sites to test the null hypothesis that there is no significant difference between them. For each intersection of study site columns and rows, a calculated p-value is shown. P-values highlighted in yellow denoted pairs of study sites where the null hypothesis was rejected; i.e., with 95% confidence there is a significant difference between the sites (p-values < 0.05). The significance of site comparisons become more apparent when addressing the Dunn's pairwise comparison result, as follows:

- Site 5 is not statistically different from any site except Site 1,
- Site 6 is statistically different from every site except Site 1, and
- No other comparisons yield significant differences between sites.

It should be noted that although these values may be statistically interesting in postulating the source of the ultra-trace furans, they are not significant from an Industrial Hygiene or Operations perspective.

Table 5-16. Dunn's Pairwise Comparison of the Combined Furans by Site (Holm-Šidák).

	Site 1	Site 2	Site 3	Site 4	Site 5	Site 6
Site 1 (Remote and upwind)						
Site 2 (SY Farm)	0.2521					
Site 3 (4th & Buffalo)	0.1103	0.6078				
Site 4 (AN Farm)	0.2714	0.3806	0.5635			
Site 5 (WTP)	0.0148*	0.5750	0.6445	0.3397		
Site 6 (395 & Clearwater)	0.2274	0.0006*	0.0000*	0.0003*	0.0000*	

P-values highlighted in yellow denote pairs of study sites where the null hypothesis was rejected; i.e., with 95% confidence there is a significant difference between the sites (p-values <0.05).

Site statistical comparisons for nitrosamines are not provided in this report due to unknown contributions from interfering chemicals. Past background studies with the PTR-MS TOF 4000 indicated significant contributions from interfering compounds particularly during smoke days. The PTR-MS TOF 6000 used in this background study may have reduced the contribution from interfering compounds; however, to what extent is unknown.

5.4.4.2 Ammonia as an Indicator of Tank Vapors

Trace quantities of ammonia are a potential indicator of tank vapors in the surrounding atmosphere. Ammonia is a major constituent of the headspace vapors in all Hanford waste storage tanks. A positive correlation of a Hanford Tank Farm COPC profile to an ammonia profile may provide a link to a waste tank emission. Additionally, elevated ammonia levels around the tank farms may be an indication of tank vapor emissions. Figure 5-28 provides a summary of hourly average ammonia concentrations by site, with the median value for each site's hourly averages shown as thick colored bars, and the overall median shown as a thin black line. First, it should be noted that the ammonia concentrations for all sites are extremely low (three orders of magnitude below its OEL of 25 ppm and well below the level of 1 ppm cited as a leading indicator action level in PNNL-27449). Ammonia concentrations for four sites [Site 1 (remote and upwind), Site 2 (SY Farm), Site 3 (4th and Buffalo) and Site 4 (AN Farm)] were consistent with global atmospheric averages (0.3 – 6 ppbv, https://www.atsdr.cdc.gov/toxprofiles/tp126-c2.pdf). The two other sites [Site 5 (WTP) and Site 6 (395 and Clearwater)] had ammonia concentrations higher than the global atmospheric average. Although these values may be statistically interesting in postulating the source of the ammonia, they are not significant from an Industrial Hygiene or Operations perspective.

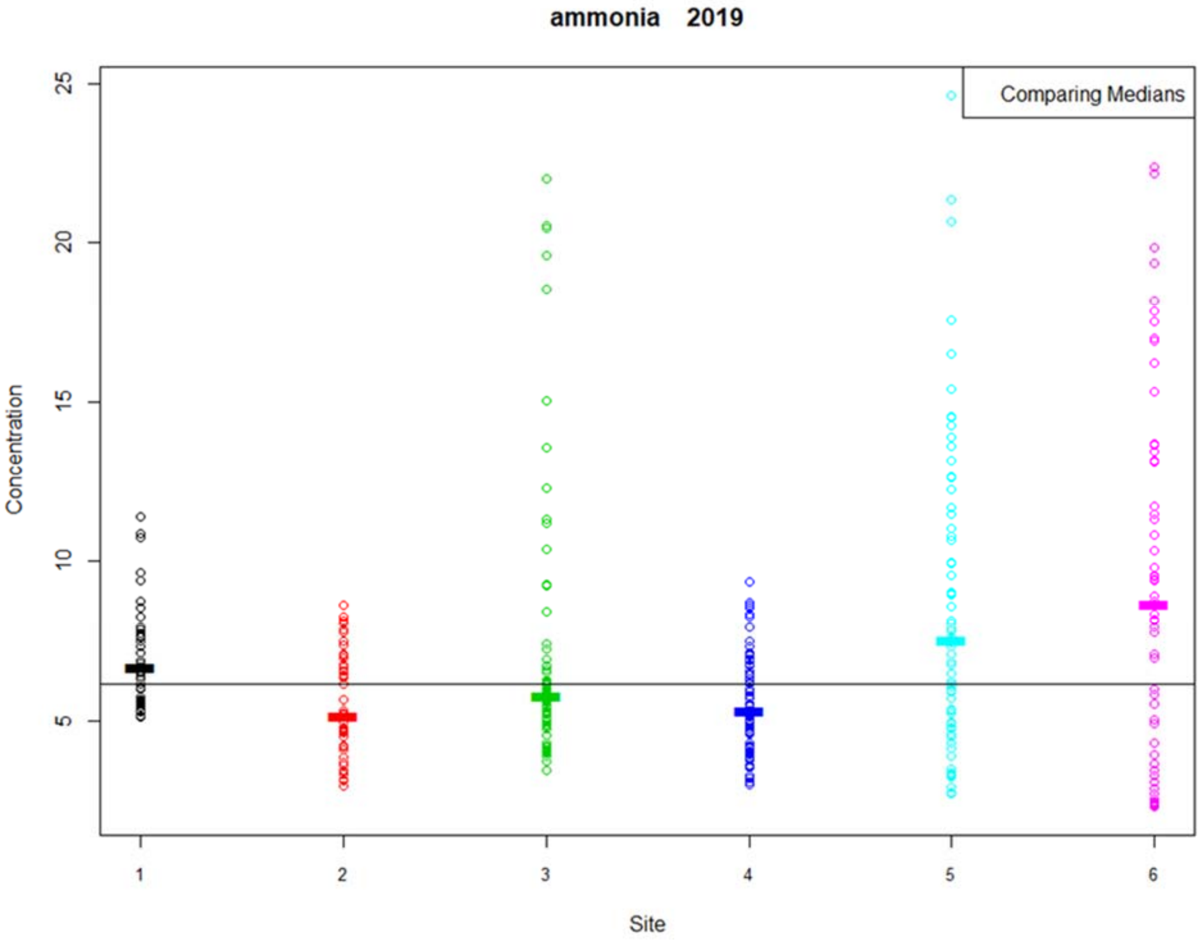

Figure 5-28. Hourly Average Ammonia Concentrations (ppbv) by Site.

Table 5-17 indicates that while Site 1 is statistically similar to Sites 3, 5, and 6, it is different from Sites 2 and 4. This is corroborated by the pairwise tests showing that Sites 1, 5 and 6 are also statistically different from Sites 2 and 4. Observing the hourly datasets in the plot above, it is visually apparent that Sites 2 and 4 have very similar medians well below the overall median, and overall tighter spreads in variance. This result aligns with the notion that there are not many local sources positively biasing the global ammonia background at either S Farms or AN Farm. Site 3 should have been statistically similar to Sites 5 and 6 as well; however, one can observe from the pairwise comparison between 3 and 5 that the statistical result were quite close to the threshold for significance at 0.0554. Additionally, from further inferences made from the plot above, Site 3 has an unaccountably higher spread in hourly averages (more in line with Sites 5 and 6), possibly brought about by the higher variance in vehicle traffic or work activities likely to take place around 4th and Buffalo on any given work shift, while still having a median below the overall median. In fact, all pairwise tests comparing Site 3 to the other study sites concluded that there is nothing pointing to Site 3 being statistically different from any of the other study sites. This is despite differences found in other pairwise tests which might indicate a difference indirectly. Since Site 3 is statistically similar to Site 1, but Site 1 is shown to be statistically different from Site 2, it might follow that, by the transitive property, that Site 3 should be different from Site 2. This is not the case with pairwise statistical tests. The overall low ammonia concentrations for all tank farm sites (near global average) support a conclusion that the observed furan concentrations around the tank farms are not due to the tank waste, but rather to vehicle traffic, diesel generators and other fugitive emissions. Further, the furan and ammonia levels at the tank farm and remote downwind monitoring locations indicate that current vapor control strategies are working (i.e., vapor control zones, stacks and stack extensions).

Table 5-17. Dunn's Pairwise Comparison of Ammonia by Site (Holm-Šidák).

	Site 1	Site 2	Site 3	Site 4	Site 5	Site 6
Site 1 (Remote and Upwind)						
Site 2 (SY Farm)	0.0026*					
Site 3 (4th & Buffalo)	0.1979	0.1341				
Site 4 (AN Farm)	0.0015*	0.6604	0.1356			
Site 5 (WTP)	0.6778	0.0001*	0.0554	0.0000*		
Site 6 (395 & Clearwater)	0.4934	0.0010*	0.1655	0.0003*	0.7434	

P-values highlighted in yellow denote pairs of study sites where the null hypothesis was rejected; i.e., with 95% confidence there is a significant difference between the sites (p-values <0.05).

5.4.4.3 Diurnal Variations

Figure 5-29 is a plot of the combined furan signal broken into one-hour averages for the entire background study. The dots represent each average taken at a given hour, from different days of the study. The thick colored bars represent the median of each of those sets of averages. The black line represents the overall median for combined furans throughout the entire data set. This plot shows very little diurnal variation in the combined furan concentrations; with minor increases in the morning and evening hours. The median hourly averages were well below 10% of the OEL. From an operational perspective, there is no significant increase in vapor hazard between day versus night given the trace concentrations.

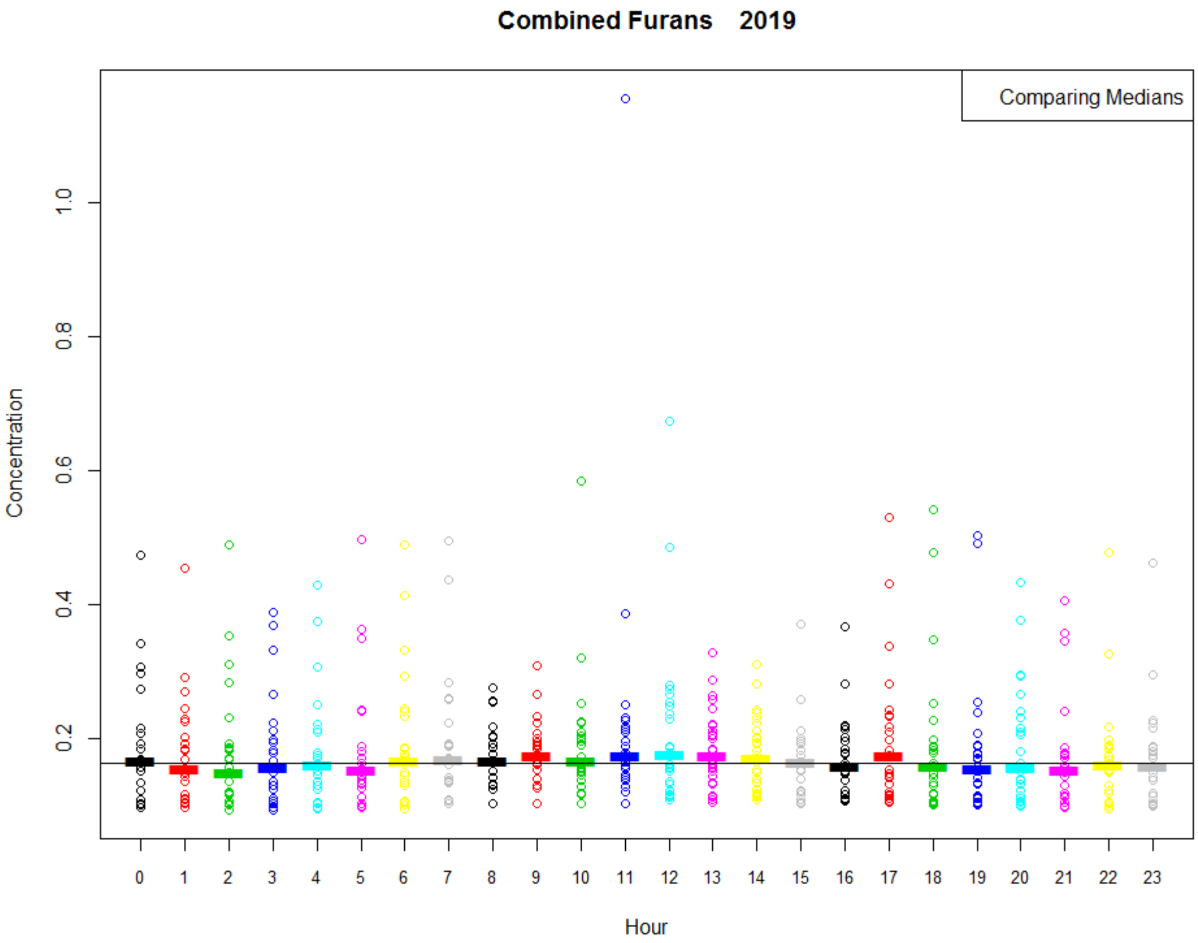

Figure 5-29. Diurnal Effects for Combined Furans (ppbv).

Figure 5-30 is a plot of the carbon dioxide signal broken into one-hour averages for the entire background study. The dots represent each average taken at a given hour, from different days of the study; the thick colored bars represent the median of each of those sets of averages. The black line represents the overall median for carbon dioxide throughout the entire data set. This plot shows the hourly median for CO_2 concentration peak around 08:00, decrease through the afternoon to a trough around 15:00, then rise throughout the night to peak again at a lower median concentration around 21:00. The cause of the variation is not known but may be partially due to the accumulation of CO_2 in the morning hours until the boundary layer breaks up.

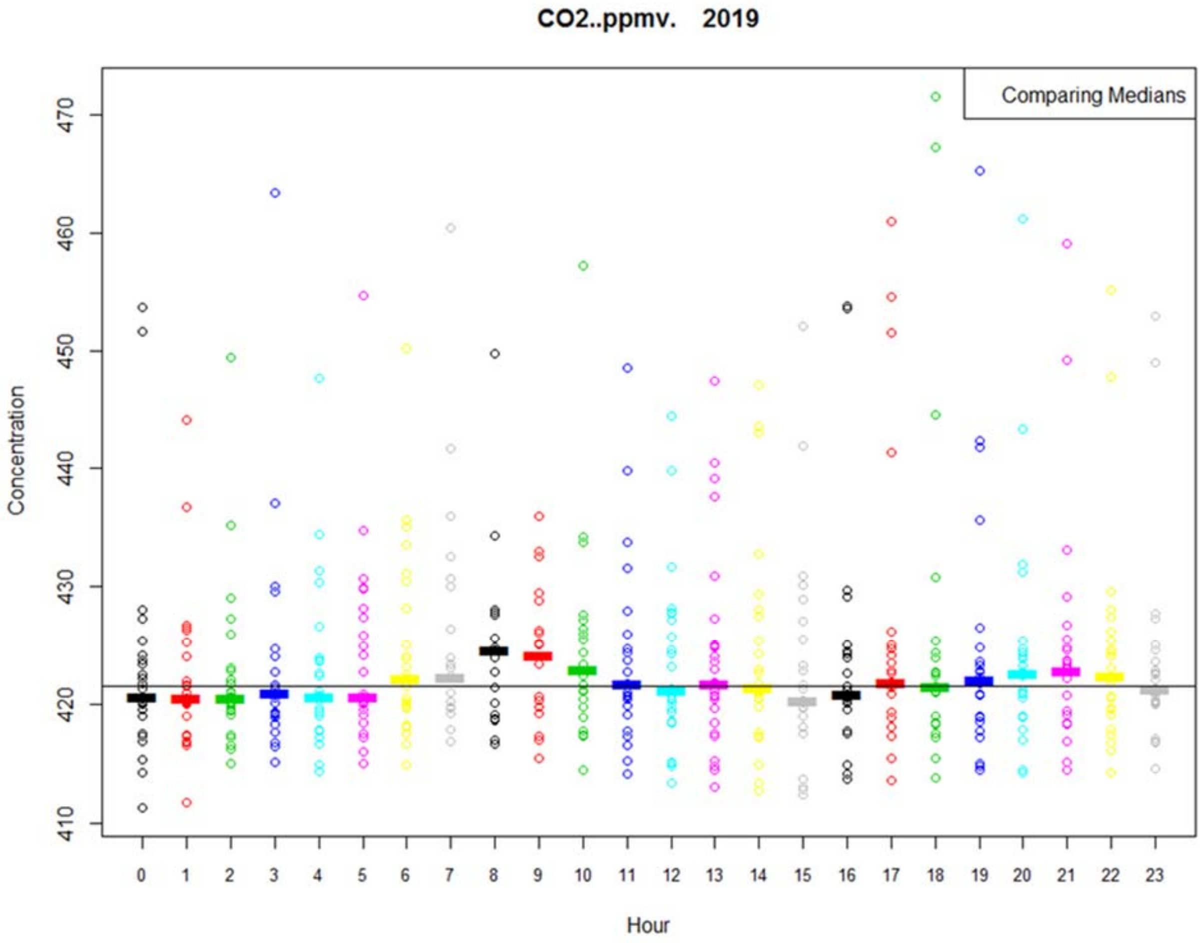

Figure 5-30. Diurnal Effects for CO_2 (ppmv).

Figure 5-31 is a plot of the ammonia signal broken into one-hour averages for the entire background study. The dots represent each average taken at a given hour. The thick colored bars represent the median of each of those sets of averages. The black line represents the overall median for ammonia throughout the entire data set. This plot shows an increase in ammonia at 08:00, decaying to a baseline level over the next ten hours.

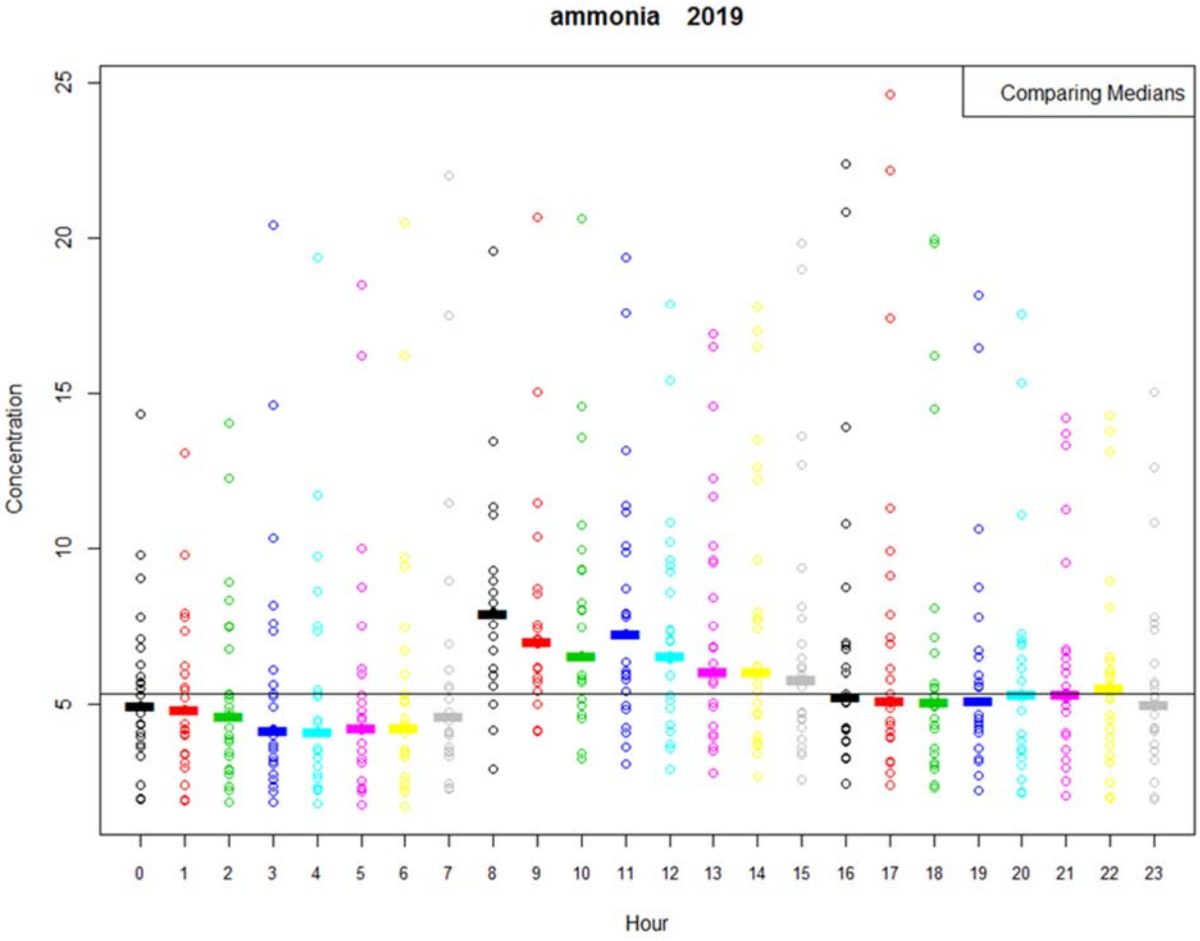

Figure 5-31. Diurnal Variation for Ammonia (ppbv).

5.4.4.4 Combustion Markers

Several PTR-MS analytes are generated as a result of combustion and can be used to help identify the source of other trace analytes (e.g., furans) also generated during combustion. Ethylamine is a good indicator of diesel combustion. While benzene and toluene are good indicators of gasoline combustion., carbon dioxide is a good indicator for all combustion sources.

Figure 5-32 provides a summary of hourly average CO_2 concentrations by site, with the median value for each site shown as a solid colored line. The dots represent each average taken at a given hour. The thick colored bars represent the median of each of those sets of averages. The black line represents the overall median for CO_2 throughout the entire data set. This plot shows one site with above average concentrations of CO_2, i.e., Site 6 (395 and Clearwater). This is consistent with the amount of traffic moving through the corner of 395 and Clearwater. The medians for Sites 1, 2, 3, 4, and 5 are all at or below the overall median level.

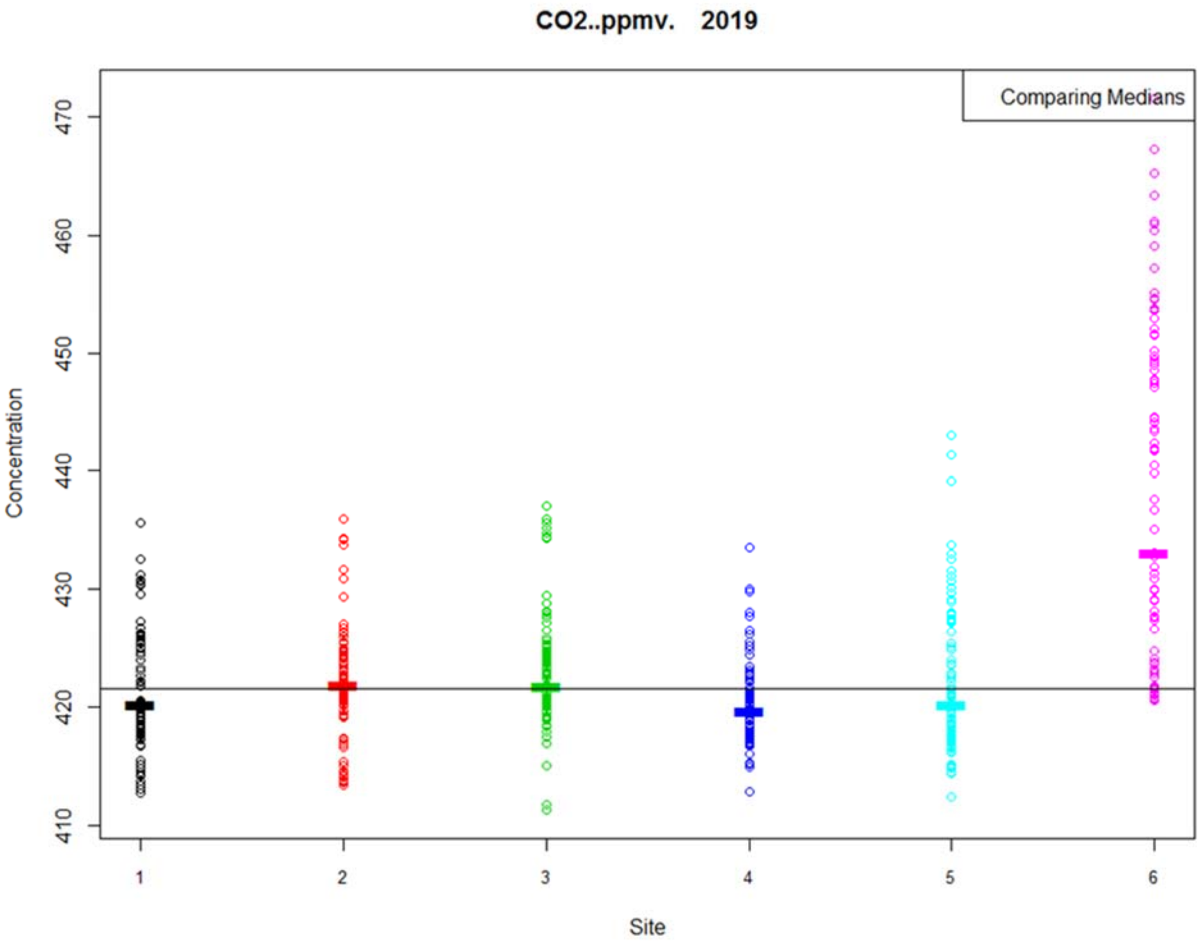

Figure 5-32. CO_2 Concentrations (ppmv) at Each Sampling Site.

6.0 NO^+ MODE ANALYSIS AND FEASIBILITY

During the background study, automated switching between H_3O^+ and NO^+ modes was performed. The purpose was to test the feasibility of operating in NO^+ mode and assess the resulting data quality. This work expands on the analysis and results presented in 53005-81-RPT-039 detail a selection of analytes that will be explored. NO^+ mode was initiated remotely at the SME's discretion, which typically occurred in the evening after the confirmatory sample sorbents were finished collecting. The confirmatory sample results are compared to the PTR-MS H_3O^+ data collected during that time. Switching between H_3O^+ and NO^+ while the confirmatory samples are collected would alter the PTR-MS results, greatly affecting the comparison. Due to the uniqueness of the ML, NO^+ mode was a newly developed sampling method and skill-of-craft process, and the SME was the only qualified ML operator; therefore, the NO^+ mode was not initiated at a consistent time in the evening. Since this was the first attempt at collecting NO^+ mode data in this manner, this responsibility was designated solely to the SME due to lack of procedure and training for the ML Operators. In addition, NO^+ mode was not initiated for a few of the days at the discretion of the SME for diagnostic reasons related to instrument performance issues.

The NO^+ results will be compared to the H_3O^+ data as a metric for assessing the quality of the NO^+ data. Before presenting the NO^+ results, it is important to explain how the H_3O^+ data was handled. Current H_3O^+ data processing procedures do not include instrument baseline subtraction. For this report, the instrument baseline is defined as the signal present at a given mass when no analytes are present. This instrument baseline is best represented when the instrument is sampling ultra-zero air during the zero/sensitivity checks. If the instrument baseline is above zero, it is important to quantify and subtract this signal from the collected data so the response in the absence does not show a signal above zero at a statistically significant level. If a high instrument baseline is present, it can lead to overestimation of an analyte if not corrected. Figure 6-1 shows a time-series of toluene collected in H_3O^+ mode during the background study with the red circles representing the average signal of toluene while sampling ultra-zero air. In the absence of toluene, there is a signal roughly between 0.01 and 0.04 ppbv, which is captured as the instrument baseline for toluene. If not accounted for this baseline signal will result in an overestimation of toluene of that magnitude, but it is at such a small level that it will be negligible under typical observations of toluene. However, during this background study, the toluene observations were at low enough concentrations that correcting for the small instrument baseline can become important in determining accurate concentrations.

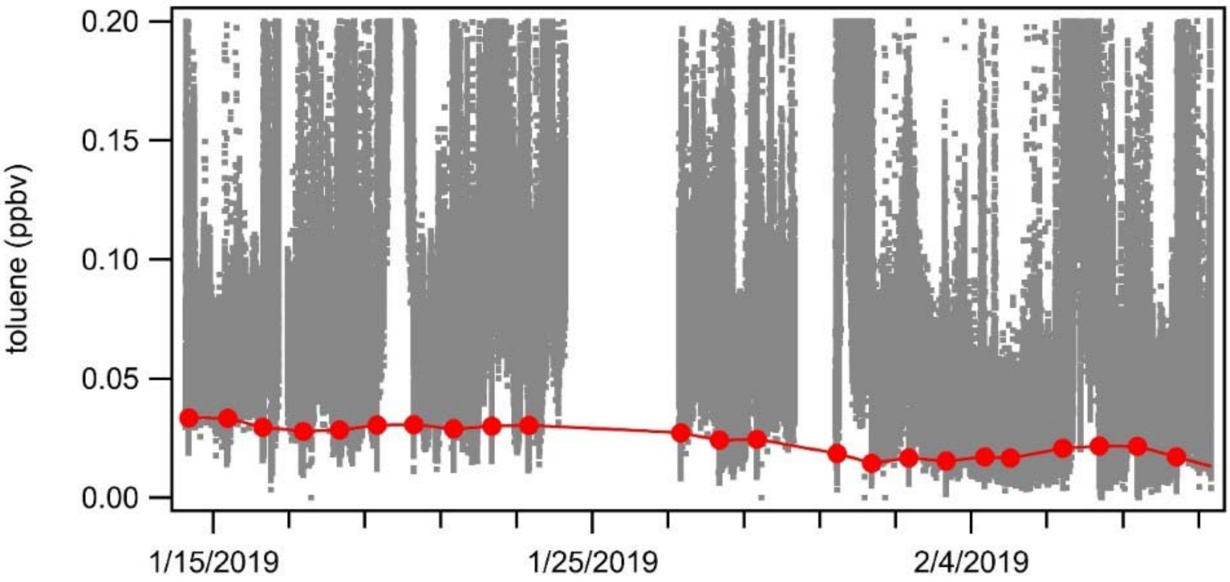

Figure 6-1. Toluene During the Winter Background Study with Red Circles Representing the Average Signal of Toluene While Sampling Ultra-zero Air.

To correct for the instrument baseline, an estimation of the baseline at any discrete point in time was derived from interpolations between the average zeros. This is represented by the red line in Figure 6-1, which is the estimated instrument baseline at each individual point for the entire dataset. The correction is implemented by subtracting the H_3O^+ data given by the interpolated instrument baseline estimation from the total toluene signal. Figure 6-2 shows toluene data before (top) and after (bottom) correcting for the instrument baseline along with the average baseline signal (red circle). The PTR-MS sampled ultra-zero air between approximately 07:51 and 08:01. After the baseline correction, the signal during this time hovers around zero, which means the instrument baseline was quantified and corrected for accurately.

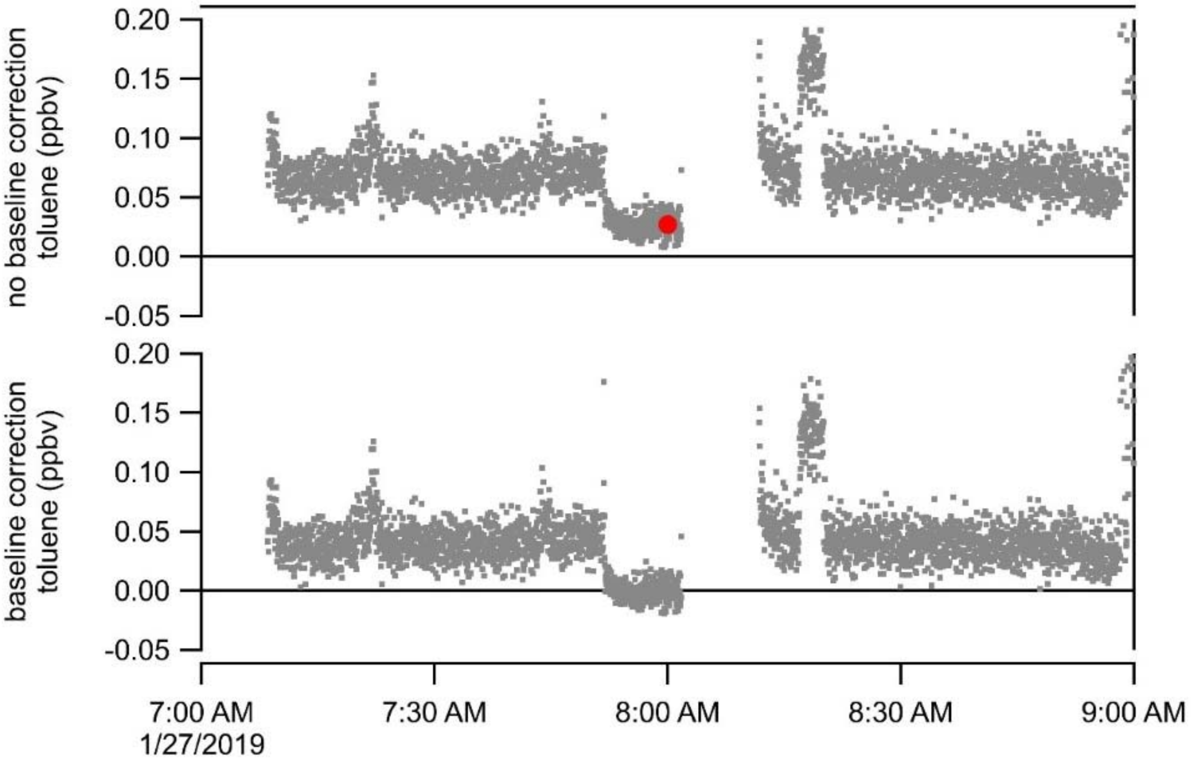

Figure 6-2. Toluene Observed in H_3O^+ Mode Before and After Instrument Baseline Correction is Applied Accompanied by the Estimation of Instrument Baseline (Red).

This level of baseline correction requires additional processing time and effort, so it is not necessary for all data sets. However, it is important when comparing to NO^+ mode data. As explained in 53005-81-RPT-039, instrument baseline correction is a required part of the NO^+ data processing routine, so it is important that the H_3O^+ data are processed in a similar manner to ensure they are comparable. The H_3O^+ data instrument baselines for analytes of interest presented in this section were evaluated and instances where the effect is not negligible the data were corrected as explained above.

The NO^+ Research & Development was processed using the same steps outlined in 53005-81-RPT-039. There were additional steps required to process the NO^+ data, but the main differences pertain to the values of the instrument baseline and the correction factors. Accurately determining them required additional steps due to limited availability of zeros and calibrations performed in NO^+ mode within the study period. Due to the nature of the study's objective of monitoring 24 hours a day, the addition of NO^+ zeros and calibration would have resulted in additional loss of data and created additional risk due to not having procedures developed and tested to handle this additional work. This was the first attempt at collecting NO^+ data of this magnitude and time resolution and will act as the primary information to generate robust procedures to handle NO^+ sampling in this manner. Due to the complexity of the process and instrumentation it is difficult to generate a procedure that would allow the Operators to confidently perform these additional zeros and calibrations without increased risk of affecting the data quality of H_3O^+ data or loss of additional data.

The NO^+ data processing uses the same steps as the H_3O^+ data processing with some parameter changes. The general process is to load and merge the files, apply a mass calibration, integrate the peaks, correct for the transmission efficiency, apply the isotopic multiplier to the reagent ion signal, and finally normalize the data to the reagent ion signal. The NO^+ data processing requires different settings for mass calibration, peak integration, and isotopic multiplication and normalization. This means there is a duplication of efforts as the NO^+ processing requires those steps to be repeated. Once these steps are completed, the output file is loaded into Igor Pro for additional processing steps. Figure 6-3 shows the toluene concentrations from the NO^+ output files for the entire duration of the study. NO^+ mode was performed five minutes out of every hour once initiated, which typically occurred after the sorbents were collected for the day. Running NO^+ mode during sorbent collection would skew the results since there would be periods of missing H_3O^+ data needed for the comparison. For the entire study, NO^+ mode was performed 328 times.

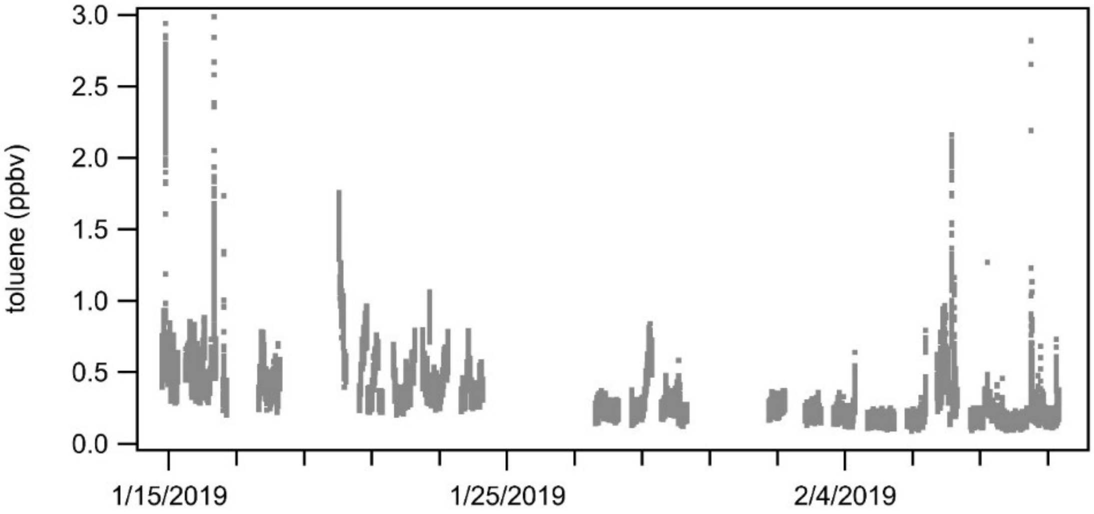

Figure 6-3. Time-series of Toluene Concentrations Monitored in NO^+ Mode Before Additional Data Processing has been Performed.

As stated previously, zeros were not performed during NO^+ mode during the study due to the complexity, time constraints, and the lack of a tested and approved procedure. Two NO^+ zeros and calibrations were performed on January 25, 2019, and February 10, 2019. These zeros will be used to quantify the instrument baseline. There is NO^+ zero prior to January 25, 2019, that would allow accurate quantification of instrument baseline in NO^+ mode between January 14, 2019, through January 24, 2019. Therefore, the instrument baseline prior to January 25, 2019, will be assumed to be the same as the instrument baseline observed on January 25, 2019. Figure 6-4 shows the resulting instrument baseline for toluene in the upper panel. An instrument baseline for each discrete data point is calculated by interpolating between the NO^+ zeros. Subtracting the interpolated instrument baseline from the toluene signal results in the baseline corrected toluene in the bottom panel in Figure 6-4. The zeros for the post-January 25, 2019, data captured the instrument baseline well, but the pre-January 25, 2019, instrument baseline seems to be higher than the January 25, 2019, baseline. There are methods to estimate the instrument baseline for the pre-January 25, 2019, data, but they are time consuming and determined to be beyond the scope of this study. The primary objective of collecting NO$^+$ data was to determine its feasibility and help shape the data processing procedure. Future implementation of the NO$^+$ mode operation will include more periodic zeros to better quantify the instrument baseline.

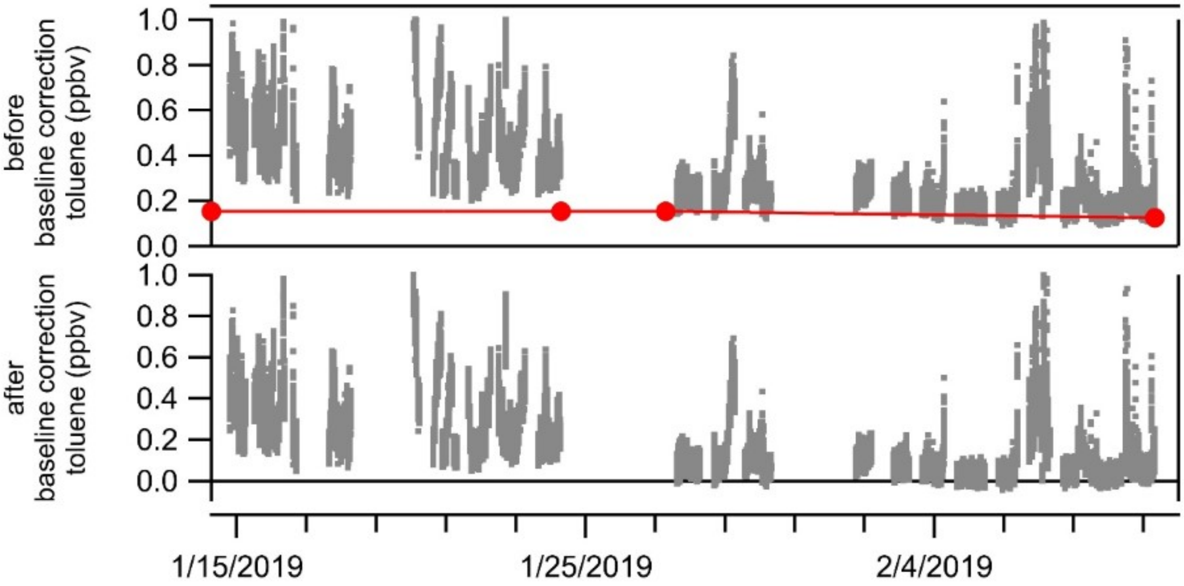

Figure 6-4. Toluene Observed in NO$^+$ Mode Before and After Instrument Baseline Correction is Applied Accompanied by the Estimation of Instrument Baseline (Red).

After the instrument baseline has been accounted for, a calibration factor to the data needs to be applied. 53005-81-RPT-039 describes how the calibration factors are determined in further detail. In summary, multi-point calibrations are used to estimate a calibration factor that estimates the effects of the transmission efficiency and reaction kinetics. This allows us to get accurate observations in NO$^+$ mode without having to understand the kinetics. Multi-point calibrations in NO$^+$ mode on January 25, 2019, and February 10, 2019, along with information from the Month 4 Report were used to determine the calibration factors for this study. Table 6-1 lists the resulting calibration factors for all species identified in the Month 4 report as species with potential for NO$^+$ mode monitoring. These calibration factors are different than those reported in 53005-81-RPT-039. During this analysis, the calibration factors were calculated using the concentration (ppbv) instead of the signal (Hz). The baseline corrected data are divided by the calibration factor to get the final concentration of the analyte.

Table 6-1. NO^+ Correction Factors for Analytes Detailed in 53005-81-RPT-039.

Analyte	m/z	Calibration
1,3-butadiene	54	2.459
dimethyl sulfide	62	0.132
furan	68a	0.836
isoprene	68b	0.106
NDMA	74	2.964
benzene	78	0.562
diethylketone	86	0.111
toluene	92	1.187
hexanone	100	0.056
C_2-benzenes	106	0.872
C_3-benzenes	120	0.829
C_4-benzenes	134	0.455
monoterpenes	136	0.040

Figure 6-5 shows the toluene concentrations processed from H_3O^+ mode (grey) and NO^+ mode (red) operations. Overall, the observations in the two modes produced similar results and both capture the same trends. The data after January 25, 2019, seem to compare better than the data prior to January 25, 2019. This is due to the instrument baseline not being captured as well as was previously described. In addition, there were instrument baseline issues detailed in Nonconformance Report (NCR-19-002). During this time, there were periods where the instrument baseline would increase and the associated NO^+ data are less accurate as a result. Given the lower quality of the NO^+ data due to these issues before January 25, 2019, the comparison between the H_3O^+ and NO^+ modes will be focused on the higher quality data collected after January 25, 2019.

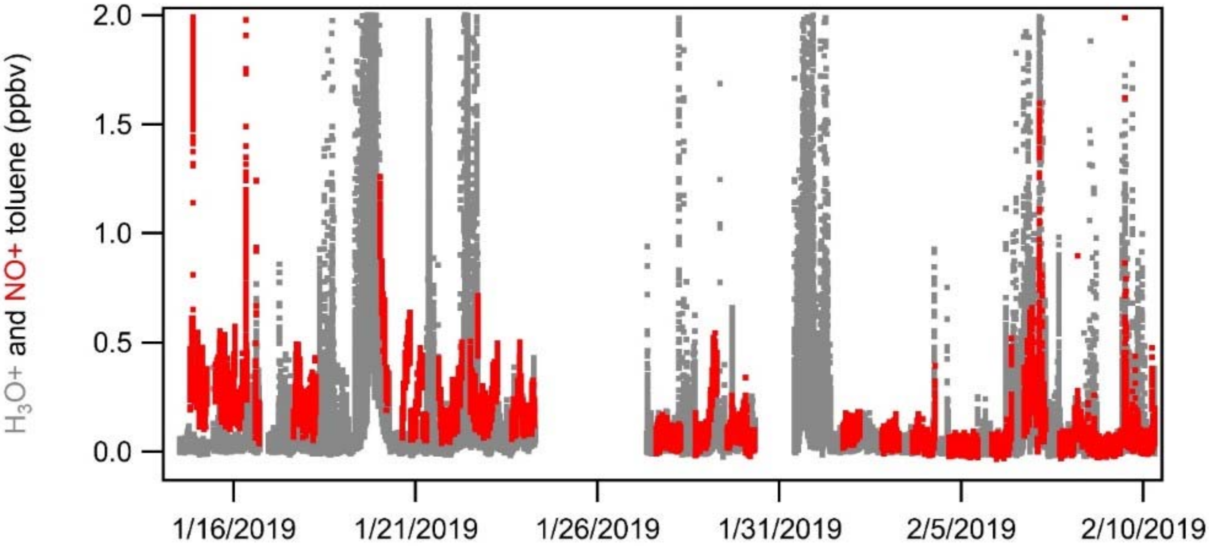

Figure 6-5. Toluene observed in H_3O^+ and NO^+ Modes During the Entire Background Study from January 14, 2019, through February 10, 2019.

Figure 6-6 shows the H_3O^+ (grey) and NO^+ (red) toluene data collected after January 25, 2019. The NO^+ data track well with the H_3O^+ data showing that both modes seem to measure toluene well. There is good agreement with both modes observing the same magnitudes in concentrations and the atmospheric background levels seem to be identical. The similarity of the atmospheric backgrounds support the conclusion that the estimation and correction of the instrument baseline in both modes is accurate. On February 6, 2019, the ML was deployed to Site 6, which is the urban site in Kennewick. Both modes saw variable levels of toluene at this site as expected due to the presence of typical sources of toluene in an urban environment. Figure 6-7 shows the toluene data for both modes while the ML was at Site 6. This shows good agreement between the two modes as the NO^+ data seem to be in sync with the H_3O^+ data as the short-lived urban plumes are observed.

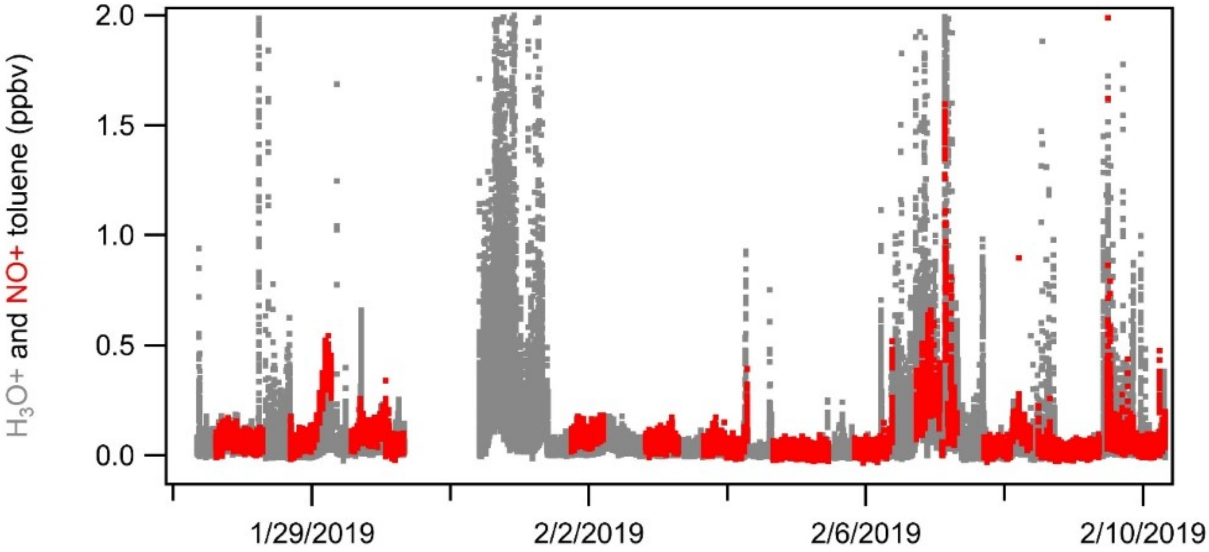

Figure 6-6. Toluene Observed in H_3O^+ and NO^+ Modes from January 27, 2019, through February 10, 2019.

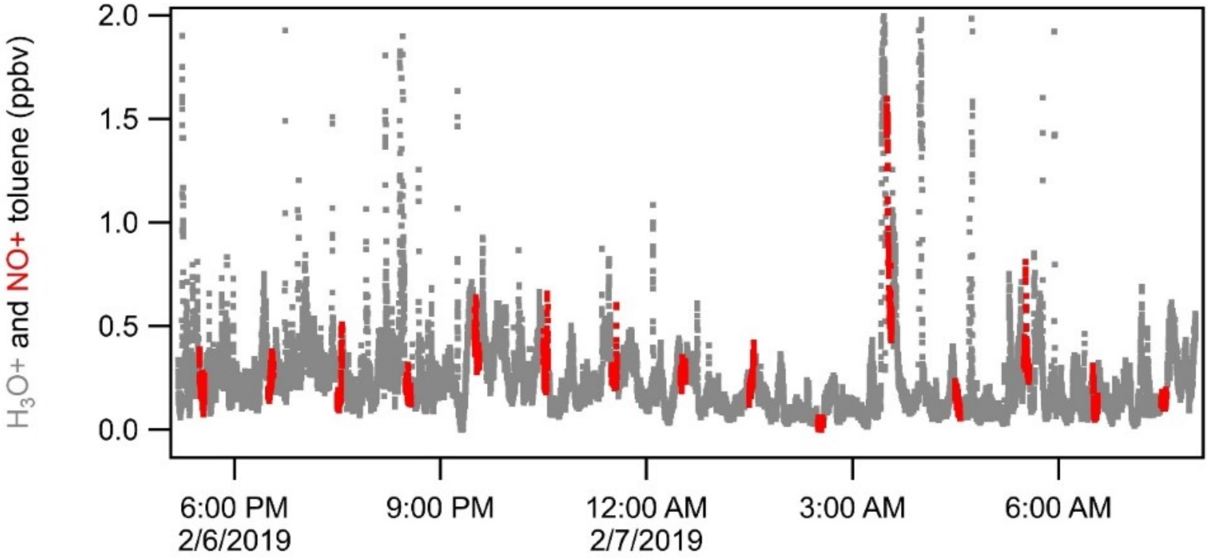

Figure 6-7. Toluene Observed in H_3O^+ and NO^+ Modes on January 6, 2019.

While the NO^+ mode observations appear to be comparable to that of H_3O^+ mode, it is also more selective than H_3O^+ mode. As 53005-81-RPT-039 shows, the NO^+ mode will be ineffective at monitoring some analytes that are easily observed in H_3O^+ mode. Therefore, it is important to quantify the advantages that NO^+ mode can offer to determine if they outweigh the disadvantage of smaller list of observable analytes. One important concept for comparison is the absolute relative sensitivity within each mode. Looking back at Figure 6-6, a relatively clean period was observed between February 1, 2019, and February 6, 2019. This relatively stable period provides a basis to compare the signal noise observed in each mode. When converted to ppbv, an analyte with a high sensitivity will have less noise than an analyte with a low sensitivity. To compare the noise of the two modes during this period, each section of NO^+ mode (~5 min) was averaged and a standard deviation was calculated. Then the H_3O^+ data before (~5 min) and after (~5 min) the NO^+ section was averaged and a standard deviation was calculated. Figure 6-8 shows the standard deviations of these averages during this period. Both modes have a very low standard deviation, but the NO^+ mode seems to be around 0.02 ppbv and approximately double the H_3O^+ standard deviation around 0.01 ppbv. This translates to the NO^+ mode having a detection limit twice as high as H_3O^+ mode. Even though both modes monitor toluene well, H_3O^+ mode remains the preferred method for toluene quantification.

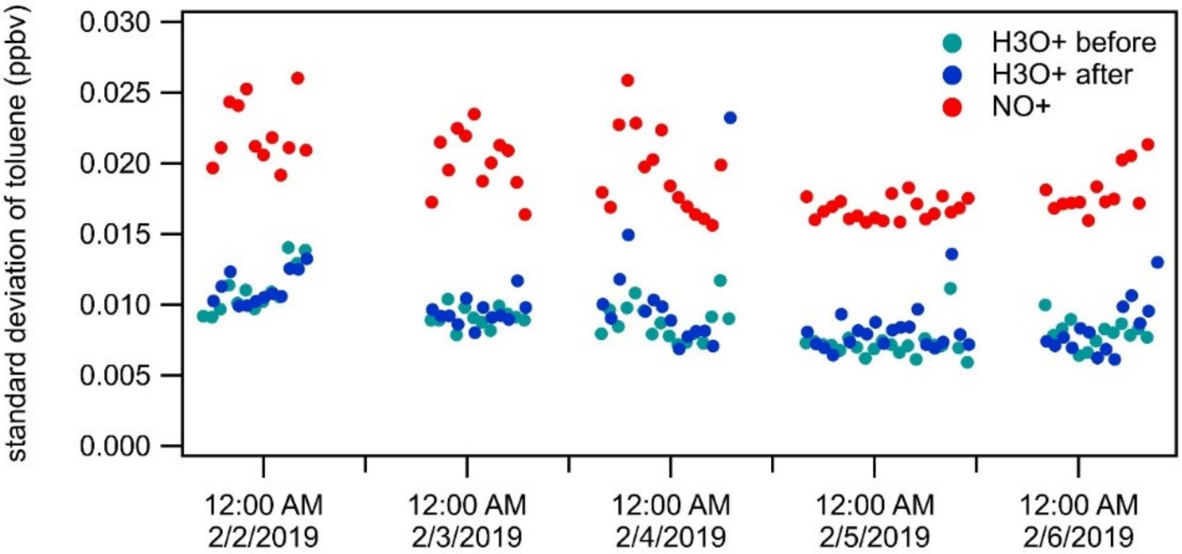

Figure 6-8. Toluene Standard Deviation of the Average NO^+ Data and Surrounding H_3O^+ Data Between February 1, 2019, and February 7, 2019.

This method of comparing the two modes will be used to assess the ability of NO^+ mode to monitor the analytes proposed in 53005-81-RPT-039 (Table 6-1). This will further refine our list of candidates for NO^+ mode monitoring and provide the initial basis for making decisions regarding when and to what capacity NO^+ mode should be implemented. The data for each analyte presented followed the same steps outlined for toluene for both modes.

6.1 1,3-butadiene (m/z 54)

Figure 6-9 shows a time-series of 1,3-butadiene in H_3O^+ (grey) and NO^+ (red). The observations after January 27, 2019, in both modes compare well and follow the same general trends. The NO^+ data prior to January 27, 20219, seem to be offset from the H_3O^+ data, which is attributed to the estimation of the instrument baseline being less accurate due to minimal zeros performed in NO^+ mode during this period.

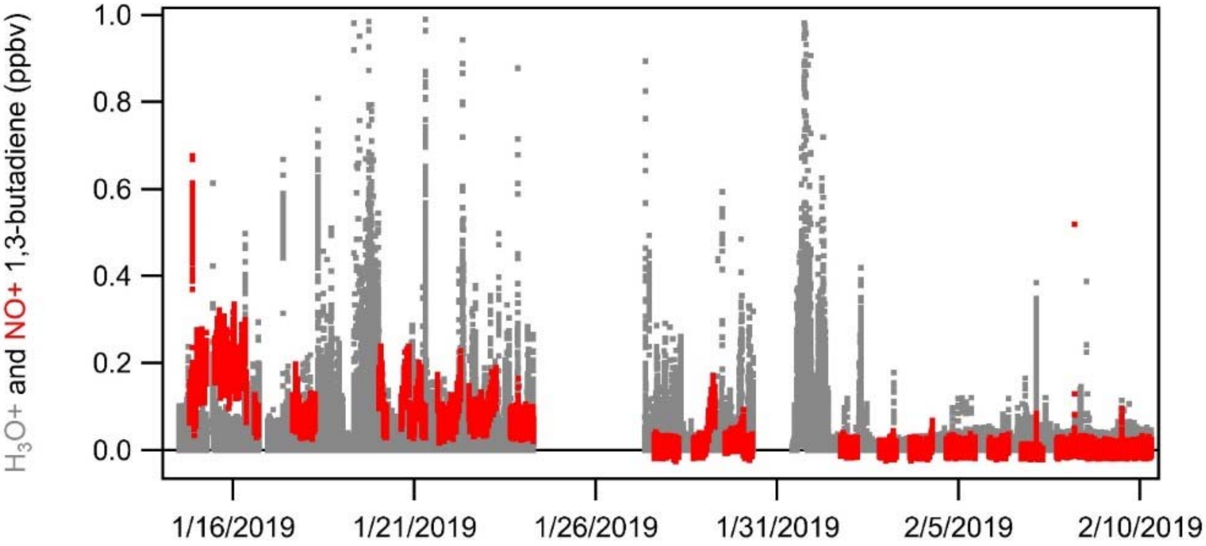

Figure 6-9. 1,3-butadiene Observed in NO^+ and H_3O^+ Modes for the Duration of the Background Study.

Figure 6-10 shows the 1,3-butadiene standard deviations of the NO^+ averages compared to the H_3O^+ standard deviations before and after the NO^+ data for the relatively clean period between January 1, 2019, and January 7, 2019. The standard deviations are low for both modes with H_3O^+ showing periods of lower standard deviation than NO^+. There would be a slight preference towards H_3O^+ mode due to this but the low magnitude of the standard deviation in NO^+ makes quantification feasible. An important factor is the potential for the water cluster present at m/z 55 interfering with H_3O^+ mode 1,3-butadiene quantification which occurs at m/z 55. Under typical operation, the water cluster at m/z 55 is relatively low and separation between the peaks is wide enough for good quantification in H_3O^+ mode. The preferred method for 1,3-butadiene observation would be NO^+ mode, but this additional separation from the water cluster will not typically outweigh the issue of a smaller observable analyte list imposed by NO^+ mode versus H_3O^+ mode.

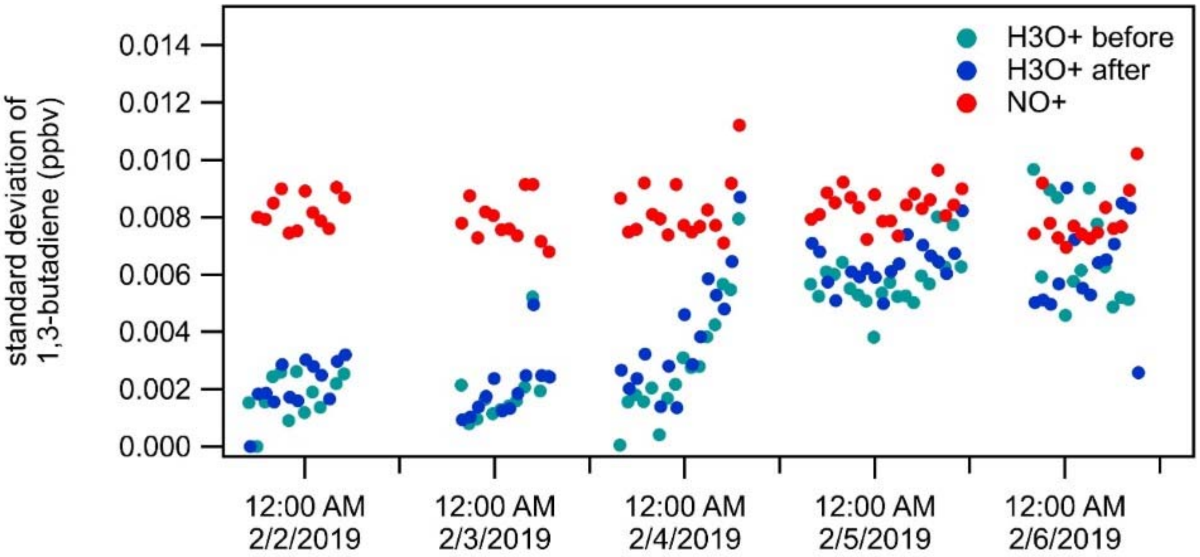

Figure 6-10. 1,3-butadiene Standard Deviation of the Average NO^+ Data and Surrounding H_3O^+ Data Between February 1, 2019, and February 7, 2019.

6.2 Dimethyl sulfide (m/z 62)

Figure 6-11 shows a time-series of dimethyl sulfide in H_3O^+ (grey) and NO^+ (red). The signal noise in NO^+ observations is much higher than in H_3O^+. This is attributed to the relatively low sensitivity of dimethyl sulfide in NO^+ mode compared to H_3O^+ mode. The NO^+ observations also appear to be offset from the H_3O^+ observations, which center around zero. This could be attributed to difficulty quantifying and correcting for instrument baseline in NO^+ mode, which could be influenced by the low sensitivity. This is more apparent with the data prior to January 27, 2019, where there is less zero information in NO^+ mode.

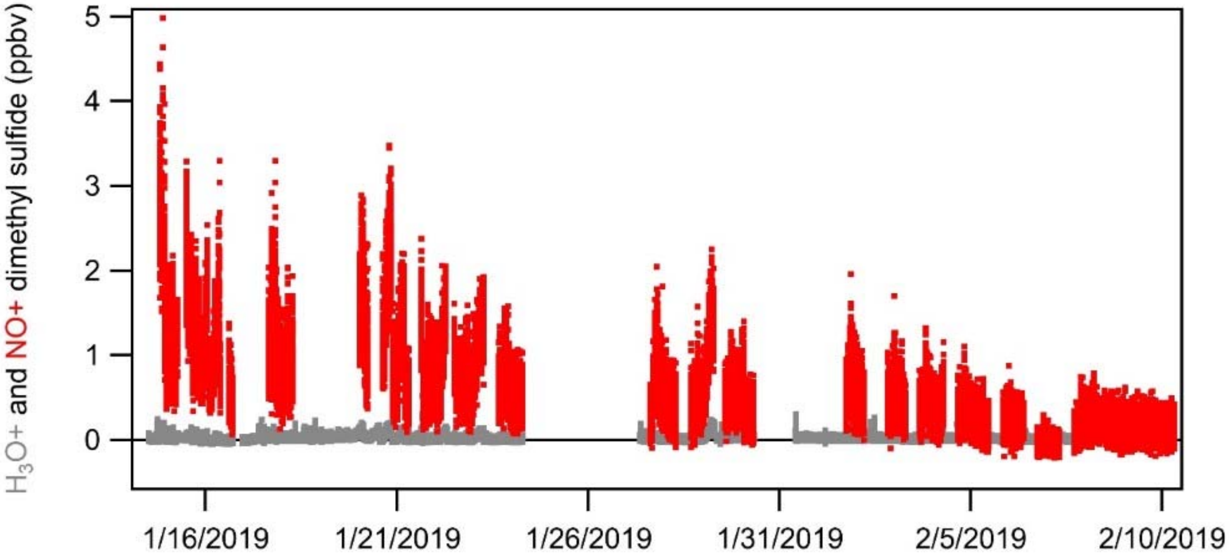

Figure 6-11. Dimethyl Sulfide Observed in NO$^+$ and H$_3$O$^+$ Modes for the Duration of the Background Study.

Figure 6-12 shows the dimethyl sulfide standard deviations of the NO$^+$ averages compared to the H$_3$O$^+$ standard deviations before and after the NO$^+$ data for the relatively clean period between January 1, 2019, and January 7, 2019. The standard deviations are almost an order of magnitude higher in NO$^+$ mode compared to H$_3$O$^+$, which was expected from the higher noise observed in Figure 6-11. Monitoring dimethyl sulfide in H$_3$O$^+$ remains the preferred method due to the lower detection limit and higher sensitivity.

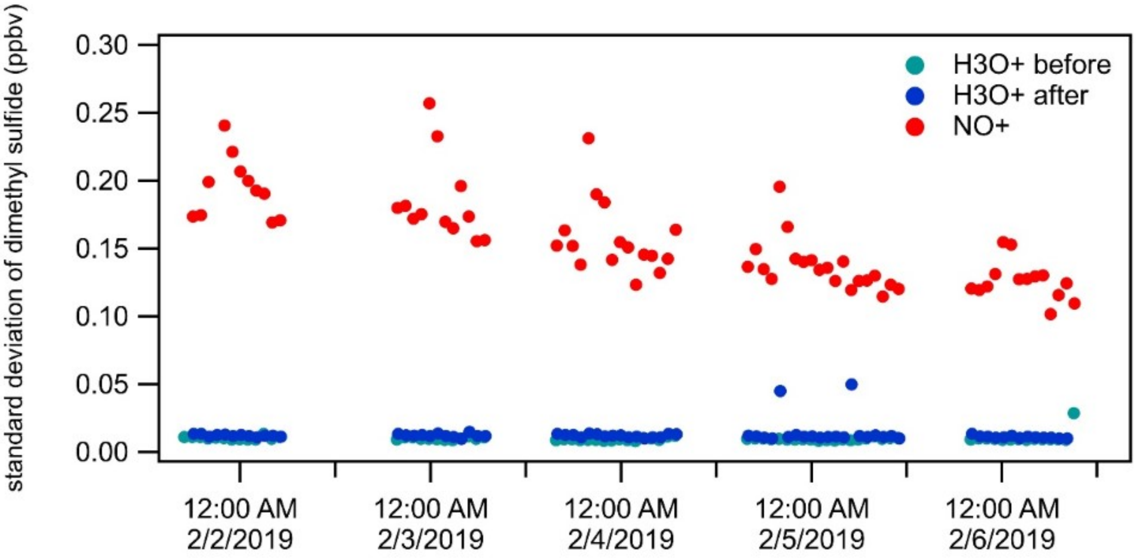

Figure 6-12. Dimethyl Sulfide Standard Deviation of the Average NO$^+$ Data and Surrounding H$_3$O$^+$ Data Between February 1, 2019, and February 7, 2019.

6.3 Furan (m/z 68a)

Figure 6-13 shows a time-series of furan in H_3O^+ (grey) and NO^+ (red). The observations after January 27, 2019, in both modes compare well and follow the same general trends. The NO^+ data prior to January 27, 2019, seem to be offset from the H_3O^+ data, which is attributed to the estimation of the instrument baseline being less accurate due to minimal zeros performed in NO^+ mode during this period.

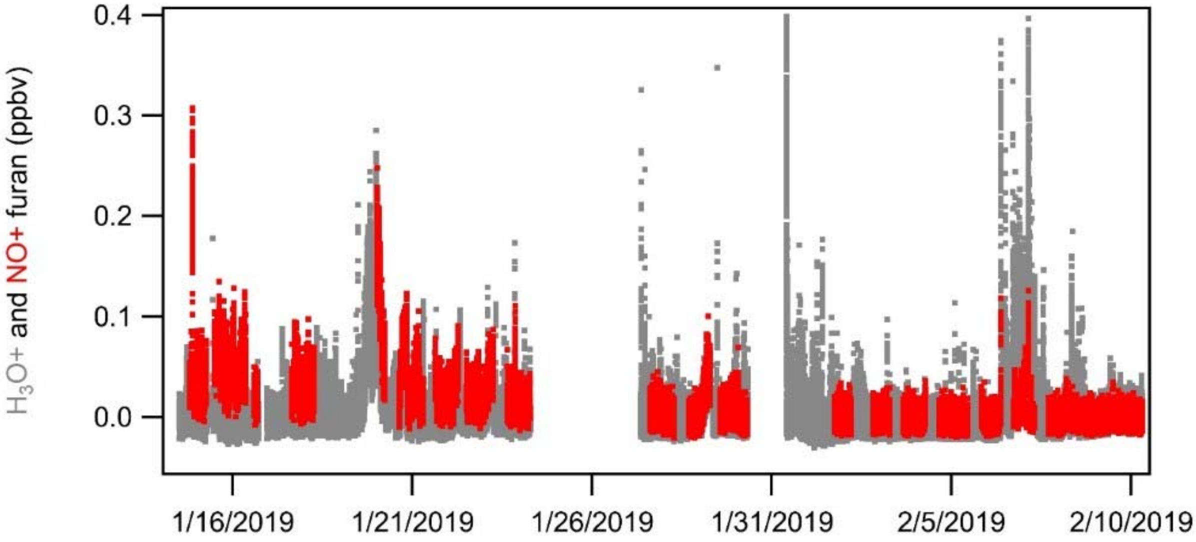

Figure 6-13. Furan Observed in NO^+ and H_3O^+ Modes for the Duration of the Background Study.

Figure 6-14 shows the furan standard deviations of the NO^+ averages compared to the H_3O^+ standard deviations before and after the NO^+ data for the relatively clean period between January 1, 2019, and January 7, 2019. The standard deviations are very similar with the NO^+ appearing to be slightly higher than the H_3O^+. This means the detection limits in NO^+ are potentially higher, but the difference would not be enough to drive preference toward either mode. One factor that is considered is the potential for isoprene as an interferent since it responds at an m/z close to furan. While the separation between the peaks is wide enough for good quantification in H_3O^+ mode, furan is much more sensitive than isoprene in NO^+ mode. The low sensitivity of isoprene in NO^+ is detailed in the next section. Given this, the preferred method for furan observation would be NO^+ mode, but this additional separation from isoprene will not typically outweigh the issue of a smaller observable analyte list imposed by NO^+ mode versus H_3O^+ mode.

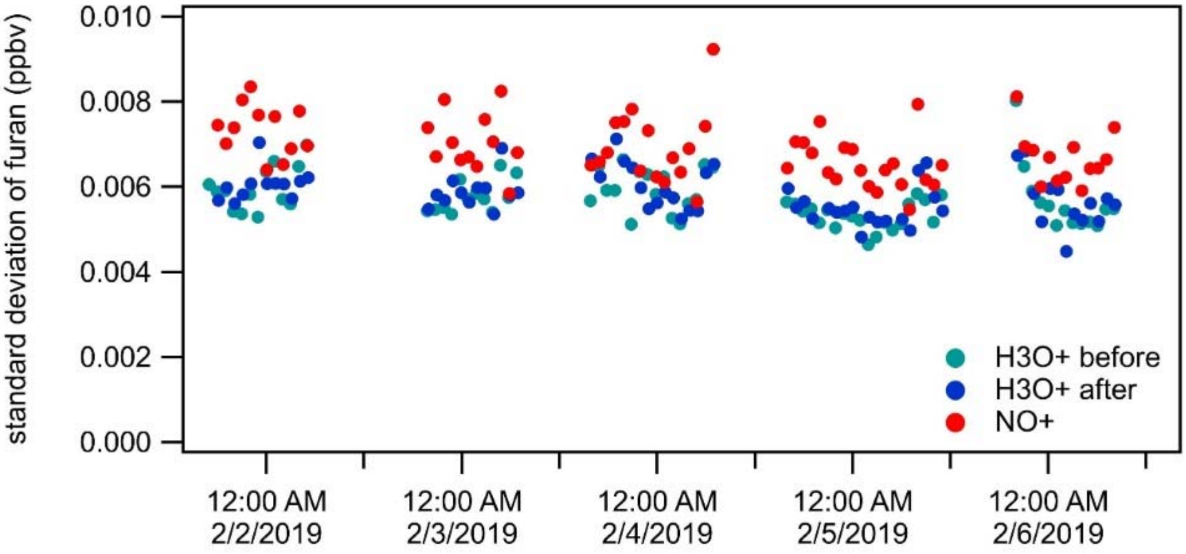

Figure 6-14. Furan Standard Deviation of the Average NO^+ Data and Surrounding H_3O^+ Data Between February 1, 2019, and February 7, 2019.

6.4 Isoprene (m/z 68b)

Figure 6-15 shows a time-series of isoprene in H_3O^+ (grey) and NO^+ (red). The signal noise in NO^+ observations is much higher than in H_3O^+. This is attributed to the relatively low sensitivity of isoprene in NO^+ mode compared to H_3O^+ mode. Despite this, the post January 27, 2019, data look to be centered around zero, which is consistent with the H_3O^+ observations. Isoprene is a biogenic and this source is effectively 'shut off' in the winter. The NO^+ data prior to January 27, 2019, looks to be offset which is attributed to difficulty quantifying and correcting for instrument baseline in NO^+ mode during this time. In addition, the instrument had periods of shifting instrument baseline which is responsible for the large increases in the pre-January 27, 2019, NO^+ data.

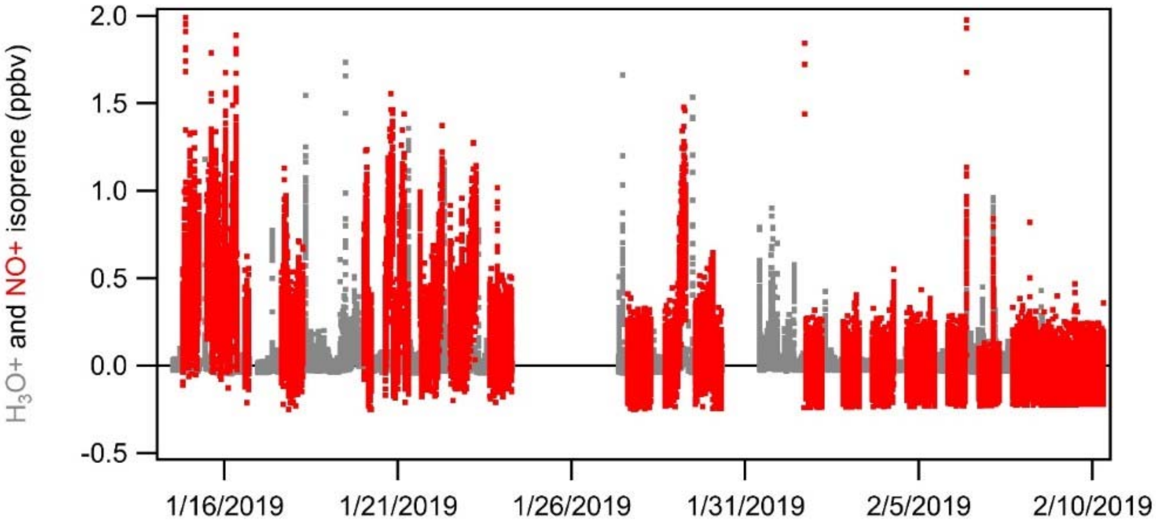

Figure 6-15. Isoprene Observed in NO$^+$ and H$_3$O$^+$ Modes for the Duration of the Background Study.

Figure 6-16 shows the isoprene standard deviations of the NO$^+$ averages compared to the H$_3$O$^+$ standard deviations before and after the NO$^+$ data for the relatively clean period between January 1, 2019, and January 7, 2019. The standard deviations are almost an order of magnitude higher in NO$^+$ mode compared to H$_3$O$^+$, which was expected from the higher noise observed in Figure 6-15. As explained earlier, isoprene is a potential interferent to furan. The larger standard deviation and lower sensitivity of isoprene would make the isoprene interference to furan negligible under most ambient conditions. The preferred method for observing isoprene is H$_3$O$^+$ mode and NO$^+$ mode provides no advantages.

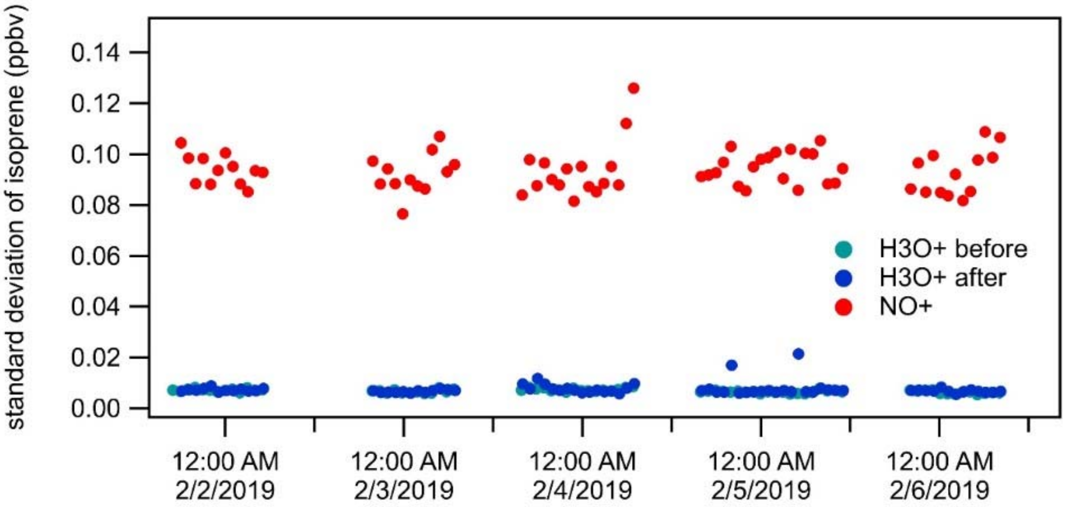

Figure 6-16. Isoprene Standard Deviation of the Average NO$^+$ Data and Surrounding H$_3$O$^+$ Data Between February 1, 2019, and February 7, 2019.

6.5 NDMA (m/z 74)

Figure 6-17 shows a time-series of NDMA in H_3O^+ (grey) and NO^+ (red). The observations in both modes compare well and follow the same general trends. The instrument baseline issues occurring before January 27, 2019, are responsible for the difference from H_3O^+ observations. In general, the instrument baseline was consistent and the estimation based on the limited zero information was adequate to capture and correct appropriately.

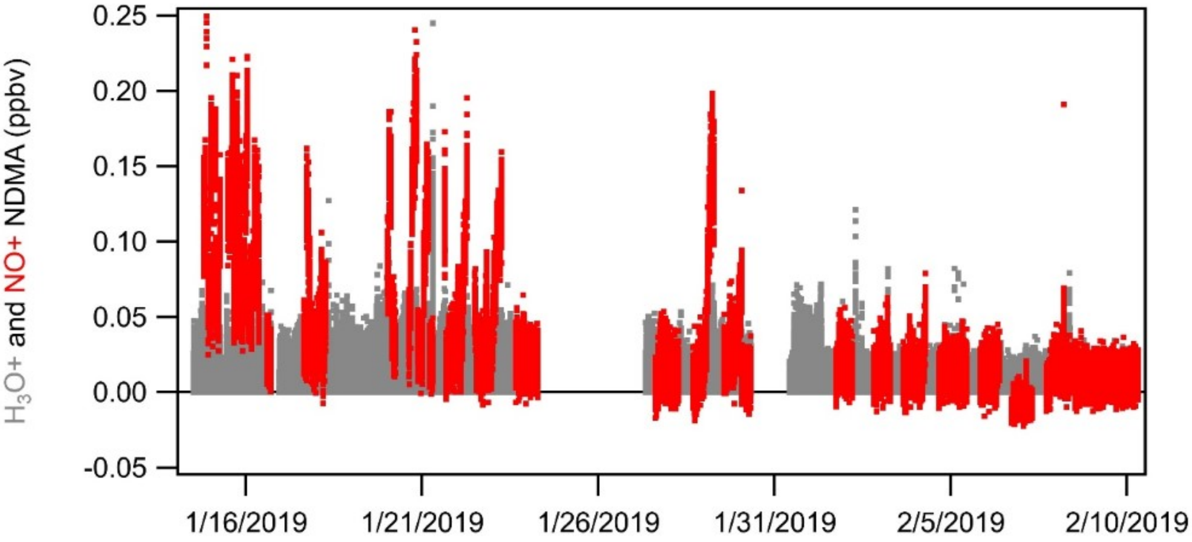

Figure 6-17. NDMA observed in NO^+ and H_3O^+ Modes for the Duration of the Background Study.

Figure 6-18 shows the NDMA standard deviations of the NO^+ averages compared to the H_3O^+ standard deviations before and after the NO^+ data for the relatively clean period between January 1, 2019, and January 7, 2019. The standard deviations in NO^+ are slightly higher than in H_3O^+, which would translate to a higher detection limit for NO^+. The advantage of NDMA in NO^+ mode lies with the ability to separate the signal from methyl acetate, which is a potential interferent in H_3O^+ mode. The ionization potential of methyl acetate is 10.25 eV, which is higher than the ionization potential of NO at 9.26 eV. This means that the electron transfer will not occur with methyl acetate so it will not produce an ion removing any potential interference from methyl acetate. The preferred method for monitoring NDMA would be NO^+ mode despite the slightly higher detection limit, but for typical monitoring activities, the removal of methyl acetate as an interferent would not outweigh the smaller observable analyte list imposed by NO^+ mode versus H_3O^+ mode.

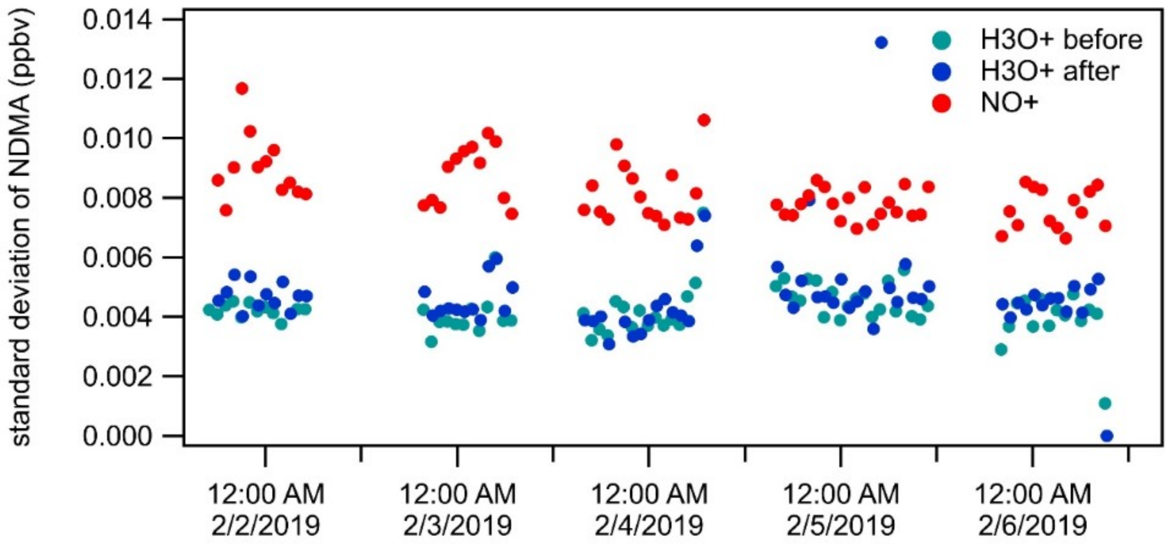

Figure 6-18. NDMA Standard Deviation of the Average NO$^+$ Data and Surrounding H$_3$O$^+$ Data Between February 1, 2019, and February 7, 2019.

6.6 Benzene (m/z 78)

Figure 6-19 shows a time-series of benzene in H$_3$O$^+$ (grey) and NO$^+$ (red). The observations after January 27, 2019, in both modes compare well and follow the same general trends. The NO$^+$ data prior to January 27, 2019, seem to be offset from the H$_3$O$^+$ data, which is attributed to the estimation of the instrument baseline being less accurate due to minimal zeros performed in NO$^+$ mode during this period. On January 6, 2019, and January 7, 2019, the ML was at the urban site (Site 6) and both modes shows increased benzene activity as expected due to a large variety of sources typical for that environment.

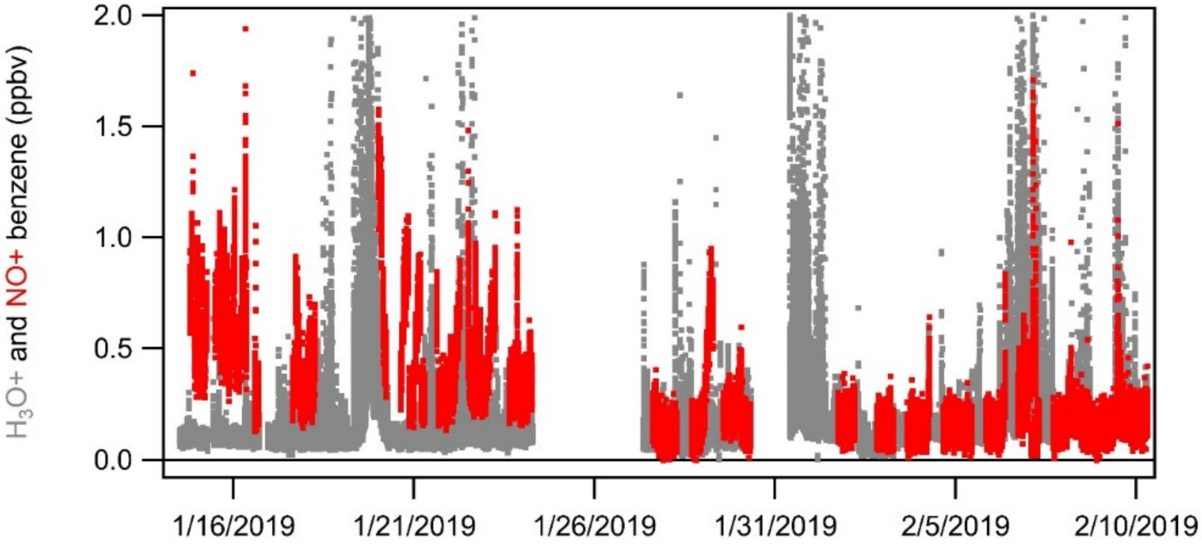

Figure 6-19. Benzene Observed in NO$^+$ and H$_3$O$^+$ Modes for the Duration of the Background Study.

Figure 6-20 shows the benzene standard deviations of the NO^+ averages compared to the H_3O^+ standard deviations before and after the NO^+ data for the relatively clean period between January 1, 2019, and January 7, 2019. The standard deviations are approximately three times higher in NO^+. This means the detection limits in NO^+ are higher. Considering this and the smaller observable analyte list imposed by NO^+ mode, the preferred mode for benzene quantification is H_3O^+ mode.

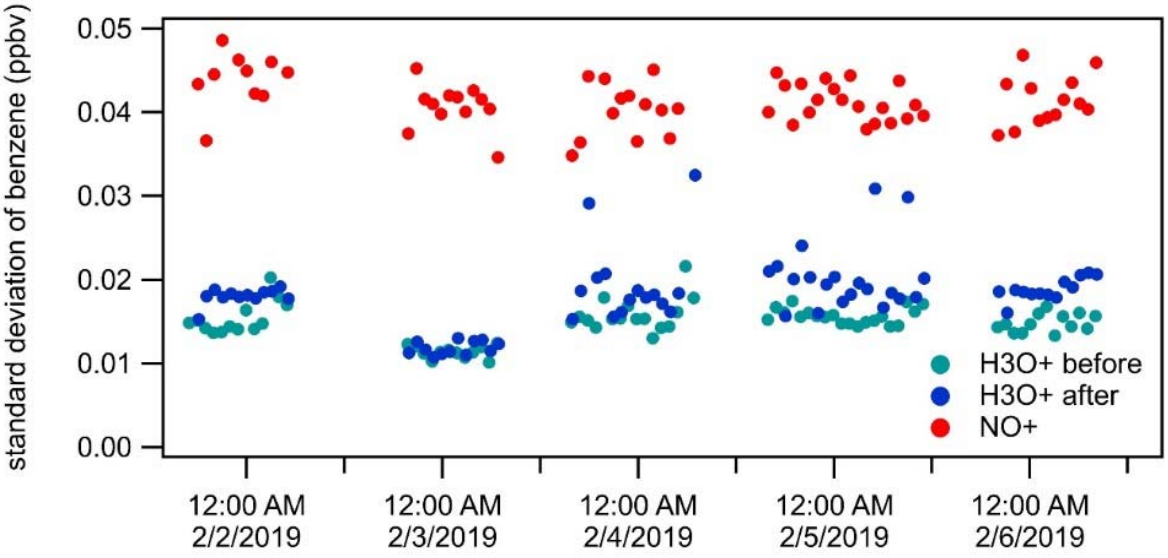

Figure 6-20. Benzene Standard Deviation of the Average NO^+ Data and Surrounding H_3O^+ Data Between February 1, 2019, and February 7, 2019.

6.7 Diethylketone (m/z 86)

Figure 6-21 shows a time-series of diethylketone in H_3O^+ (grey) and NO^+ (red). The noise in the NO^+ signal is much higher than in H_3O^+. This is attributed to the relatively low sensitivity of diethylketone in NO^+ mode compared to H_3O^+ mode. Despite this, the post January 27, 2019, data look to be centered around zero, which is consistent with the H_3O^+ observations. The NO^+ data prior to January 27, 2019, look to be offset which is attributed to difficulty quantifying and correcting for instrument baseline in NO^+ mode during this time. In addition, the instrument had periods of shifting instrument baseline which is responsible for the large increases in the pre-January 27, 2019, NO^+ data.

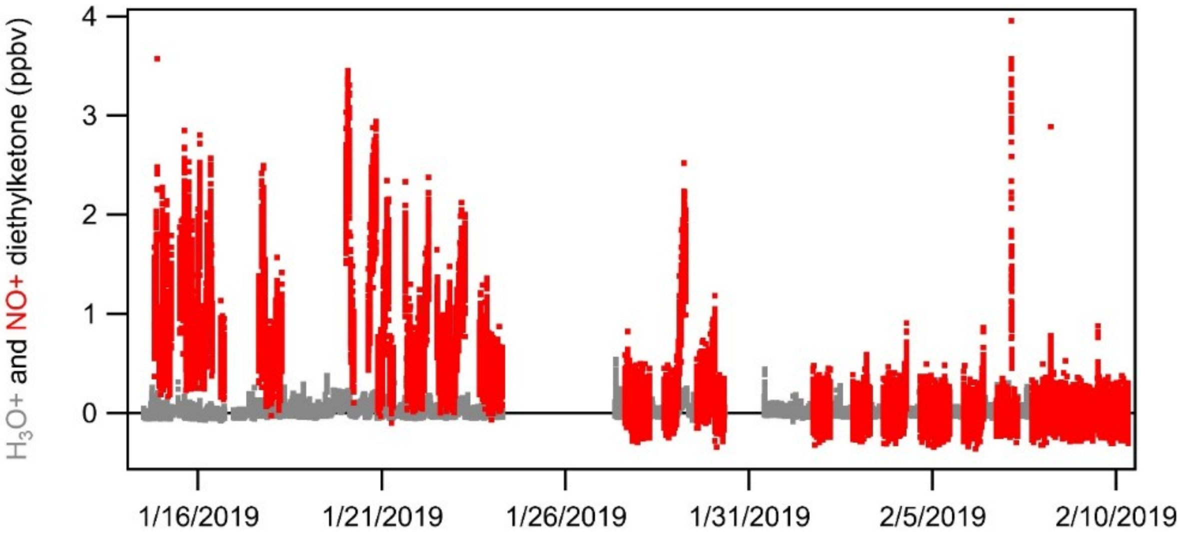

Figure 6-21. Diethylketone Observed in NO$^+$ and H$_3$O$^+$ Modes for the Duration of the Background Study.

Figure 6-22 shows the diethylketone standard deviations of the NO$^+$ averages compared to the H$_3$O$^+$ standard deviations before and after the NO$^+$ data for the relatively clean period between January 1, 2019, and January 7, 2019. The standard deviations are approximately an order of magnitude higher in NO$^+$ mode compared to H$_3$O$^+$, which was expected from the higher noise observed in Figure 6-21. Monitoring diethylketone in H$_3$O$^+$ remains the preferred method due to the lower detection limit and higher sensitivity.

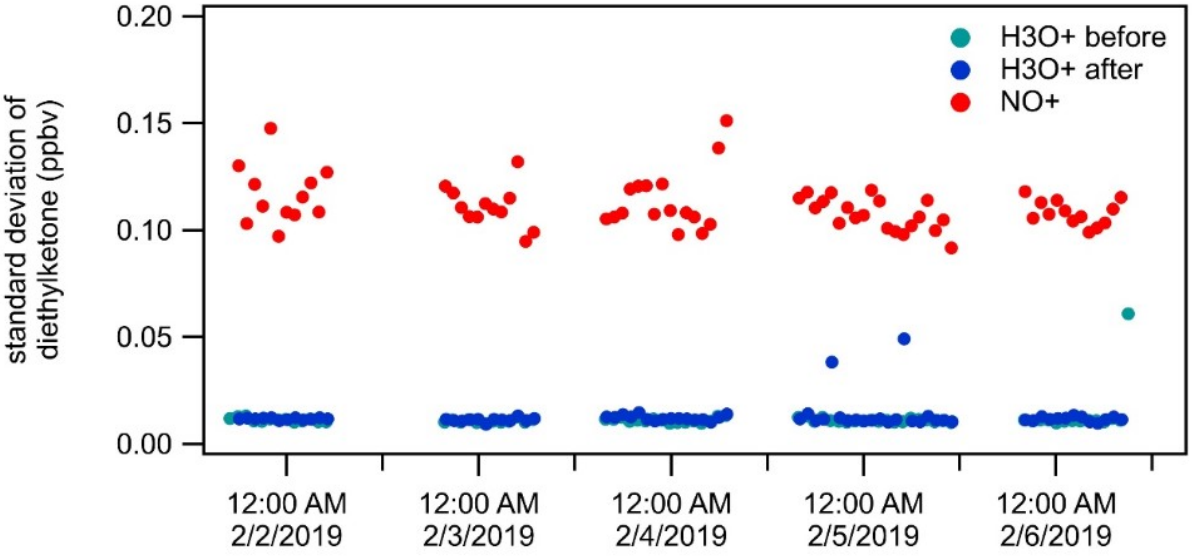

Figure 6-22. Diethylketone Standard Deviation of the Average NO$^+$ Data and Surrounding H$_3$O$^+$ Data Between February 1, 2019, and February 7, 2019.

6.8 Toluene (m/z 92)

Figure 6-23 shows a time-series of toluene in H_3O^+ (grey) and NO^+ (red). The observations after January 27, 2019, in both modes compare well and follow the same general trends. The NO^+ data prior to January 27, 2019, seem to be offset from the H_3O^+ data, which is attributed to our estimation of the instrument baseline being less accurate due to minimal zeros performed in NO^+ mode during this period. On January 6, 2019, and January 7, 2019, the ML was at the urban site (Site 6) and both modes show increased toluene activity as expected due to a large variety of sources typical for that environment.

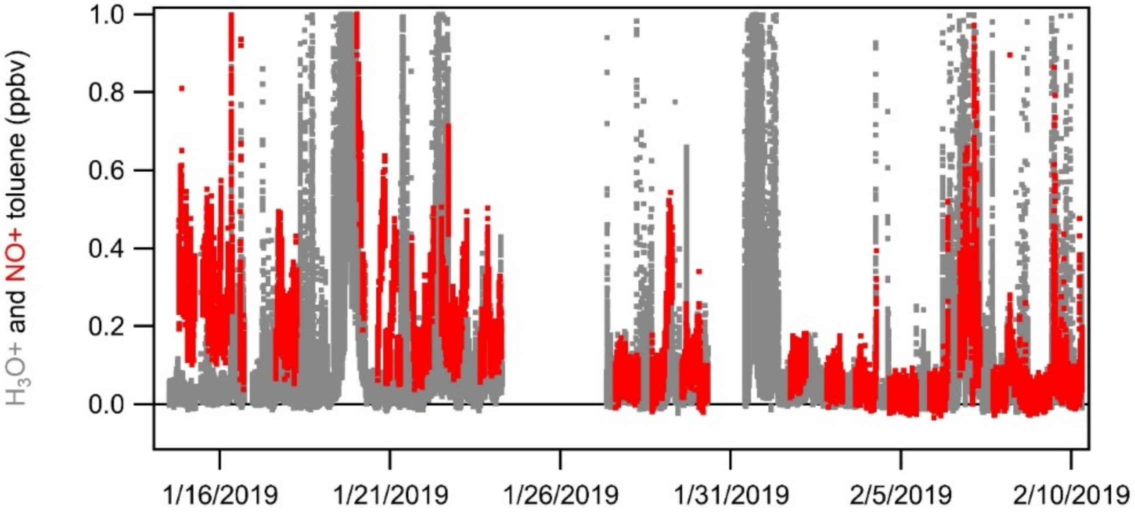

Figure 6-23. Toluene Observed in NO^+ and H_3O^+ Modes for the Duration of the Background Study.

Figure 6-24 shows the toluene standard deviations of the NO^+ averages compared to the H_3O^+ standard deviations before and after the NO^+ data for the relatively clean period between January 1, 2019, and January 7, 2019. The standard deviations are approximately twice as high in NO^+ compared to H_3O^+ mode. This means the detection limits in NO^+ are higher. Considering this and the smaller observable analyte list imposed by NO^+ mode, the preferred mode for toluene quantification is H_3O^+ mode.

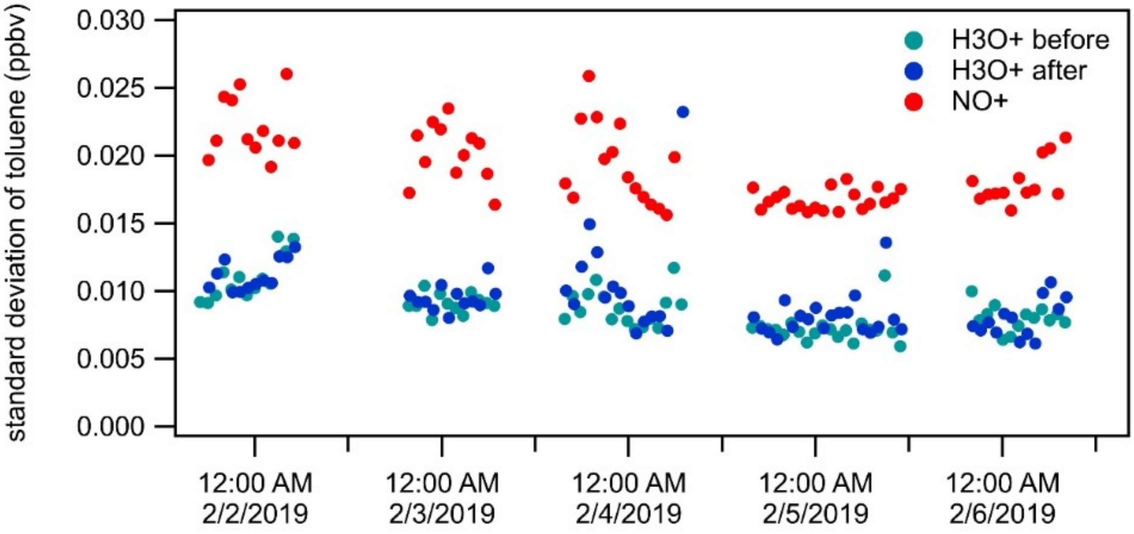

Figure 6-24. Toluene Standard Deviation of the Average NO$^+$ Data and Surrounding H$_3$O$^+$ Data Between February 1, 2019, and February 7, 2019.

6.9 hexanone (m/z 100)

Figure 6-25 shows a time-series of hexanone in H$_3$O$^+$ (grey) and NO$^+$ (red). The signal noise in NO$^+$ observations is much higher than in H$_3$O$^+$. This is attributed to the relatively low sensitivity of hexanone in NO$^+$ mode compared to H$_3$O$^+$ mode. Despite this, the post January 27, 2019, data look to be centered around zero, which is consistent with the H$_3$O$^+$ observations. The NO$^+$ data prior to January 27, 2019, look to be offset which is attributed to difficulty quantifying and correcting for instrument baseline in NO$^+$ mode during this time. In addition, the instrument had periods of shifting instrument baseline which is responsible for the large increases in the pre-January 27, 2019, NO$^+$ data.

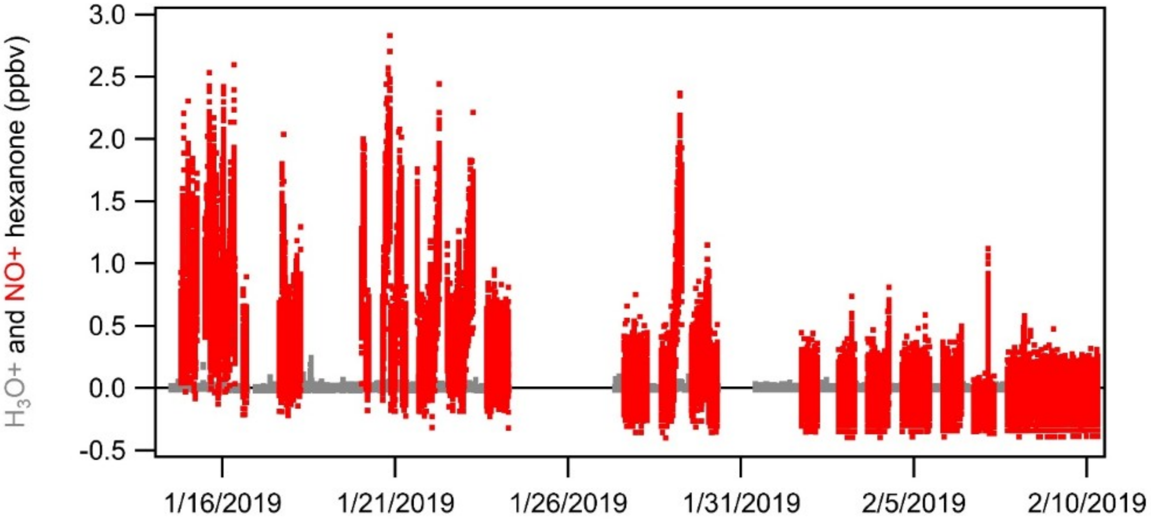

Figure 6-25. Hexanone Observed in NO$^+$ and H$_3$O$^+$ Modes for the Duration of the Background Study.

Figure 6-26 shows the hexanone standard deviations of the NO^+ averages compared to the H_3O^+ standard deviations before and after the NO^+ data for the relatively clean period between January 1, 2019, and January 7, 2019. The standard deviations are approximately an order of magnitude higher in NO^+ mode compared to H_3O^+, which was expected from the higher noise observed in Figure 6-25. Monitoring hexanone in H_3O^+ remains the preferred method due to the lower detection limit and higher sensitivity.

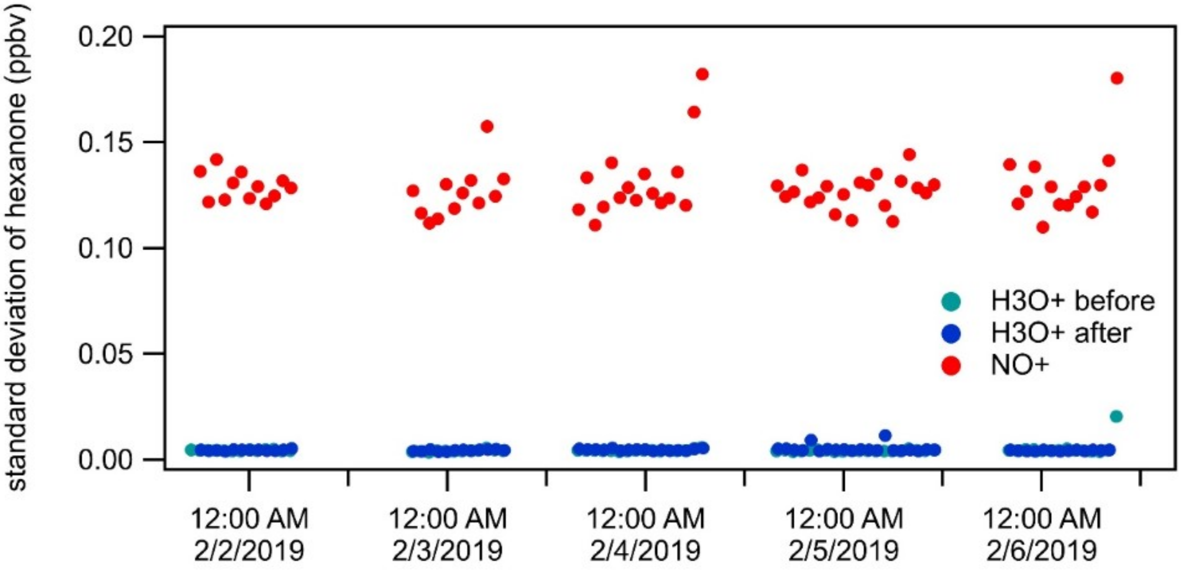

Figure 6-26. Hexanone Standard Deviation of the Average NO^+ Data and Surrounding H_3O^+ Data Between February 1, 2019, and February 7, 2019.

6.10 C_2-benzenes (m/z 106)

Figure 6-27 shows a time-series of C_2-benzenes in H_3O^+ (grey) and NO^+ (red). The observations after January 27, 2019, in both modes compare well and follow the same general trends. The NO^+ data prior to January 27, 2019, seem to be offset from the H_3O^+ data, which is attributed to the estimation of the instrument baseline being less accurate due to minimal zeros performed in NO^+ mode during this period. On January 6, 2019, and January 7, 2019, the ML was at the urban site (Site 6) and both modes show increased C_2-benzene activity as expected due to a large variety of sources typical for that environment.

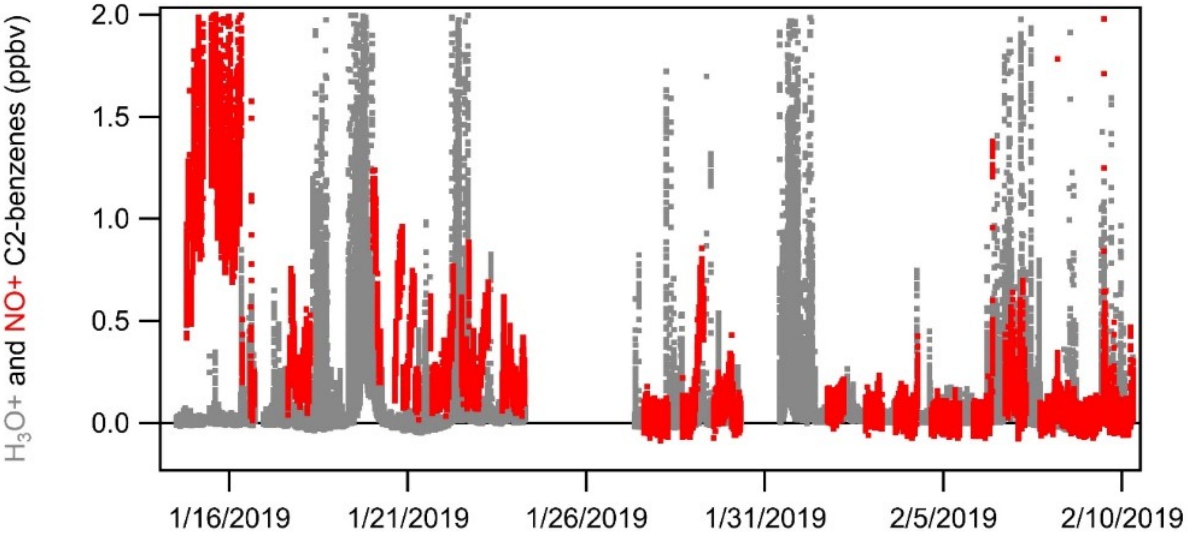

Figure 6-27. C_2-benzenes Observed in NO^+ and H_3O^+ Modes for the Duration of the Background Study.

Figure 6-28 shows the C_2-benzene standard deviations of the NO^+ averages compared to the H_3O^+ standard deviations before and after the NO^+ data for the relatively clean period between January 1, 2019, and January 7, 2019. The standard deviations are approximately three times higher in NO^+ compared to H_3O^+ mode. This means the detection limits in NO^+ are higher. Considering this and the smaller observable analyte list imposed by NO^+ mode, the preferred mode for C_2-benzene quantification is H_3O^+ mode.

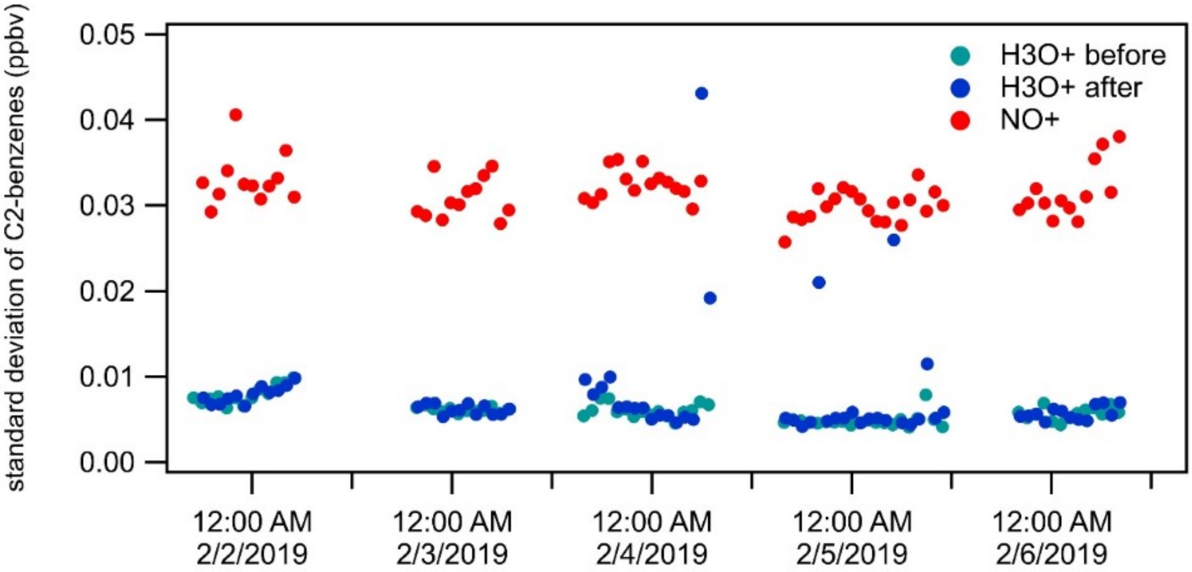

Figure 6-28. C_2-benzene Standard Deviation of the Average NO^+ Data and Surrounding H_3O^+ Data Between February 1, 2019, and February 7, 2019.

6.11 C_3-benzenes (m/z 120)

Figure 6-29 shows a time-series of C_3-benzenes in H_3O^+ (grey) and NO^+ (red). The observations after January 27, 2019, in both modes compare well and follow the same general trends. The NO^+ data prior to January 27, 2019, seems to be offset from the H_3O^+ data, which is attributed to our estimation of the instrument baseline being less accurate due to minimal zeros performed in NO^+ mode during this period. On January 6, 2019, and January 7, 2019, the ML was at the urban site (Site 6) and both modes shows increased C_3-benzene activity as expected due to a large variety of sources typical for that environment.

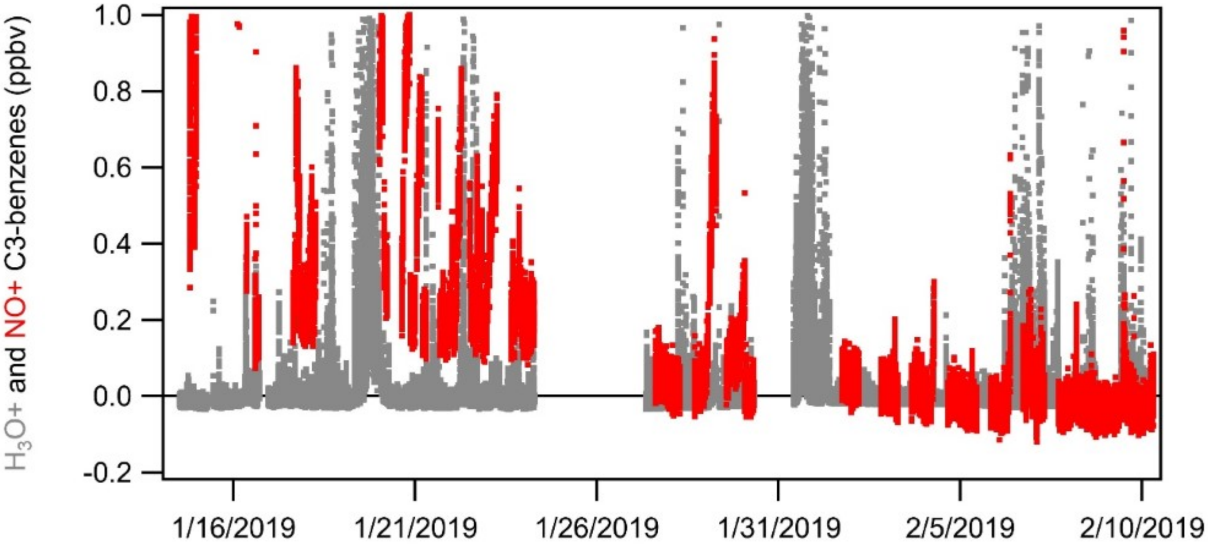

Figure 6-29. C_3-benzenes Observed in NO^+ and H_3O^+ Modes for the Duration of the Background Study.

Figure 6-30 shows the C_3-benzene standard deviations of the NO^+ averages compared to the H_3O^+ standard deviations before and after the NO^+ data for the relatively clean period between January 1, 2019, and January 7, 2019. The standard deviations are approximately six times higher in NO^+ compared to H_3O^+ mode. This means the detection limits in NO^+ are higher. Considering this and the smaller observable analyte list imposed by NO^+ mode, the preferred mode for C_3-benzene quantification is H_3O^+ mode.

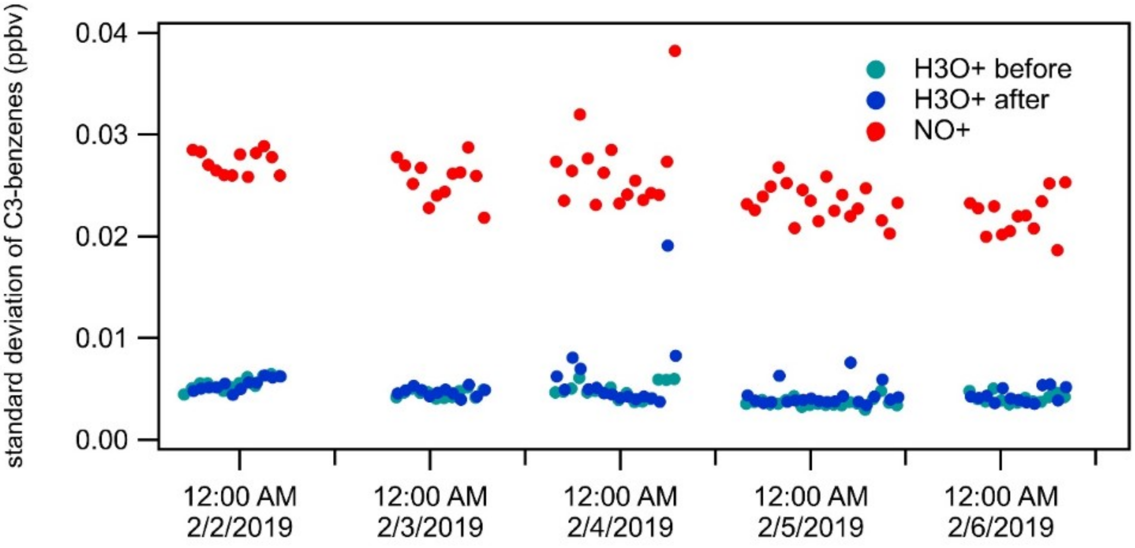

Fig 6-30. C_3-benzene Standard Deviation of the Average NO^+ Data and Surrounding H_3O^+ Data Between February 1, 2019, and February 7, 2019.

6.12 C_4-benzenes (m/z 134)

Figure 6-31 shows a time-series of C_4-benzenes in H_3O^+ (grey) and NO^+ (red). The observations after January 27, 2019, in both modes compare well and follow the same general trends. The NO^+ data prior to January 27, 2019, seem to be offset from the H_3O^+ data, which is attributed to our estimation of the instrument baseline being less accurate due to minimal zeros performed in NO^+ mode during this period. On January 6, 2019, and January 7, 2019, the ML was at the urban site (Site 6) and both modes show increased C_4-benzene activity as expected due to a large variety of sources typical for that environment.

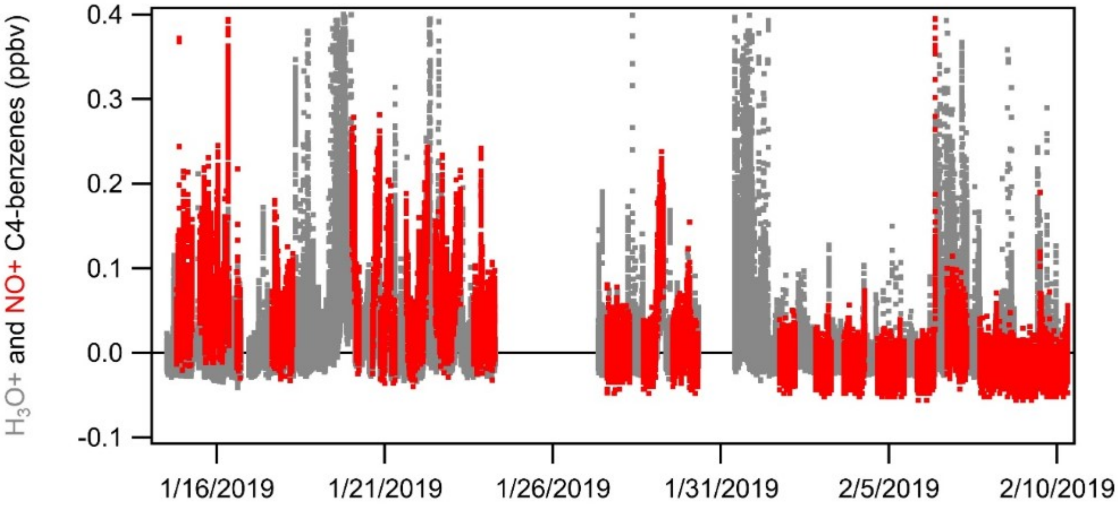

Figure 6-31. C_4-benzenes Observed in NO^+ and H_3O^+ Modes for the Duration of the Background Study.

Figure 6-32 shows the C4-benzene standard deviations of the NO^+ averages compared to the H_3O^+ standard deviations before and after the NO^+ data for the relatively clean period between January 1, 2019, and January 7, 2019. The standard deviations are approximately twice as high in NO^+ compared to H_3O^+ mode. This means the detection limits in NO^+ are higher. Considering this and the smaller observable analyte list imposed by NO^+ mode, the preferred mode for C4-benzene quantification is H_3O^+ mode.

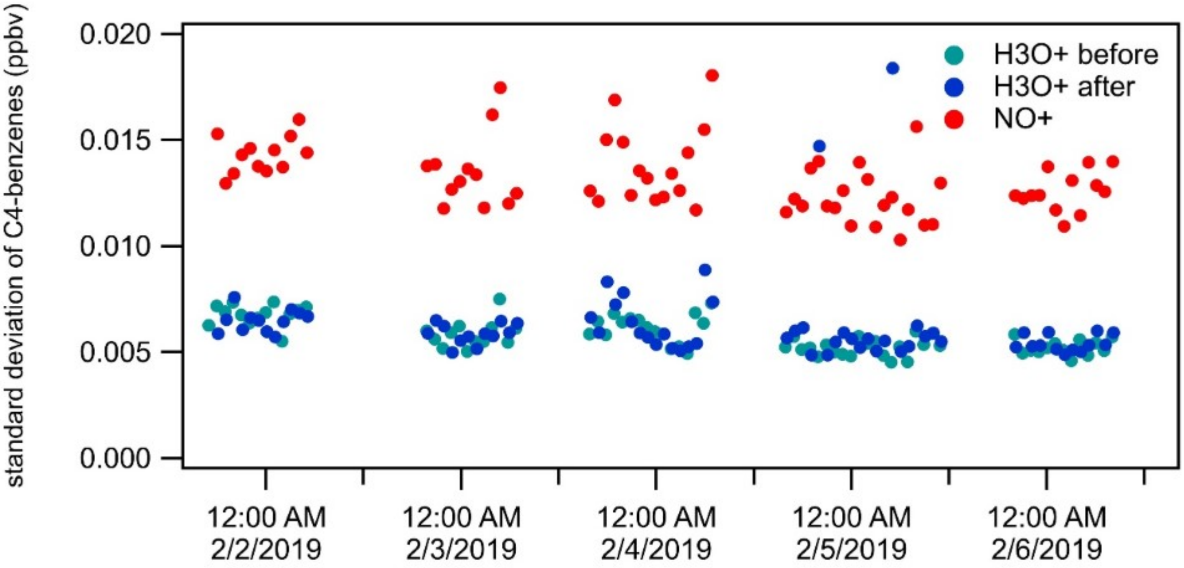

Figure 6-32. C_4-benzene Standard Deviation of the Average NO^+ Data and Surrounding H_3O^+ Data Between February 1, 2019, and February 7, 2019.

6.13 Monoterpenes (m/z 136)

Figure 6-33 shows a time-series of monoterpenes in H_3O^+ (grey) and NO^+ (red). The signal noise in NO^+ observations is much higher than in H_3O^+. This is attributed to the relatively low sensitivity of monoterpenes in NO^+ mode compared to H_3O^+ mode. Despite this, the post January 27, 2019, data look to be centered around zero, which is consistent with the H_3O^+ observations. The NO^+ data prior to January 27, 2019, look to be offset which is attributed to difficulty quantifying and correcting for instrument baseline in NO^+ mode during this time. In addition, the instrument had periods of shifting instrument baseline which is responsible for the large increases in the pre-January 27, 2019, NO^+ data.

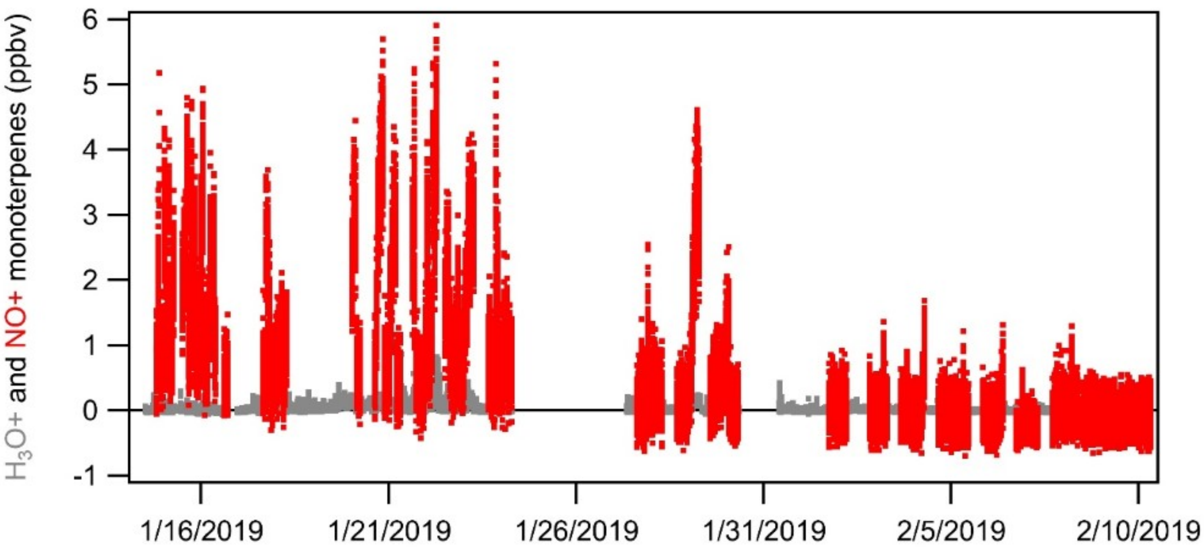

Figure 6-33. Monoterpenes Observed in NO^+ and H_3O^+ Modes for the Duration of the Background Study.

Figure 6-34 shows the monoterpene standard deviations of the NO^+ averages compared to the H_3O^+ standard deviations before and after the NO^+ data for the relatively clean period between January 1, 2019, and January 7, 2019. The standard deviations are approximately an order of magnitude higher in NO^+ mode compared to H_3O^+, which was expected from the higher noise observed in Figure 6-33. Monitoring monoterpenes in H_3O^+ remains the preferred method due to the lower detection limit and higher sensitivity.

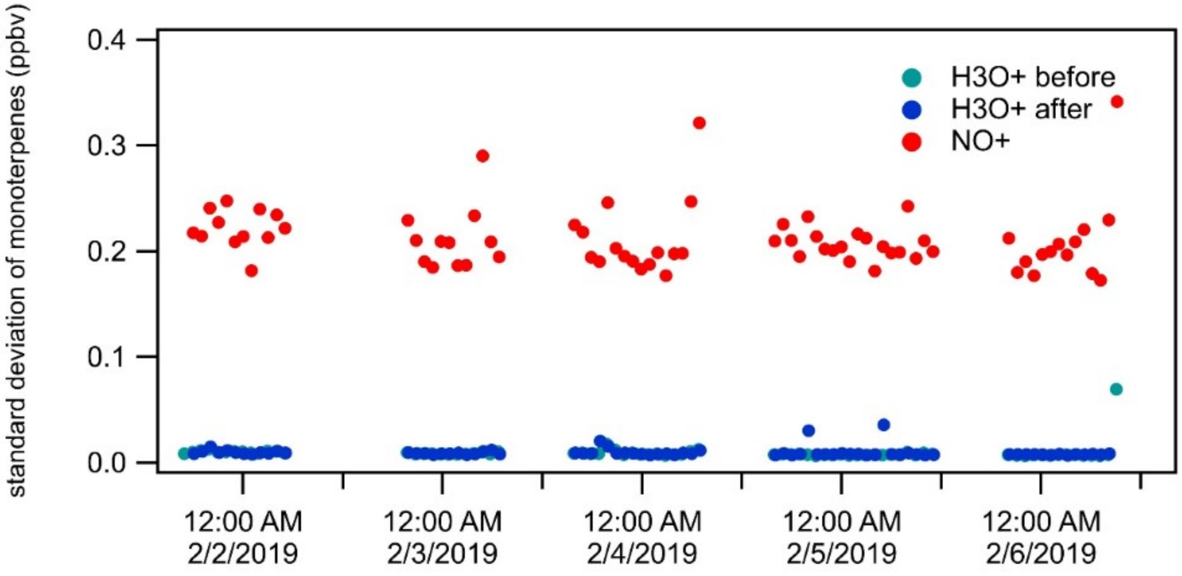

Figure 6-34. Monoterpene Standard Deviation of the Average NO^+ Data and Surrounding H_3O^+ Data Between February 1, 2019, and February 7, 2019.

6.14 Overview

Table 6-2 shows a summary of the current feasibility of NO^+ mode. This includes species that were found to be non-reactive with NO^+ in 53005-81-RPT-039. The analytes detailed above were organized into three levels of feasibility. The high feasibility classification includes species that would have benefits from NO^+ mode under certain conditions. The fair feasibility classification includes species that are reasonably quantified in NO^+ mode but show better results in H_3O^+ mode. The low feasibility classification includes species that have a response in NO^+ but quantification is very limited due to low sensitivity and high detection limit. The list of analytes feasible for NO^+ mode further decreased from those listed in 53005-81-RPT-039. Of the studied analytes, only 1,3-butadiene, furan, and NDMA are the only ones that seem to benefit from NO^+ mode over H_3O^+ mode, but even for them the smaller list of observable analytes imposed by NO^+ mode would typically outweigh this advantage. The benefit of NO^+ mode for sampling 1,3-butadiene, furan and NDMA would be removing the potential interferences that can be present in H_3O^+ mode. NO^+ mode would remove the potential water cluster interference from 1,3-butadiene, reduce the potential for isoprene interference with furan, and remove the potential the methyl acetate interference from NDMA. For most monitoring activities, the small advantage provided by NO^+ for a select few analytes comes at the sacrifice of no measurement for a large list of analytes. Given this, NO^+ mode can be useful in specific studies, but will likely be supplemental information to H_3O^+ mode observations.

Table 6-2. Feasibility of Monitoring Select Analytes in NO^+ Mode.

Species	m/z	NO^+ Feasibility	Reason
methanol	32	None	No reaction with NO^+
acetonitrile	41	None	No reaction with NO^+
acetaldehyde	44	None	No reaction with NO^+
1,3-butadiene	54	High	
1-butene	56	None	No reaction with NO^+
acetone	58	None	No reaction with NO^+
dimethylsulfide	62	Low	Low Sensitivity, High MDL
furan	68a	High	
isoprene	68b	Low	Low Sensitivity, High MDL
methyl vinyl ketone	70	None	No reaction with NO^+
methyl ethyl ketone	72	None	No reaction with NO^+
NDMA	74	High	
benzene	78	Fair	Higher MDL than H_3O^+
diethylketone	86	Low	Low Sensitivity, High MDL
toluene	92	Fair	Higher MDL than H_3O^+
3-hexanone	100	Low	Low Sensitivity, High MDL
p-xylene	106	Fair	Higher MDL than H_3O^+
1,3,5-trimethylbenzene	120	Fair	Higher MDL than H_3O^+
1,2,3,5-tetramethylbenzene	134	Fair	Higher MDL than H_3O^+
alpha pinene	136	Low	Low Sensitivity, High MDL

One result of monitoring ambient background concentrations is the limited response for most of the analytes. This low response is expected at Sites 1 through 5 with observed source plumes being often short-lived and requiring ideal meteorological conditions. As pointed out previously, this is not the case with the urban Site 6, which contains a large quantity and variety of sources. This site provides better data to look further into how well NO^+ and H_3O^+ data compared. Figure 6-35 shows the data collected for toluene, benzene, C_2-benzenes, and furan at Site 6 from 01:00 to 08:00 on January 6, 2019. All four of these species have a fair NO^+ feasibility except for furan, which is high, and seem to capture the trends and plumes comparable to H_3O^+. In general, the NO^+ data compliments the H_3O^+ data and they appear to flow well together with most transitions between the two modes looking seamless. One exception seems to be that under lower concentrations the NO^+ observations seem to be a bit lower. This could be attributed to less zero information in NO^+ than H_3O^+ meaning the NO^+ estimation of instrument baseline could be offset.

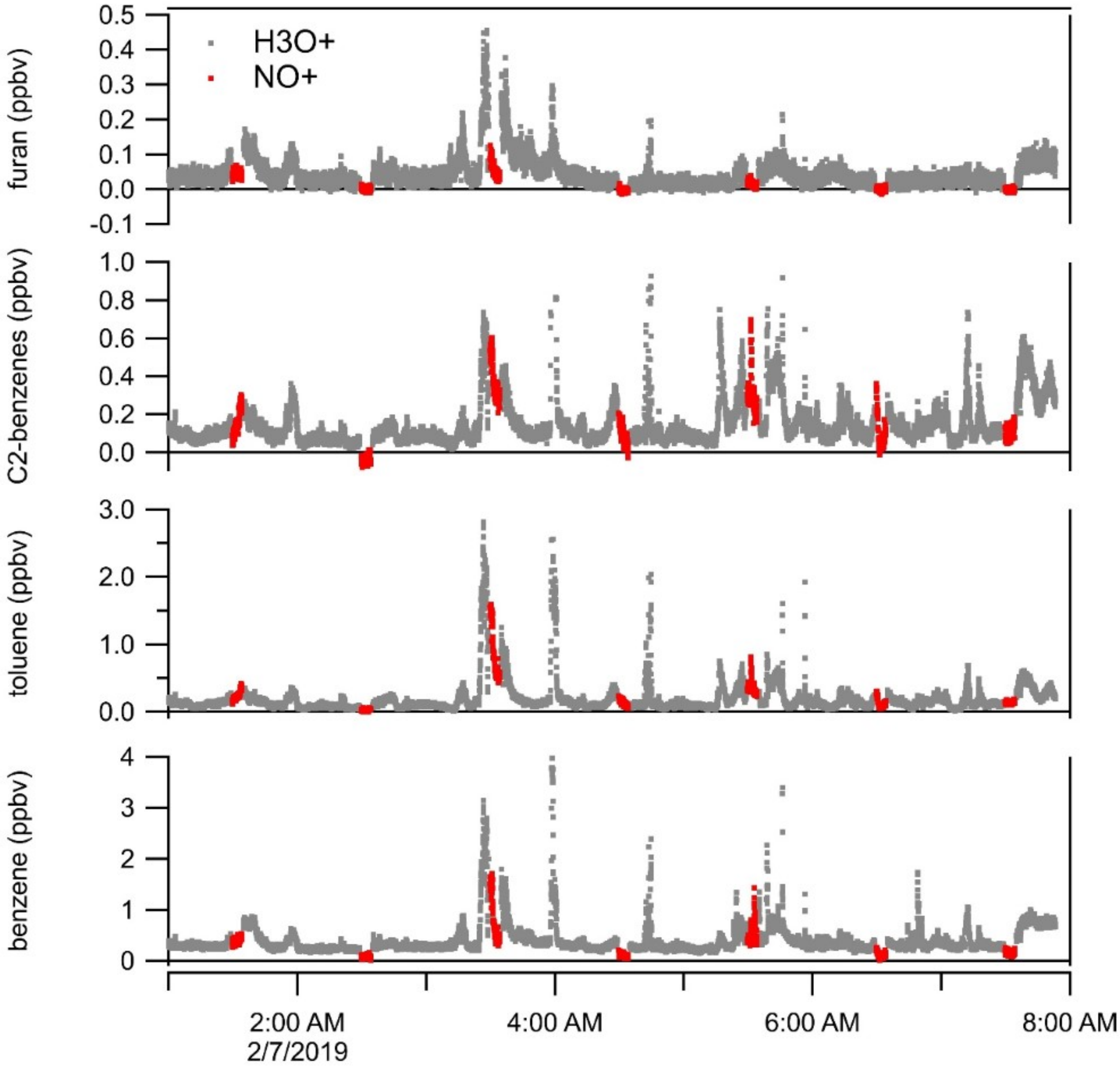

Figure 6-35. Observations of Benzene, Toluene, C$_2$-benzenes, and Furan in H$_3$O$^+$ and NO$^+$ Modes at Site 6 on January 6, 2019.

6.15 Recommendations and Considerations

Due to requiring different peak tables, collecting both H$_3$O$^+$ and NO$^+$ data will require twice the data processing time than just collecting in one mode. In addition, the time required for analysis will double at a minimum.

- Automated switching between NO$^+$ and H$_3$O$^+$ modes can complicate the live interpretation of data and has potential to cause issues with the live mass calibration. Manually switching limits these issues, but will require additional training, procedures, and result in minor data loss.

- NO^+ mode only provides better data for a small set of analytes at the expense of losing information for a large list of analytes. Implementation of NO^+ mode will likely result in supplemental data to H_3O^+ monitoring.

- Operating in NO^+ mode requires its own zero/sensitivity check. This means two would be performed if both H_3O^+ and NO^+ modes are utilized.

- If time resolution is not critical, the strengths of multiple ion modes can be combined using IONICON's Automated Measurement and Evaluation (AME) software. In this mode of operation, an instrument cycles between many different ionization modes and compares all results to a library of standard spectra for pure substances to make use of the most effective quantification approach and gain additional qualitative assignments to peaks that suffer interference. Setting up an AME requires some time to build the appropriate library and limits time resolution to no faster than about 2 minutes but alleviates the concerns in the bullets above. Partially quality assured (QA'd) data is made available immediately so live interpretation is stronger than normal operation and automation is easy to proceduralize.

7.0 QUALITY ASSESSMENT

During the January 14, 2019, to February 9, 2019, monitoring campaign, quality control procedures were followed by the TerraGraphics Vapor Team: Data Collection and Data Processing. Data were collected and quality documents completed according to Procedure 66409-RPT-004. All data were accepted, processed, and reported according to the Procedure 17124-DOE-HS-102, "Mobile Laboratory Data Processing – Analysis." All exceptions have been noted and any potential quality-affecting issues were resolved prior to report or are noted in this report. All potential quality-affecting deviations have been captured in Deficiency Reports (DRs) and are summarized below with some interpretation.

During the January 14, 2019, to February 9, 2019, monitoring campaign, there were five (5) DRs. DR19-001 documents the failed zero air and sensitivity checks on the PTR-MS on January 14, 2019. DR19-002 records the instance of a full data hard drive on January 16, 2019, which resulted in 5 to 6 hours of unsaved PTR-MS data. DR19-003 notes an incorrect sampling system configuration recorded in 66409-RPT-004 for Thermosorb-N cartridges. DR19-004 documents an unexpected closure of the DAQFactory program on February 5, 2019. DR19-005 addresses two events of a frozen screen on the PTR-MS software on January 31, 2019 and February 2, 2019. See Appendix C for the full deficiency reports.

During the January 14, 2019, to February 9, 2019, monitoring campaign, there were two (2) Nonconformance Reports. NCR19-001 documents the PTR-MS experiencing periods of increased instrument baseline readings. NCR19-002 records the same increase in instrument background discussed in NCR19-001 which returned on 01/28/19. See Appendix D for the full Nonconformance Reports.

7.1 Lessons Learned – DR19-001

On January 14, 2019, the PTR-MS failed its daily zero and sensitivity check which prompted the ML Operators to contact the SME. The SME remotely logged into the PTR-MS to verify that the instrument was operating correctly. The WRPS Project Manager was notified of the deficiency and instructed to continue with ML data collection. The PTR-MS failed its sensitivity check again on January 15, 2019, and it was determined that a transmission efficiency shift caused the failure. Previously on January 11, 2019, the PTR-MS had been retuned by an IONICON representative and the change was not captured correctly in live data interpretation.

The SME conducted a multi-point VOC calibration, which was used to calculate a new transmission efficiency. This new transmission efficiency was input into the instrument settings before deployment on January 16, 2019. The zero and sensitivity checks on the PTR-MS passed on January 16, 2019, after the new transmission efficiency was applied.

7.2 Lessons Learned – DR19-002

On January 16, 2019, the PTR-MS's data collection hard drive was full and the software was unable to record data properly. This resulted in approximately 5-6 hours of data not being recorded. The SME relocated older PTR-MS files to allow space for new data to be saved. At 22:59, a new file was created (BKG_3_190116_F). During this background study, the PTR-MS has been collecting a high volume of data causing the hard drive storage space to be exhausted more quickly than expected.

Revision 11 of 66409-RPT-004 will include a step for the computer hard drive to be checked by the ML Operators to mitigate occurrences of a full hard drive in the future.

7.3 Lessons Learned – DR19-003

On January 30, 2019, it was determined that the "Alternative Media Sampling" section in procedure 66409-RPT-004 stated the incorrect orientation of Thermosorb-N cartridges. The procedure stated that the cartridges should be attached to the sample line with the "male end facing down (into sample line);" therefore, following the procedure resulted in incorrect installation of the Thermosorb tubes. The consequence of sampling with this orientation is the possibility of getting false positives. The presence of amines or NOx can lead to generation of nitrosamines within the sorbent. Proper orientation of the Thermosorb directs the sample air through an amine trap first, then to the nitrosamine trap. This removes the amines and eliminates the chance of them generating a false positive. To date, no false positives have occurred because none of the Thermosorb results from ALS have been reported above their detection limit.

To avoid further confusion, labels will be added to the sampling system, further training on the correct orientation of the Thermosorbs for ML Operators will occur, and the ML procedure will be changed to reflect the correct installation ("male end facing up (into the sampling line)."

7.4 Lessons Learned – DR19-004

On January 5, 2019, it was discovered that the DAQFactory program had unexpectantly closed at 08:51. After investigation, the SME determined that approximately four hours of data were lost from this closure. The SME restarted the DAQFactory program and it began collecting data again. There are no specific actions identified to preclude recurrence at this time. The reported condition is currently being treated as an anomaly. Should the condition persist, further analysis will be performed to determine the extent of condition and identify appropriate actions to preclude recurrence.

7.5 Lessons Learned – DR19-005

On January 30, 2019, and February 2, 2019, the PTR-MS software froze, stopping the data collection that was in process. In both instances, the PTR-MS was immediately restarted and continued collecting data as normal. There are no specific actions identified to preclude recurrence at this time. The reported condition is currently being treated as an anomaly. Should the condition persist, further analysis will be performed to determine the extent of condition and identify appropriate actions to preclude recurrence.

7.6 Lessons Learned – NCR19-001

During the winter background study, the PTR-MS began experiencing periods of increased instrument baseline readings, as a result of the MCP module not performing to optimal specifications. During increased instrument baseline, the detection limits of the instrument also increased. Data were not affected beyond the increased detection limits and the possibility that the instrument baseline could be misinterpreted as a shift in concentration. The instrument was determined to still be viable and would be monitored routinely to ensure that the issue would not worsen. When increased baseline occurred, the PTR-MS was tuned via the MCP F setting. A new MCP module was installed on January 24, 2019, and tested the following day. With this installation, the SME determined that the PTR-MS was back to normal operation, but that the instrument would continue to be monitored routinely. The client Technical Lead and Quality Assurance Representative were informed of this issue via phone, DR19-001 and DR19-001_Rev. 01, and during the weekly meeting.

7.7 Lessons Learned – NCR19-002

On January 28, 2019, the PTR-MS began experiencing an increase in instrument background, the same as described in NCR19-001. In order to complete the background study, increasing the frequency of monitoring and MCP F tuning was enacted to reduce the intervals of increased instrument background. IONICON suggested an invasive investigation into the issue. After the January 31, 2019, weekly ML discussion meeting, it was determined that these solutions were acceptable as long as the transmission efficiency continued to be resolved. Approval for continued use of the PTR-MS was captured via the phone and the weekly ML discussion meeting.

7.8 Overall Assessment of Data Quality and Quality Assurance Recommendations

All operational anomalies and exceptions of potential negative impact on data quality were documented, addressed, and corrected using root cause analysis. Data presented in this report have passed acceptance criteria.

8.0 CONCLUSION AND RECOMMENDATIONS

The ML was assigned to the following Hanford Site activities:

- Stationary air monitoring at six study sites: five on the secured Hanford Site, one within the City of Kennewick.

The ML was also involved in the following off-site activities in preparation for the background study campaign:

- ML instrument and vehicle maintenance, verifications, and testing.

The TerraGraphics ML operated for 24 days between January 14, 2019, and February 9, 2019, across six study sites ranging from remote, to onsite, to urban influences. During this time, the ML was monitoring 54 COPCs with a focus on a subset of 21 compounds, some of which overlap and are reported as a composite sum. This subset is of interest due to low OELs and historical difficulty with using traditional methods to monitor the Hanford Site. Throughout the course of the study, the site averages for all COPCs never exceeded their respective OELs.

During the AP pump removal on January 24, 2019, there was no response observed in ammonia or nitrosamines. There were spikes in concentration observed for furan and the but-3-en-2-one + 2,3-dihydrofuran + 2,5-dihydrofuran signals; however, all of them were below the OEL and only a few increased above 50% the OEL. There were several diesel generators operating upwind of the ML during the pump removal and the diesel combustion markers had the same pattern of response as observed in the furan and the but-3-en-2-one + 2,3-dihydrofuran + 2,5-dihydrofuran signals. Furan is a known constituent of diesel exhaust which appears to be the only source of COPCs during the duration of this monitoring.

The septic testing on January 30, 2019, was conducted with a primary goal of identifying any large molecular species in addition to the standard source fingerprint analysis. Sampling within the septic tank showed strong signal from methyl mercaptan, dihydrogen sulfide, and the OSC frag at m/z 93 as observed in previous septic emission monitoring. These tests did identify responses at larger masses with m/z 145 being reasonably prominent with a minor but non-negligible response at m/z 201, 223, 239, 281, 297, and 299. Identification of the species causing these responses requires further testing and research. Comparing the resulting septic fingerprint to previous reports also showed some variability among the most abundant species. It appears that methyl mercaptan, dihydrogen sulfide, and the OSC frag at m/z 93 are always present, but their relative abundances are not consistent. This could suggest that there are temporal variations within the septic test and further testing at different times of day, week, and year would provide further insight.

Confirmatory samples were collected for EPA TO-17, EPA TO-11A, and NIOSH Method 2522 analysis by ALS. For the TO-17 results, 68% of the measurements were reported not detectable, which was comparable to the 73% of the PTR-MS measurements simultaneous with confirmatory sample collection being below the detection limit. Acetone, benzene, and toluene had enough detects to warrant further comparison; however, these detects were typically between the MDL and RL which creates some uncertainty leading to poor precision with the TO-17 results. For the TO-11A results, 46% of the measurements were reported not detectable, but

82% of the PTR-MS measurements simultaneous with confirmatory sample collection were below the detection limit. The PTR-MS was experiencing an issue of high instrument baseline, which resulted in a higher estimation of MDLs. Acetone was the only species with enough detects to warrant further comparison, but the conclusion was similar to the TO-17 with the signal generally being between the MDL and RL leading to poor precision with TO-11A results. For the NIOSH 2522 results, none of the ALS or PTR-MS results were above the respective MDLs; therefore, no further comparisons could be made. Overall, the lack of detects greatly reduced the opportunities for comparative analysis. The objective of the study was to quantify ambient background levels, which are expected to be extremely low, so the limited number of detects supports the other data in this report showing a very low background for most of the monitored species. To shed light on isobaric interferences, alternative sampling and analysis methods were used, consisting of NIOSH 2522, EPA TO-17, and EPA TO-11A. While these methods do not provide the same temporal resolution as PTR-MS, they do provide speciation and corroboration of PTR-MS results.

Comparing the averages and standard deviations of the sites during the background study showed that there are only minor differences with background concentrations across all sites being very comparable. Site 6 is expected to have higher averages and variability due to its urban location and from an overall perspective, this held true. The averages and standard deviations were not exclusively the highest for each species. Site 3 showed higher variability for 2-heptylfuran, 6-(2-furanly)-6-methyl-2-heptanone, and furfural acetophenone. The NDEA, 2-methylfuran, and 2,5-dimethylfuran at Site 1 had high averages. Site 5 had some of the lowest averages and variability. Overall, the differences between the sites were relatively minimal and the magnitude of all the averages was very low. Only ammonia saw average concentrations in the ppbv range with everything else being well below 100 pptv. This study further supports the previous observations that the ambient background levels on site are generally in the tens of pptv with some species being even lower.

The comparison of average background concentrations between the different study periods emphasized the difference in FY17 due to the wildfires. However, the FY19 fall and winter study averages exceeded the averages in FY17 for NDEA, 2-heptylfuran, 6-(2-furanyl)-6-methyl-2-heptanone, and furfural acetophenone. The FY18 study generally showed the lowest averages with the FY19 winter study being comparable except for the four species just mentioned.

Collecting NO^+ data throughout the background study provided a great deal of insight into its capabilities and drawbacks. Of the 20 species initially investigated in 53005-81-RPT-039, only three were determined to have a high feasibility (1,3-butadiene, furan, NDMA) for NO^+ mode monitoring. The five aromatics tested (benzene, toluene, p-xylene, 1,3,5-trimethylbenzene, 1,2,3,5-tetramethylbenzene) showed a reasonable response and demonstrated the NO^+ monitoring of aromatics is feasible, but H_3O^+ mode is still preferred. When monitoring at the urban Site 6, the NO^+ furan, benzene, toluene, and C_2-benzenes meshed well with their H_3O^+ counterparts demonstrating that NO^+ mode operation for these species can capture trends and producing similar results in a dynamic environment.

The following recommendations are offered for consideration for future septic tank monitoring:

- The high concentrations within the tank resulted in some saturation. In the time since this test was performed, a sample dilution system has been developed and tested that allows the ML Operators to eliminate or reduce any saturation. The sample dilution system should be utilized for sampling within the septic tank or under circumstances that result in high concentrations.

The following recommendations are offered for consideration concerning future NO^+ monitoring (as stated previously in Section 6.0):

- Automated switching between NO^+ and H_3O^+ modes can complicate the live interpretation of data and has potential to cause issues with the live mass calibration. Manually switching limits these issues, but will require additional training, procedures, and result in minor data loss.

- NO^+ mode only provides better data for a small set of analytes at the expense of losing information for a large list of analytes. Implementation of NO^+ mode will likely be as supplemental data to H_3O^+ monitoring.

- Operating in NO^+ mode requires its own zero/sensitivity check. This means two would be performed if both H_3O^+ and NO^+ modes are utilized.

- If time resolution is not critical, the strengths of multiple ion modes can be combined using IONICON’s AME software. In this mode of operation, an instrument cycles between many different ionization modes and compares all results to a library of standard spectra for pure substances to make use of the most effective quantification approach and gain additional qualitative assignments to peaks that suffer interference. Setting up an AME requires some time to build the appropriate library and limits time resolution to no faster than about 2 minutes but alleviates the concerns in the bullets above. Partially QA’d data are made available immediately; therefore, live interpretation is stronger than normal operation and automation is easy to proceduralize.

9.0 REFERENCES

17124-DOE-HS-102, 2018, “Mobile Laboratory Data Processing – Analysis,” Revision 2, TerraGraphics Environmental Engineering, Inc., Pasco, Washington.

53005-81-RPT-007, 2018, *PTR-MS Mobile Laboratory Vapor Monitoring Background Study, (3/18/2018 – 4/20/2018)*, Revision 0, TerraGraphics Environmental Engineering, Inc., Pasco, Washington.

53005-81-RPT-027, 2018, *PTR-MS Mobile Laboratory Vapor Monitoring Monthly Report – Month 2*, Revision A, TerraGraphics Environmental Engineering, Inc., Pasco, Washington.

53005-81-RPT-039, 2018, *PTR-MS Mobile Laboratory Vapor Monitoring Monthly Report – Month 4*, Revision A, TerraGraphics Environmental Engineering, Inc., Pasco, Washington.

66409-18-ML-003, 2018, *Sampling Manifold Sketch*, TerraGraphics Environmental Engineering, Inc., Pasco, Washington.

66409-18-ML-004, 2018, *Mobile Lab Schematics*, TerraGraphics Environmental Engineering, Inc., Pasco, Washington.

66409-RPT-003, 2018, *Mobile Laboratory Operational Acceptance Testing Plan*, Revision 0, TerraGraphics Environmental Engineering, Inc., Pasco, Washington.

66409-RPT-004, 2018, *Mobile Laboratory Operational Procedure*, Revisions 9 and 10, TerraGraphics Environmental Engineering, Inc., Pasco, Washington.

66409-RPT-007, 2018, *Mobile Laboratory Operational Project Test Plan FY2019 (Test Plan)*, Revision 0, TerraGraphics Environmental Engineering, Inc., Pasco, Washington.

EPA TO-11A, 1999, “Determination of Formaldehyde in Ambient Air Using Adsorbent Cartridge Followed by High Performance Liquid Chromatography (HPLC),” U.S. Environmental Protection Agency, Washington, D.C.

EPA TO-17, 1999, “Determination of Volatile Organic Compounds in Ambient Air Using Active Sampling Onto Sorbent Tubes,” U.S. Environmental Protection Agency, Washington, D.C.

Fiscal Year 2017 Mobile Laboratory Vapor Monitoring at the Hanford Site: Monitoring During Waste Disturbing Activities and Background Study, 2017, RJ Lee Group, Inc., Pasco, Washington.

NIOSH 2522, 1994, “Nitrosamines,” National Institute of Occupational Safety and Health, Washington, D.C.

PNNL-27449, 2018, *FY18 Leading Indicator Phase 2 Report*, Pacific Northwest National Laboratory, Richland, Washington.

APPENDIX A

COMPARISON OF PTR-MS TO CONFIRMATORY SAMPLES

The table below shows comparison between Carbotrap-300 sorbent samples as analyzed by TO--17 modified and average PTR-MS data taken over the corresponding time period as the sample was drawn. Reporting limits for TO-17 modified analysis were provided by ALS. Reporting limits for PTR-MS were calculated using a Method Detection Limit Study, as described in Section 4.2.

Table A-1. Key.

🟨	Tentatively Identified Compound (TIC)
▨	between RL and MDL
🟧	Non-Detect (ND)
🟥	ND of a TIC

Table A-2. Comparison of TO-17 Results to Proton Transfer Reaction – Mass Spectrometer for Selected Analytes. (2 Sheets)

Date Taken	Study Site	Media Type	Analyte	ALS RL (ppbv)	PTR RL (ppbv)	ALS Result (ppbv)	PTR Avg. Result (ppbv)	Relative % diff
01/14/2019	Site 1	Carbotrap-300	benzene	0.078	0.690	0.097	0.108	N/A
			acetone	0.105	1.196	0.422	0.419	0.604
			toluene	0.066	0.183	ND	0.068	N/A
01/16/2019	Site 3	Carbotrap-300	benzene	0.101	0.690	0.154	0.122	23.019
			acetone	0.136	1.196	0.534	0.470	12.680
			toluene	0.086	0.183	0.110	0.093	17.003
01/18/2019	Site 5	Carbotrap-300	benzene	0.081	0.690	0.171	0.121	N/A
			acetone	0.109	1.196	2.132	0.614	110.621
			toluene	0.069	0.183	0.250	0.085	98.380
01/21/2019	Site 2	Carbotrap-300	benzene	0.081	0.690	0.091	0.112	N/A
			acetone	0.109	1.196	0.871	0.266	N/A
			toluene	0.069	0.183	0.439	0.165	90.909
01/23/2019	Site 4	Carbotrap-300	benzene	0.081	0.690	0.177	0.098	N/A
			acetone	0.108	1.196	0.520	0.322	N/A
			toluene	0.068	0.183	0.115	0.065	55.004
01/28/2019	Site 3	Carbotrap-300	benzene	0.079	0.690	0.217	0.079	N/A
			acetone	0.106	1.196	0.718	0.384	N/A
			toluene	0.067	0.183	0.128	0.059	N/A
01/30/2019	Site 5	Carbotrap-300	benzene	0.079	0.690	0.384	0.188	N/A
			acetone	0.106	1.196	1.192	0.645	59.518
			toluene	0.067	0.183	0.349	0.165	71.533

Table A-2. Comparison of TO-17 Results to Proton Transfer Reaction – Mass Spectrometer for Selected Analytes. (2 Sheets)

Date Taken	Study Site	Media Type	Analyte	ALS RL (ppbv)	PTR RL (ppbv)	ALS Result (ppbv)	PTR Avg. Result (ppbv)	Relative % diff
01/31/2019	Site 6 (Blank)	Carbotrap-300	benzene	N/A	0.690	ND	N/A	N/A
			acetone	N/A	1.196	ND	N/A	N/A
			toluene	N/A	0.183	ND	N/A	N/A
01/31/2019	Site 6	Carbotrap-300	benzene	0.080	0.690	0.544	0.355	42.181
			acetone	0.108	1.196	1.506	0.709	71.934
			toluene	0.068	0.183	0.950	0.356	90.947
01/31/2019	Site 6 (Duplicate)	Carbotrap-300	benzene	0.080	0.690	0.512	0.355	40.721
			acetone	0.108	1.196	1.720	0.709	76.017
			toluene	0.068	0.183	1.139	0.356	90.610
02/01/2019	Site 1	Carbotrap-300	benzene	0.080	0.690	0.209	0.138	N/A
			acetone	0.108	1.196	0.993	0.446	76.017
			toluene	0.068	0.183	0.128	0.048	N/A
02/02/2019	Site 2	Carbotrap-300	benzene	0.081	0.690	0.239	0.075	N/A
			acetone	0.109	1.196	1.216	0.486	85.808
			toluene	0.063	0.183	0.271	0.074	114.520
02/04/2019	Site 4	Carbotrap-300	benzene	0.079	0.690	0.224	0.140	N/A
			acetone	0.106	1.196	0.551	0.331	N/A
			toluene	0.067	0.183	0.086	0.034	N/A
02/06/2019	Site 6	Carbotrap-300	benzene	0.079	0.690	0.472	0.292	47.062
			acetone	0.106	1.196	1.101	0.558	65.493
			toluene	0.067	0.183	0.801	0.114	150.223
02/06/2019	Site 6 (Duplicate)	Carbotrap-300	benzene	0.078	0.690	0.470	0.292	46.582
			acetone	0.105	1.196	1.180	0.558	71.584
			toluene	0.066	0.183	0.744	0.114	146.904
02/07/2019	Site 3	Carbotrap-300	benzene	0.078	0.690	ND	0.154	N/A
			acetone	0.105	1.196	0.544	0.492	10.102
			toluene	0.066	0.183	ND	0.033	N/A

The table below shows comparison between Thermosorb-N samples as analyzed by NIOSH 2522 modified and average PTR-MS data taken over the corresponding time period as the sample was drawn. Reporting limits for TO-17 modified analysis were provided by ALS. Reporting limits for PTR-MS were calculated using a Method Detection Limit Study, as described in Section 4.2.

Table A-3. Comparison of NIOSH 2522 Results to PTR-MS. (2 Sheets)

Date Taken	Study Site	Media Type	Analyte	ALS RL (ppbv)	PTR RL (ppbv)	ALS Result (ppbv)	PTR Avg. Result (ppbv)	Relative % diff
01/26/2019	Site 1	Thermosorb	NDEA	0.012	0.069	ND	0.007	N/A
			NDMA	0.008	0.060	ND	0.011	N/A
			NEMA	0.007	0.082	ND	0.010	N/A
			NMOR	0.005	0.050	ND	0.003	N/A
01/27/2019	Site 2	Thermosorb	NDEA	0.012	0.069	ND	0.007	N/A
			NDMA	0.008	0.060	ND	0.007	N/A
			NEMA	0.007	0.082	ND	0.008	N/A
			NMOR	0.005	0.050	ND	0.004	N/A
01/27/2019	Site 2 (Duplicate)	Thermosorb	NDEA	0.012	0.069	ND	0.007	N/A
			NDMA	0.008	0.060	ND	0.007	N/A
			NEMA	0.007	0.082	ND	0.008	N/A
			NMOR	0.005	0.050	ND	0.004	N/A
01/27/2019	Site 3 (Blank)	Thermosorb	NDEA	0.012	0.069	ND	N/A	N/A
			NDMA	0.008	0.060	ND	N/A	N/A
			NEMA	0.007	0.082	ND	N/A	N/A
			NMOR	0.005	0.050	ND	N/A	N/A
01/29/2019	Site 4	Thermosorb	NDEA	0.012	0.069	ND	0.006	N/A
			NDMA	0.008	0.060	ND	0.004	N/A
			NEMA	0.007	0.082	ND	0.006	N/A
			NMOR	0.005	0.050	ND	0.003	N/A
01/30/2019	Site 5	Thermosorb	NDEA	0.012	0.069	ND	0.006	N/A
			NDMA	0.008	0.060	ND	0.005	N/A
			NEMA	0.007	0.082	ND	0.007	N/A
			NMOR	0.005	0.050	ND	0.003	N/A
01/31/2019	Site 6	Thermosorb	NDEA	0.012	0.069	ND	0.006	N/A
			NDMA	0.008	0.060	ND	0.017	N/A
			NEMA	0.007	0.082	ND	0.011	N/A
			NMOR	0.005	0.050	ND	0.007	N/A

Table A-3. Comparison of NIOSH 2522 Results to PTR-MS. (2 Sheets)

Date Taken	Study Site	Media Type	Analyte	ALS RL (ppbv)	PTR RL (ppbv)	ALS Result (ppbv)	PTR Avg. Result (ppbv)	Relative % diff
02/01/2019	Site 1	Thermosorb	NDEA	0.012	0.069	ND	0.005	N/A
			NDMA	0.008	0.060	ND	0.011	N/A
			NEMA	0.007	0.082	ND	0.009	N/A
			NMOR	0.005	0.050	ND	0.009	N/A
02/02/2019	Site 2	Thermosorb	NDEA	0.012	0.069	ND	0.005	N/A
			NDMA	0.008	0.060	ND	0.003	N/A
			NEMA	0.007	0.082	ND	0.004	N/A
			NMOR	0.005	0.050	ND	0.003	N/A
02/03/2019	Site 3	Thermosorb	NDEA	0.012	0.069	ND	0.004	N/A
			NDMA	0.008	0.060	ND	0.003	N/A
			NEMA	0.007	0.082	ND	0.003	N/A
			NMOR	0.005	0.050	ND	0.003	N/A
02/04/2019	Site 4	Thermosorb	NDEA	0.012	0.069	ND	0.004	N/A
			NDMA	0.008	0.060	ND	0.003	N/A
			NEMA	0.007	0.082	ND	0.004	N/A
			NMOR	0.005	0.050	ND	0.003	N/A
02/05/2019	Site 5	Thermosorb	NDEA	0.012	0.069	ND	0.004	N/A
			NDMA	0.008	0.060	ND	0.003	N/A
			NEMA	0.007	0.082	ND	0.004	N/A
			NMOR	0.005	0.050	ND	0.002	N/A
02/06/2019	Site 6	Thermosorb	NDEA	0.012	0.069	ND	0.004	N/A
			NDMA	0.008	0.060	ND	0.003	N/A
			NEMA	0.007	0.082	ND	0.004	N/A
			NMOR	0.005	0.050	ND	0.002	N/A
02/06/2019	Site 6	Thermosorb	NDEA	0.012	0.069	ND	0.004	N/A
			NDMA	0.008	0.060	ND	0.003	N/A
			NEMA	0.007	0.082	ND	0.004	N/A
			NMOR	0.005	0.050	ND	0.004	N/A
02/07/2019	Site 3	Thermosorb	NDEA	0.012	0.069	ND	0.004	N/A
			NDMA	0.008	0.060	ND	0.003	N/A
			NEMA	0.007	0.082	ND	0.004	N/A
			NMOR	0.005	0.050	ND	0.004	N/A

The table below shows comparison between DNPH sorbent samples as analyzed by TO-11A modified and average PTR-MS data taken over the corresponding time period as the sample was drawn. Reporting limits for TO-17 modified analysis were provided by ALS. Reporting limits for PTR-MS were calculated using a Method Detection Limit Study, as described in Section 4.2.

Table A-4. Comparison of TO-11A Results to PTR-MS. (3 Sheets)

Date Taken	Study Site	Media Type	Analyte	ALS RL (ppbv)	PTR-MS RL (ppbv)	ALS Result (ppbv)	PTR-MS Avg. Result (ppbv)	% diff
01/14/2019	1	LpDNPH	Formaldehyde	0.205	3.907	ND	0.359	N/A
			Acetaldehyde	0.140	6.209	ND	0.828	N/A
			Acetone	0.106	1.196	0.87	0.498	-54.236%
			Acrolein	0.110	0.943	ND	0.095	N/A
			Butyraldehyde	0.085	0.190	ND	0.063	N/A
01/16/2019	3	LpDNPH	Formaldehyde	0.210	3.907	0.33	0.398	N/A
			Acetaldehyde	0.143	6.209	0.34	0.687	N/A
			Acetone	0.109	1.196	1.54	0.465	-107.269%
			Acrolein	0.112	0.943	ND	0.075	N/A
			Butyraldehyde	0.087	0.190	ND	0.058	N/A
01/18/2019	5	LpDNPH	Formaldehyde	0.211	3.907	0.97	0.337	N/A
			Acetaldehyde	0.144	6.209	0.72	0.605	N/A
			Acetone	0.109	1.196	1.42	0.569	-85.452%
			Acrolein	0.113	0.943	ND	0.074	N/A
			Butyraldehyde	0.088	0.190	ND	0.059	N/A
01/21/2019	2	LpDNPH	Formaldehyde	0.211	3.907	0.31	0.335	N/A
			Acetaldehyde	0.144	6.209	0.43	0.417	N/A
			Acetone	0.109	1.196	1.68	0.241	N/A
			Acrolein	0.113	0.943	ND	0.044	N/A
			Butyraldehyde	0.088	0.190	ND	0.038	N/A
01/23/2019	4	LpDNPH	Formaldehyde	0.209	3.907	0.38	0.308	N/A
			Acetaldehyde	0.142	6.209	0.60	0.462	N/A
			Acetone	0.108	1.196	0.89	0.308	N/A
			Acrolein	0.112	0.943	ND	0.045	N/A
			Butyraldehyde	0.087	0.190	ND	0.043	N/A

Table A-4. Comparison of TO-11A Results to PTR-MS. (3 Sheets)

Date Taken	Study Site	Media Type	Analyte	ALS RL (ppbv)	PTR-MS RL (ppbv)	ALS Result (ppbv)	PTR-MS Avg. Result (ppbv)	% diff
01/28/2019	3	LpDNPH	Formaldehyde	0.205	3.907	0.82	0.272	N/A
			Acetaldehyde	0.140	6.209	0.78	0.437	N/A
			Acetone	0.106	1.196	0.64	0.405	-44.317%
			Acrolein	0.110	0.943	ND	0.040	N/A
			Butyraldehyde	0.085	0.190	ND	0.034	N/A
01/31/2019	6		Formaldehyde	0.209	3.907	0.54	0.488	-41.062%
		LpDNPH	Acetaldehyde	0.143	6.209	0.43	1.041	N/A
			Acetone	0.108	1.196	1.02	0.671	N/A
			Acrolein	0.112	0.943	ND	0.111	N/A
			Butyraldehyde	0.087	0.190	ND	0.075	N/A
01/31/2019	6 (Duplicate)	LpDNPH	Formaldehyde	0.210	3.907	2.01	0.488	N/A
			Acetaldehyde	0.143	6.209	1.20	1.041	N/A
			Acetone	0.108	1.196	1.65	0.671	-84.181%
			Acrolein	0.112	0.943	ND	0.111	N/A
			Butyraldehyde	0.087	0.190	ND	0.075	N/A
01/31/2019	6 (Blank)	LpDNPH	Formaldehyde	0.210	3.907	ND	N/A	N/A
			Acetaldehyde	0.143	6.209	ND	N/A	N/A
			Acetone	0.108	1.196	ND	N/A	N/A
			Acrolein	0.112	0.943	ND	N/A	N/A
			Butyraldehyde	0.087	0.190	ND	N/A	N/A
02/01/2019	1	LpDNPH	Formaldehyde	0.209	3.907	0.54	0.235	N/A
			Acetaldehyde	0.143	6.209	0.74	0.414	N/A
			Acetone	0.108	1.196	0.74	0.447	-48.867%
			Acrolein	0.112	0.943	ND	0.036	N/A
			Butyraldehyde	0.087	0.190	ND	0.038	N/A
02/02/2019	2	LpDNPH	Formaldehyde	0.211	3.907	0.93	0.228	N/A
			Acetaldehyde	0.144	6.209	0.69	0.425	N/A
			Acetone	0.109	1.196	0.61	0.493	-21.424%
			Acrolein	0.113	0.943	ND	0.047	N/A
			Butyraldehyde	0.088	0.190	ND	0.035	N/A

Table A-4. Comparison of TO-11A Results to PTR-MS. (3 Sheets)

Date Taken	Study Site	Media Type	Analyte	ALS RL (ppbv)	PTR-MS RL (ppbv)	ALS Result (ppbv)	PTR-MS Avg. Result (ppbv)	% diff
02/04/2019	4	LpDNPH	Formaldehyde	0.207	3.907	ND	0.262	N/A
			Acetaldehyde	0.141	6.209	0.59	0.320	N/A
			Acetone	0.107	1.196	1.18	0.326	N/A
			Acrolein	0.111	0.943	ND	0.031	N/A
			Butyraldehyde	0.086	0.190	ND	0.034	N/A
02/05/2019	5	LpDNPH	Formaldehyde	0.207	3.907	0.46	0.278	N/A
			Acetaldehyde	0.141	6.209	0.59	0.329	N/A
			Acetone	0.107	1.196	1.87	0.409	-128.074%
			Acrolein	0.111	0.943	ND	0.034	N/A
			Butyraldehyde	0.086	0.190	ND	0.039	N/A
02/06/2019	6	LpDNPH	Formaldehyde	0.206	3.907	0.37	0.243	N/A
			Acetaldehyde	0.140	6.209	0.56	0.376	N/A
			Acetone	0.106	1.196	1.08	0.637	-51.902%
			Acrolein	0.110	0.943	ND	0.109	N/A
			Butyraldehyde	0.086	0.190	ND	0.033	N/A
02/06/2019	6	LpDNPH	Formaldehyde	0.206	3.907	2.06	0.243	N/A
			Acetaldehyde	0.140	6.209	1.37	0.376	N/A
			Acetone	0.106	1.196	2.55	0.637	-120.027%
			Acrolein	0.110	0.943	ND	0.109	N/A
			Butyraldehyde	0.086	0.190	ND	0.033	N/A
02/07/2019	3	LpDNPH	Formaldehyde	0.204	3.907	0.61	0.294	N/A
			Acetaldehyde	0.139	6.209	0.69	0.418	N/A
			Acetone	0.105	1.196	1.83	0.498	-114.538%
			Acrolein	0.109	0.943	ND	0.047	N/A
			Butyraldehyde	0.085	0.190	ND	0.038	N/A

APPENDIX B

SITE COMPARISONS ADDITIONAL PLOTS

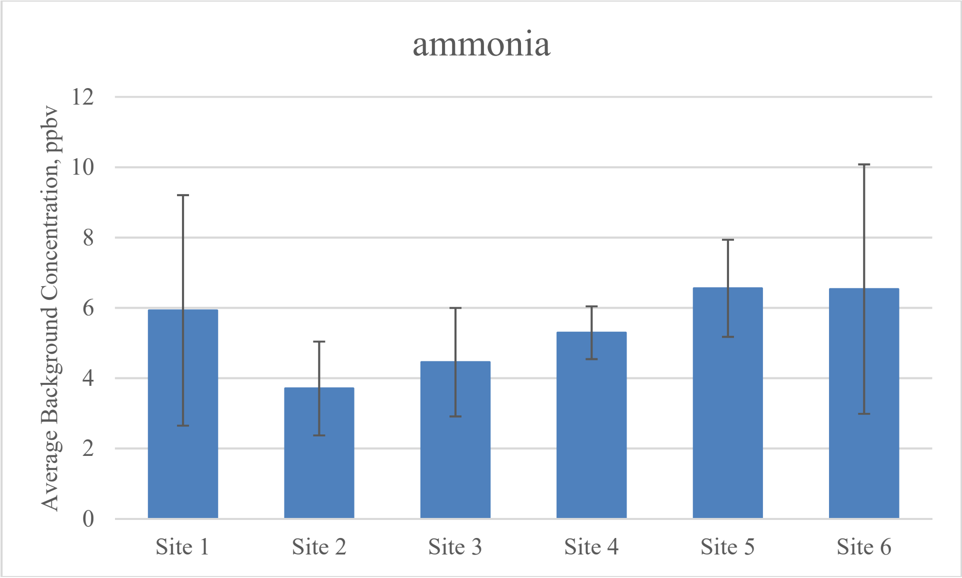
ammonia
Average Background Concentration, ppbv
0
2
4
6
8
10
12
Site 1
Site 2
Site 3
Site 4
Site 5
Site 6

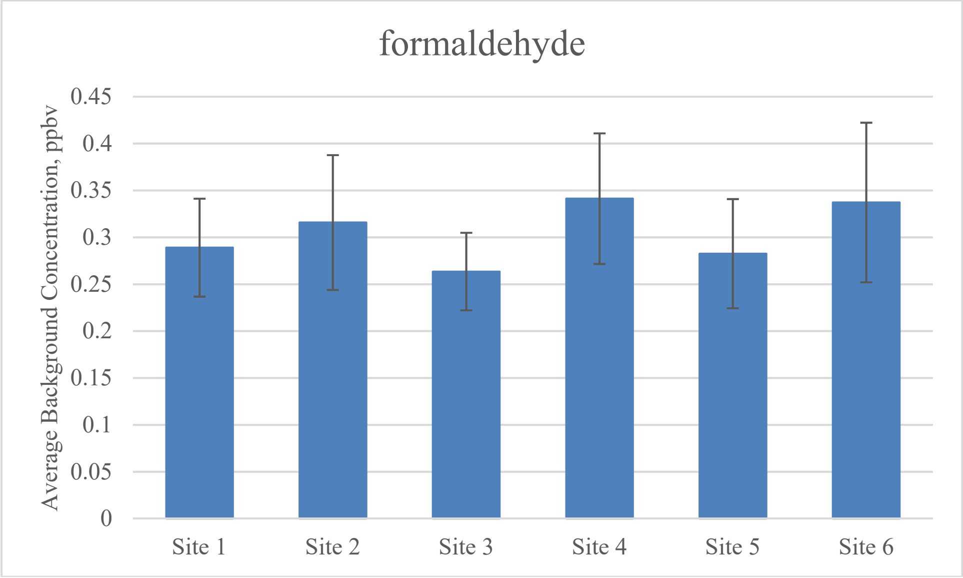
formaldehyde
Average Background Concentration, ppbv
0
0.05
0.1
0.15
0.2
0.25
0.3
0.35
0.4
0.45
Site 1
Site 2
Site 3
Site 4
Site 5
Site 6

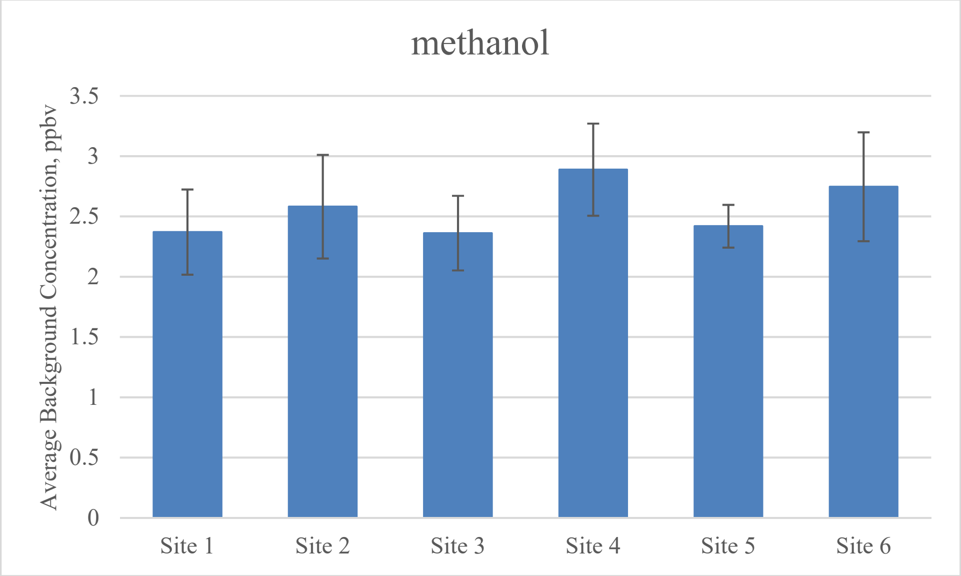
methanol
Average Background Concentration, ppbv
3.5
3
2.5
2
1.5
1
0.5
0
Site 1
Site 2
Site 3
Site 4
Site 5
Site 6

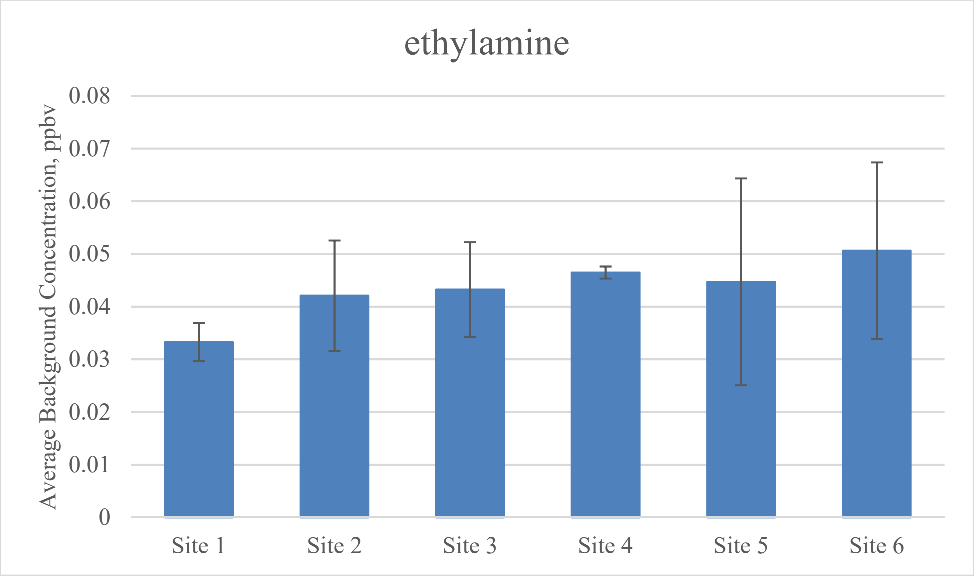
ethylamine
Average Background Concentration, ppbv
0.08
0.07
0.06
0.05
0.04
0.03
0.02
0.01
0
Site 1
Site 2
Site 3
Site 4
Site 5
Site 6

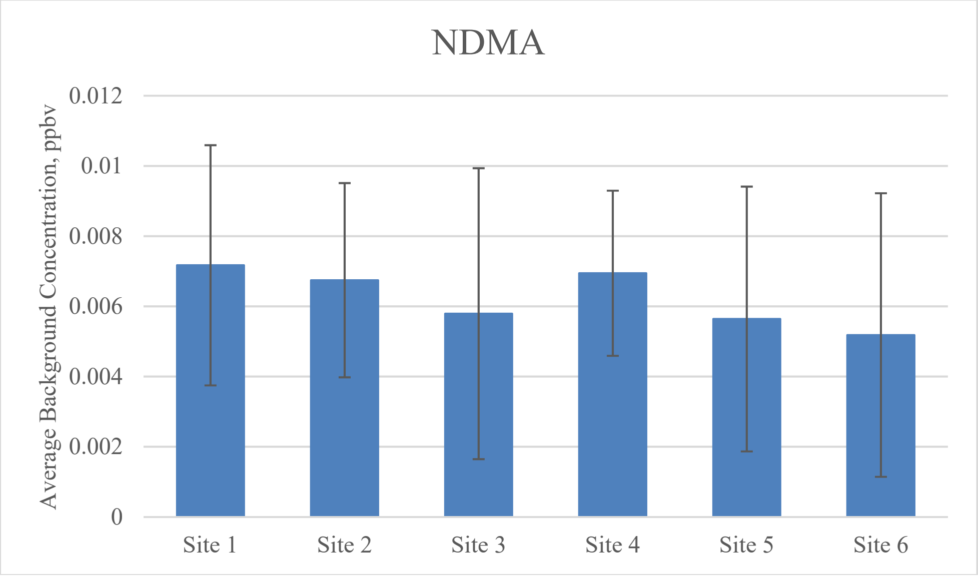
NDMA
Average Background Concentration, ppbv
0.012
0.01
0.008
0.006
0.004
0.002
0
Site 1
Site 2
Site 3
Site 4
Site 5
Site 6

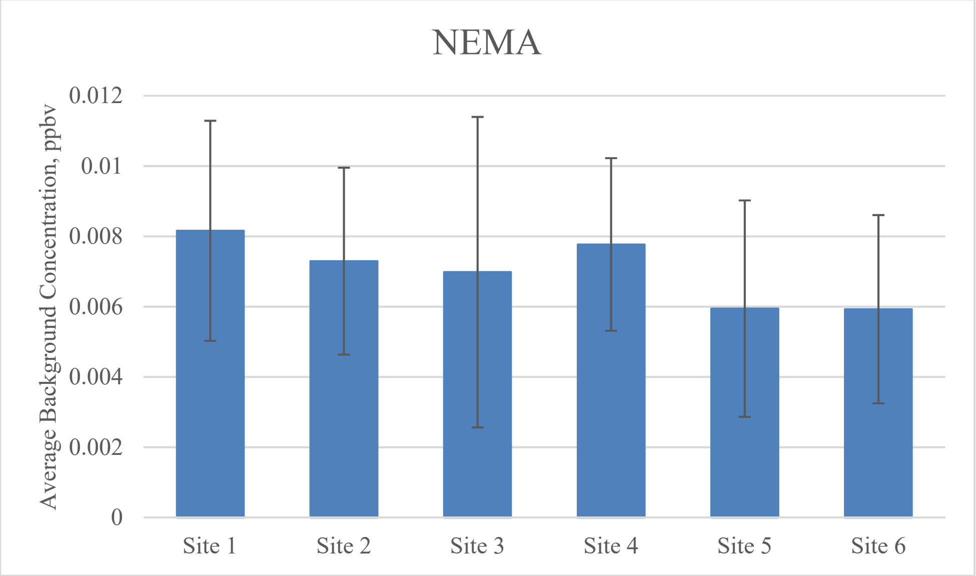
NEMA
Average Background Concentration, ppbv
0.012
0.01
0.008
0.006
0.004
0.002
0
Site 1
Site 2
Site 3
Site 4
Site 5
Site 6

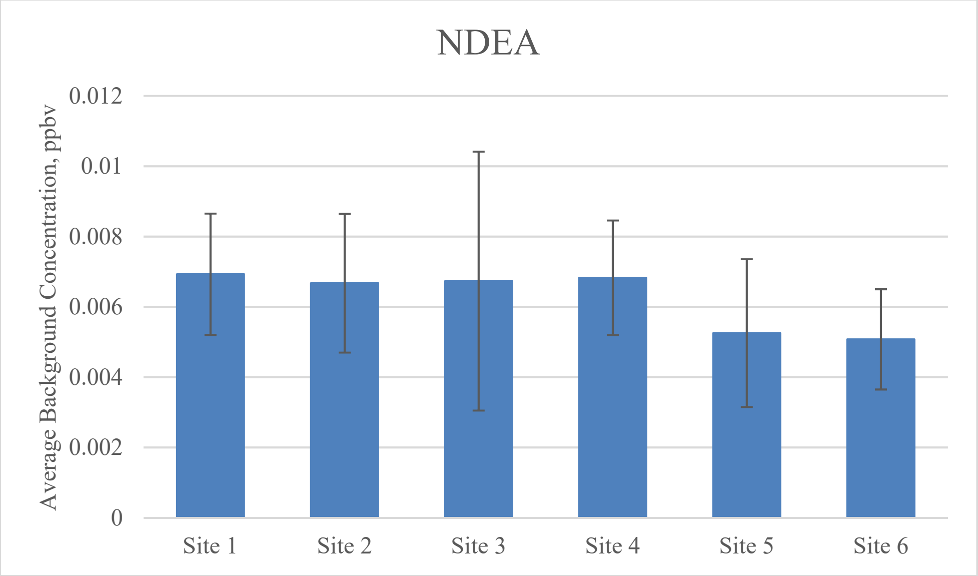
NDEA
Average Background Concentration, ppbv
0.012
0.01
0.008
0.006
0.004
0.002
0
Site 1
Site 2
Site 3
Site 4
Site 5
Site 6


NMOR
Average Background Concentration, ppbv
0.004
0.0035
0.003
0.0025
0.002
0.0015
0.001
0.0005
0
Site 1
Site 2
Site 3
Site 4
Site 5
Site 6

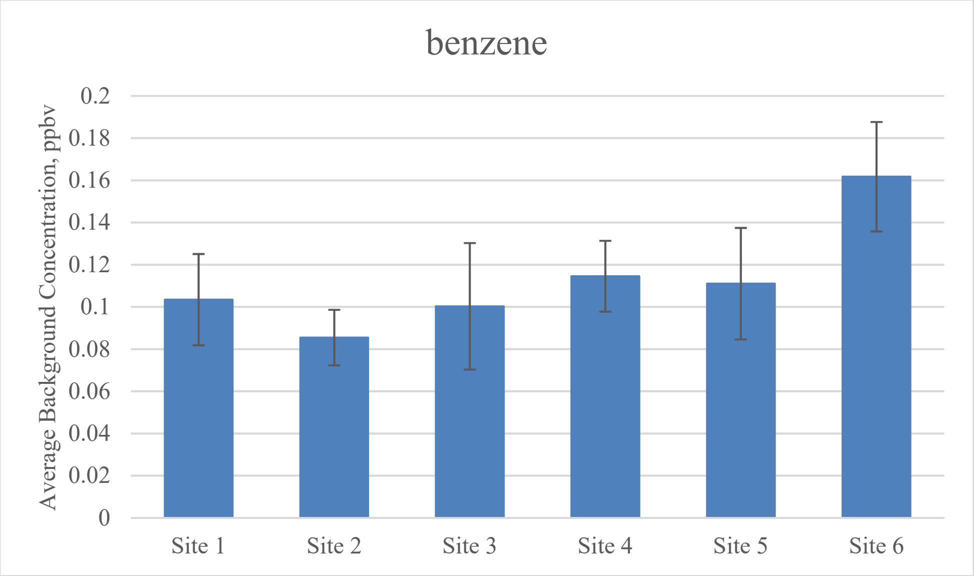
benzene
Average Background Concentration, ppbv
0.2
0.18
0.16
0.14
0.12
0.1
0.08
0.06
0.04
0.02
0
Site 1
Site 2
Site 3
Site 4
Site 5
Site 6

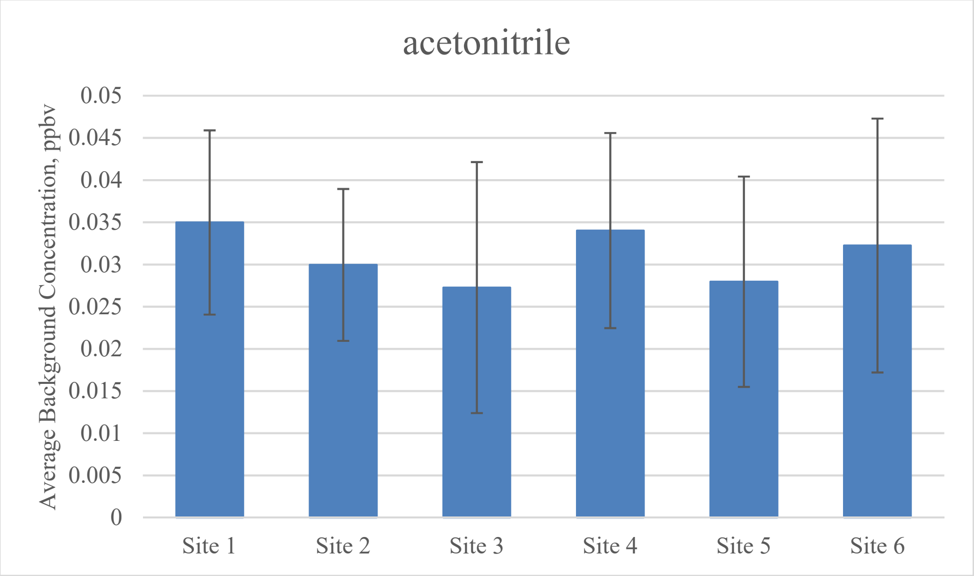
acetonitrile
Average Background Concentration, ppbv
0.05
0.045
0.04
0.035
0.03
0.025
0.02
0.015
0.01
0.005
0
Site 1
Site 2
Site 3
Site 4
Site 5
Site 6

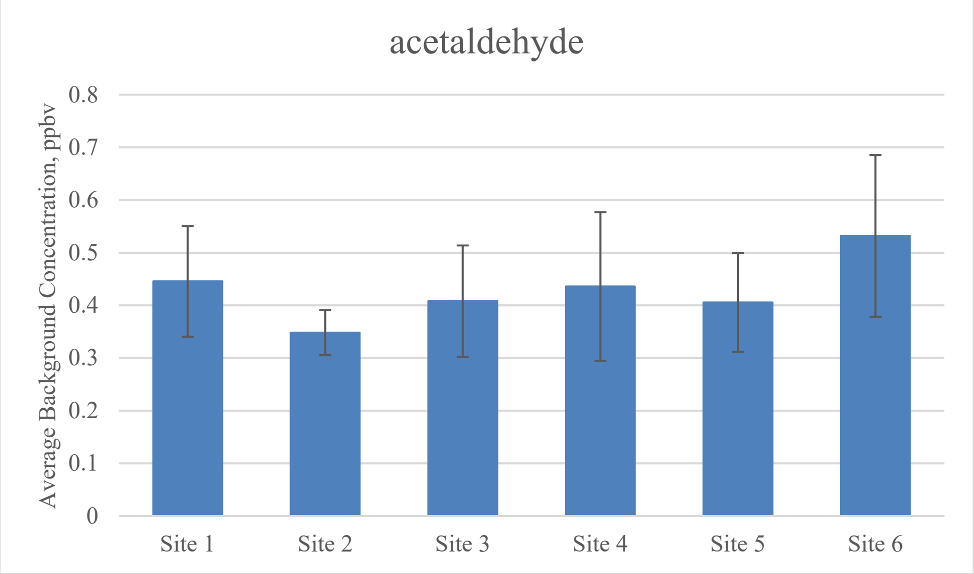
acetaldehyde
Average Background Concentration, ppbv
0.8
0.7
0.6
0.5
0.4
0.3
0.2
0.1
0
Site 1
Site 2
Site 3
Site 4
Site 5
Site 6

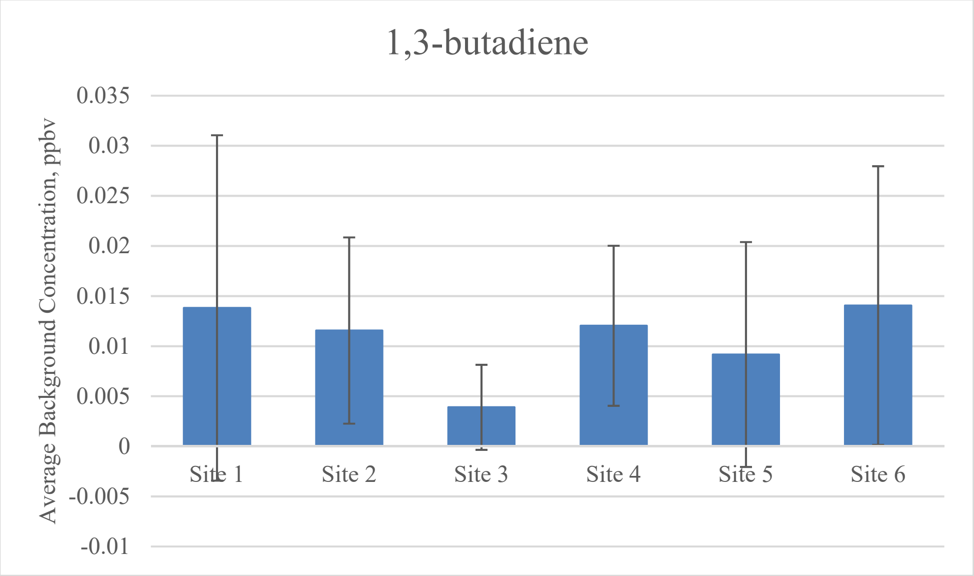
1,3-butadiene
Average Background Concentration, ppbv
0.035
0.03
0.025
0.02
0.015
0.01
0.005
0
-0.005
-0.01
Site 1
Site 2
Site 3
Site 4
Site 5
Site 6

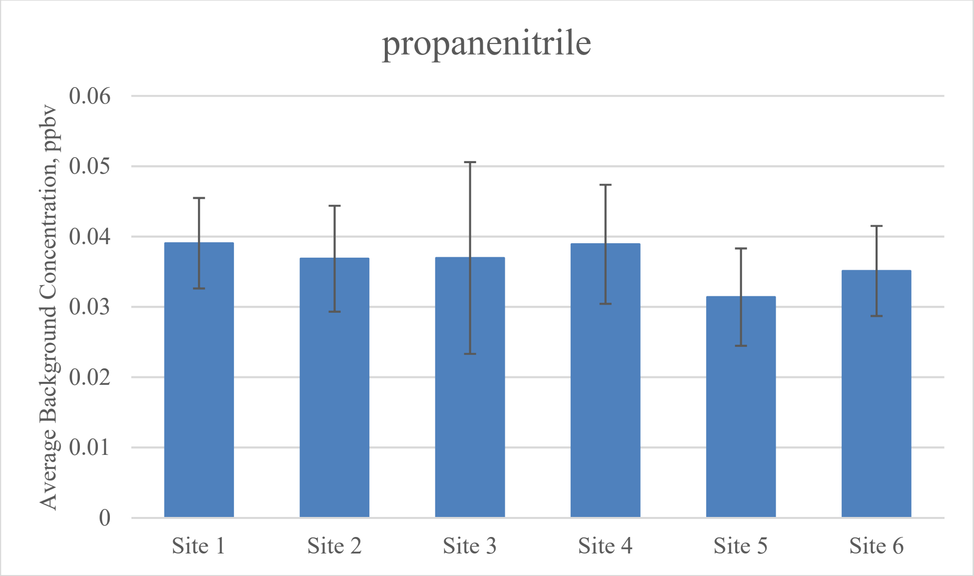
propanenitrile
Average Background Concentration, ppbv
0.06
0.05
0.04
0.03
0.02
0.01
0
Site 1
Site 2
Site 3
Site 4
Site 5
Site 6

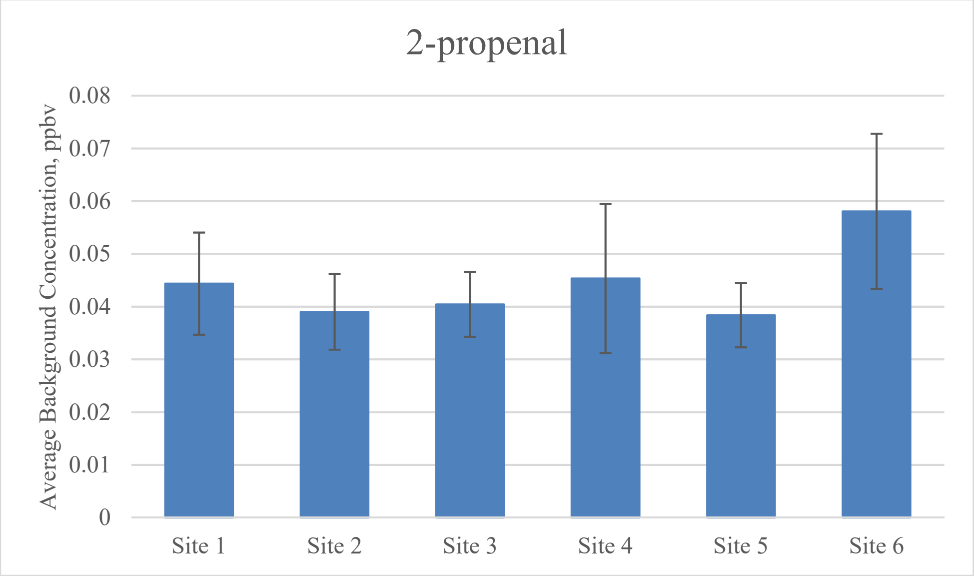
2-propenal
Average Background Concentration, ppbv
0.08
0.07
0.06
0.05
0.04
0.03
0.02
0.01
0
Site 1
Site 2
Site 3
Site 4
Site 5
Site 6

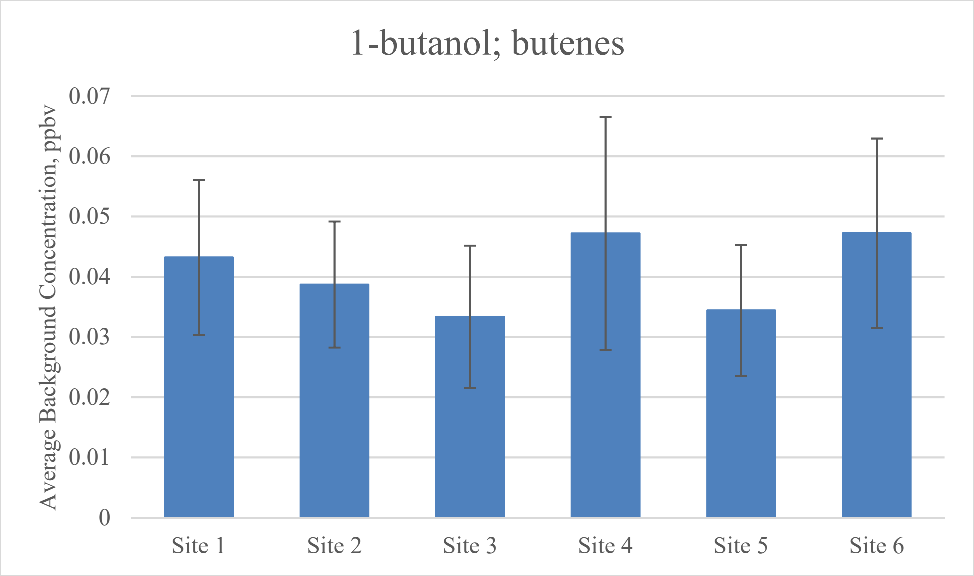
1-butanol; butenes
Average Background Concentration, ppbv
0.07
0.06
0.05
0.04
0.03
0.02
0.01
0
Site 1
Site 2
Site 3
Site 4
Site 5
Site 6

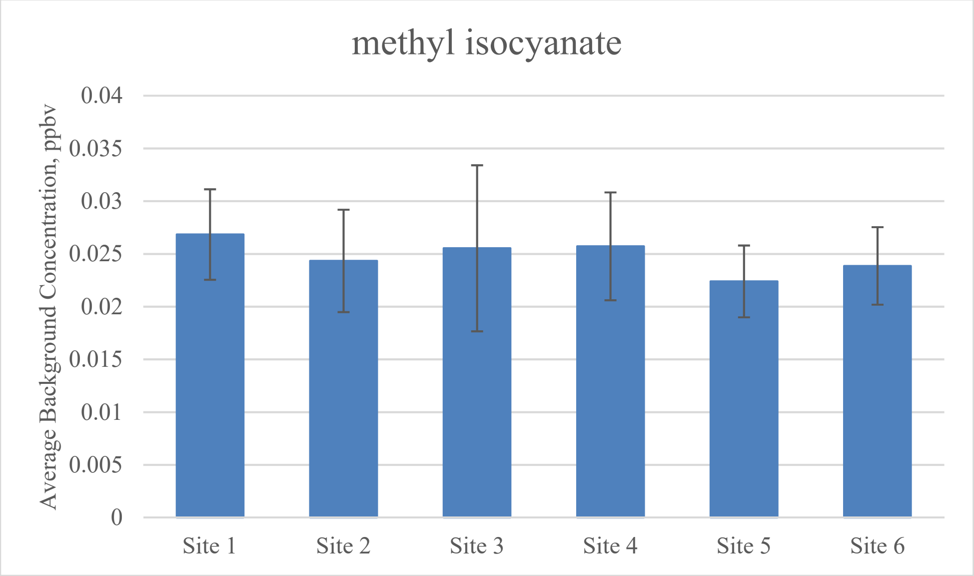
methyl isocyanate
Average Background Concentration, ppbv
0.04
0.035
0.03
0.025
0.02
0.015
0.01
0.005
0
Site 1
Site 2
Site 3
Site 4
Site 5
Site 6

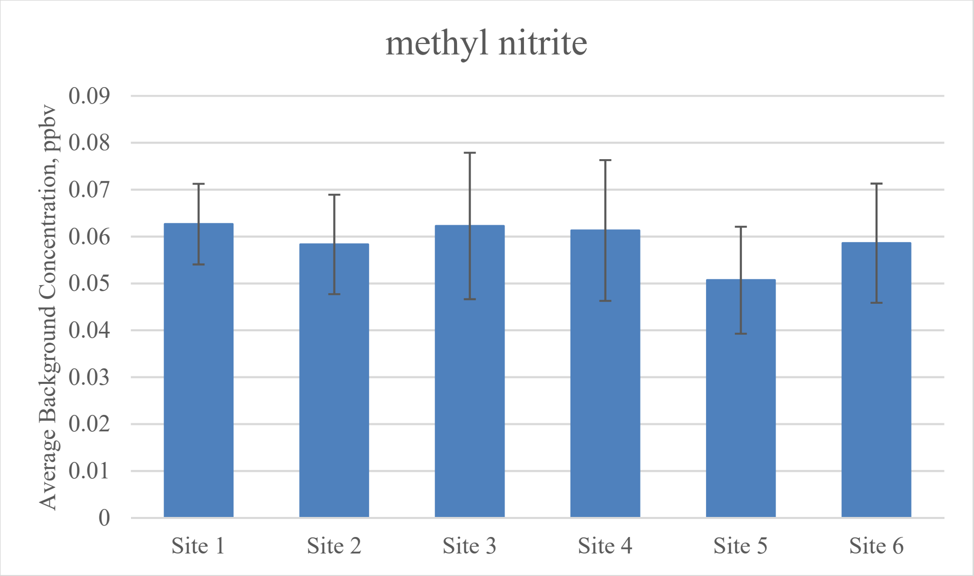
methyl nitrite
Average Background Concentration, ppbv
0.09
0.08
0.07
0.06
0.05
0.04
0.03
0.02
0.01
0
Site 1
Site 2
Site 3
Site 4
Site 5
Site 6

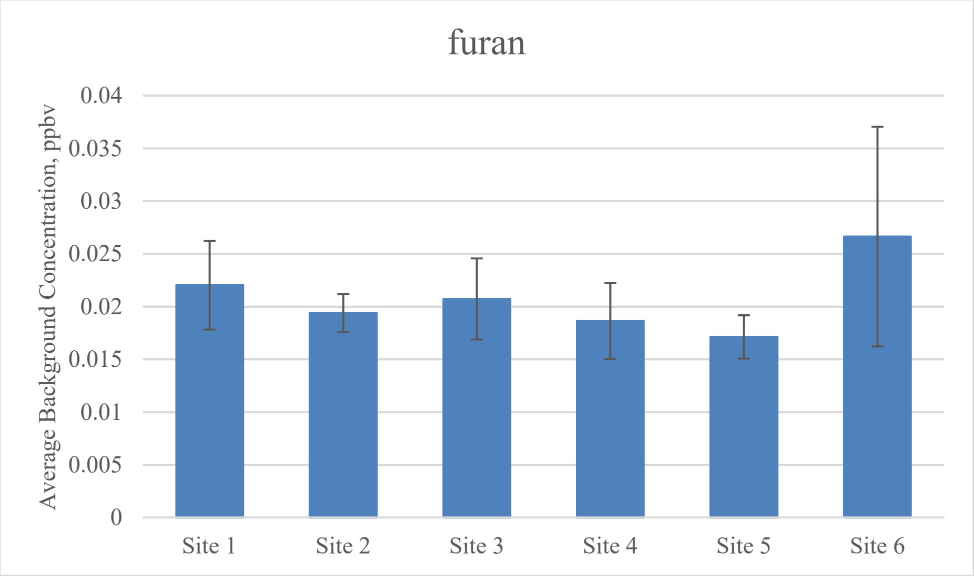
furan
Average Background Concentration, ppbv
0.04
0.035
0.03
0.025
0.02
0.015
0.01
0.005
0
Site 1
Site 2
Site 3
Site 4
Site 5
Site 6

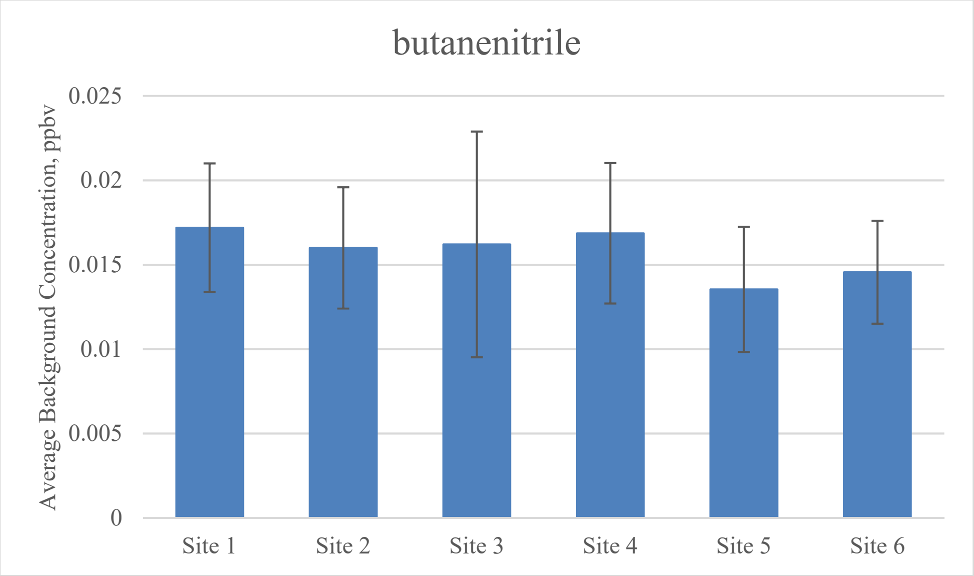
butanenitrile
Average Background Concentration, ppbv
0.025
0.02
0.015
0.01
0.005
0
Site 1
Site 2
Site 3
Site 4
Site 5
Site 6

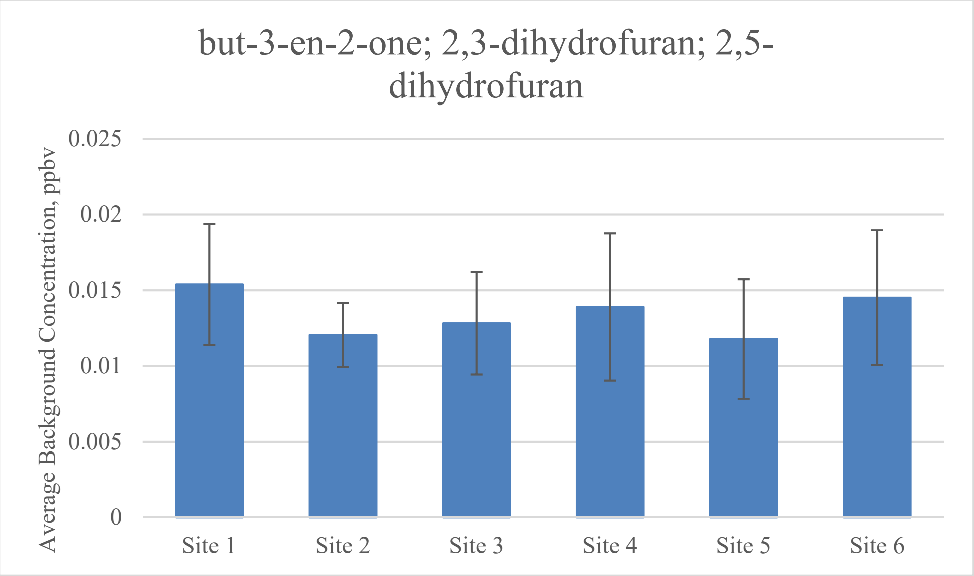
but-3-en-2-one; 2,3-dihydrofuran; 2,5-dihydrofuran
Average Background Concentration, ppbv
0.025
0.02
0.015
0.01
0.005
0
Site 1
Site 2
Site 3
Site 4
Site 5
Site 6

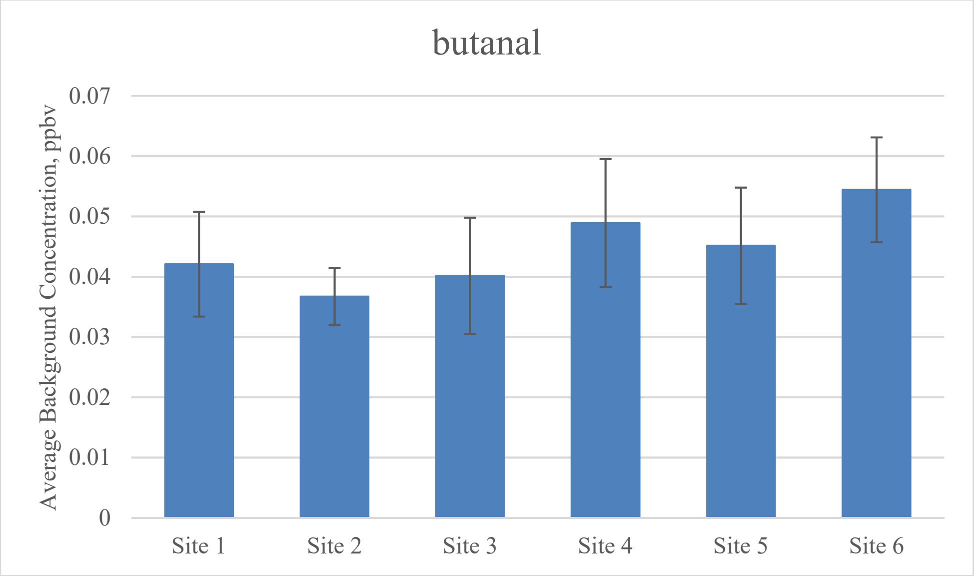
butanal
Average Background Concentration, ppbv
0.07
0.06
0.05
0.04
0.03
0.02
0.01
0
Site 1
Site 2
Site 3
Site 4
Site 5
Site 6

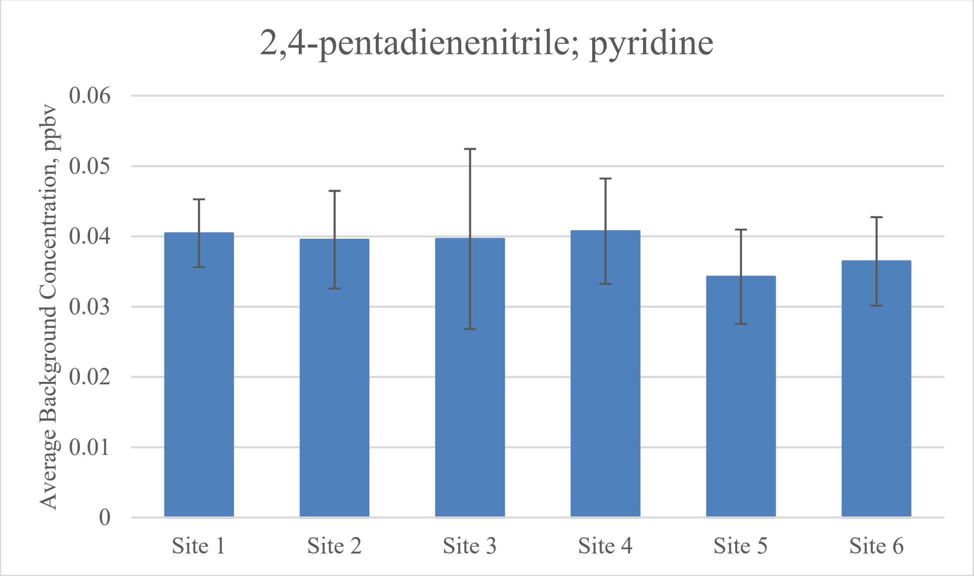
2,4-pentadienenitrile; pyridine
Average Background Concentration, ppbv
0.06
0.05
0.04
0.03
0.02
0.01
0
Site 1
Site 2
Site 3
Site 4
Site 5
Site 6

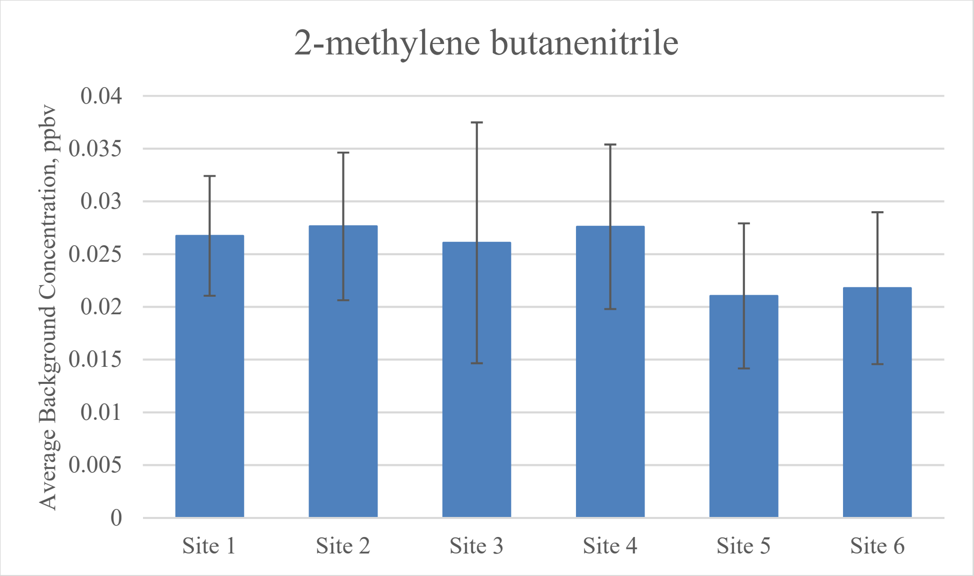
2-methylene butanenitrile
Average Background Concentration, ppbv
0.04
0.035
0.03
0.025
0.02
0.015
0.01
0.005
0
Site 1
Site 2
Site 3
Site 4
Site 5
Site 6

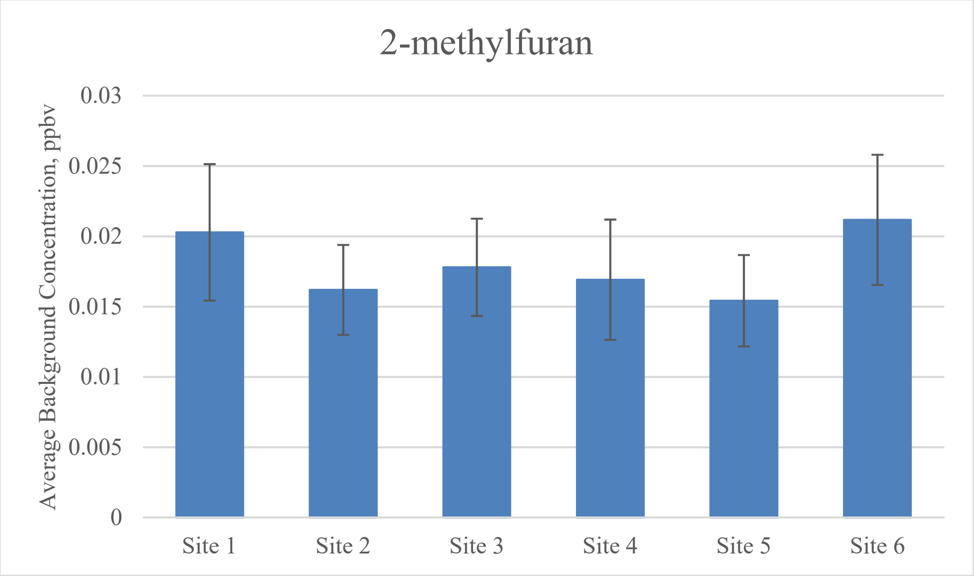
2-methylfuran
Average Background Concentration, ppbv
0.03
0.025
0.02
0.015
0.01
0.005
0
Site 1
Site 2
Site 3
Site 4
Site 5
Site 6

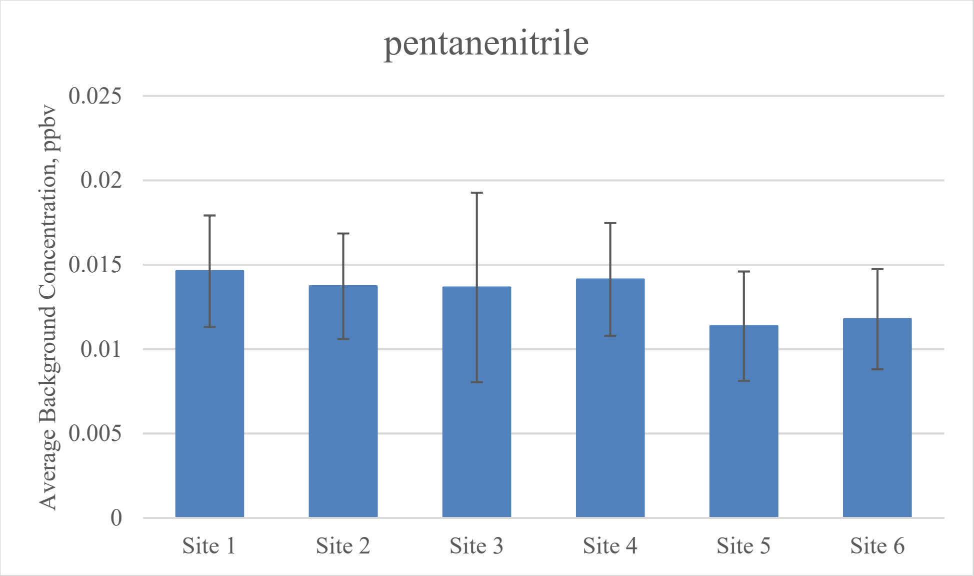
pentanenitrile
Average Background Concentration, ppbv
0.025
0.02
0.015
0.01
0.005
0
Site 1
Site 2
Site 3
Site 4
Site 5
Site 6

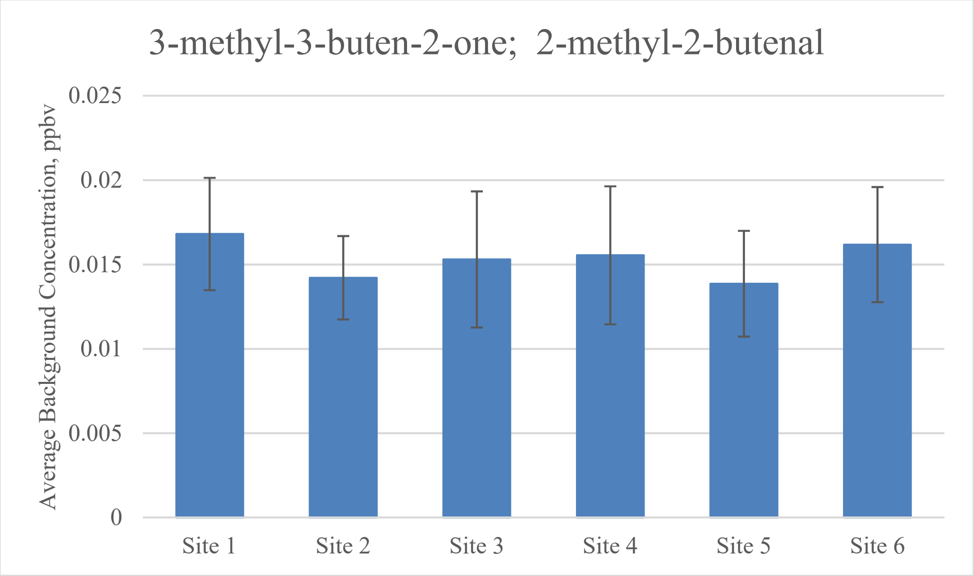
3-methyl-3-buten-2-one; 2-methyl-2-butenal
Average Background Concentration, ppbv
0.025
0.02
0.015
0.01
0.005
0
Site 1
Site 2
Site 3
Site 4
Site 5
Site 6

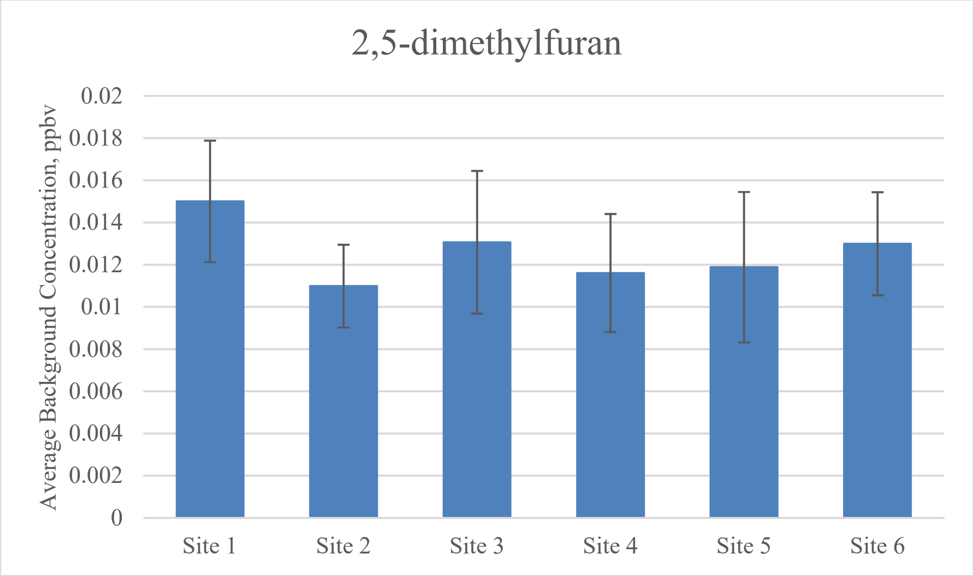
2,5-dimethylfuran
Average Background Concentration, ppbv
0.02
0.018
0.016
0.014
0.012
0.01
0.008
0.006
0.004
0.002
0
Site 1
Site 2
Site 3
Site 4
Site 5
Site 6

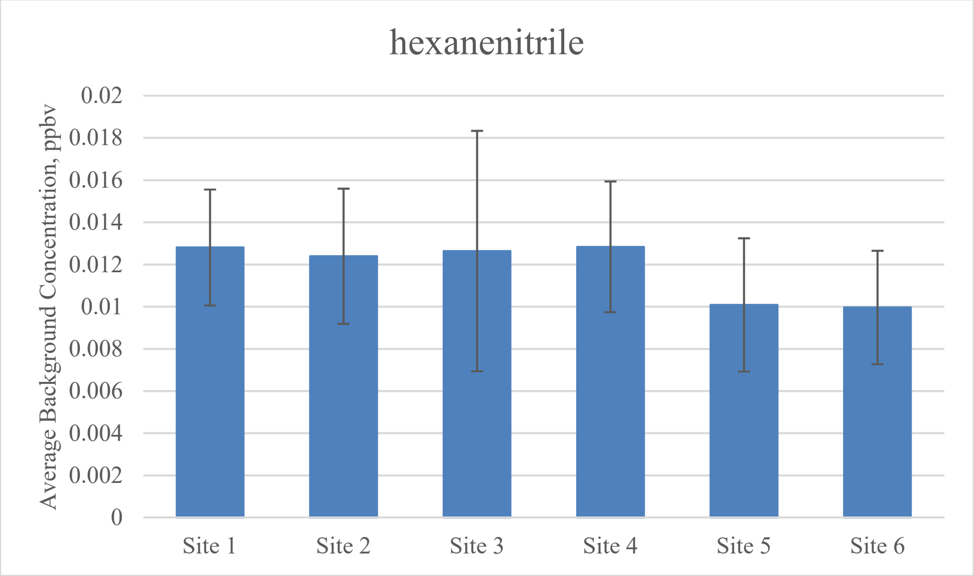
hexanenitrile
Average Background Concentration, ppbv
0.02
0.018
0.016
0.014
0.012
0.01
0.008
0.006
0.004
0.002
0
Site 1
Site 2
Site 3
Site 4
Site 5
Site 6

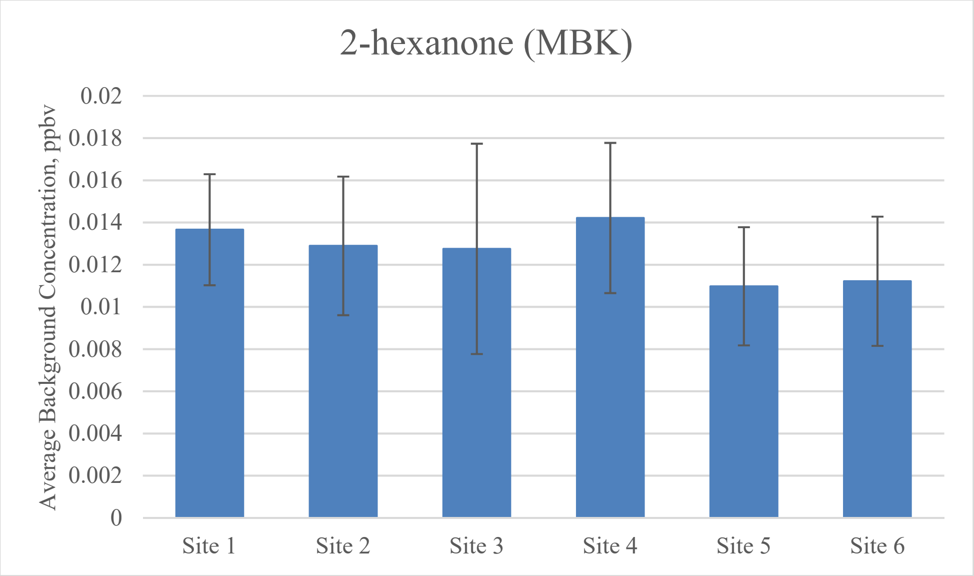
2-hexanone (MBK)
Average Background Concentration, ppbv
0.02
0.018
0.016
0.014
0.012
0.01
0.008
0.006
0.004
0.002
0
Site 1
Site 2
Site 3
Site 4
Site 5
Site 6

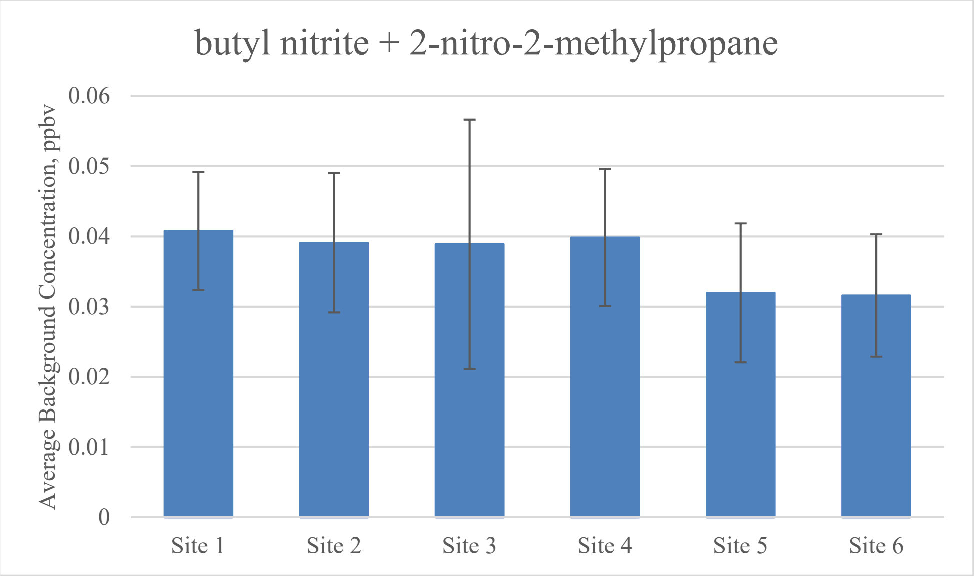
butyl nitrite + 2-nitro-2-methylpropane
Average Background Concentration, ppbv
0.06
0.05
0.04
0.03
0.02
0.01
0
Site 1
Site 2
Site 3
Site 4
Site 5
Site 6

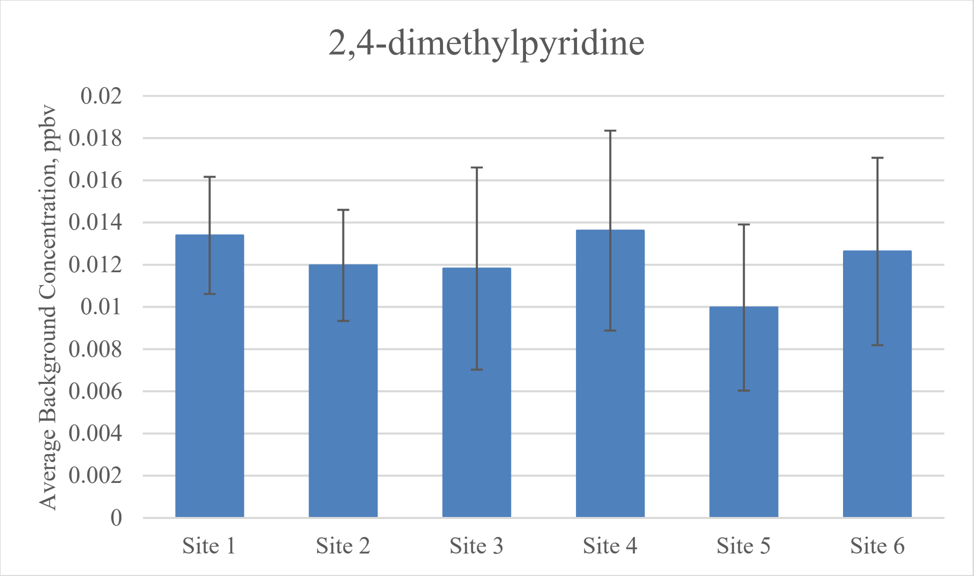
2,4-dimethylpyridine
Average Background Concentration, ppbv
0.02
0.018
0.016
0.014
0.012
0.01
0.008
0.006
0.004
0.002
0
Site 1
Site 2
Site 3
Site 4
Site 5
Site 6

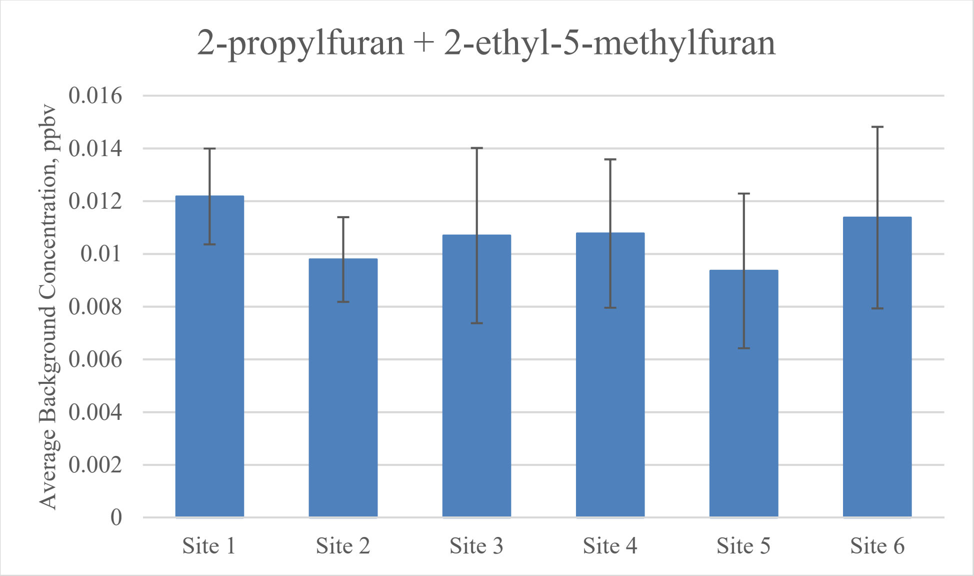
2-propylfuran + 2-ethyl-5-methylfuran
Average Background Concentration, ppbv
0.016
0.014
0.012
0.01
0.008
0.006
0.004
0.002
0
Site 1
Site 2
Site 3
Site 4
Site 5
Site 6

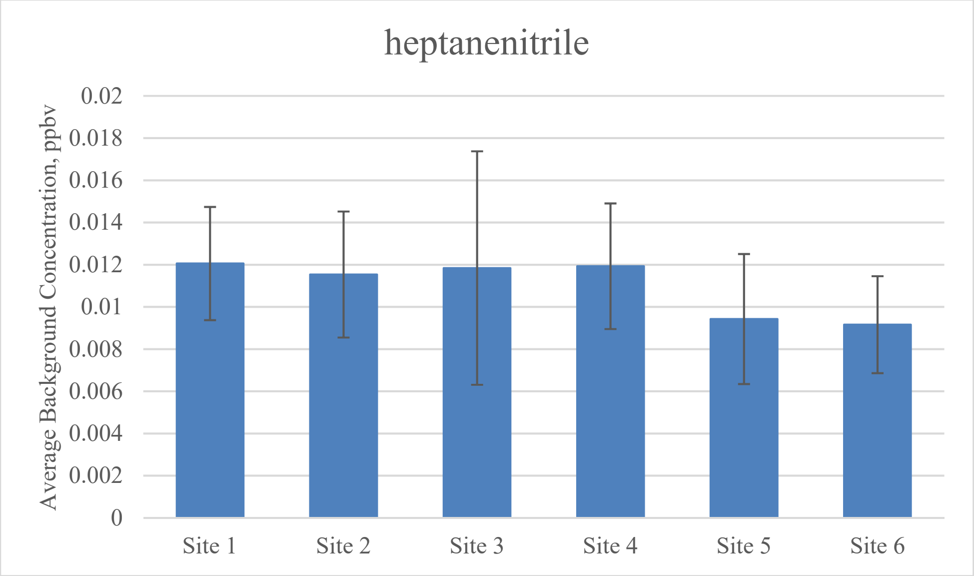
heptanenitrile
Average Background Concentration, ppbv
0.02
0.018
0.016
0.014
0.012
0.01
0.008
0.006
0.004
0.002
0
Site 1
Site 2
Site 3
Site 4
Site 5
Site 6

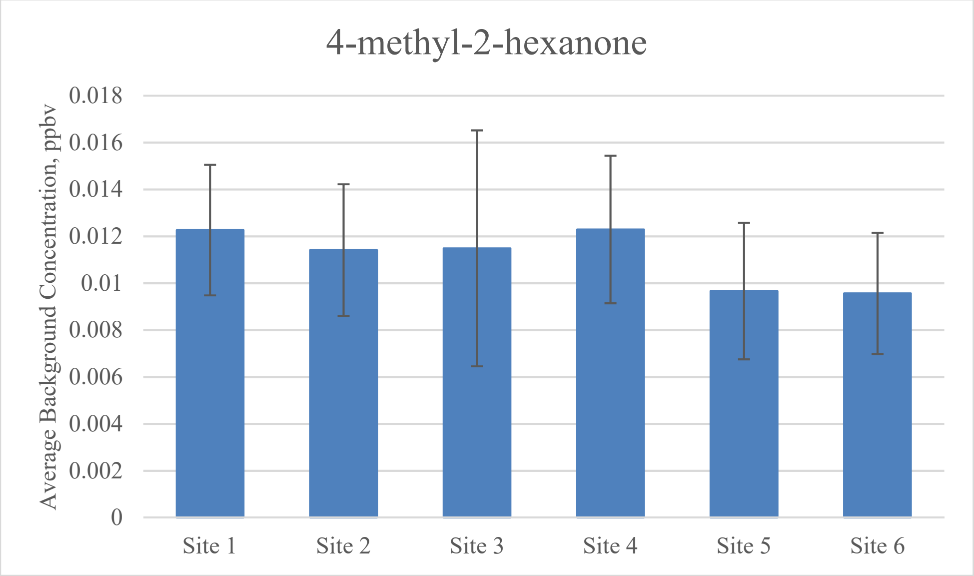
4-methyl-2-hexanone
Average Background Concentration, ppbv
0.018
0.016
0.014
0.012
0.01
0.008
0.006
0.004
0.002
0
Site 1
Site 2
Site 3
Site 4
Site 5
Site 6

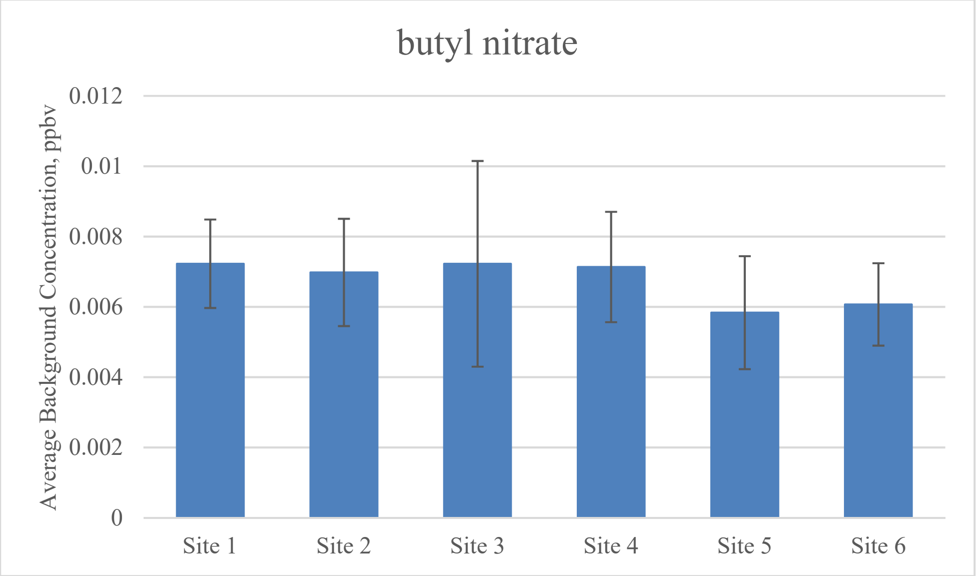
butyl nitrate
Average Background Concentration, ppbv
0.012
0.01
0.008
0.006
0.004
0.002
0
Site 1
Site 2
Site 3
Site 4
Site 5
Site 6

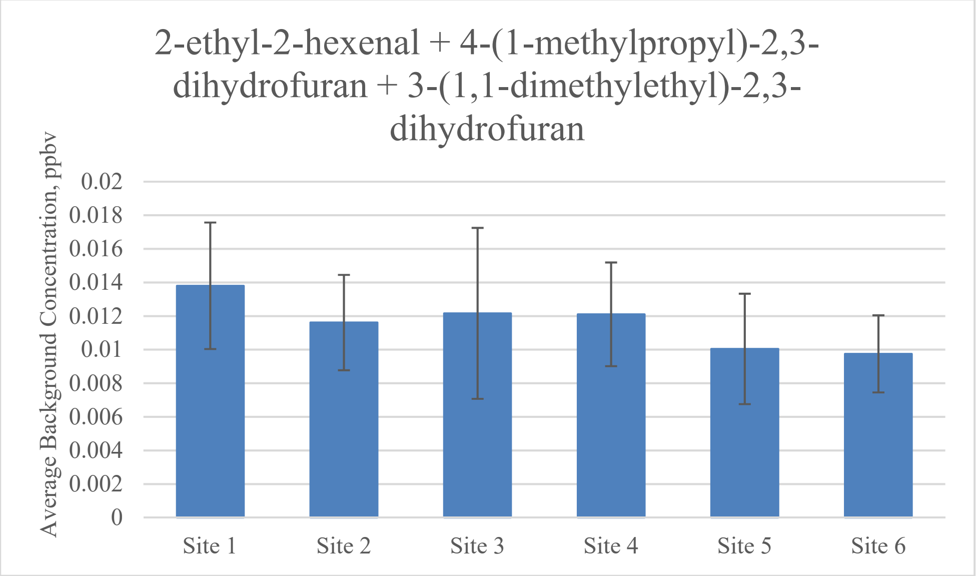
2-ethyl-2-hexenal + 4-(1-methylpropyl)-2,3-dihydrofuran + 3-(1,1-dimethylethyl)-2,3-dihydrofuran
Average Background Concentration, ppbv
0.02
0.018
0.016
0.014
0.012
0.01
0.008
0.006
0.004
0.002
0
Site 1
Site 2
Site 3
Site 4
Site 5
Site 6

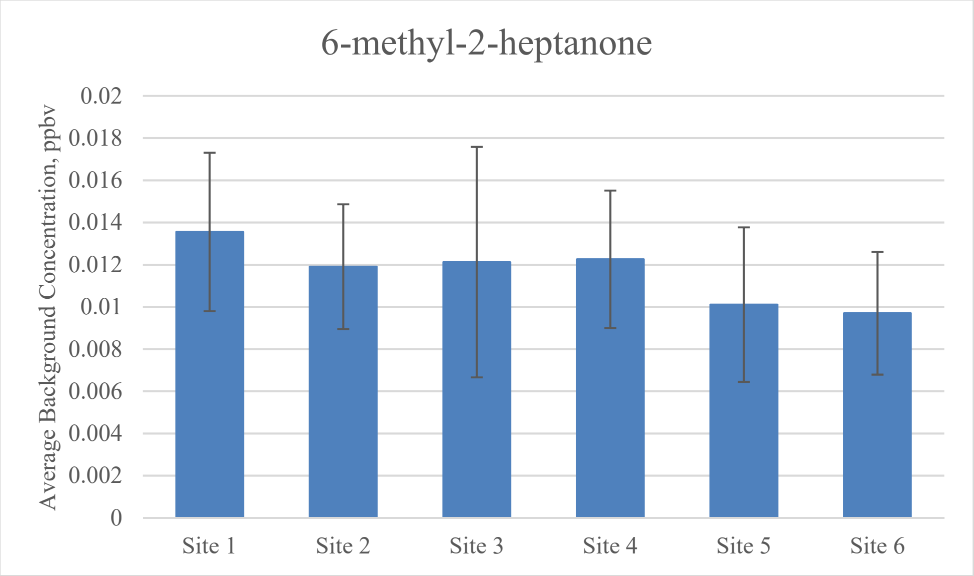
6-methyl-2-heptanone
Average Background Concentration, ppbv
0.02
0.018
0.016
0.014
0.012
0.01
0.008
0.006
0.004
0.002
0
Site 1
Site 2
Site 3
Site 4
Site 5
Site 6

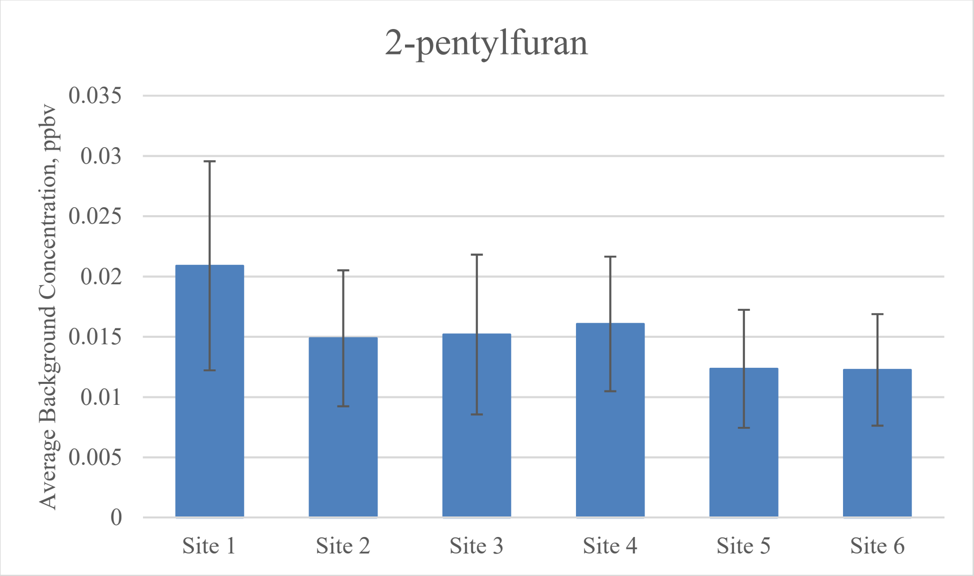
2-pentylfuran
Average Background Concentration, ppbv
0.035
0.03
0.025
0.02
0.015
0.01
0.005
0
Site 1
Site 2
Site 3
Site 4
Site 5
Site 6

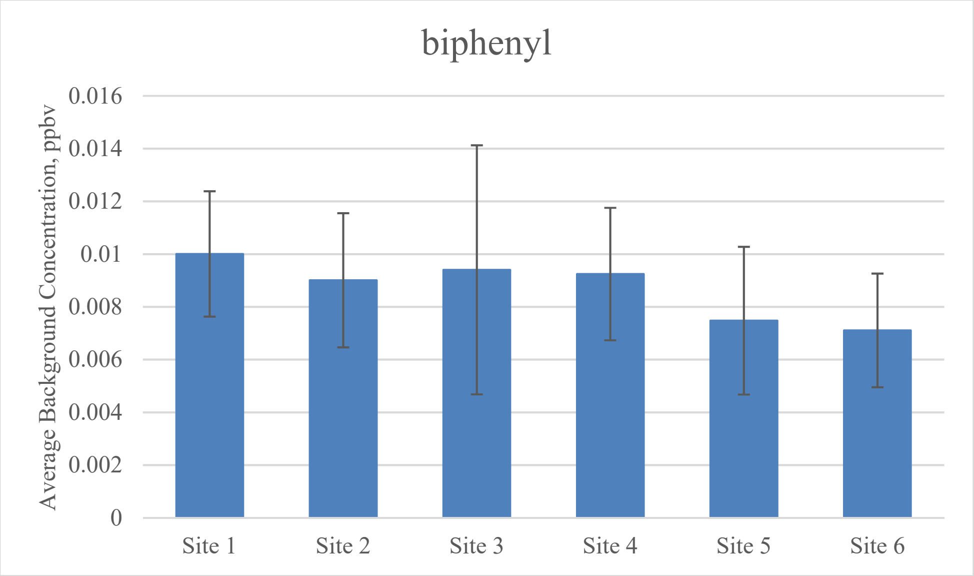
biphenyl
Average Background Concentration, ppbv
0.016
0.014
0.012
0.01
0.008
0.006
0.004
0.002
0
Site 1
Site 2
Site 3
Site 4
Site 5
Site 6

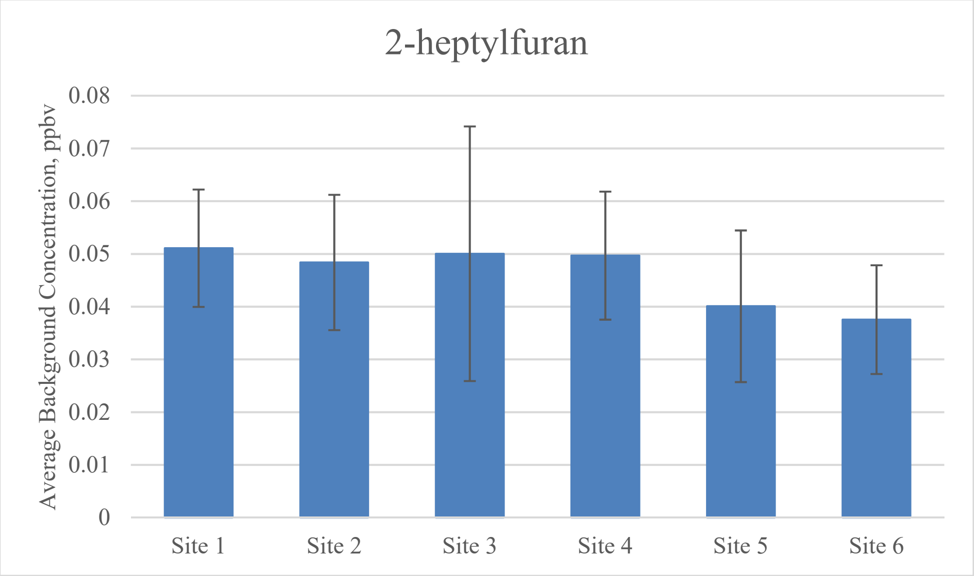
2-heptylfuran
Average Background Concentration, ppbv
0.08
0.07
0.06
0.05
0.04
0.03
0.02
0.01
0
Site 1
Site 2
Site 3
Site 4
Site 5
Site 6

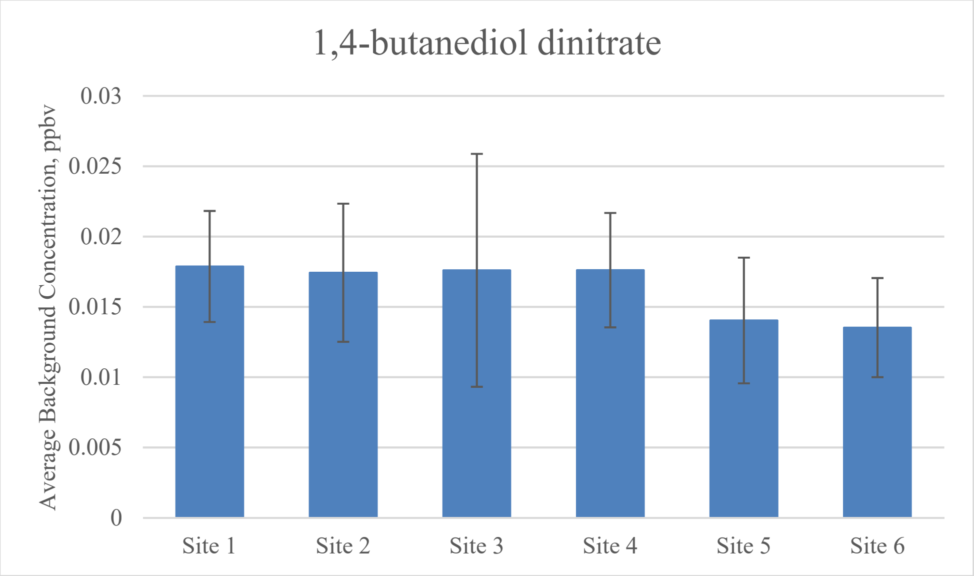
1,4-butanediol dinitrate
Average Background Concentration, ppbv
0.03
0.025
0.02
0.015
0.01
0.005
0
Site 1
Site 2
Site 3
Site 4
Site 5
Site 6

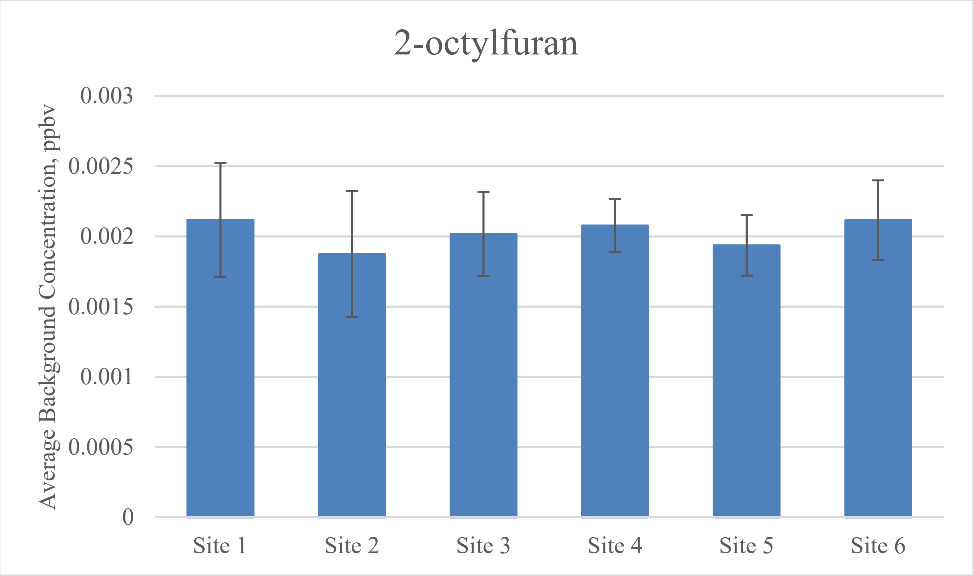
2-octylfuran
Average Background Concentration, ppbv
0.003
0.0025
0.002
0.0015
0.001
0.0005
0
Site 1
Site 2
Site 3
Site 4
Site 5
Site 6

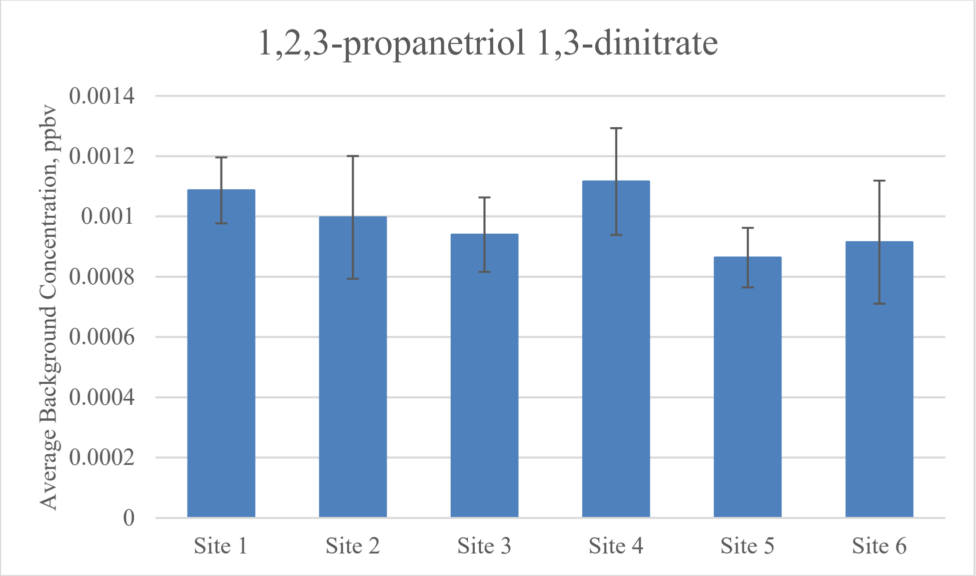
1,2,3-propanetriol 1,3-dinitrate
Average Background Concentration, ppbv
0.0014
0.0012
0.001
0.0008
0.0006
0.0004
0.0002
0
Site 1
Site 2
Site 3
Site 4
Site 5
Site 6

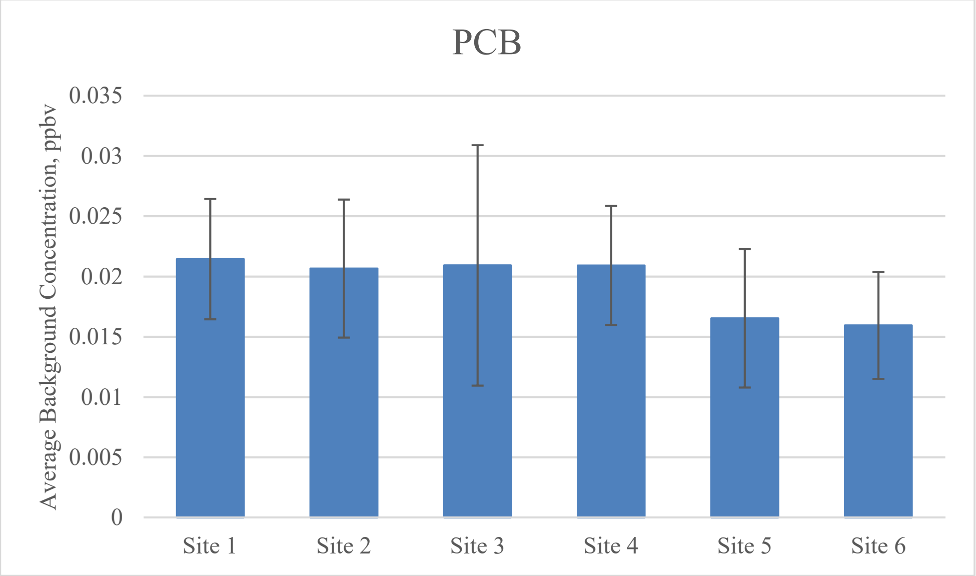
PCB
Average Background Concentration, ppbv
0.035
0.03
0.025
0.02
0.015
0.01
0.005
0
Site 1
Site 2
Site 3
Site 4
Site 5
Site 6

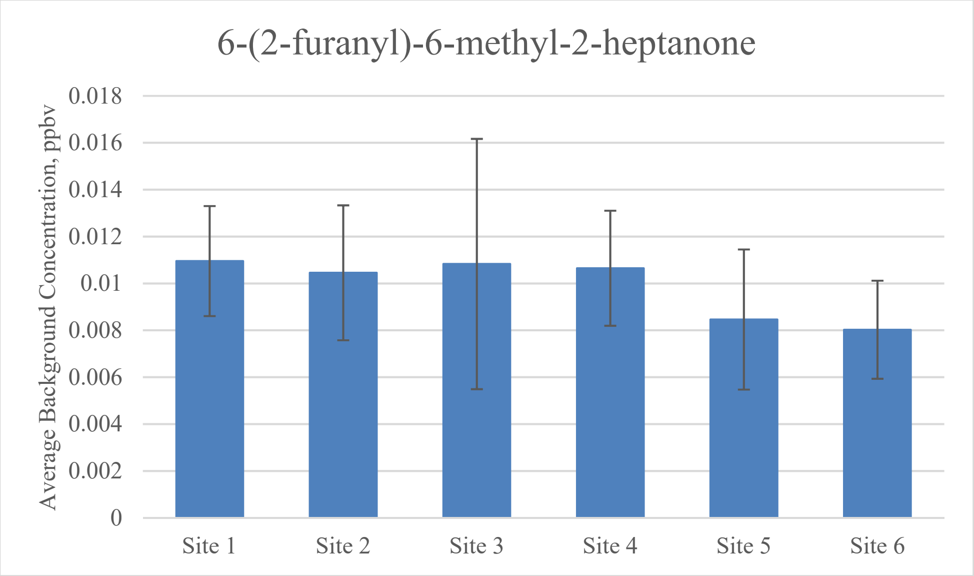
6-(2-furanyl)-6-methyl-2-heptanone
Average Background Concentration, ppbv
0.018
0.016
0.014
0.012
0.01
0.008
0.006
0.004
0.002
0
Site 1
Site 2
Site 3
Site 4
Site 5
Site 6

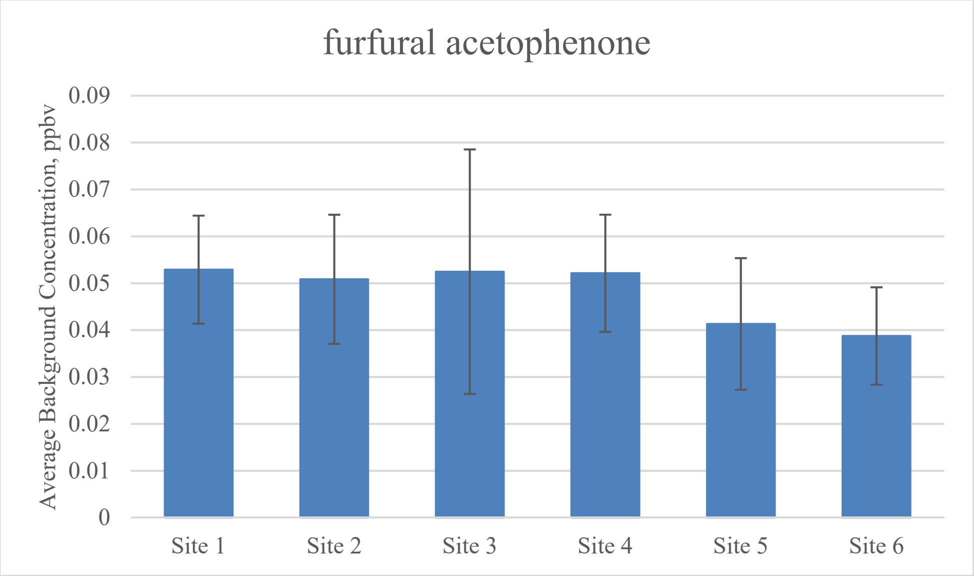
furfural acetophenone
Average Background Concentration, ppbv
0.09
0.08
0.07
0.06
0.05
0.04
0.03
0.02
0.01
0
Site 1
Site 2
Site 3
Site 4
Site 5
Site 6

APPENDIX C

DEFICIENCY REPORTS

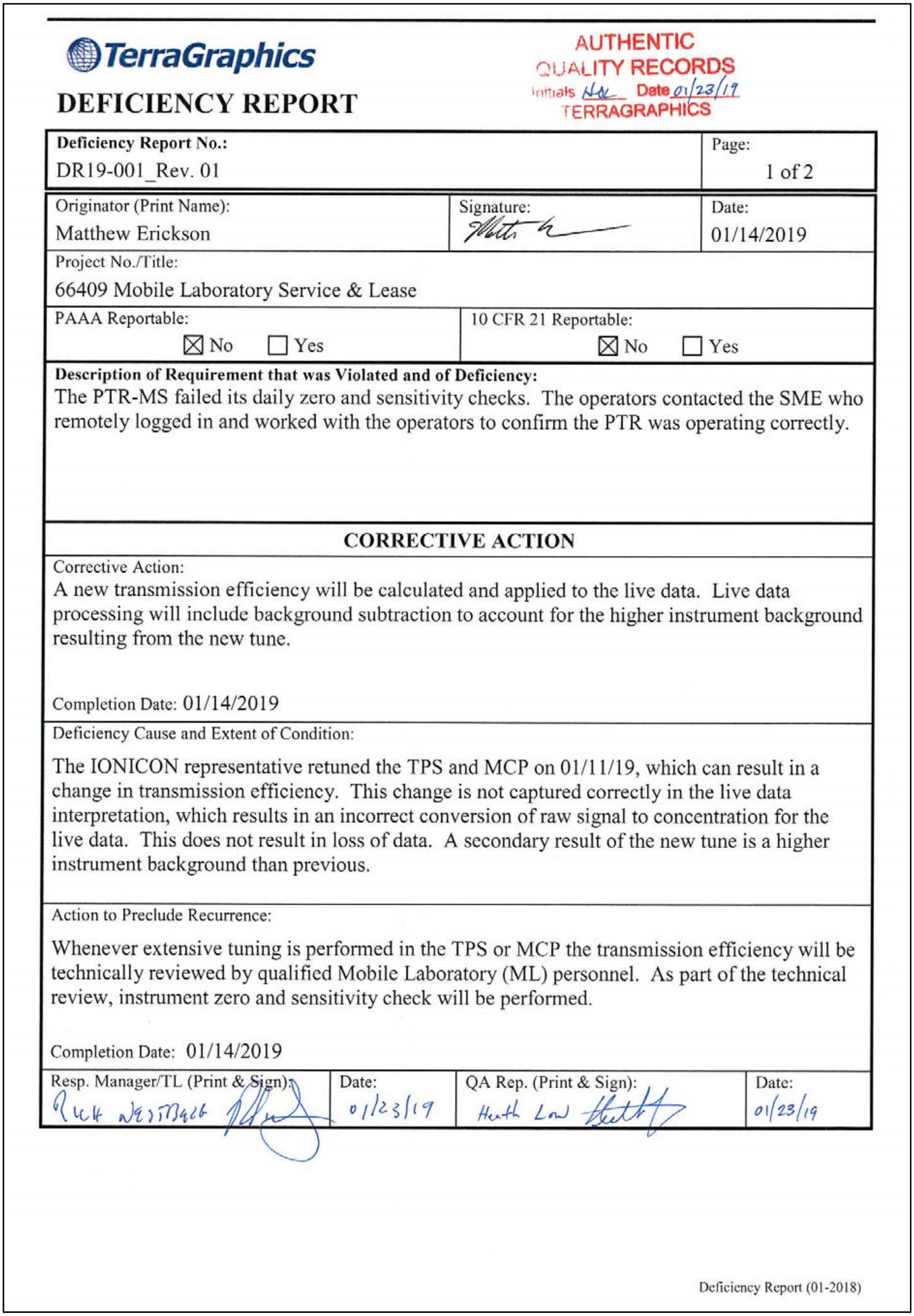

TerraGraphics

DEFICIENCY REPORT

AUTHENTIC
QUALITY RECORDS
Initials HL Date 01/23/19
TERRAGRAPHICS

Deficiency Report No.: DR19-001_Rev. 01	Page: 1 of 2

Originator (Print Name): Matthew Erickson	Signature:	Date: 01/14/2019

Project No./Title:
66409 Mobile Laboratory Service & Lease

PAAA Reportable: ☒ No ☐ Yes	10 CFR 21 Reportable: ☒ No ☐ Yes

Description of Requirement that was Violated and of Deficiency:
The PTR-MS failed its daily zero and sensitivity checks. The operators contacted the SME who remotely logged in and worked with the operators to confirm the PTR was operating correctly.

CORRECTIVE ACTION

Corrective Action:
A new transmission efficiency will be calculated and applied to the live data. Live data processing will include background subtraction to account for the higher instrument background resulting from the new tune.

Completion Date: 01/14/2019

Deficiency Cause and Extent of Condition:

The IONICON representative retuned the TPS and MCP on 01/11/19, which can result in a change in transmission efficiency. This change is not captured correctly in the live data interpretation, which results in an incorrect conversion of raw signal to concentration for the live data. This does not result in loss of data. A secondary result of the new tune is a higher instrument background than previous.

Action to Preclude Recurrence:

Whenever extensive tuning is performed in the TPS or MCP the transmission efficiency will be technically reviewed by qualified Mobile Laboratory (ML) personnel. As part of the technical review, instrument zero and sensitivity check will be performed.

Completion Date: 01/14/2019

Resp. Manager/TL (Print & Sign): Rick Westmack	Date: 01/23/19	QA Rep. (Print & Sign): Heath Low	Date: 01/23/19

Deficiency Report (01-2018)

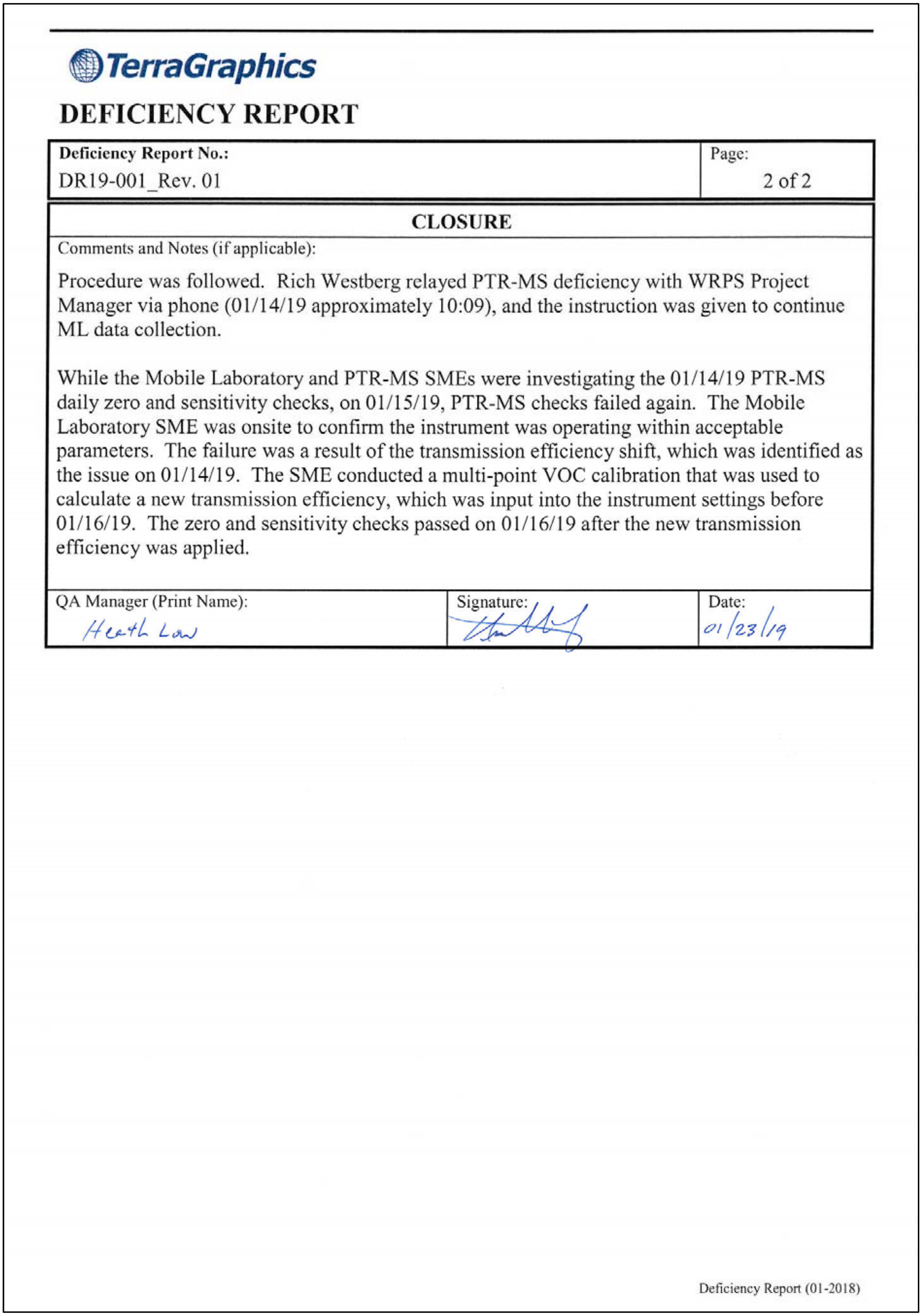

TerraGraphics

DEFICIENCY REPORT

Deficiency Report No.: DR19-001_Rev. 01	Page: 2 of 2

CLOSURE

Comments and Notes (if applicable):

Procedure was followed. Rich Westberg relayed PTR-MS deficiency with WRPS Project Manager via phone (01/14/19 approximately 10:09), and the instruction was given to continue ML data collection.

While the Mobile Laboratory and PTR-MS SMEs were investigating the 01/14/19 PTR-MS daily zero and sensitivity checks, on 01/15/19, PTR-MS checks failed again. The Mobile Laboratory SME was onsite to confirm the instrument was operating within acceptable parameters. The failure was a result of the transmission efficiency shift, which was identified as the issue on 01/14/19. The SME conducted a multi-point VOC calibration that was used to calculate a new transmission efficiency, which was input into the instrument settings before 01/16/19. The zero and sensitivity checks passed on 01/16/19 after the new transmission efficiency was applied.

QA Manager (Print Name): Heath Low	Signature:	Date: 01/23/19

Deficiency Report (01-2018)

TerraGraphics

AUTHENTIC
QUALITY RECORDS
Initials HAL Date 01/22/19
TERRAGRAPHICS

DEFICIENCY REPORT

Deficiency Report No.: DR19-002	Page: 1 of 1

Originator (Print Name): Matthew Erickson	Signature:	Date: 01/17/2019

Project No./Title:
66409 Mobile Laboratory Services and Lease

PAAA Reportable: ☒ No ☐ Yes	10 CFR 21 Reportable: ☒ No ☐ Yes

Description of Requirement that was Violated and of Deficiency:

The PTR-MS's data collection hard drive was full. The software was unable to record data properly and approximately 5-6 hours were not recorded.

CORRECTIVE ACTION

Corrective Action:

On 01/16/2019, older files were relocated to allow space for new files. At 22:59, a new PTR-MS file was created (BKG_3_190116_F).

Completion Date: 01/16/2019

Deficiency Cause and Extent of Condition:

The PTR-MS has been collecting a high volume of data, almost 4-6 GBs per Mobile Laboratory deployment.

Action to Preclude Recurrence:

The next revision (11) of 66409-RPT-004, *Mobile Laboratory Operational Procedure*, will include a computer hard drive check. Mobile Laboratory Operators will check hard drive space.

Completion Date: 01/24/2019

Resp. Manager/TL (Print & Sign): RICH WESTBERG	Date: 01/22/19	QA Rep. (Print & Sign): Heath Low	Date: 01/17/19

CLOSURE

Comments and Notes (if applicable):

QA Manager (Print Name): Heath Low	Signature:	Date: 01/17/19

Deficiency Report (01-2018)

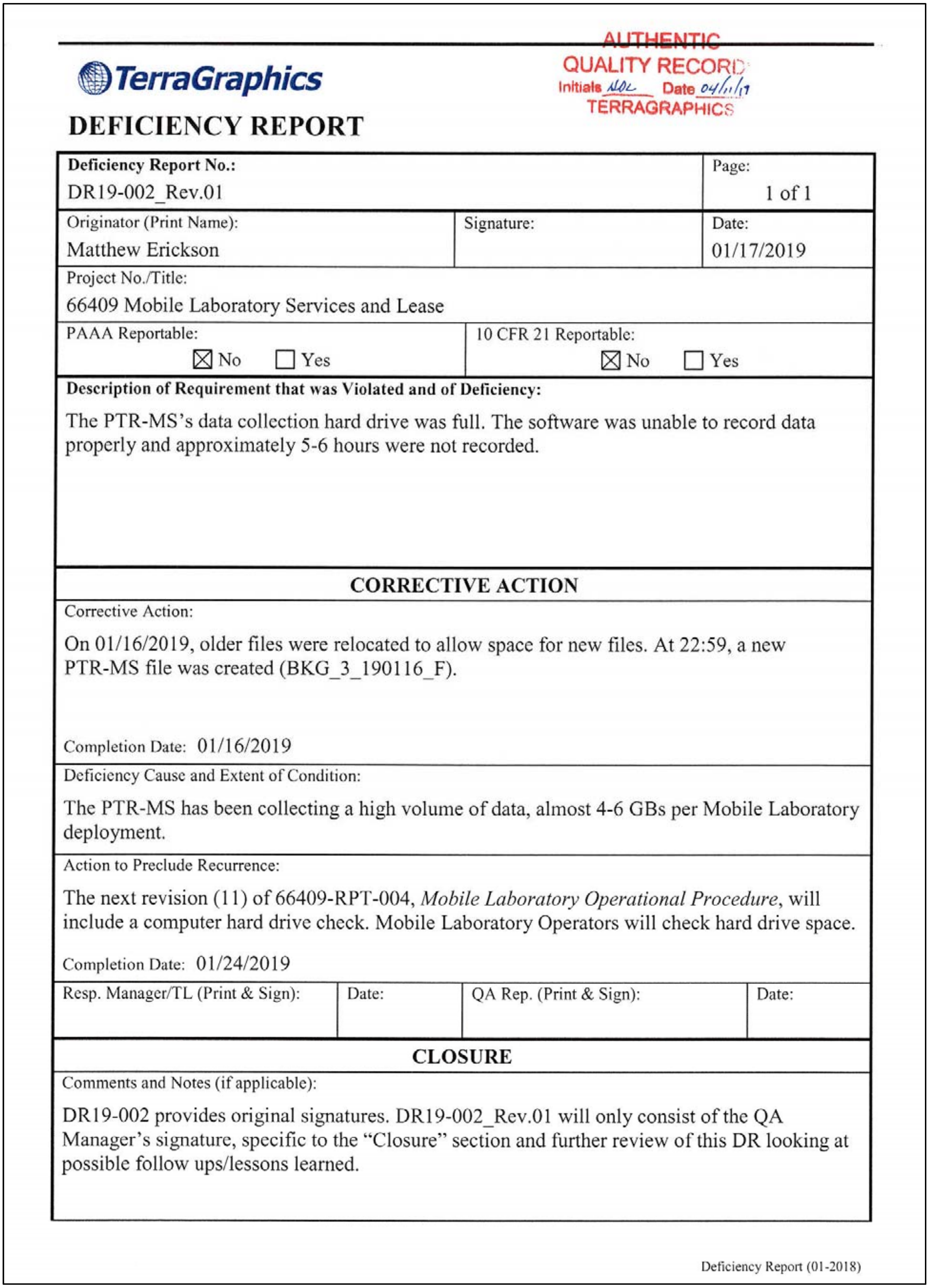

TerraGraphics

AUTHENTIC
QUALITY RECORD
Initials NDL Date 04/11/19
TERRAGRAPHICS

DEFICIENCY REPORT

Deficiency Report No.: DR19-002_Rev.01		Page: 1 of 1
Originator (Print Name): Matthew Erickson	Signature:	Date: 01/17/2019

Project No./Title:
66409 Mobile Laboratory Services and Lease

PAAA Reportable: ☒ No ☐ Yes

10 CFR 21 Reportable: ☒ No ☐ Yes

Description of Requirement that was Violated and of Deficiency:

The PTR-MS's data collection hard drive was full. The software was unable to record data properly and approximately 5-6 hours were not recorded.

CORRECTIVE ACTION

Corrective Action:

On 01/16/2019, older files were relocated to allow space for new files. At 22:59, a new PTR-MS file was created (BKG_3_190116_F).

Completion Date: 01/16/2019

Deficiency Cause and Extent of Condition:

The PTR-MS has been collecting a high volume of data, almost 4-6 GBs per Mobile Laboratory deployment.

Action to Preclude Recurrence:

The next revision (11) of 66409-RPT-004, *Mobile Laboratory Operational Procedure*, will include a computer hard drive check. Mobile Laboratory Operators will check hard drive space.

Completion Date: 01/24/2019

Resp. Manager/TL (Print & Sign):	Date:	QA Rep. (Print & Sign):	Date:

CLOSURE

Comments and Notes (if applicable):

DR19-002 provides original signatures. DR19-002_Rev.01 will only consist of the QA Manager's signature, specific to the "Closure" section and further review of this DR looking at possible follow ups/lessons learned.

Deficiency Report (01-2018)

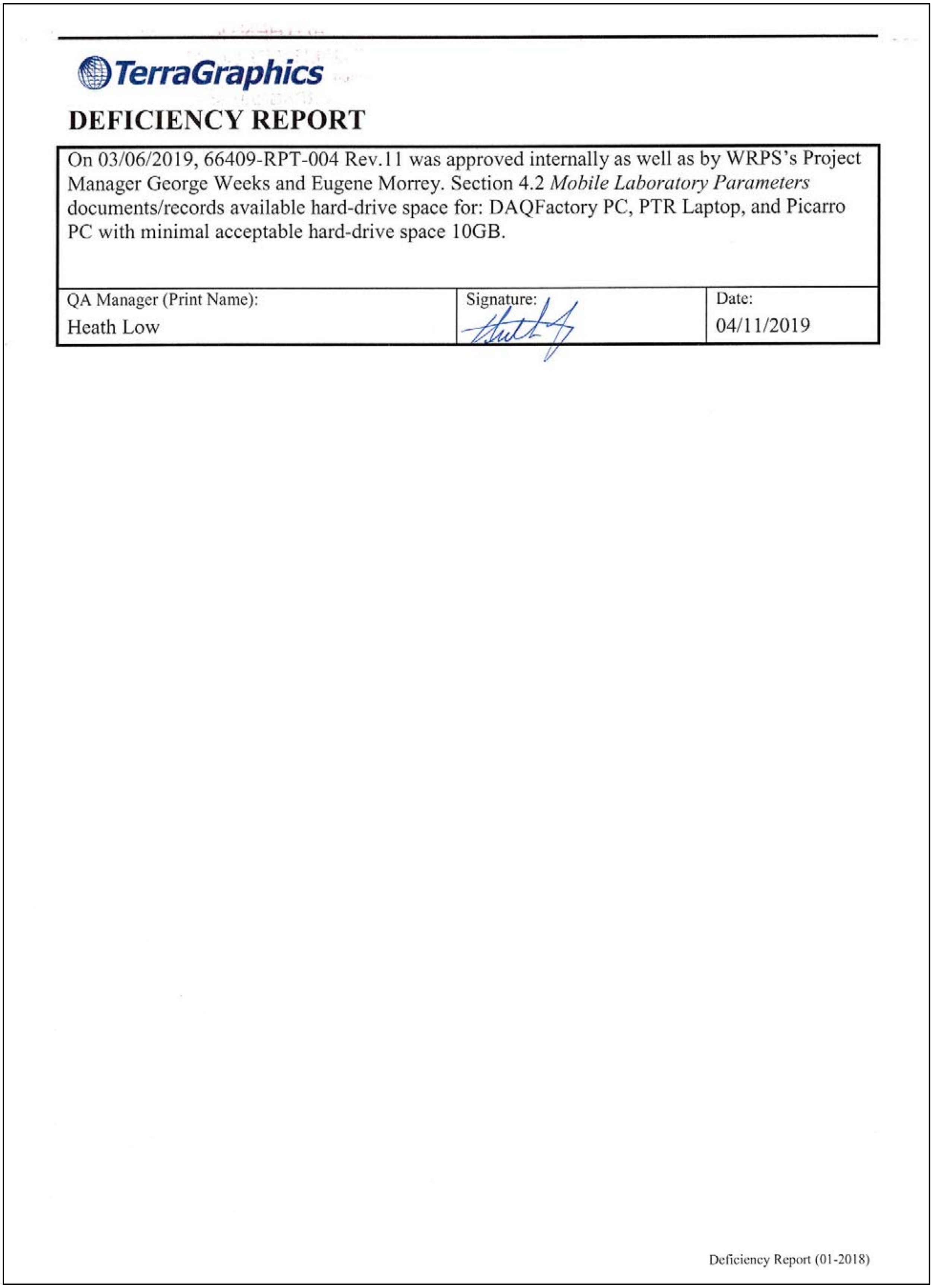

TerraGraphics

DEFICIENCY REPORT

On 03/06/2019, 66409-RPT-004 Rev.11 was approved internally as well as by WRPS's Project Manager George Weeks and Eugene Morrey. Section 4.2 *Mobile Laboratory Parameters* documents/records available hard-drive space for: DAQFactory PC, PTR Laptop, and Picarro PC with minimal acceptable hard-drive space 10GB.

QA Manager (Print Name): Heath Low	Signature:	Date: 04/11/2019

Deficiency Report (01-2018)

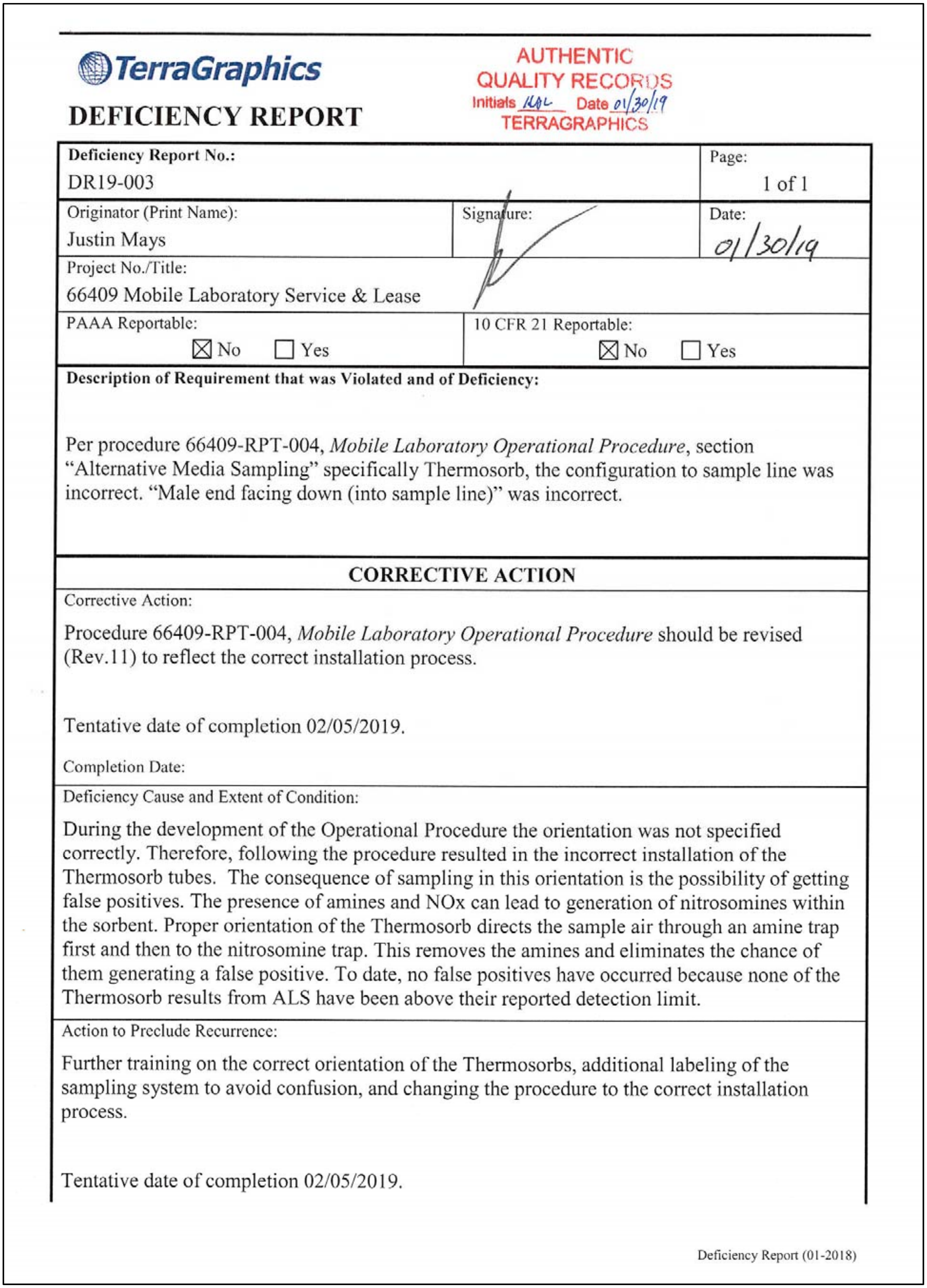

TerraGraphics

DEFICIENCY REPORT

AUTHENTIC
QUALITY RECORDS
Initials KAL Date 01/30/19
TERRAGRAPHICS

Deficiency Report No.: DR19-003	Page: 1 of 1

Originator (Print Name): Justin Mays
Signature:
Date: 01/30/19

Project No./Title: 66409 Mobile Laboratory Service & Lease

PAAA Reportable: ☒ No ☐ Yes

10 CFR 21 Reportable: ☒ No ☐ Yes

Description of Requirement that was Violated and of Deficiency:

Per procedure 66409-RPT-004, *Mobile Laboratory Operational Procedure*, section "Alternative Media Sampling" specifically Thermosorb, the configuration to sample line was incorrect. "Male end facing down (into sample line)" was incorrect.

CORRECTIVE ACTION

Corrective Action:

Procedure 66409-RPT-004, *Mobile Laboratory Operational Procedure* should be revised (Rev.11) to reflect the correct installation process.

Tentative date of completion 02/05/2019.

Completion Date:

Deficiency Cause and Extent of Condition:

During the development of the Operational Procedure the orientation was not specified correctly. Therefore, following the procedure resulted in the incorrect installation of the Thermosorb tubes. The consequence of sampling in this orientation is the possibility of getting false positives. The presence of amines and NOx can lead to generation of nitrosomines within the sorbent. Proper orientation of the Thermosorb directs the sample air through an amine trap first and then to the nitrosomine trap. This removes the amines and eliminates the chance of them generating a false positive. To date, no false positives have occurred because none of the Thermosorb results from ALS have been above their reported detection limit.

Action to Preclude Recurrence:

Further training on the correct orientation of the Thermosorbs, additional labeling of the sampling system to avoid confusion, and changing the procedure to the correct installation process.

Tentative date of completion 02/05/2019.

Deficiency Report (01-2018)

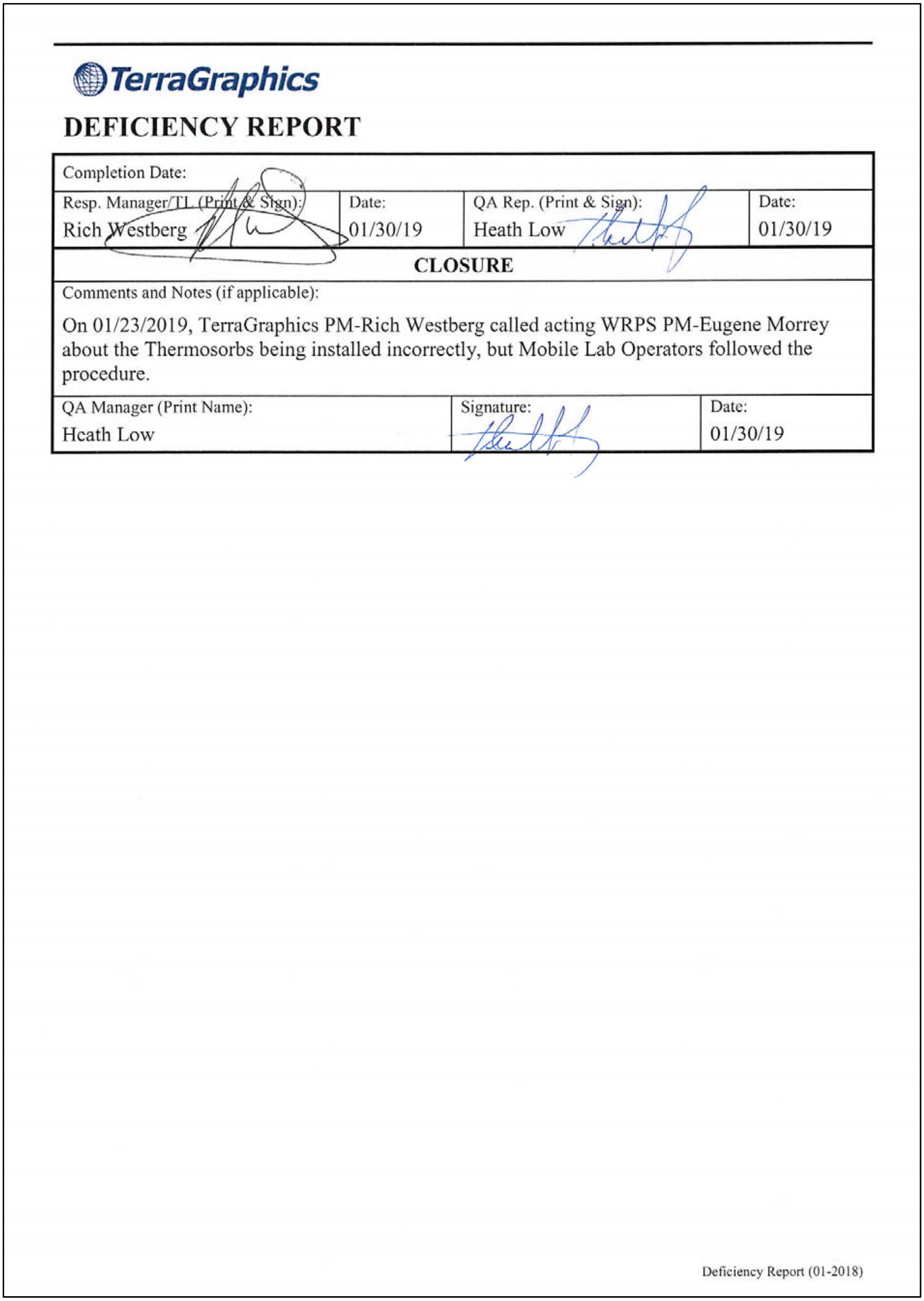

TerraGraphics

DEFICIENCY REPORT

Completion Date:			
Resp. Manager/TL (Print & Sign): Rich Westberg	Date: 01/30/19	QA Rep. (Print & Sign): Heath Low	Date: 01/30/19

CLOSURE

Comments and Notes (if applicable):

On 01/23/2019, TerraGraphics PM-Rich Westberg called acting WRPS PM-Eugene Morrey about the Thermosorbs being installed incorrectly, but Mobile Lab Operators followed the procedure.

QA Manager (Print Name): Heath Low	Signature:	Date: 01/30/19

Deficiency Report (01-2018)

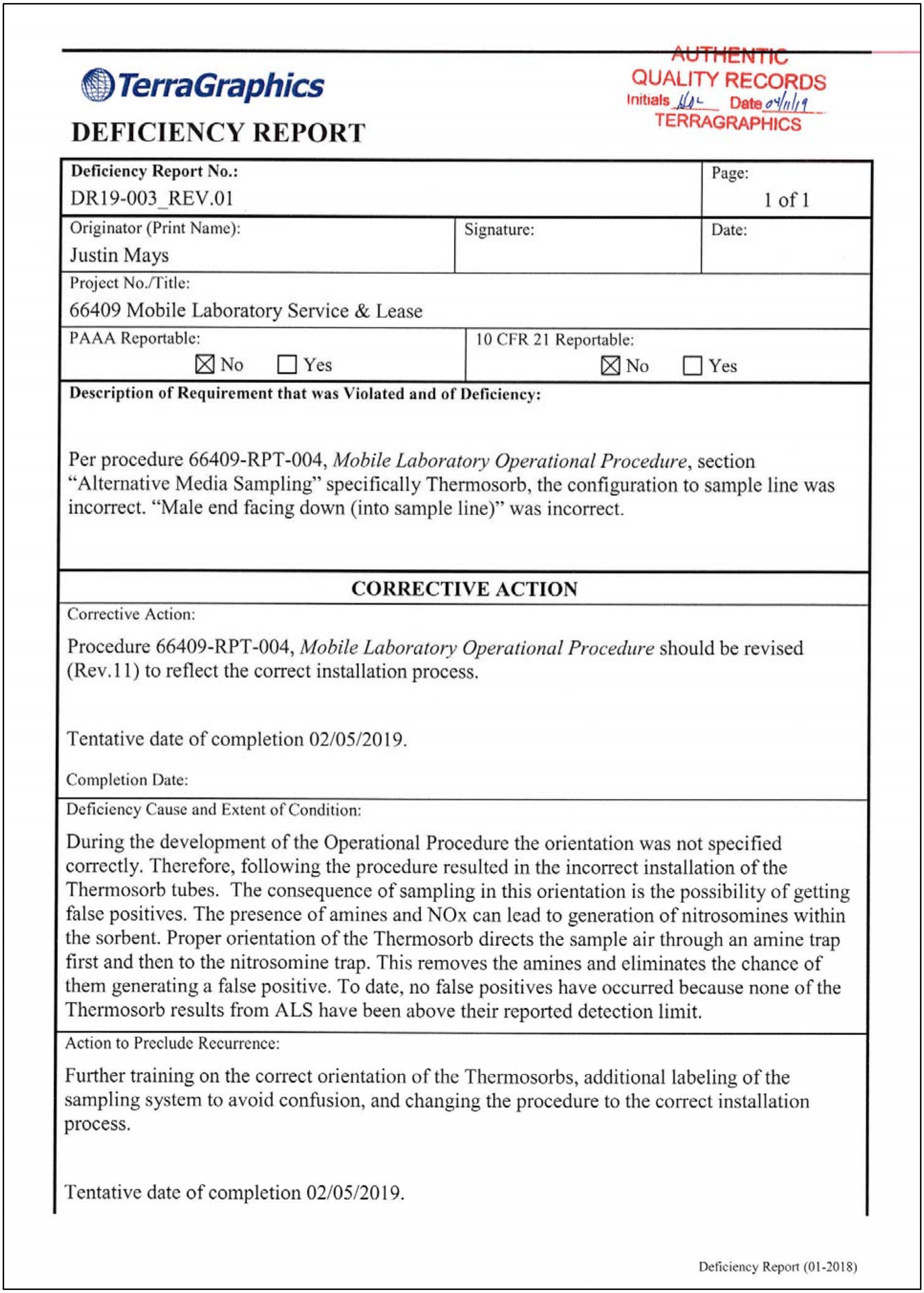

TerraGraphics

AUTHENTIC
QUALITY RECORDS
Initials Date 04/11/19
TERRAGRAPHICS

DEFICIENCY REPORT

Deficiency Report No.: DR19-003_REV.01		Page: 1 of 1
Originator (Print Name): Justin Mays	Signature:	Date:
Project No./Title: 66409 Mobile Laboratory Service & Lease		
PAAA Reportable: ☒ No ☐ Yes	10 CFR 21 Reportable: ☒ No ☐ Yes	

Description of Requirement that was Violated and of Deficiency:

Per procedure 66409-RPT-004, *Mobile Laboratory Operational Procedure*, section "Alternative Media Sampling" specifically Thermosorb, the configuration to sample line was incorrect. "Male end facing down (into sample line)" was incorrect.

CORRECTIVE ACTION

Corrective Action:

Procedure 66409-RPT-004, *Mobile Laboratory Operational Procedure* should be revised (Rev.11) to reflect the correct installation process.

Tentative date of completion 02/05/2019.

Completion Date:

Deficiency Cause and Extent of Condition:

During the development of the Operational Procedure the orientation was not specified correctly. Therefore, following the procedure resulted in the incorrect installation of the Thermosorb tubes. The consequence of sampling in this orientation is the possibility of getting false positives. The presence of amines and NOx can lead to generation of nitrosomines within the sorbent. Proper orientation of the Thermosorb directs the sample air through an amine trap first and then to the nitrosomine trap. This removes the amines and eliminates the chance of them generating a false positive. To date, no false positives have occurred because none of the Thermosorb results from ALS have been above their reported detection limit.

Action to Preclude Recurrence:

Further training on the correct orientation of the Thermosorbs, additional labeling of the sampling system to avoid confusion, and changing the procedure to the correct installation process.

Tentative date of completion 02/05/2019.

Deficiency Report (01-2018)

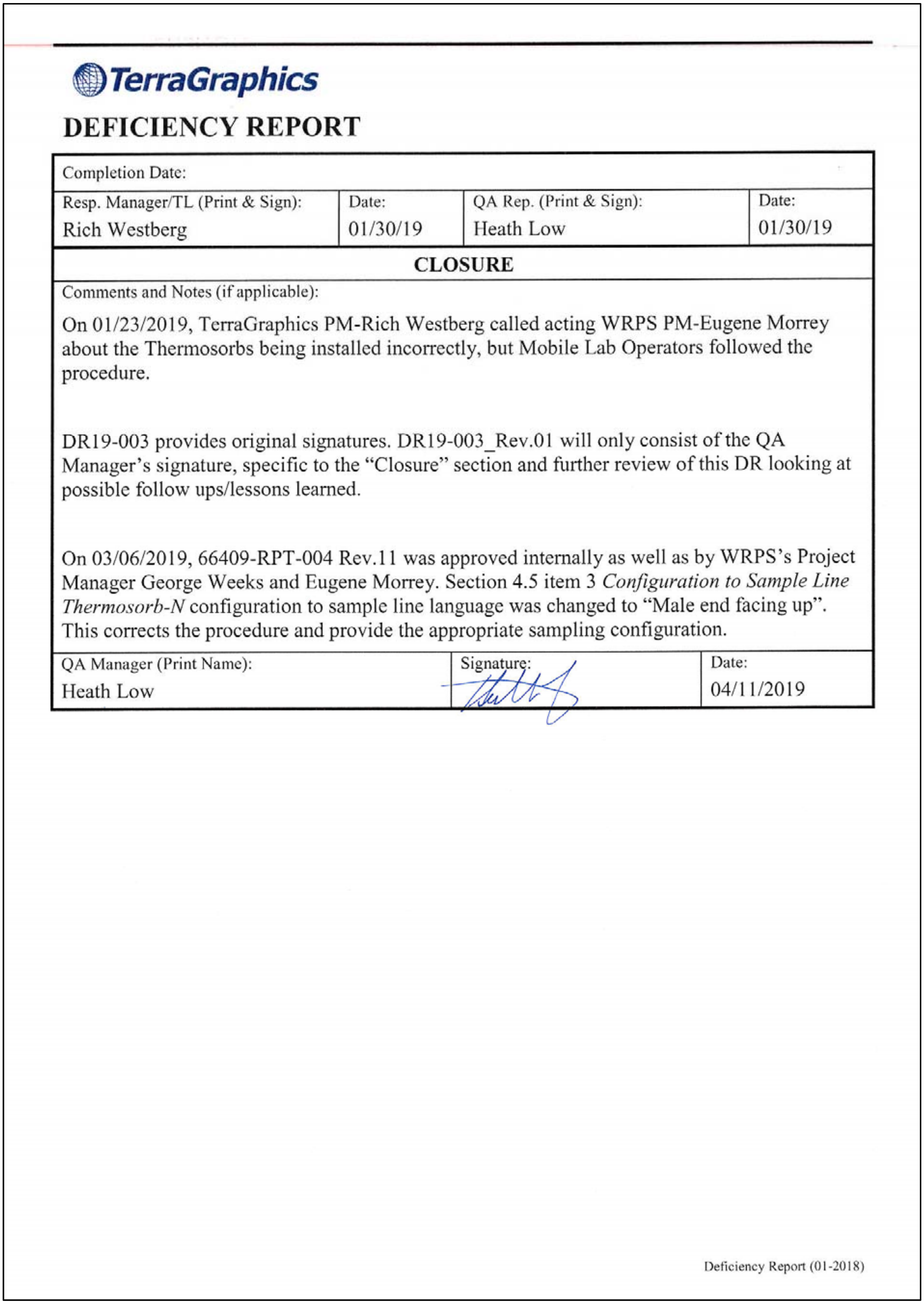

TerraGraphics

DEFICIENCY REPORT

Completion Date:			
Resp. Manager/TL (Print & Sign): Rich Westberg	Date: 01/30/19	QA Rep. (Print & Sign): Heath Low	Date: 01/30/19

CLOSURE

Comments and Notes (if applicable):

On 01/23/2019, TerraGraphics PM-Rich Westberg called acting WRPS PM-Eugene Morrey about the Thermosorbs being installed incorrectly, but Mobile Lab Operators followed the procedure.

DR19-003 provides original signatures. DR19-003_Rev.01 will only consist of the QA Manager's signature, specific to the "Closure" section and further review of this DR looking at possible follow ups/lessons learned.

On 03/06/2019, 66409-RPT-004 Rev.11 was approved internally as well as by WRPS's Project Manager George Weeks and Eugene Morrey. Section 4.5 item 3 *Configuration to Sample Line Thermosorb-N* configuration to sample line language was changed to "Male end facing up". This corrects the procedure and provide the appropriate sampling configuration.

QA Manager (Print Name): Heath Low	Signature:	Date: 04/11/2019

Deficiency Report (01-2018)

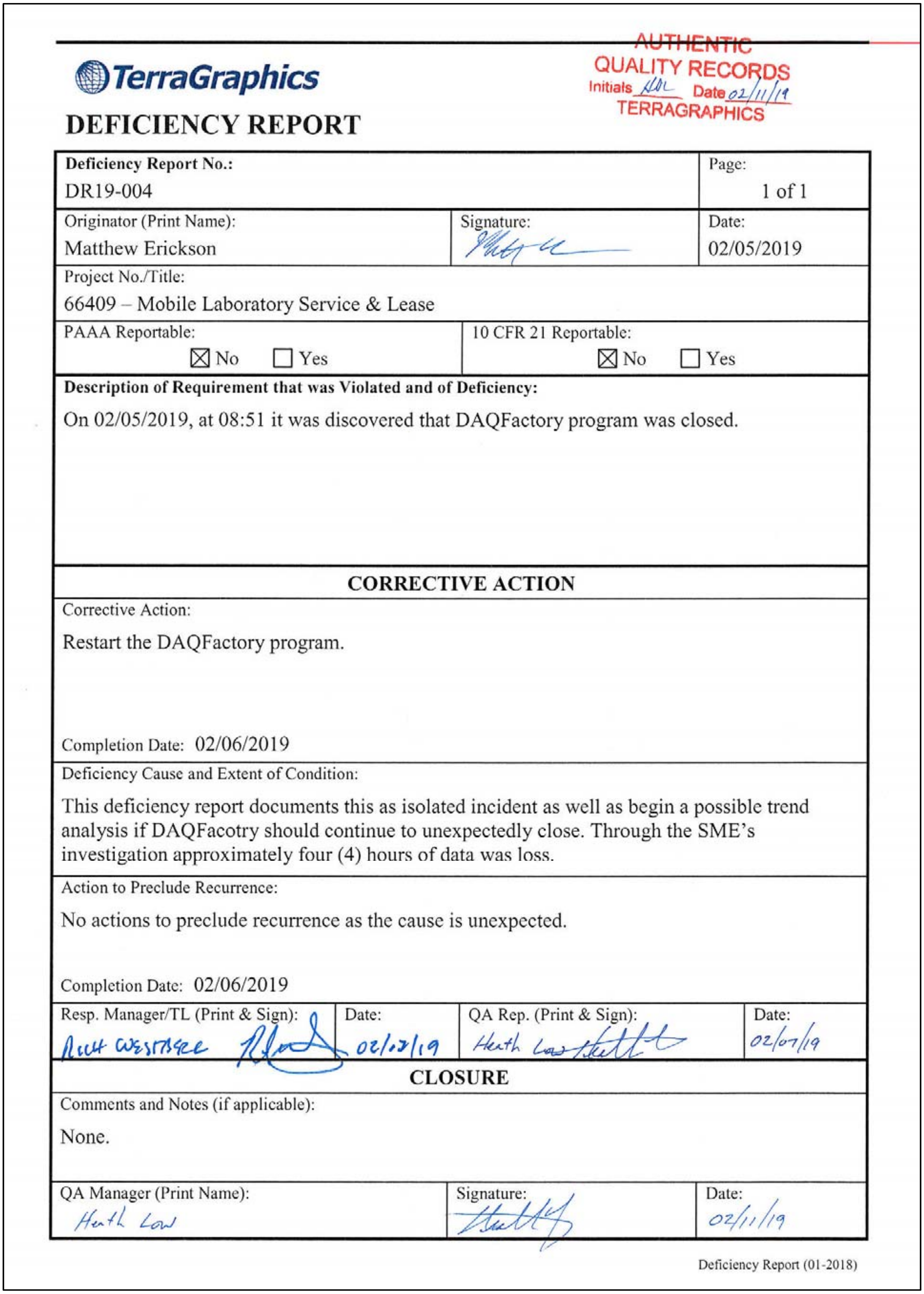

AUTHENTIC
QUALITY RECORDS
Initials HDL Date 02/11/19
TERRAGRAPHICS

TerraGraphics

DEFICIENCY REPORT

Deficiency Report No.: DR19-004	Page: 1 of 1

Originator (Print Name): Matthew Erickson	Signature:	Date: 02/05/2019

Project No./Title:
66409 – Mobile Laboratory Service & Lease

PAAA Reportable: ☒ No ☐ Yes	10 CFR 21 Reportable: ☒ No ☐ Yes

Description of Requirement that was Violated and of Deficiency:

On 02/05/2019, at 08:51 it was discovered that DAQFactory program was closed.

CORRECTIVE ACTION

Corrective Action:

Restart the DAQFactory program.

Completion Date: 02/06/2019

Deficiency Cause and Extent of Condition:

This deficiency report documents this as isolated incident as well as begin a possible trend analysis if DAQFacotry should continue to unexpectedly close. Through the SME's investigation approximately four (4) hours of data was loss.

Action to Preclude Recurrence:

No actions to preclude recurrence as the cause is unexpected.

Completion Date: 02/06/2019

Resp. Manager/TL (Print & Sign): Rich Westberg	Date: 02/07/19	QA Rep. (Print & Sign): Heath Low	Date: 02/07/19

CLOSURE

Comments and Notes (if applicable):

None.

QA Manager (Print Name): Heath Low	Signature:	Date: 02/11/19

Deficiency Report (01-2018)

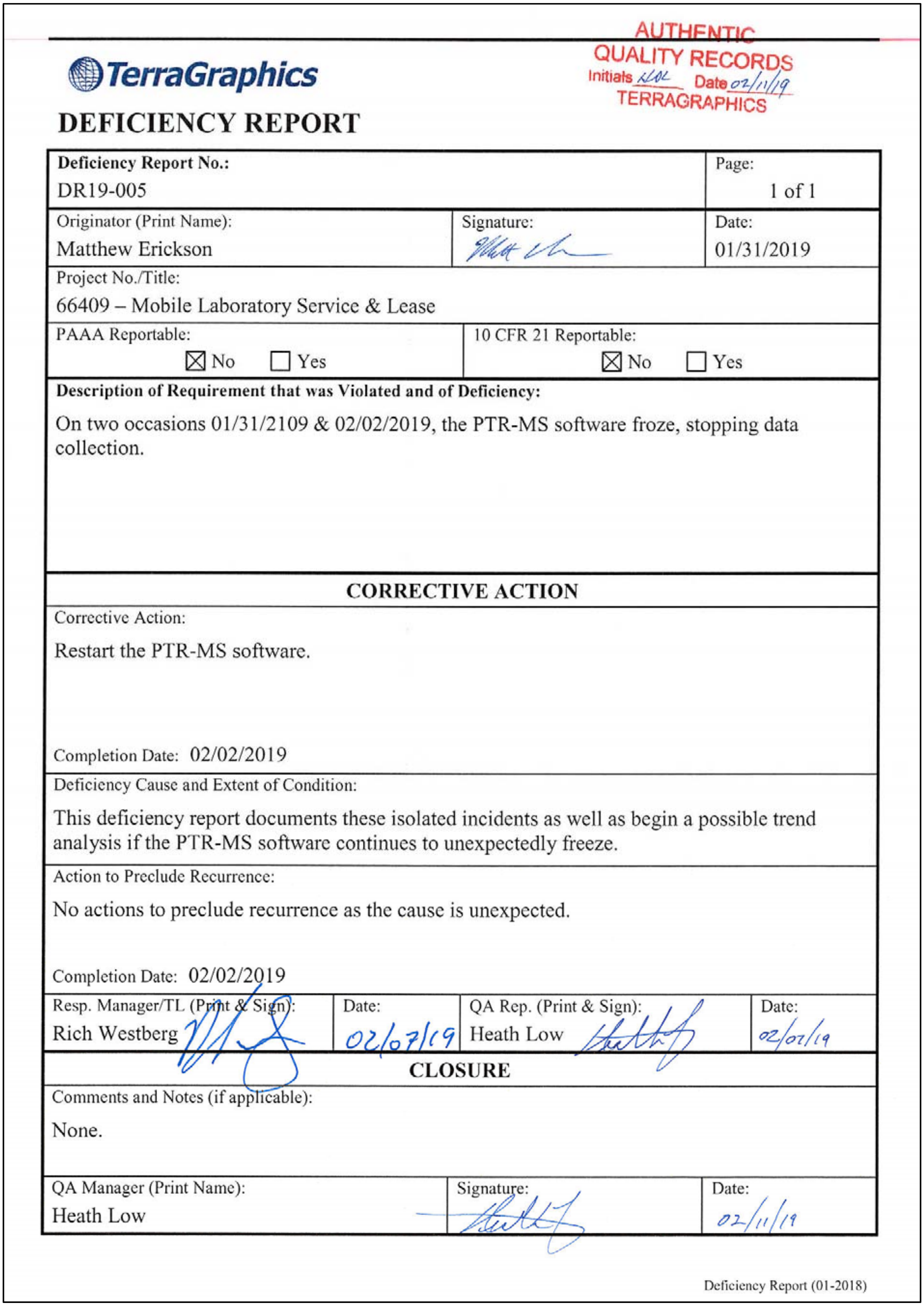

TerraGraphics

AUTHENTIC
QUALITY RECORDS
Initials HDL Date 02/11/19
TERRAGRAPHICS

DEFICIENCY REPORT

Deficiency Report No.: DR19-005	Page: 1 of 1

Originator (Print Name): Matthew Erickson	Signature:	Date: 01/31/2019

Project No./Title:
66409 – Mobile Laboratory Service & Lease

PAAA Reportable: ☒ No ☐ Yes	10 CFR 21 Reportable: ☒ No ☐ Yes

Description of Requirement that was Violated and of Deficiency:

On two occasions 01/31/2109 & 02/02/2019, the PTR-MS software froze, stopping data collection.

CORRECTIVE ACTION

Corrective Action:

Restart the PTR-MS software.

Completion Date: 02/02/2019

Deficiency Cause and Extent of Condition:

This deficiency report documents these isolated incidents as well as begin a possible trend analysis if the PTR-MS software continues to unexpectedly freeze.

Action to Preclude Recurrence:

No actions to preclude recurrence as the cause is unexpected.

Completion Date: 02/02/2019

Resp. Manager/TL (Print & Sign): Rich Westberg	Date: 02/07/19	QA Rep. (Print & Sign): Heath Low	Date: 02/07/19

CLOSURE

Comments and Notes (if applicable):

None.

QA Manager (Print Name): Heath Low	Signature:	Date: 02/11/19

Deficiency Report (01-2018)

APPENDIX D

NONCONFORMANCE REPORTS

NCR19-001

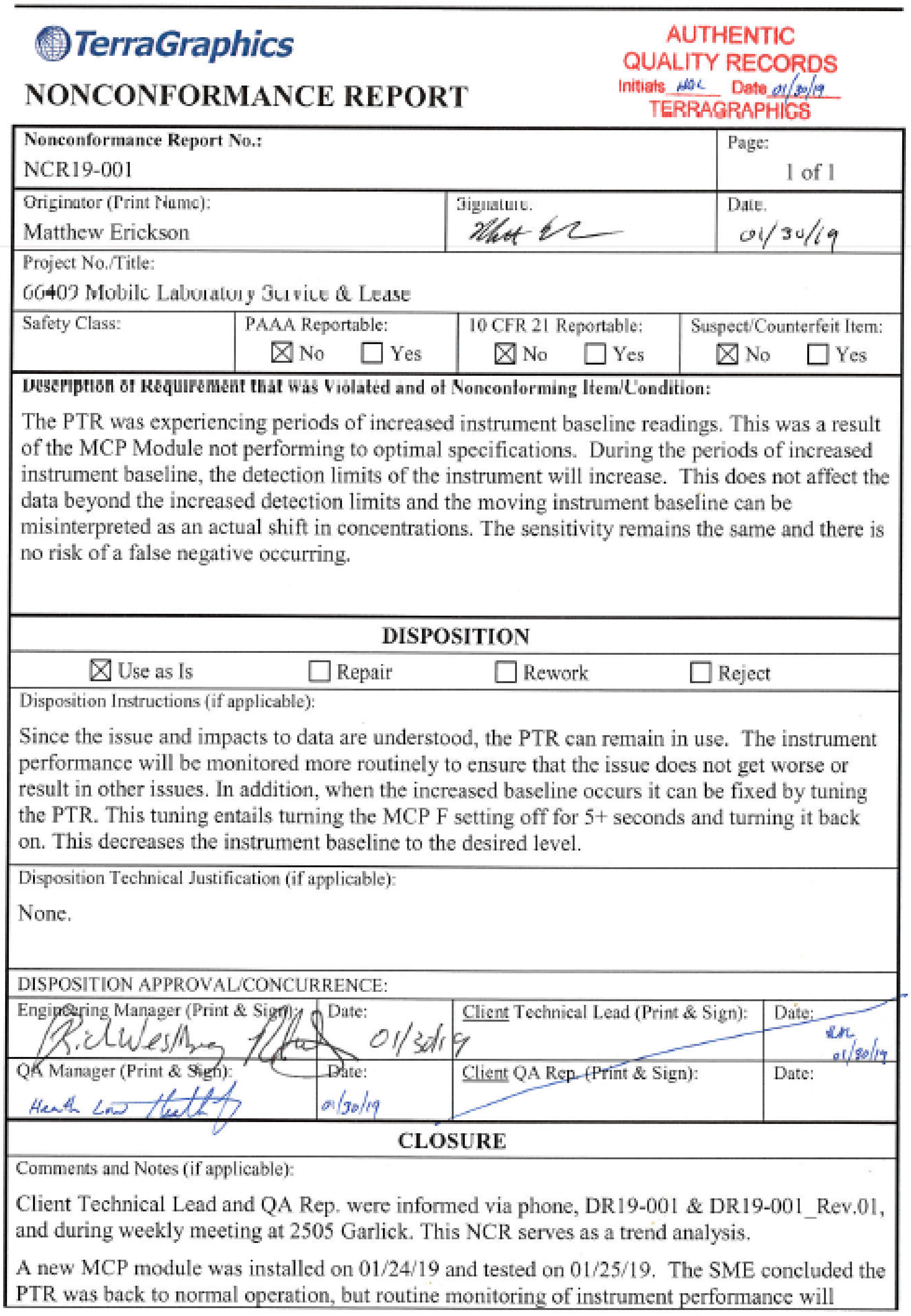

TerraGraphics

NONCONFORMANCE REPORT

AUTHENTIC
QUALITY RECORDS
Initials HDL Date 01/30/19
TERRAGRAPHICS

Nonconformance Report No.: NCR19-001			Page: 1 of 1
Originator (Print Name): Matthew Erickson	Signature:		Date: 01/30/19
Project No./Title: 66409 Mobile Laboratory Service & Lease			
Safety Class:	PAAA Reportable: ☒ No ☐ Yes	10 CFR 21 Reportable: ☒ No ☐ Yes	Suspect/Counterfeit Item: ☒ No ☐ Yes

Description of Requirement that was Violated and of Nonconforming Item/Condition:

The PTR was experiencing periods of increased instrument baseline readings. This was a result of the MCP Module not performing to optimal specifications. During the periods of increased instrument baseline, the detection limits of the instrument will increase. This does not affect the data beyond the increased detection limits and the moving instrument baseline can be misinterpreted as an actual shift in concentrations. The sensitivity remains the same and there is no risk of a false negative occurring.

DISPOSITION

☒ Use as Is ☐ Repair ☐ Rework ☐ Reject

Disposition Instructions (if applicable):

Since the issue and impacts to data are understood, the PTR can remain in use. The instrument performance will be monitored more routinely to ensure that the issue does not get worse or result in other issues. In addition, when the increased baseline occurs it can be fixed by tuning the PTR. This tuning entails turning the MCP F setting off for 5+ seconds and turning it back on. This decreases the instrument baseline to the desired level.

Disposition Technical Justification (if applicable):

None.

DISPOSITION APPROVAL/CONCURRENCE:

Engineering Manager (Print & Sign): [illegible]	Date: 01/30/19	<u>Client</u> Technical Lead (Print & Sign):	Date: RN 01/30/19
QA Manager (Print & Sign): Heath Low	Date: 01/30/19	<u>Client</u> QA Rep. (Print & Sign):	Date:

CLOSURE

Comments and Notes (if applicable):

Client Technical Lead and QA Rep. were informed via phone, DR19-001 & DR19-001_Rev.01, and during weekly meeting at 2505 Garlick. This NCR serves as a trend analysis.

A new MCP module was installed on 01/24/19 and tested on 01/25/19. The SME concluded the PTR was back to normal operation, but routine monitoring of instrument performance will

Nonconformance Report (03-2017)

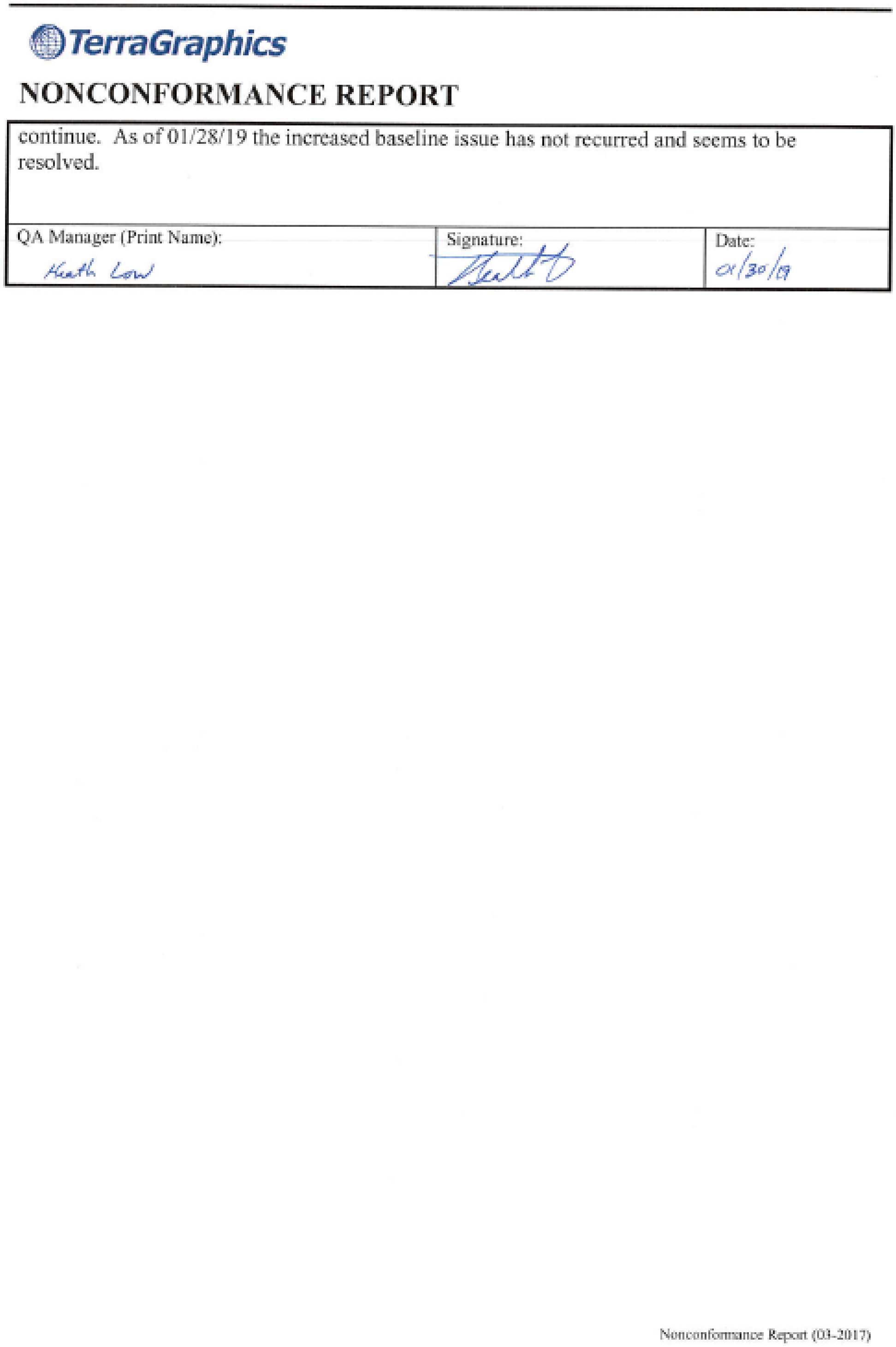

TerraGraphics

NONCONFORMANCE REPORT

continue. As of 01/28/19 the increased baseline issue has not recurred and seems to be resolved.

QA Manager (Print Name): Heath Low	Signature:	Date: 01/30/19

Nonconformance Report (03-2017)

NCR19-002

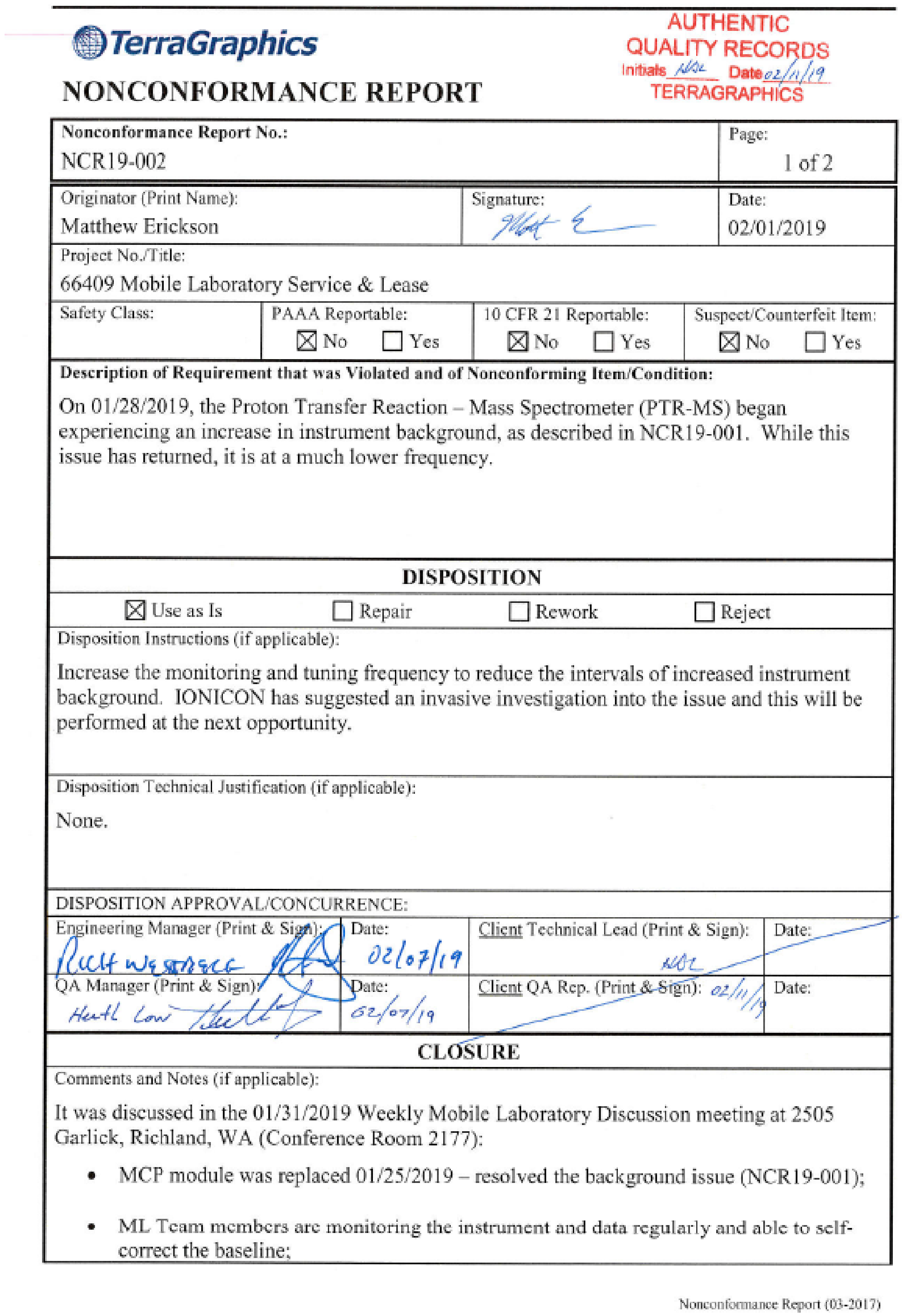

TerraGraphics

AUTHENTIC
QUALITY RECORDS
Initials NAL Date 02/11/19
TERRAGRAPHICS

NONCONFORMANCE REPORT

Nonconformance Report No.: NCR19-002	Page: 1 of 2

Originator (Print Name): Matthew Erickson	Signature: Matt E	Date: 02/01/2019

Project No./Title:
66409 Mobile Laboratory Service & Lease

Safety Class:	PAAA Reportable: ☒ No ☐ Yes	10 CFR 21 Reportable: ☒ No ☐ Yes	Suspect/Counterfeit Item: ☒ No ☐ Yes

Description of Requirement that was Violated and of Nonconforming Item/Condition:

On 01/28/2019, the Proton Transfer Reaction – Mass Spectrometer (PTR-MS) began experiencing an increase in instrument background, as described in NCR19-001. While this issue has returned, it is at a much lower frequency.

DISPOSITION

☒ Use as Is ☐ Repair ☐ Rework ☐ Reject

Disposition Instructions (if applicable):

Increase the monitoring and tuning frequency to reduce the intervals of increased instrument background. IONICON has suggested an invasive investigation into the issue and this will be performed at the next opportunity.

Disposition Technical Justification (if applicable):

None.

DISPOSITION APPROVAL/CONCURRENCE:

Engineering Manager (Print & Sign): Rich [illegible]	Date: 02/07/19	Client Technical Lead (Print & Sign): NAL	Date:
QA Manager (Print & Sign): Heath Low	Date: 02/07/19	Client QA Rep. (Print & Sign): 02/11/19	Date:

CLOSURE

Comments and Notes (if applicable):

It was discussed in the 01/31/2019 Weekly Mobile Laboratory Discussion meeting at 2505 Garlick, Richland, WA (Conference Room 2177):

- MCP module was replaced 01/25/2019 – resolved the background issue (NCR19-001);
- ML Team members are monitoring the instrument and data regularly and able to self-correct the baseline;

Nonconformance Report (03-2017)

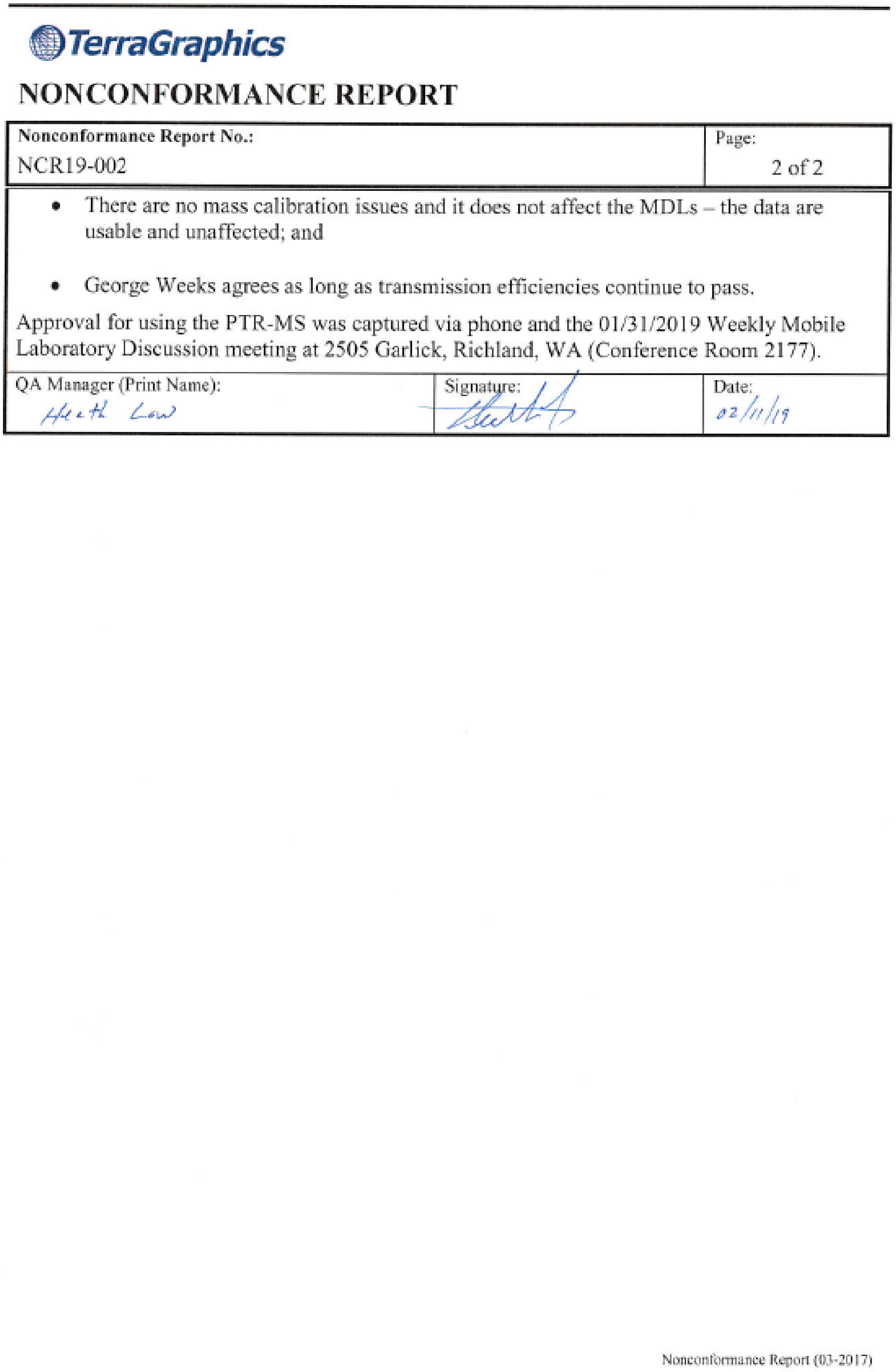

TerraGraphics

NONCONFORMANCE REPORT

Nonconformance Report No.: NCR19-002	Page: 2 of 2

- There are no mass calibration issues and it does not affect the MDLs – the data are usable and unaffected; and
- George Weeks agrees as long as transmission efficiencies continue to pass.

Approval for using the PTR-MS was captured via phone and the 01/31/2019 Weekly Mobile Laboratory Discussion meeting at 2505 Garlick, Richland, WA (Conference Room 2177).

QA Manager (Print Name): Heath Low	Signature:	Date: 02/11/19

Nonconformance Report (03-2017)